A COMPARISON OF DIFFERENT HEATING AND COOLING ENERGY DELIVERY SYSTEMS AND THE INTEGRATED COMMUNITY ENERGY AND HARVESTING SYSTEM IN HEATING DOMINANT COMMUNITIES

A COMPARISON OF DIFFERENT HEATING AND COOLING ENERGY DELIVERY SYSTEMS AND THE INTEGRATED COMMUNITY ENERGY AND HARVESTING SYSTEM IN HEATING DOMINANT COMMUNITIES

By BRENDAN SULLIVAN, B.Eng.

A Thesis Submitted to the School of Graduate Studies in Partial Fulfilment of the Requirements for the Degree Master of Applied Science

Master of Applied Science 2020 McMaster University

Mechanical Engineering Hamilton, Ontario, Canada

TITLE: A COMPARISON OF DIFFERENT HEATING AND COOLING ENERGY DELIVERY SYSTEMS AND THE INTEGRATED COMMUNITY ENERGY AND HARVESTING SYSTEM IN HEATING DOMINANT COMMUNITIES

AUTHOR: Brendan Sullivan

B.Eng. (Mechanical Engineering)

McMaster University, Hamilton, Ontario, Canada

SUPERVISORS: Dr. James Cotton and Dr. Marilyn Lightstone

NUMBER OF PAGES: ***CXCVI, 196***

Abstract

The building sector is one of the largest consumers of energy and producers of greenhouse gas emissions in Ontario, representing 13% of the province's emissions. Recently, countries have been looking to decrease their emissions in response to climate change. The electrification of space heating and domestic hot water preparation has gained traction in reducing emissions in countries with low emission electricity grids. This thesis proposes a novel energy delivery system called the Integrated Community Energy and Harvesting (ICE-Harvest) system. The ICE-Harvest system is a modified 5th Generation District Heating and Cooling (5GDHC) system. An ICE-Harvest system, much like a 5GDHC system, is a district energy system that incorporates heat pumps to couple the thermal and electrical energy demands of buildings. The ICE-Harvest system uses heat pumps to supply both heating and cooling from a one pipe thermal distribution network. The ICE-Harvest system has unidirectional mass flow in a ring arrangement with branches at each building. Bidirectional energy flow between the network and buildings is permitted, meaning that heat rejection from cooling processes can be recovered in the network to reduce the total system heating load. This concept is referred to as energy sharing.

The energy needs of the network, and thus the buildings, are serviced through a centralized generation station referred to as the Energy Management Center (EMC). The EMC regulates the supply temperature of the network to the controlled setpoint. Within the EMC, the primary generation source is a Combined Heat and Power (CHP) unit. The purpose of this CHP is to offset the existing centralized natural gas generators on the Ontario electrical grid. These gas generators operate intermittently and inefficiently as a form of dispatchable generation to stabilize the provincial electrical grid. In this research, it is proposed that ICE-Harvest systems with on-site CHPs could replace these gas generators while providing the same support to the electrical grid at

a much higher energy utilization ratio. For an accurate comparison, the CHP is constrained to only turn on according to the electricity system operator's gas generator dispatching schedule. An auxiliary boiler is included in the EMC to provide heat when the CHP is not permitted to operate. However, the possibility for Thermal Energy Storage (TES) to replace this boiler is also explored.

An ICE-Harvest system's ideal design depends on the market conditions, building energy demands, and available waste energy sources. This research presents an ICE-Harvest system in a heating demand dominated community located in Ontario, Canada. The community consists of five buildings. The ICE-Harvest system is compared to conventional and alternative building energy systems using the energy consumption data of these buildings. The systems are compared according to their energy consumption, emissions produced, and impact on the electrical grid at both the distribution and transmission levels. The topic of using thermal energy storage in ICE-Harvest systems is also discussed, and a parameter sweep is performed on the thermal energy storage capacity. The results show that the ICE-Harvest system offers demand management opportunities to electricity system operators, substantially reduces annual emissions, and offers improved energy utilization compared to conventional systems.

Acknowledgments

Research can not happen in isolation, and our results mean nothing without great minds to share them with. I would like to acknowledge and thank the many great minds I enjoyed learning from and collaborating with while producing this work.

In no particular order, my deepest gratitude goes to:

- Dr. James Cotton
- Dr. Marilyn Lightstone
- Dr. Yasser Abdelsalam
- Chantel Millar
- Ryan Rogers
- Dr. Vickram Lakhian
- Jessica Whittaker
- Brian McCrindle
- Erik Reimers
- My loving parents Kevin Sullivan and Karen Clarke and dearest brother Conor Sullivan

You have all made this an enlightening, enriching, and much less agonizing experience. Without your mentorship and friendship, I could not have reached this accomplishment. Thank you all very much.

Brendan Sullivan

Table of Contents

Notations and Abbreviations

Nomenclature

k	Gain of the controller [unitless]
$\dot{m}$	Mass flow rate [kg/s]
P	Power [W]
Q	Heat flow rate [W]
T	Temperature [°C] or [K]
Ti	Time constant of the controller integrator [s]
V	Volume [m^3]

Subscripts

B	Relating to a building
boiler	Relating to the boiler
bottom	Measured from the bottom of the Thermal Energy Storage
C	Relating to a cooling process
Carnot	Operating under Carnot conditions (ideal, reversible)
CHP	Relating to a CHP
con	Relating to the condenser
eva	Relating to the evaporator
H	Relating to a heating process
HP	Relating to a heat pump
max	Maximum allowed or expected value
min	Minimum allowed or expected value
nominal	Relating to the nominal operating condition
scaling	Parameter is used for scaling
setpoint	Relating to a controller setpoint
supplied	Energy supplied to the system
TES	Relating to the Thermal Energy Storage
th	Relating to thermal energy
top	Measured from the top of the Thermal Energy Storage

wasted	Energy wasted from the system

Abbreviations

5GDHC	5th Generation District Heating and Cooling
AEF	Average Emission Factor
AFUE	Annual Fuel Utilization Efficiency
ATD	Aggregate Thermal Demand
ATES	Aquifer Thermal Energy Storage
BF	Baufield
BTES	Borehole Thermal Energy Storage
BUR	Boiler Utilization Ratio
CCHP	Combined Cooling Heating and Power
CDH	Cold District Heating
CHP	Combined Heat and Power
CHCP	Combined Heating Cooling and Power
CHWS	Chilled Water Supply
CHWSR	Chilled Water Supply and Return
CO_2e	Carbon Dioxide Equivalent
COP	Coefficient of Performance
DC	District Cooling
DH	District Heating
DHC	District Heating and Cooling
EER	Energy Efficiency Ratio
ε-NTU	Effectiveness Net Transfer Units
EMC	Energy Management Center
EUR	Energy Utilization Ratio
FEL	Following the Electrical Load
FHL	Following the Hybrid Load
FTL	Following the Thermal Load
GFRP	Glass Fiber Reinforced Plastic
GSHP	Ground Source Heat Pump

HOEP	Hourly Ontario Electricity Price
HRHP	Heat Recovery Heat Pump
HWS	Hot Water Supply
HWSR	Hot Water Supply and Return
HVAC	Heating Ventilation and Air Conditioning
IBPSA	International Building Performance Simulation Association
ICE	Integrated Community Energy
IEA	International Energy Agency
IESO	Independent Electricity System Operator
IPCC	Intergovernmental Panel on Climate Change
LTDHC	Low-temperature District Heating and Cooling
LTN	Low-temperature Networks
MEF	Marginal Emission Factor
MILP	Mixed Integer Linear Programming
MR	Maximum Rectangle
PCM	Phase Change Material
PEC	Primary Energy Consumption
PI	Proportional-Integral
PTES	Pit Thermal Energy Storage
PV	Photovoltaic
PVT	Photovoltaic Thermal collector
SBG	Surplus Baseload Generation
SEER	Seasonal Energy Efficiency Ratio
SPF	Seasonal Performance Factor
TAC	Thermally Activated Cooling
TES	Thermal Energy Storage
TMY	Typical Meteorological Year
TTES	Tank Thermal Energy Storage
WSHP	Water Source Heat Pump

List of Tables

List of Figures

Chapter 1

1 Introduction and Problem Statement

The building sector is one of Canada's largest energy consumers and greenhouse gas producers [1]. With temperatures as low as -40 °C in many major cities, Canadians rely upon space heating to maintain comfortable living spaces. In 2016, Canadians consumed 1885 PJ of energy for thermal comfort (heating and cooling) and domestic hot water purposes. In consuming this energy, the buildings sector produced 82 Mt of CO_2 equivalent (CO_2e) (a term for describing the impact of different greenhouse gases under a common unit [2]), which makes it the third-largest source of emissions behind oil and gas production, and transportation [3]. If Canada is to meet its stated emissions reduction targets by 2030 [4], improvements must be made in the building sector.

Electrification of space heating and domestic hot water preparation has risen to prominence in numerous countries seeking to reduce their emissions impact [5]. The Canadian province of Ontario has a uniquely positioned electrical grid that could take advantage of this technology. Since phasing out coal powerplants in the province [6], emissions from the electrical sector have been decreasing steadily. In 2019, approximately 93% of Ontario electricity was generated by non-emissive sources [7]. A large share of the non-emissive electricity comes from nuclear and hydropower, which produces 86% of the energy supplied. However, the province still struggles to incorporate larger shares of variable renewable generators such as wind and solar. Despite representing 13% of the installed capacity, wind and solar generators supplied less than 8% of the electricity demand. Also, 2,581 GWh (22% of the province's demand) of wind and solar generation was curtailed which indicates that the renewable resources are not being used to their full potential [7]. Energy curtailment on an electrical grid is detrimental to the adoption of renewable energy projects worldwide, leading to lower capacity factors for generators and raising issues for system

operators [8]. System operators are exploring electrical energy storage systems to increase the utilization of renewable energy resources, but they are currently too costly to be implemented outside of subsidized pilot projects [9].

The electrification of space heating and domestic hot water preparation would introduce a sizeable new load to the electrical system. Intelligent controls and operations are necessary to avoid overloading the transmission and generation infrastructure. Fortunately, thermal energy demands are more straightforward to forecast due to predictable weather patterns. They are also more flexible than typical electrical loads allowing for demand response strategies such as preheating or precooling buildings and load deferment using thermal energy storage [10]. The problem is that heating and cooling are currently managed at the building level with no oversight from a system operator who could coordinate consumers' actions. Also, the energy demands of individual buildings are inconsequentially small compared to the grid energy demands. Thus, the response of individual consumers would have little impact on such an extensive system.

The need for coordination between a set of buildings with energy demands large enough to be non-trivial has shifted the focus towards district energy systems. District energy systems provide heating, cooling, and electricity to multiple buildings through underground piping networks. The thermal and the electrical energy are typically generated at one location and distributed to the district's customers. District energy systems have existed commercially since the 1880s, and they were first introduced to reduce the risk of boiler explosions in individual buildings [11]. District energy systems have evolved over the years since the 1970s, and today they are classified according to the temperature level of the transport media and the assets involved in energy production [12]. The 4^{th} and 5^{th} generations of District Heating and Cooling (DHC) systems are currently being explored for their ability to become part of a holistic, smart energy system [13].

Fifth Generation District Heating and Cooling (5GDHC) systems use heat pumps at each building to deliver heating and cooling from a low temperature piping network [14]. The use of heat pumps introduces a coupling between the thermal and the electrical energy demands that can be used by system operators to control the electrical demand. Since heat pumps require electricity to operate, electricity demands will be linked to the thermal energy required. The ratio between the amount of thermal energy delivered or extracted versus the amount of electricity consumed is measured by the Coefficient of Performance (COP) of the heat pump. The COP of a heat pump is a function of the temperature difference between the heat pump's evaporator and condenser. In building applications, the condenser's temperature is fixed according to the required supply temperature of the building hot water system. Conversely, the evaporator temperature is set according to the supply temperature of the building chilled water system. For simplicity, the discussion will focus on heating operation. Therefore, the COP of the heat pump can be controlled by changing the temperature on the evaporator side of the heat pump.

Typically, heat pumps are connected to a quasi-infinite source such as the air or ground, whose temperatures are mostly unaffected by the heat pump energy consumption. However, in 5GDHC systems, the heat pump can be connected to a closed-circuit network where the temperature can be controlled by a system operator. Depending on the size, and thus thermal mass, of the network, changing the temperature can be within the timescale of minutes to hours.

In this research, a modified 5GDHC system is compared to other building energy delivery systems. The system is referred to as the Integrated Community Energy and Harvesting (ICE-Harvest) system. The ICE-Harvest system uses Water Source Heat Pumps (WSHPs) at each building connected to a single pipe thermal distribution network with an Energy Management

Center (EMC) to control the network's supply temperature. A schematic of the system is provided in Figure 1.1.

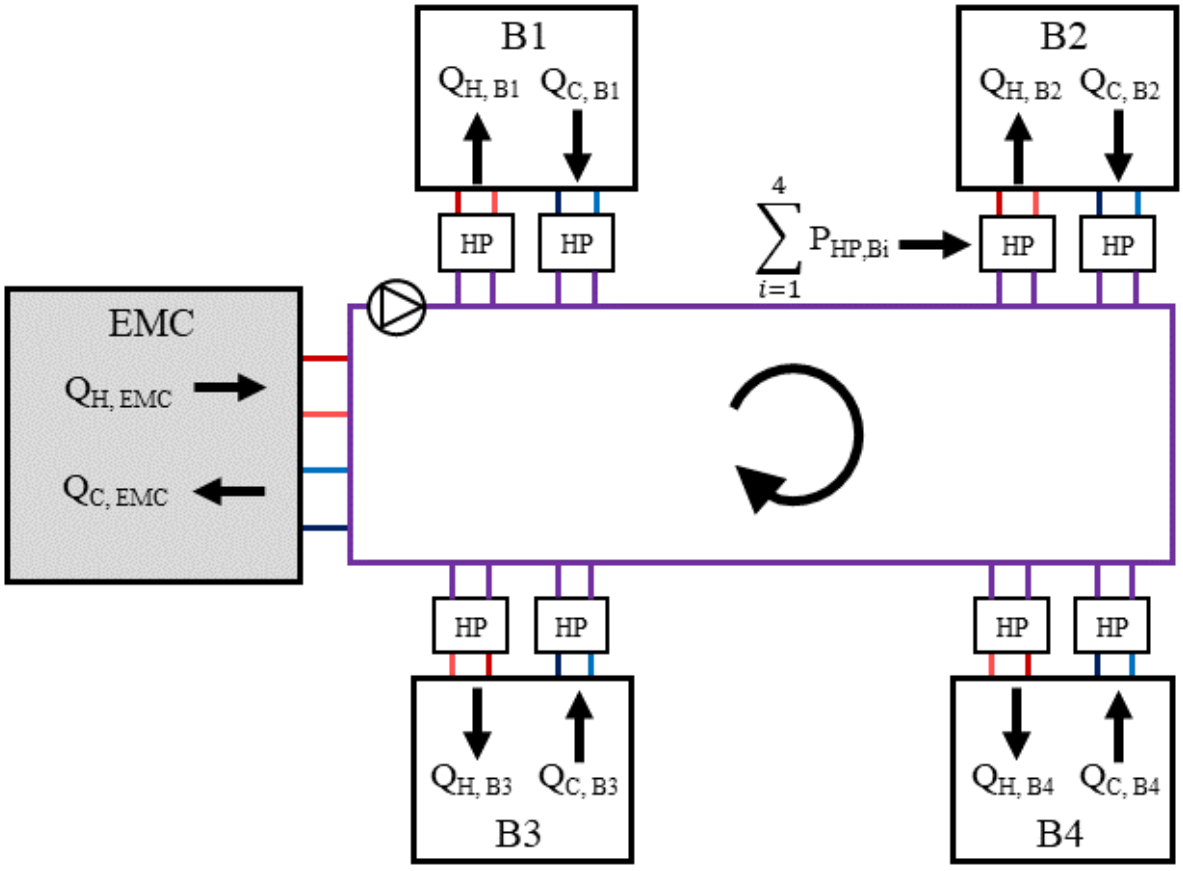

Figure 1.1: Schematic of the ICE-Harvest system. Energy flows are shown and categorized according to thermal energy (Q) and electrical energy (P).

The single pipe network is connected to each building in series without separate piping for supply and return. This arrangement allows for heat recovery from building cooling processes to be used directly by neighbouring buildings in the network. The EMC adds or removes energy to or from the network as required to maintain a specific temperature setpoint. The piping of this network is different from conventional DHC systems where four separate pipes are used. The four pipes in a conventional DHC system are separated according to temperature level, typically using a hot water supply, hot water return, chilled water supply, and chilled water return. The benefit of

using a single pipe network is that heating and cooling come from the same pipe allowing for bidirectional energy flow.

While there are numerous options for equipment to use within the EMC, this research will focus on using the waste heat from gas generators as the primary heat source. Gas generators account for 29% of Ontario's installed generation capacity, yet they produce only 6% of the delivered power [15]. This discrepancy between capacity and generation is because gas generators are mainly used for dispatchable generation. Dispatchable generation means that the gas generators respond to supply or demand changes to balance the electrical grid. Therefore, the gas generators are contracted to operate for short periods (typically 1 to 3 hours) at infrequent intervals throughout the year. The generators generally are contracted to operate according to the one day ahead schedule created by the electricity system operator. The number of contracted generators varies depending on market conditions such as the predicted wind and solar availability, sudden increases in demand, or outages from other generating equipment. For example, the gas generators tend to operate more frequently during the summer months when there is high variability in demand due to cooling equipment energy demands. Furthermore, the amount of generation can also change annually. For example, gas generation increased substantially during 2015 and 2016 due to the nuclear powerplants entering refurbishment [16].

These gas generators have low efficiencies, typically only converting 30% to 40% of the fuel they consume into electricity [17]. The heat produced by the generators is exhausted to the ambient as waste. This research proposes moving the gas generators into communities where the heat they produce can be used in a local thermal distribution network. This will be accomplished through the use of decentralized Combined Heat and Power (CHP) units installed in the EMC. The concept is similar to the CHP units that are commonly used in District Heating (DH) systems [18].

However, the ICE-Harvest CHP will operate according to a one day ahead schedule provided by the electricity system operator rather than in response to the local energy demands.

The novelty of this approach is that CHPs typically operate by either:

- Following the Thermal Load (FTL)
- Following the Electrical Load (FEL)
- Following the Hybrid Load (FHL)
- Following an optimized scheduling software

The downside of these operating strategies is that they do not consider using the CHP to offset grid-level natural gas generators. The waste heat produced by these gas generators represents a large untapped thermal resource in the province of Ontario.

The ICE-Harvest CHP schedule is predetermined according to gas generator operating hours in the Ontario energy market. The Ontario energy market is used in this thesis because it has a large capacity of renewable and emission-free generation that is supported by dispatchable gas generators. This type of market has become increasingly common as more countries switch to renewable energy resources but have difficulties managing the energy supply. Thus, the concept presented in this research can be applied to any similar market. The historical gas generator hours for 2015 through 2018 are shown in Figure 1.2. The gas generators are considered to be “On” when their combined output is greater than or equal to 1000 MW, approximately 10% of the installed gas generator capacity. This threshold was chosen because 1000 MW of capacity is sufficiently large such that demand response measures could be coordinated.

There were significantly more gas generator hours in 2015 and 2016 than in 2017 and 2018, attributed to increased energy conservation measures, consumer price incentives, and an increase

in embedded generation [19]. All of these factors contribute to reducing the amount of grid-level gas generation required. The CHP will be restricted to only operate during these hours. The results will indicate what would happen if the gas generators' heat were used in a thermal distribution network rather than being wasted by enforcing this restriction. The quantification of the possible fuel and emission savings will provide insight into whether it is worthwhile to relocate gas generators closer to the communities that they serve. The CHP heat will be used to supply energy to the thermal distribution network, which acts as the source for the building heat pumps.

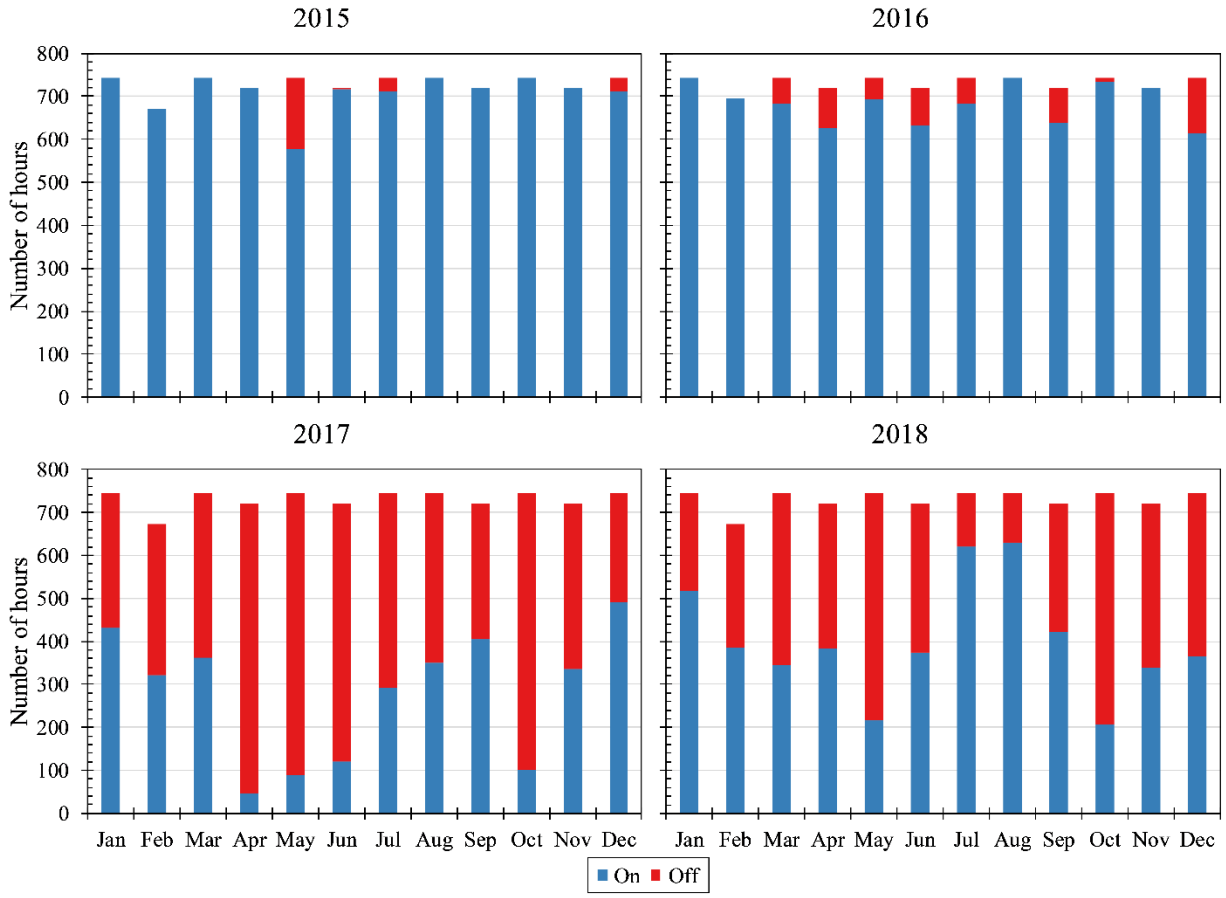

Figure 1.2: IESO gas generator operating hours in Ontario for the years 2015 through 2018. Hours are grouped according to the month of the year. The threshold for the gas generation to be considered "On" is 1000 MW of capacity. One "On" hour corresponds to one hour of 1000 MW or more gas generation on the grid.

This scheduling limitation will result in a decoupling of the supply and demand of energy. For example, the CHP could be contracted to operate during the summer when there is no heating

demand in the network. Also, it is more challenging to decide upon the CHP capacity. Typically, the CHP capacity is determined by the energy demands of the buildings being serviced. Methodologies commonly used include the Maximum Demand Rectangle method [20], the Aggregate Thermal Demand (ATD) [21], or optimized sizing according to a specific objective function [22]–[25]. Since the ICE-Harvest CHP does not respond to local energy demands, an alternative sizing strategy must be developed.

In this research, the CHP is sized according to the total heating demand in the network and the number of operating hours the CHP is scheduled to run in a year. This sizing methodology was chosen as it provided good system performance and reasonable equipment capacities. As a result of this sizing methodology the CHP capacity is undersized for the largest heating demand necessitating a boiler for increased heat output capacity. Thermal Energy Storage (TES) is also considered to increase the heat output capacity. In some cases, TES was shown to be capable of replacing the boiler entirely.

The ICE-Harvest system is compared to other building energy systems. The alternative options discussed are a conventional system of individual heating and cooling equipment at each building, a DH system where a centralized CHP delivers heat according to a FTL control strategy, and a Ground Source Heat Pump (GSHP) system with individual geothermal borehole fields at each building. The systems are compared according to their energy consumption, emissions produced, and impact on the electrical grid. The comparison is made using Dymola, a system simulation software that uses libraries developed as part of the International Energy Agency (IEA) Annex 60 [26] and International Building Performance Simulation Association (IBPSA) Project 1 [27] projects. This work aims to quantify the ICE-Harvest system's potential to utilize the heat

currently being wasted from grid-level gas generators and prove that demand response is achievable through a coupled smart energy system.

An overview of the work is as follows. Chapter 2 provides a literature review of topics related to 5GDHC. This review includes the history of DHC systems, a background on energy markets in Ontario, a discussion of energy modelling tools and software, and examples of TES projects. Chapter 3 presents the methodology for the research. This section outlines the assumptions made during modelling and shows verification of the system performance. Chapter 4 is the results section of the work. In this chapter, results are shown comparing the ICE-Harvest system to a conventional, district heating, and GSHP system. The systems are compared according to their electricity demands, electricity supply, impact on the hourly electricity demand, heating energy supplied, utilization of waste heat, equipment capacities required, and emissions produced. A parameter sweep on the TES volume is also performed, and the impact of CHP scheduling is examined using a set of the historical gas generator operating hours in Ontario. Chapter 5 discusses the emissions and energy consumption reductions of each system and the potential for electrical demand management. The chapter also shows the energy balances of the GSHP borehole fields and the TES's temperature and heat loss measurements. Chapter 6 provides conclusions and recommendations for future work.

Chapter 2

2 Literature Review

This literature review will cover topics related to the current state of Ontario energy markets, the evolution of DHC systems, a survey of comparable 5GHDC systems found in literature, examples of software used for energy system modelling, and a discussion on TES technologies and practices.

2.1 The current state of Ontario energy markets

2.1.1 Heating, cooling, and domestic hot water

The building sector consists of all human-made structures that require Heating, Ventilation, and Air Conditioning (HVAC) to maintain the thermal comfort and safety of its occupants. The Intergovernmental Panel on Climate Change (IPCC) divides the building sector into residential and commercial [28]. In 2010, the residential sector accounted for 24% of global energy consumption while the commercial sector accounted for 8%, totalling 32% of global energy consumption or 32.4 PWh of energy [29]. There are over five million occupied private dwellings in Ontario, with the majority (54.3%) being single detached houses [30]. In these buildings, 61.7% of energy is used for space heating, 19.7% for domestic hot water preparation and 3.4% for space cooling [31]. As shown in Figure 2.1, non-renewable based fuels accounted for 73.5% of all space and water heating energy use in the residential sector [1]. Most households use natural gas because of the robust distribution network present in most Canadian cities. Natural gas is an affordable option for homes located in dense urban centers where numerous customers can use the same distribution piping. The province of Ontario is currently looking to expand natural gas distribution

infrastructure in northern and remote communities [32]. The projects are eligible for $130 million in funding with an expected annual fuel cost savings of $800 to $2500 per household.

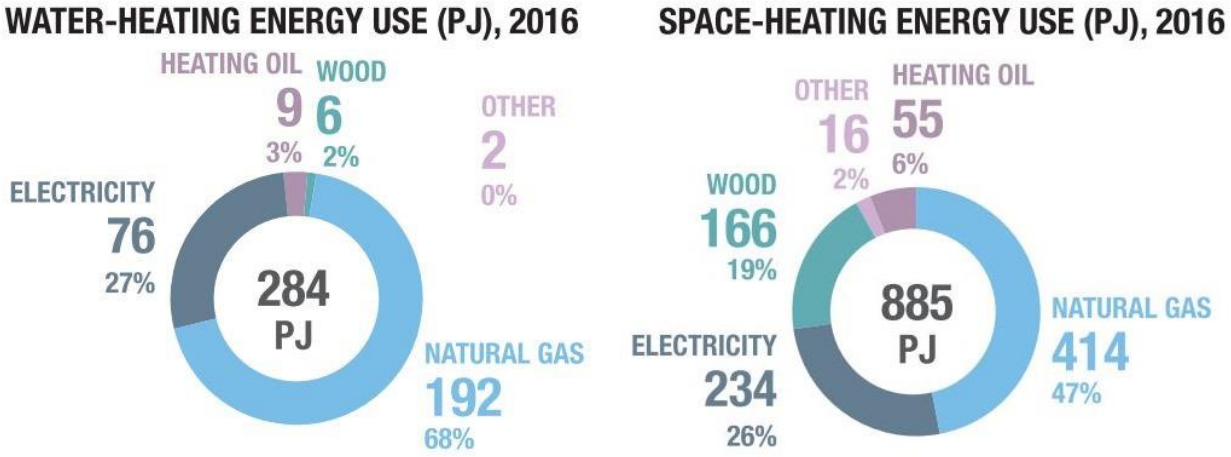

Figure 2.1: Space and water heating energy use by fuel source across Canada in the residential sector [1]

The high shares of non-renewable fuel sources used in space and water heating are responsible for most of the emissions from the building sector. In 2017, space and water heating accounted for 84% of all emissions from Ontario's residential sector [31].

Forced air furnaces are the most common primary heating system in Canadian households making up 55% of all heating equipment [33]. The efficiencies of furnaces and boilers have increased considerably in the past decades. New high-efficiency furnaces have Annual Fuel Utilization Efficiencies (AFUEs) of 90% to 98.5% compared to older furnaces with AFUEs between 56% and 70% [34]. In the interest of improving energy efficiency, government programs have been put in place to subsidize the cost of high-efficiency furnaces for homeowners [35]. Electric-based heating sources such as baseboard heaters, radiant heaters, and heat pumps represent 31% of all heating equipment, with 26% being baseboard heaters, 4% heat pumps, and 1% radiant heaters. Currently, electric heating sources are most common in Northern communities where there is no access to natural gas piping networks.

Space cooling demands are much smaller in the province than space heating demands. In 2017, the cooling demand across Ontario in the residential sector was only 18.7 PJ compared to the 336.1 PJ used for space heating [31], which is an 18 times difference. The commercial and institutional sector is not much different, with 25.1 PJ of space cooling and 240.5 PJ used for space heating, which is a 9.6 times difference [36]. The actual energy consumption for space cooling is difficult to measure because cooling equipment uses electricity to meet a thermal demand. To get an accurate estimate of the energy consumption the cooling equipment must be sub-metered to monitor the individual energy consumption which is rarely done. The European Cooling Index was established to estimate and understand the variations in space cooling demands across Europe [37].

A cooling process's efficiency is referred to as the Energy Efficiency Ratio (EER), which varies depending on climatic conditions, building temperature setpoints, and equipment technology. The Seasonal Energy Efficiency Ratio (SEER) is used to benchmark cooling equipment performance on an annual basis accounting for differences in climatic conditions. The Canadian government publishes Energy Efficiency regulations for cooling equipment that manufacturers must satisfy to be eligible for sale [38]. For example, the minimum SEER for single package central air conditioners is 12.0 (for through-wall air conditioners) to 14.0 (for others). This efficiency corresponds to a COP of 3.1 to 3.5, which means approximately three Joules of heat are removed from the conditioned space for each Joule of electricity consumed.

While cooling demands are currently much smaller than heating demands, they are predicted to increase in the coming years. In 2016, commercial and residential buildings' space cooling accounted for an estimated 2.02 PWh of electricity consumption [39]. That demand is predicted to increase by approximately 7% annually up until 2100 [40]. Cooling demands are

expected to grow due to a global rise in average temperature and increased accessibility to electricity in the developing world [41].

While the total cooling demand appears small amongst all buildings, there are some specialized buildings with considerably high cooling demands. For example, grocery stores have an average energy use intensity of 530 kWh/m^2/year, double that of comparable commercial buildings. The energy use is large due to the need for refrigerated storage which is 2.1 times more energy-intensive than non-refrigerated storage [42]. Additionally, researchers at CanmetENERGY found that ice rinks have double the average annual energy use intensity as other municipal buildings (500 kWh/m^2/year versus 236 kWh/m^2/year) [43]. This is due to the energy required to maintain the frozen skating surfaces. Of this energy consumption, 50% was used for refrigeration with only 10% of the refrigeration waste energy being recovered. They concluded that the refrigeration system rejected three times the energy required to meet the building heating requirements, signifying the potential for an improved waste heat recovery program.

Another building category with large cooling demands is data centers. Data centers are essential in the field of information technology for storing and transmitting data. Between 2010 and 2018, internet traffic increased by over ten-fold and data center storage capacity increased by 25 times to keep up with demand [44]. Data centers require electricity to operate and the power they consume is dissipated through the circuitry as heat. Shehabi et al. reported that 43% of all electricity consumed in data centers in the United States is used for cooling and power provision systems [45]. These energy-intensive buildings with high cooling demands offer opportunities for localized heat recovery strategies. Amazon was one of the first companies to take advantage of this opportunity by partnering with a neighbouring telecom building to recycle approximately 4 million kWh of heat each year [46].

2.1.2 Electricity

Ontario's electricity market consists of numerous power producers and power plants managed by a centralized electricity system operator. The system operator in Ontario is called the Independent Electricity System Operator (IESO) and they are responsible for managing the delivery of power from the power plants to the customers. Their primary concern is balancing the supply and demand of power on a near-instantaneous basis to avoid overloading the transmission infrastructure. They accomplish this through supply and demand predictions based on historical energy consumption and weather data.

The Ontario supply mix consists of nuclear, hydro, gas, wind, solar and biofuel. Most producers are considered transmission connected generation that transmit power from their centralized sites to local distribution companies through high voltage transmission lines (50 kV and above). Transmission connected generators are eligible to sell power on the grid at the rates determined by the IESO Hourly Ontario Electricity Price (HOEP) [47]. The HOEP is determined dynamically. It is used as a leveraging tool to incentivize producers with higher production costs to produce power profitability during increased demand or decreased supply. There are also distribution connected generators, which are small-scale generators that provide electricity to nearby buildings such that the demands are managed locally. The purpose of distribution connected generators is to offset demand from the transmission grid, which avoids capacity enhancements and system bottlenecks. The majority of Ontario's solar power generation is distribution connected generation with 2195 MW of distribution connected capacity compared to 478 MW of transmission connected capacity [48].

The supply mix refers to the group of producers providing power at a given moment in time. The mix of producers is continuously changing in response to changes in demand or resource

availability. Figure 2.2 shows the hourly Ontario supply mix for June 11th to June 17th, 2020. The nuclear generation is shown in orange, hydro in light blue, gas in dark blue, wind in green, solar in yellow, and biofuel in dark red.

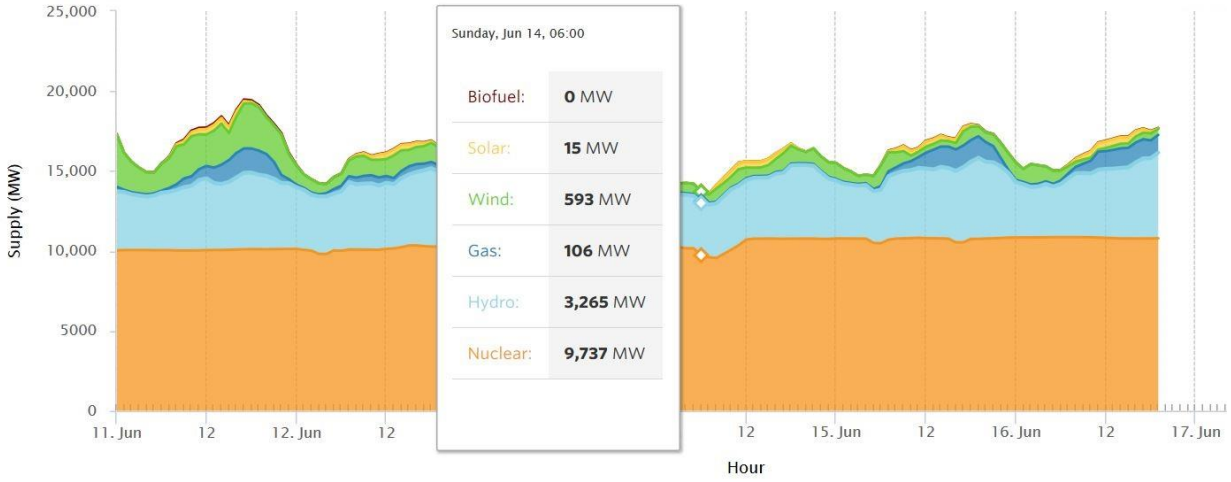

Figure 2.2: Hourly Ontario supply mix for June 11th, 2020 through June 17th, 2020 [49]

Most of the electricity generated comes from nuclear and hydro. These two resources provide what is known as baseload power. Baseload power provides a stable level of power to the grid to meet a large portion of the electricity demand, allowing flexible generators (for example, gas power plants) to meet the transient electrical demands. Nuclear is selected for this purpose because of its high output and stable production. The drawback of these plants is that they are inflexible to variations in demand. Reducing a nuclear reactor's output, referred to as a nuclear manoeuvre, is when the turbine is bypassed and the fuel energy is not used to produce power [50]. Evidence of a nuclear manoeuvre can be seen in Figure 2.2 at approximately 7:00 AM on June 14th, 2020 when the nuclear supply decreases in response to a decrease in demand.

To solve this problem, system operators rely upon variable and dispatchable generators. Renewable resources such as wind and solar are classified as variable generators because operators cannot control their output. The utilization of these resources is encouraged because the energy

source is emission-free and has no associated fuel costs. The intermittent nature of variable generators leads to problems when there is insufficient supply during peak demands or surplus supply during low demands. Dispatchable generators are used to mitigate this problem by rapidly responding to fluctuations in output. Natural gas generators are the primary form of dispatchable generation on the Ontario electrical grid. Gas generators represent 26% (11,317 MW) of the installed capacity and only 6% (9.5 TWh) of the supplied electricity [7]. A large capacity of gas generators is maintained as a redundancy measure for other generators. In the event of maintenance or failure, gas generators are used to maintain a stable power supply while the problem is addressed. There is also an estimated 1053 MW capacity of behind the meter CHP in Ontario [51]. Behind the meter refers to the fact that the power produced by the CHPs is used entirely on-site and they do not supply or sell to the grid. These projects are popular with businesses and institutions that have large energy demands to reduce their energy costs.

The difficulty in predicting the output of variable generation resources serves as a severe barrier to widespread adoption [52]. This difficulty has led to the belief that wind and solar cannot exceed a limit of 20% to 25% of all generation [53]. However, some researchers believe that higher renewable energy penetration is possible through decoupling the generation and consumption using energy storage [54]. The Ontario IESO is currently investigating this opportunity and as of 2016 has procured 21 energy storage projects with a total installed power capacity of 50 MW [9]. Results from the report highlight the ability for energy storage systems to withdraw Surplus Baseload Generation (SBG) from the grid, which is later reinjected or used in a commercial process. While the report did not comment on the economics of energy storage, a report done in California assessed the stacked economic benefits of energy storage projects [55]. They found that by combining multiple revenue streams such as increased transmission / distribution capacity,

spinning reserves, frequency regulation, and generation capacity, batteries could be valued at $280/kW-year. Battery prices, however, range of $200 to $500/kW-year and the revenue streams discussed are not guaranteed in all markets. Until the reliability of renewable generators can be improved, dispatchable generation is necessary on the power grid.

The variability in the supply mix of the Ontario electrical grid leads to a highly dynamic emissions factor. For example, some hours will have all the power provided by emission-free sources, whereas other hours could have significant shares of gas generation on the grid. The Atmospheric Fund publishes an annual report detailing the Average and Marginal Emission Factors for the province [56]. The Average Emission Factor (AEF) is the average carbon intensity of electricity consumed from the Ontario grid based on the weighted average of each producer's output for that hour and its corresponding emission factor. The Marginal Emission Factor (MEF) is the change in carbon emissions from a change in electricity consumption in each hour. The MEF is distinguished from the AEF because energy conservation measures are expected to disproportionately reduce the use of highly emissive sources (such as gas generators).

Figure 2.3 shows the MEF and AEF for Ontario in 2018. The MEF is always greater than the AEF because the gas generators that are producing on the margin are the largest source of emissions from the electricity sector. The Atmospheric Fund recommends using the AEF for calculating current or historical emissions on an hourly basis and the MEF to calculate the emission saving potential of a demand intervention project such as installing solar panels or battery storage.

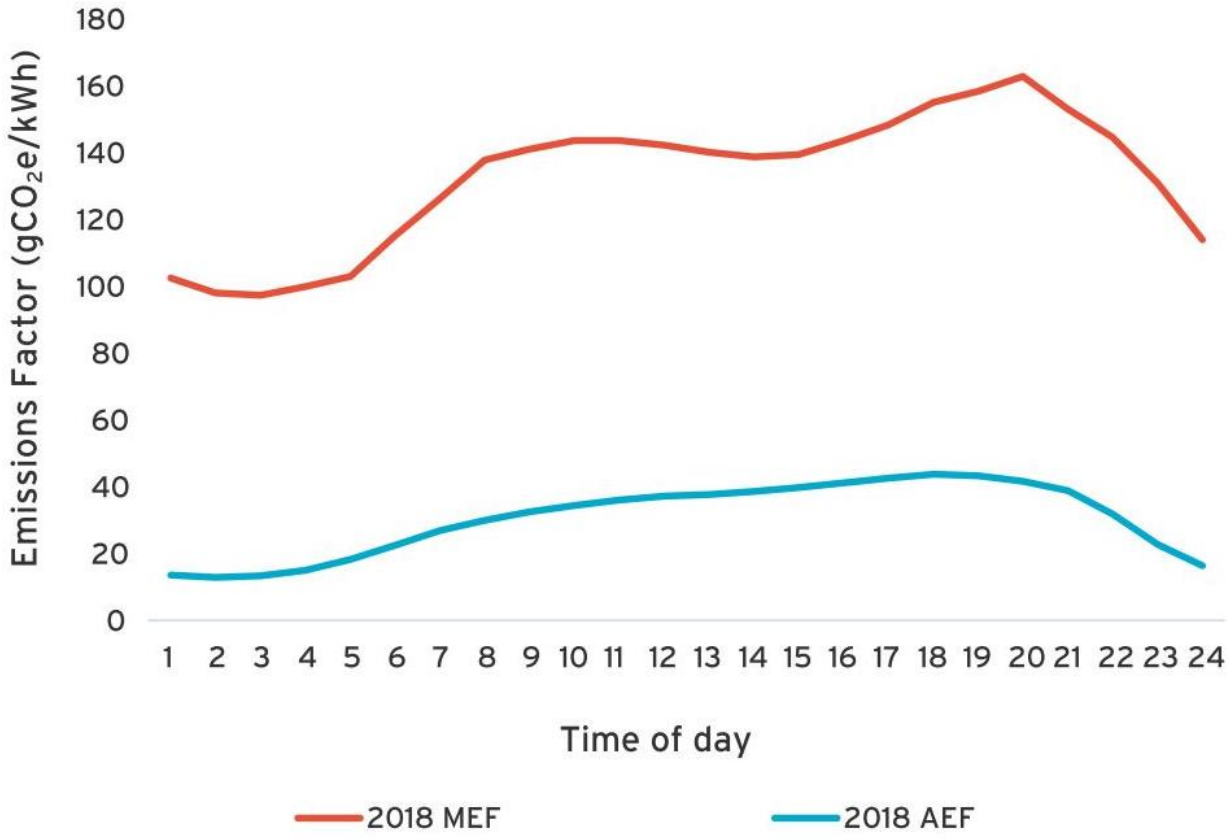

Figure 2.3: Ontario 2018 Average and Marginal Emission Factors [56]

Emissions from the electrical sector have been steadily declining in Ontario since the phase-out of coal-fired power plants [6]. In 2019, over 96% of all transmission connected power supplied in Ontario came from emission-free sources [7]. Therefore, there is significant potential to reduce emissions from the buildings sector by using emission-free electricity for heating, cooling, and domestic hot water production instead of fossil fuels.

2.2 The evolution of district heating and cooling

There are four categories of district energy systems: DH, District Cooling (DC), DHC, and trigeneration systems. The central components of all the systems are identical. Some buildings act as the consumers of energy, a distribution network to deliver the energy to the buildings, and energy producers that supply heating and cooling to the network. DH systems only deliver heating,

DC systems only deliver cooling, DHC systems deliver heating and cooling, and trigeneration systems deliver heating, cooling, and power [57]. Trigeneration is also referred to as Combined Cooling Heating and Power (CCHP) [58], Combined Heating Cooling and Power (CHCP) [21], or multi-energy systems [59].

2.2.1 District heating

DH systems are the most common of the four categories. DH systems are divided into five generations according to their network supply temperature, transportation medium, heating and cooling equipment.

2.2.1.1 1st through 3rd generation

The first generation of commercial DH emerged in the period of the 1870s to 1880s [11]. These systems were established in Lockport and New York, USA. The systems consisted of an underground piping network that transported high-temperature steam to buildings from centralized boiler plants. The primary motivation for developing DH systems was to reduce the risk of boiler explosions in individual apartments. Other benefits include the economies of scale from using larger capacity equipment and easier maintenance due to fewer assets to manage. However, these DH systems suffered from drawbacks, including frequent bursts requiring extensive network maintenance and high distribution temperatures that led to high heat losses in the network. Almost all DH systems built up until the 1930s used the first-generation design. The DH system in New York is still operational today and provides steam service to roughly 1700 commercial and residential customers [60].

The second generation of DH emerged in the 1930s and used high-temperature water instead of steam as the heat carrier medium. The pressurized water temperature was typically at or

above 100 °C and used pressurized piping to avoid vaporization [13]. With the introduction of the 2nd generation of DH came new installations in the Soviet Union and China who adopted the technology in the 1930s and 1950s, respectively. Switching to a lower network supply temperature reduced the network heat losses and increase fuel savings. By lowering the supply temperature, suppliers were able to use CHP units. CHP-based DH systems can increase primary energy utilization by up to 40% compared to traditional power plants [61]. By using the fuel energy to produce both power and heat, CHPs effectively use the otherwise wasted heat, thereby increasing fuel utilization [62]. CHP-based DH systems are some of the most common types of DH systems in the world. For example, in Finland (which supplies 50% of its resident's heating requirements using DH), CHP-based DH makes up 73% of all DH systems [63].

The third generation of DH was introduced in the 1970s, and it continued to lower supply temperatures below 100 °C. This temperature level is still appropriate for direct heat delivery to buildings through a heat exchanger, but the lower temperature further decreased heat losses in the network. The 3rd generation of DH is the most popular form of DH system used today; most new systems installed or extended in North America, Europe, and Asia use this technology [13]. It became possible to prefabricate the networks' components, which reduced costs and increased adoption rates. The Oil Crisis of the 1970s shifted many countries' focus towards energy security and energy efficiency [64]. DH systems were well-suited for this purpose as CHP units have high energy utilization and can use various fuel sources.

There are currently an estimated 80,000 DH systems installed worldwide [65]. The DH market amounted to 11.5 EJ[1] of heat delivered in 2014 [66]. Of this amount, 51% of the heat was

[1] 1 EJ (Exa Joule) = 10^{18} Joules

delivered to buildings, 45% to industries, and 4% to other sectors. Most of the district heat energy delivered is in Russia, China, and Europe, which make up 85% of all heating consumed. However, it is worth noting that heat deliveries in North America are higher than reported by the IEA because many North American DH systems are operated by end-users such as hospitals and universities, which is not included in the IEA energy balance. Internationally, recycled heat from fossil fuel-based CHPs and industries makes up most fuel consumption in DH networks, followed closely by the direct use of fossil fuels [13]. Renewable energy sources such as geothermal energy, biomass, and waste comprise just a small percentage of the heat supplied by DH systems internationally. In the European Union, however, renewable sources represent a larger market share than the direct use of fossil fuels. This results from an increased focus on emissions reductions and renewable energy sources in the European Union.

2.2.1.2 4th generation and beyond

The 4th generation of DH is distinct from previous generations because it introduces the idea of DH as part of a holistic energy concept. Researchers have shown that CHPs together with renewable energy resources offer important synergies between thermal and electrical energy [13], [67]. The 4th generation builds on previous generations by supplying water at lower temperatures, but more importantly, it introduces DH as part of a smart energy system [5]. The smart energy concept entails cross-sectoral integration of energy (i.e.., thermal and electrical sectors) to maximize the possible energy saving synergies. Benefits include the active regulation of CHP plants using TES, integrating heat pumps into DH networks, and including CHPs as part of a grid stabilization strategy.

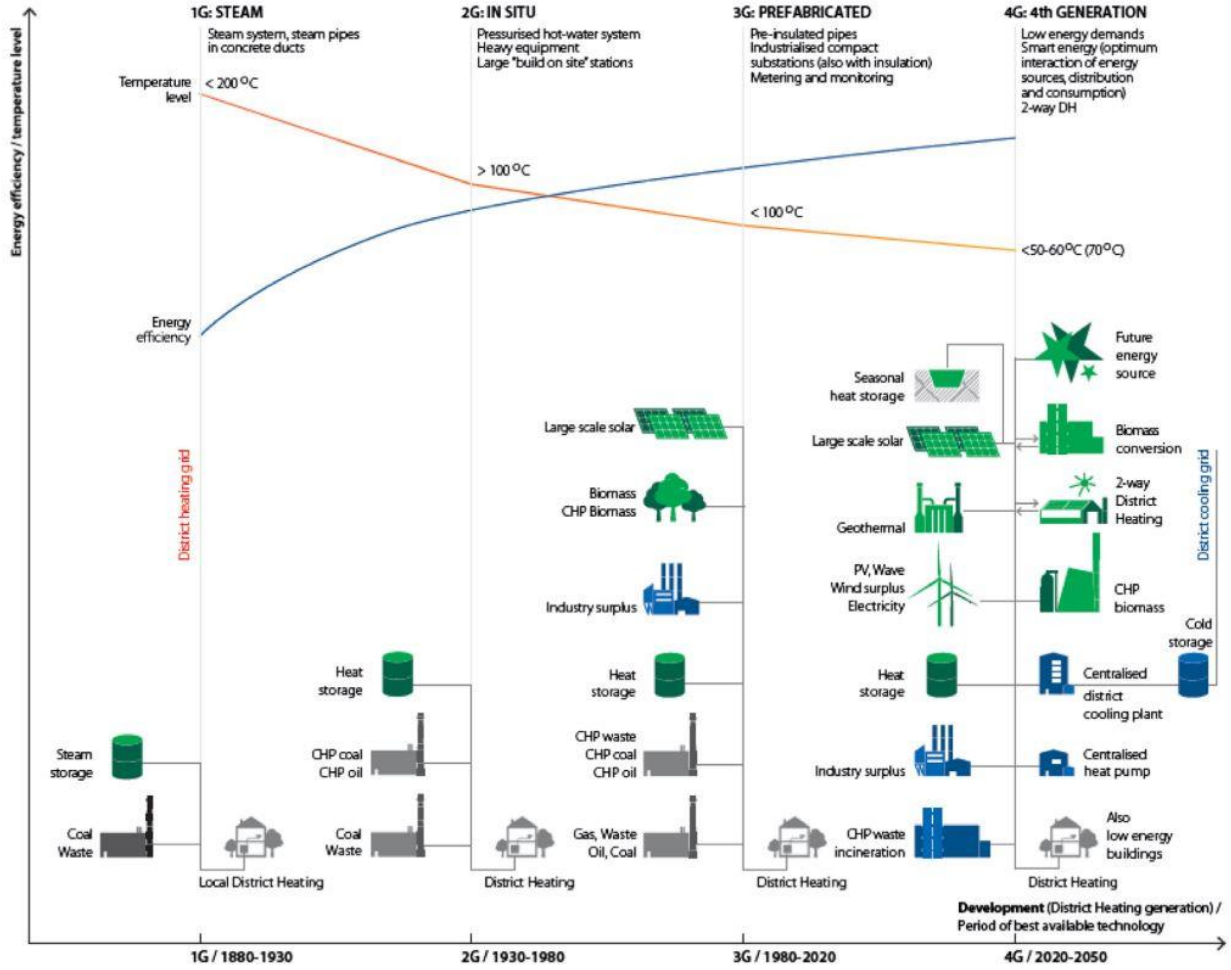

Figure 2.4: Evolution of DH from the 1st to 4th generation [13]

Figure 2.4 depicts the evolution of DH systems from the 1880s to the present day. As depicted on the y-axis, the temperature level steadily decreases with each successive generation while the energy efficiency increases due to lower heat losses. Along the x-axis, there are also pictures indicating the resources involved in the system. As the generations evolve, more resources are incorporated. Initially, DH systems relied on the direct use of fossil fuels such as coal and oil to create heat energy to be delivered to customers. In 4th generation systems, there are no generators that only produce heat using fossil fuels. Examples of energy suppliers are industry waste heat sources, CHP waste incinerators, and centralized heat pumps. These sources are connected to external markets such as industrial processes, waste disposal, and power generation that go beyond

simply delivering thermal energy. The resources shown in green (renewable surplus electricity, large scale solar, geothermal) indicate that the 4th generation of DH is part of the overall energy market including electricity.

Increasing renewable energy penetration levels is one of the largest problems facing electricity system operators today. Painuly outlined the major barriers associated with renewable energy penetration [68]. These barriers include technical issues such as intermittent generation and difficulties in forecasting demands to financial barriers caused by the lack of existing market structure for financing renewable energy projects. The greatest potential for facilitating the integration of these resources has been found through coordinating thermal and electrical energy demands [69].

The most recent generation of DH is the 5th generation of DH [14]. The 5th generation DH systems use supply temperatures lower than that of building hot water systems. 5th generation systems require water-source heat pumps (WSHPs) to deliver energy to the buildings at the desired temperature level. WSHPs at each building allow 5th generation systems to deliver both heating and cooling from the same pipe. For this reason, the 5th generation of DH is referred to as the 5th Generation District Heating and Cooling (5GDHC).

Buffa et al. conducted a survey of DHC systems in Europe, of which there are 40 5GDHC systems currently in operation [14]. Before the classification as 5GDHC, numerous systems were using different names to describe the same technology. 5GDHC has also been referred to as Low-temperature District Heating and Cooling (LTDHC) [70], [71], Low-temperature Networks (LTNs) [71]–[74], Cold District Heating (CDH) [75], [76] and Anergy networks. According to the definition of 5GDHC provided by Buffa et al.:

> *A 5GDHC network is a thermal energy supply grid that uses water or brine as a carrier medium and hybrid substations with Water Source Heat Pumps (WSHP). It operates at temperatures so close to the ground that it is not suitable for direct heating purpose. The low temperature of the carrier medium gives the opportunity to exploit directly industrial and urban excess heat and the use of renewable heat sources at low thermal exergy content. The possibility to reverse the operation of the customer substations permits to cover simultaneously and with the same pipelines both the heating and cooling demands of different buildings. Through hybrid substations, 5GDHC technology enhances sector coupling of thermal, electrical and gas grids in a decentralised smart energy system* [14].

5GDHC will be the primary focus of this research as the proposed system falls into the classification provided above. Further discussions will be limited to 5GDHC systems and their operation.

2.3 5th generation district heating and cooling

There is no single design of 5GDHC systems. Instead, systems are divided into numerous classifications depending on the type of loop, the number of distribution pipes, and the direction of energy and medium flow in the network. The types of loops are divided into open-loop and closed-loop systems similar to GSHP systems [77], [78]. Open-loop systems pump the transport medium from a quasi-infinite source (ex. lakes or groundwater) and closed-loop systems circulate the transport medium in a piping circuit. The number of distribution pipes is counted according to the number of pipes at different temperature levels in the network [79], [80]. For example, a traditional DHC system with pipes for hot and chilled water supply and return is classified as a four-pipe network. The direction of energy flow refers to whether buildings are consumers or

prosumers of energy [81]. Prosumers can add energy into the network to be used for heating in other buildings. Systems with distributed pumping stations can reverse the transport medium's direction in the network, which distinguishes these systems from traditional systems where the flow direction is unidirectional and managed by a centralized pumping station. Table 2.1 provides a summary of the different 5GDHC classifiers with descriptions of each term.

Table 2.1: Summary of 5GDHC classifiers (adapted from [14]*).*

Classifier				
Type of loop	**Open-loop**: the transport medium is extracted from a quasi-infinite source, passed through the network then discharged to the same source		**Closed-loop**: the transport medium is circulated in a closed circuit where energy is added and extracted	
Number of distribution pipes	**One-pipe**: supply only, no return pipe	**Two-pipe**: the supply temperature is greater than the return in heating mode and less than the return in cooling mode	**Three-pipe**: like the two-pipe design but a third pipe is included at a temperature suitable for direct heating or cooling	**Four-pipe**: separate supply and return for heating and cooling
The direction of energy and medium flow	**Unidirectional energy flow – Unidirectional medium flow**: traditional DH/DC system where one producer supplies energy to be used by consumers	**Unidirectional energy flow – directional medium flow**: traditional DH/DC system with multiple producers leading to changes in the flow direction in some network branches	**Directional energy flow – Unidirectional medium flow**: centralized pumping system but users can add and reject energy into the same network	**Directional energy flow – directional medium flow**: decentralized pumping system allowing for flow reversal and users can add and reject energy into the same network

In their survey, Buffa et al. [14] showed that 29 of the 40 systems use a regenerative energy source for supplying energy to the network. Examples of regenerative energy sources are open-loop systems like Aquifer Thermal Energy Storage (ATES), lakes, oceans, and geothermal borehole fields. The remaining systems use non-regenerative systems where the source's thermal energy is not regenerated naturally. Examples of this are waste heat recovery and fossil fuel-based heat sources.

Most of the systems (62.5%) are supplied by only a single energy source. Single energy source systems are typically open-loop systems that extract or inject energy into the transport medium before discharging it back to the source. Examples of this are the “Genève-Lac-Nations” and “La Tour-de-Peilz” systems that use deep lake water for free cooling and also as a heat source during winter months [82]. Rivers are another viable energy source. There are two river-based 5GDHC heating systems, one in Ohrberg, Germany, that provides energy for 82 building units [83], and another in Leuven, Belgium [84].

Research is lacking, however, around multisource 5GDHC systems. Multisource systems include at least two thermal energy sources that provide energy to the distribution network. There is a significant gap concerning multisource 5GDHC systems that use excess and recycled heat as a major energy system component. Of the 40 systems surveyed by Buffa et al., only fifteen are classified as multisource energy systems. Of those fifteen, only three systems use excess heat sources such as biomass boilers or CHP plants. None of these systems consider changing the network's supply temperature based on CHP operation or integrating the CHP as a grid level service provider, which is a primary feature of this research. With such a strong presence of CHP systems throughout the history of DH, there is an immediate need to incorporate this equipment as part of the 5th generation framework.

2.3.1 Waste heat recovery

The objective of this research is to quantify the potential for an ICE-Harvest system in Ontario market conditions. The proposed system will use waste heat produced by gas generators on the electrical grid and waste heat from cooling processes to provide heating to a cluster of buildings. In this space, two projects are the most similar to the proposed system.

The first project similar to the proposed system is the FLEXYNETS project out of Europe [85]. The project is part of the European Union's Horizon 2020 [86] research and innovation programme, and it is coordinated by EURAC research [87]. The project is currently working with three early adopter projects located in Heilbronn (Germany), Høje Taastrup (Denmark), and Trento (Italy) [88].

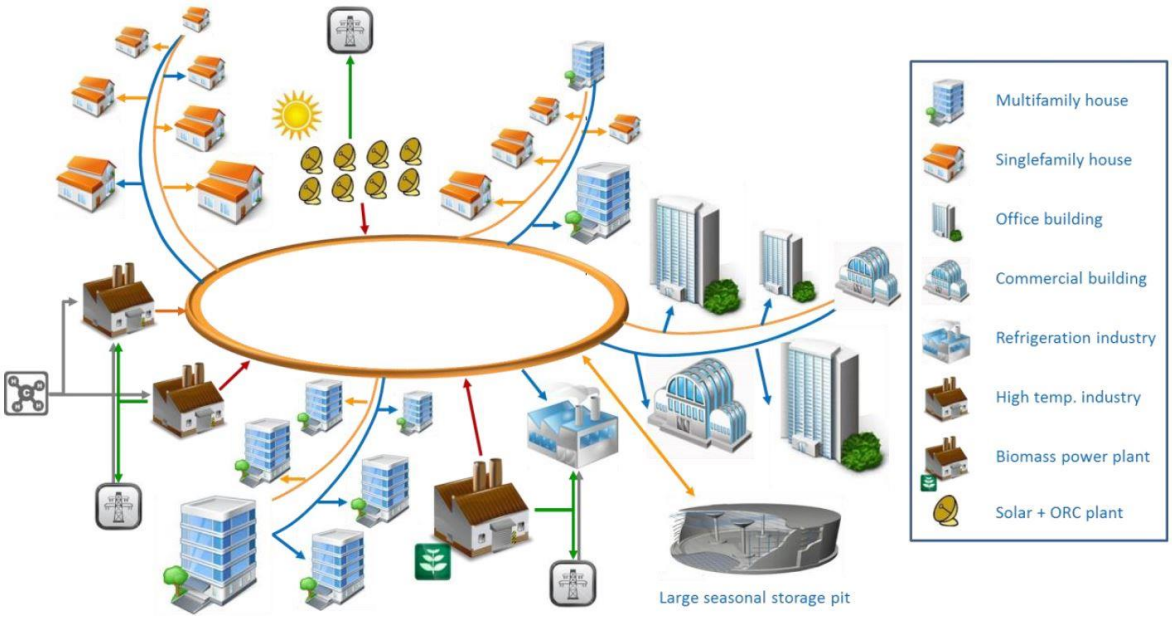

Figure 2.5: Network schematic of a FLEXYNETS system [89]

Figure 2.5 shows the network schematic of a FLEXYNETS system. The FLEXYNETS system is a 5GDHC network using a ring-based distribution structure. The ring connects to various building types, including multi-family and single-family houses, offices, commercial buildings, refrigeration units, high-temperature industrial sources, and solar thermal plants. The primary purpose of the FLEXYNETS system is to capture renewable and low-grade waste heat that is rejected by cooling systems in urban centers. This is accomplished by operating the network temperature between 10 °C and 30 °C while WSHPs exchange heat with the same pipeline. Large scale seasonal TES is used to balance out the seasonal energy supply imbalances. The research's

primary objective is to exploit the synergetic primary energy savings potential of an integrated energy system and develop the business models for a heat trading market.

Results from the early adopter case studies show that FLEXYNETS network heat losses are reduced by 75% over the conventional system just by using a lower network supply temperature [89]. On the financial side, the FLEXYNETS system is approximately 50% more expensive than conventional DH networks, but costs can be reduced considerably by integrating more inexpensive waste energy sources such as supermarkets and datacenters. The project also hypothesizes that there is significant potential for demand response services on the electrical grid through the coupling of thermal and electrical demands. This is hugely beneficial to electricity system operators and contributes to a more stable electricity grid with greater potential for renewable resource integration. The project also reports significant emissions reduction potential (up to 95% over the conventional system) using large scale TES [90]. The use of TES reduces the need for auxiliary energy sources, which has been found to lower annual CO_2 emissions and heat costs.

The second project similar to the proposed system is the Life4HeatRecovery project, which started in 2018 in three cities across Europe [91]. The project has four main objectives. Firstly, to demonstrate the opportunity for waste heat recovery from urban sources such as air conditioners and industrial processes. Second, to demonstrate management strategies for DH networks that prioritize the harvesting of waste energy sources and interact with the electricity grid to benefit both the utility owners and customers. Third, to demonstrate energy trading schemes wherein customers act as both producers and consumers of energy. Finally, to develop the financial schemes that produce a replicable and reliable business case in various investment markets. The project is currently under development and is gathering results from four demonstration sites. The

first is a foundry in Italy, the second is a hospital in the Netherlands, the third is a detergent factory in the Netherlands, and the final project is a sewer waste heat recovery project in Germany. Once the sites' data has been compiled and analyzed, the Life4HeatRecovery project will publish its results. The results will focus on the effectiveness of using prefabricated skids and will produce a database of the DH network solutions, waste heat sources, energy trading schemes, and financial schemes developed.

2.4 Experimentation and modelling of 5GDHC

There are two main categories of 5GDHC systems: physical systems with data gathered from instrumentation and modelled systems with data gathered from numerical simulations. Physical systems are preferred because they provide real information about the system operation subject to real-world conditions. The challenge with physical systems is that they are costly and difficult to implement, typically requiring coordination from multiple stakeholders to operate successfully. This barrier to entry has limited the development of most 5GDHC systems to smaller-scale pilot projects which seek to verify a single component of the system operation. To avoid significant capital expenses, some researchers have chosen to create models of 5GDHC systems that can be simulated to estimate the real system performance. The challenge with models is that the quality of the results depends entirely on the quality of the inputs and assumptions used in mathematical modelling. Inaccuracies in modelling can lead to significant variance between the estimated and actual system performance.

2.4.1 Physical systems

There are 40 documented 5GDHC systems currently in operation in Europe [14]. Vetterli et al. [92] analyzed the monitored data from the 5GDHC system in the Surstoffi district located in

Risch Rotkreuz, Switzerland. The district currently consists of nineteen low-energy commercial and residential buildings with approximately 32 buildings scheduled for future development. Examples of buildings included in the development are kindergartens, community centers, residential buildings, and offices. The buildings within the district are clustered into groups referred to as Baufields (BFs). The BFs have their heating and cooling demands serviced using a low-temperature thermal network. A schematic of the network is provided in Figure 2.6.

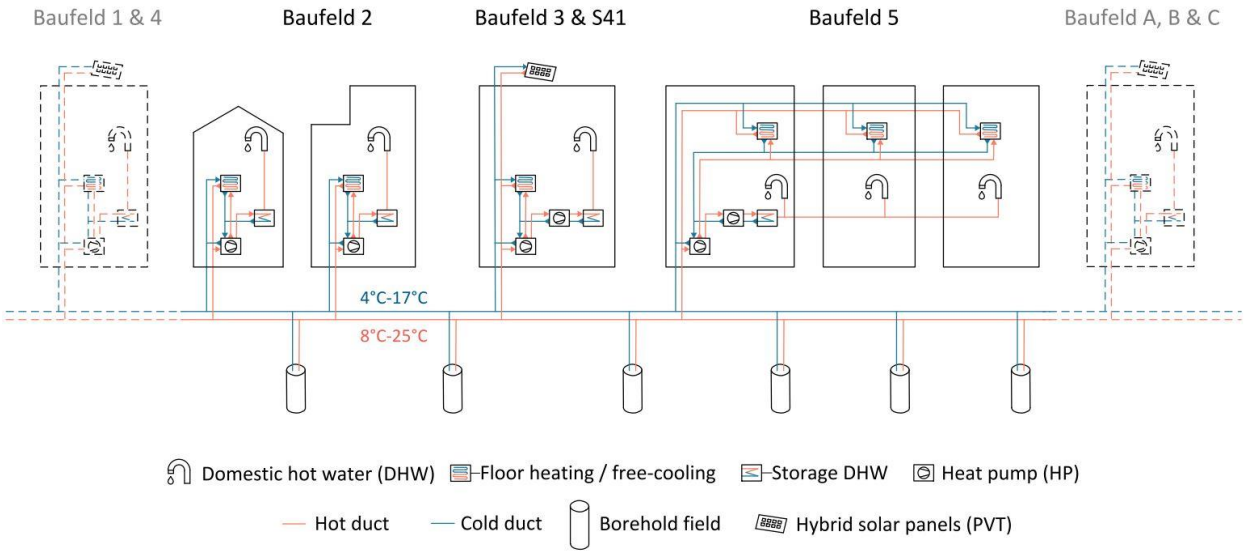

Figure 2.6: Schematic of the 5GDHC system in the Suurstoffi district [92]

The network consists of 215 boreholes at a 150 m depth connected to the BFs through decentralized heat pumps and heat exchangers [92]. The geothermal borehole field functions as seasonal storage that permits bidirectional mass flow throughout the network. There are Photovoltaic (PV) and Photovoltaic Thermal collector (PVT) systems located at the buildings to provide electricity for the heat pumps, circulating pumps, and other building-level electrical loads. The heat produced by the PVT system and the heat recovered from building space cooling is used to regenerate the borehole field's heat content. The first construction phase of the project was completed in 2012. Energy and temperature monitoring devices were included in the construction

to gather data on the system operation. The energy fluxes for heating and cooling, typical system-temperatures, and itemized power demands are recorded by over 300 measurement devices at 15-minute intervals, and the data is aggregated weekly. Between the years 2012 and 2017, the project gathered five years worth of operational data, which was analyzed by Vetterli et al. to quantify the performance gap between the design calculations and the measurements [92].

The monitored data exposed numerous inconsistencies between the design and actual system performance. Namely, the heat consumption for space heating was underestimated by 127%, the power consumed by circulating pumps was underestimated by as high as 233% in one BF, and the power consumed by the distributed heat pumps was underestimated by 49%. This enormous discrepancy highlighted the need for improved performance monitoring and sub-metering in 5GDHC systems. For example, the circulating pump power difference was attributed to the circulating pump constantly operating regardless of whether the heat pump was operating or not. This conclusion was only noticeable due to sub-metering the circulating pump and heat pump separately. Despite inaccuracies in absolute measurements, the Seasonal Performance Factor (SPF), a ratio of the heating energy delivered to the power consumed, was only different by 6% with a design value of 4.1 and a measured value of 4.4.

The monitoring of physical systems is essential in accurately reporting energy consumption and fluxes in 5GDHC systems. A major component of 5GDHC systems is waste heat recovery from cooling processes. Sub-metering of cooling equipment such as chillers and air conditioners is essential in monitoring the waste heat recovery of this equipment. This sub-metering is not typically done in buildings [12], making it difficult to monitor cooling systems' energy flows. As Vetterli et al. [92] demonstrated, monitored consumption data can be significantly different from design values.

2.4.2 Modelled systems

Modelled systems are the alternative to monitoring physical 5GDHC networks. Modelled systems are beneficial in the design and proof of concept stage of a technology because modelled systems are inexpensive to develop, iterate, and can evolve as the design changes or is disproven. The downside of modelled systems is that the results are significantly impacted by the quality and accuracy of the models and inputs. This can be problematic in systems such as 5GDHC, where there is limited monitored data for whole system performance. Fortunately, the underlying technologies that comprise 5GDHC systems, such as heat pumps, heat exchangers, pumps, and piping, are well understood, and verified models readily exist. Therefore, it is possible to simulate 5GDHC systems of validated component models that can predict the overall system performance to a reasonable degree of accuracy.

Numerous software programs are capable of modelling 5GDHC systems. Connolly et al. reviewed 37 different software programs to simulate the integration of renewable energy into various energy systems [93]. Many of the software programs listed in this paper are suitable for the simulation of 5GDHC systems. Examples include EnergyPLAN [94], energyPRO [95], HOMER [96], and TRNSYS [97]. Of these software tools, TRNSYS is the one most used by researchers in the DHC field. TRNSYS has been used for the modelling of CHP with Thermally Activated Cooling (TAC) in a DHC system [98] and exergy analysis of DHC systems [99]. The FLEXYNETS project uses TRNSYS to simulate different 5GDHC components to determine profitability and annual total emissions [90]. TRNSYS has difficulties in modelling large DHC networks with multiple building nodes due to the software's computational limitations, and it also does not easily incorporate the monitoring of energy across different streams (thermal and electrical).

Other researchers use equation-based solvers such as IBM CPLEX and GAMS to simulate DHC systems. The systems that are simulated using these tools are typically linear systems of equations that are classified under the field of Mixed Integer Linear Programming (MILP). The systems are typically governed by the flow of energy from one component to another and neglect the transport medium's temperatures in each component. The temperature levels between various components are assumed to be sufficiently large to allow for heat transfer in the desired direction and at the desired rate. The benefit of this simplification is that it allows for extremely fast simulation, which is necessary for system optimization. Therefore, these software tools are typically used when the objective is to optimize the DHC network design or operation. Common objective functions include Primary Energy Consumption (PEC), annual total emissions, and annual total cost. For example, Prasanna et al. [74] optimized the Suurstoffi DH system's operation with the objective function of minimizing annual carbon emissions. Ahmadisedigh and Gosselin [100] optimized the operation and design of a DHC system (referred to as an “energy hub”) with the dual objective function of minimizing both cost and emissions. Evins [22] used a multi-objective genetic algorithm to optimize the design of a DHC system and a MILP to optimize the system operation to reduce emissions, capital costs, and running costs.

Recently, there has been rising interest in using the Modelica [101] coding language to design 5GDHC systems. In 2016, the IBPSA announced the start of the IBPSA Project 1 project [27]. The project builds on the work accomplished as part of the IEA Annex 60 project [26], where four libraries developed in Modelica were amalgamated and standardized for inter-library compatibility. The libraries are: the Buildings library developed by the Lawrence Berkeley National Laboratory [102], AIXLib developed by RWTH Aachen, Germany [103], BuildingSystems developed by UdK Berlin [104], Germany, and IDEAS developed by KU

Leuven, Belgium [105]. These libraries are composed of verified and validated equipment models commonly used in DHC systems. The three main tasks of the IBPSA Project 1 are to develop unified Modelica libraries, develop building and city quarter models, and to demonstrate the project through application and dissemination of the results. Research is still ongoing, with a project timeline of 2017 to 2022.

Numerous researchers have used the Modelica libraries developed by the IEA Annex 60 and IBPSA Project 1 teams to do simulation work in 5GDHC systems. For example, Rogers [106] used the library models alongside some custom models to compare a modified 5GDHC system's performance as a retrofit solution to an existing DHC network. Pass et al. [107] used the models developed to perform a thermodynamic analysis of a 5GDHC system with bi-directional medium and energy flow. Bünning et al. [72] used the models to test an agent-based control strategy on a 5GDHC system to better manage and coordinate distributed energy resources. The benefit of using the Modelica language for the development of 5GDHC systems is that it is an acausal modelling language. Acausal modelling means that relationships between components are expressed according to their physical or mathematical relationship, thus eliminating the need to define the inputs and outputs [108] explicitly. The simulations are solved dynamically using an equation-based solver that can efficiently solve large systems of equations. Therefore, it can be concluded that Modelica is a viable option for simulating 5GDHC networks.

2.5 Thermal energy storage

2.5.1 Introduction

TES is an important component of many 5GDHC systems. TES is applied to store excess thermal energy for use at a later time. The two primary types of TES are sensible and latent energy

storage [108]. Sensible TES stores heat in a medium by raising the temperature of the medium. Examples of this include hot water tanks, solar walls, and pre-heating building air. Latent TES stores heat in a medium by changing the phase of the medium. Examples of this include ice storage and Phase Change Materials (PCMs), such as paraffin wax.

Sensible energy storages are by far the most common type of TES used in the buildings industry today. The most common medium used in sensible TES is water because of its relatively high heat capacity, ease of transport (inert and stable), and appropriate liquid phase temperature range for most building energy requirements. Latent TES is typically used in solar thermal applications where the system's performance depends on the system temperature. Since phase change occurs at a constant temperature, latent TES offers more stable operating temperatures than sensible TES [109]. Latent TES also has a higher energy density than sensible TES, which allows for storage of the same amount of energy in smaller storage volumes. Researchers have reported as high as three times reduction in storage volume across small temperature differences [110]. Latent TES can also shift electrical loads when coupled with a heat pump [111]. However, because sensible TES is currently the most common type of TES, it will be the focus of this research.

Sensible TES can come in many forms, but the primary TES for DHC applications are Tank Thermal Energy Storage (TTES), Pit Thermal Energy Storage (PTES), Borehole Thermal Energy Storage (BTES), and ATES. Schematics of each storage type and their typical energy densities (kWh/m^3) are provided in Figure 2.7.

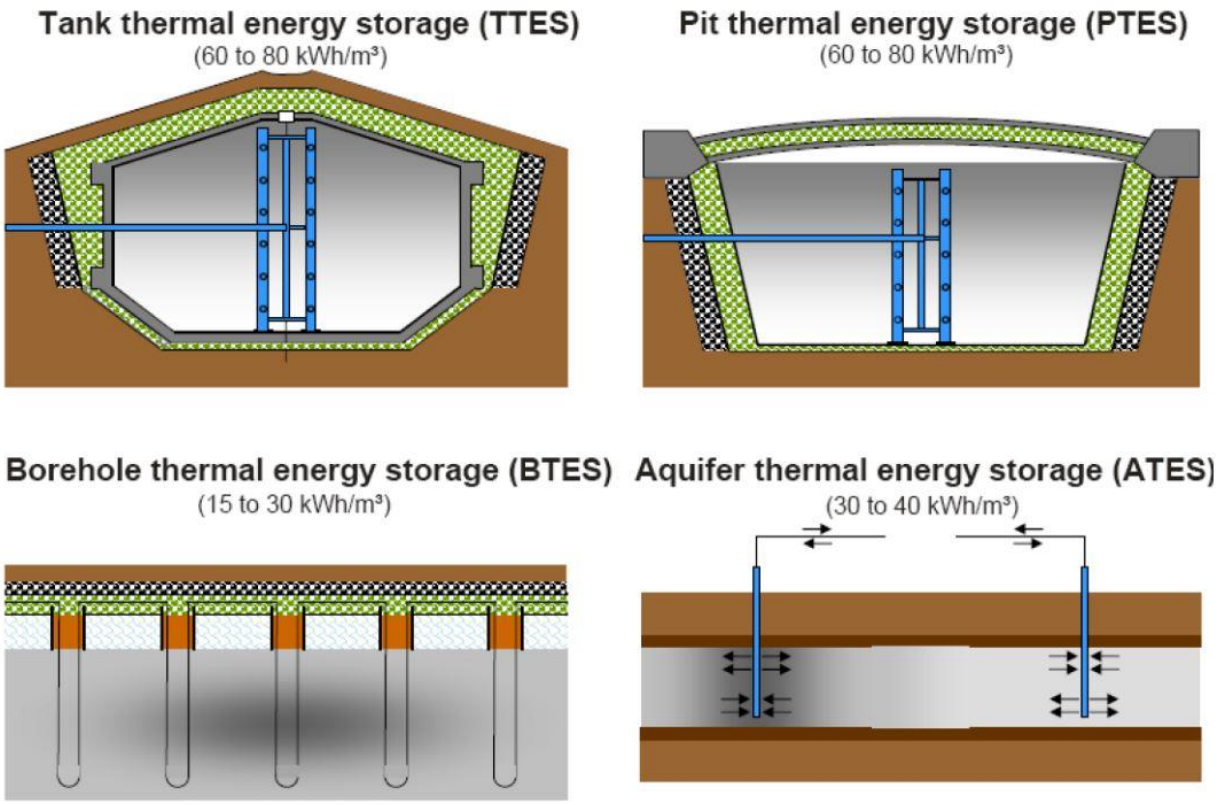

Figure 2.7: Schematics of the four most common TESs used in DHC systems. Figure reproduced from [112].

TTES is the most common of the four TES systems. Nearly 300 Danish DH plants have TTES with an average storage volume of approximately 3000 m^3, with the largest measuring approximately 70,000 m^3 [113]. The tanks are, on average, operated from 35 to 95 °C. TTES can be made from stainless steel, concrete, or Glass Fiber Reinforced Plastic (GFRP), use mineral wool for insulation, and water as a storage medium. Most TTES are located above ground level and occupy a large amount of surface area. Some TTES are buried below ground level, such as the one shown in Figure 2.7, where the area on top of the tank can be used for other purposes. TTES can achieve low heat losses with sufficient insulation. TTES also have a higher energy density than other storage options for district energy applications because the heat does not need to be transferred into a storage medium. TTES have good economies of scale up to 5000 m^3, but it is not a favourable option for installations larger than this volume due to having higher costs per unit of capacity than alternative storage options.

PTES uses a large waterproof membrane to store water inside a pit that is dug into the ground. The membrane is uninsulated and prevents the water from leaking into the soil. The surrounding soil is used as insulation for the pit's sides and bottom, while an insulated lid is used on the top. PTES is the most common large-scale storage system in Denmark with multiple locations built with storage volumes above 10,000 m^3, the largest of which is in the town of Vojens with a volume of more than 200,000 m^3 [90]. PTES operates in similar temperature ranges to TTES within the range of 35 to 95 °C for district heating purposes. The large storage volumes make PTES a suitable solution for seasonal energy storage. PTES has a lower efficiency than TTES due to slightly higher heat losses, however, PTES has lower specific investment costs because the pit provides most of the storage structure. The type of lid chosen has a significant impact on the heat losses and cost of the project. Some lids can be designed such that structures can be built on top of the PTES, thus reducing the spatial requirements for the storage.

BTES systems are composed of numerous boreholes buried in the ground which transfer heat from buried pipes into the surrounding soil. BTES acts like a heat exchanger where the storage is charged by running hot water through the pipes which transfer heat into the soil. The heat is extracted by running cooler water through the pipes which transfer heat from the soil. The heat transfer rate into and out of the field is governed by the temperature difference between the pipe medium (typically water or a water-glycol mixture) and the soil. It is important to balance the amount of energy transferred into and out of BTES systems to avoid introducing a temperature drift to the soil. Temperature drifts result in annual increases or decreases to the average soil temperature due to improper energy balancing. For example, the 5GDHC system in the Surrstoffi district had to add solar thermal collectors after one year of operation to avoid drifting the temperature downwards [92]. The efficiency and energy density of BTES is dependent on a variety

of geological factors. Ideally, BTES should be in soils with high heat capacities and limited groundwater flow.

ATES is constructed using a natural or human-made aquifer located underground. Typically, ATES systems use two drilled wells where one well is used for heat storage, and the other is used for cold storage. Water is pumped from the hot well during the heating season, and heat is extracted in the network before being dumped into the cold storage well. The process is then reversed during the cooling seasons. ATES is a highly financially viable option of large-scale TES, however, they can only be constructed in locations where impermeable aquifers exist, which limits their application.

A summary of TES technologies can be found in Table 2.2. A summary of existing international TES projects with equipment, capacities, and storage volumes can be found in Appendix A.

Table 2.2: Summary of TES technologies. Reprinted from [90].

Type	TTES	PTES	BTES	ATES
Storage medium	Water	Water or gravel-water	Soil	Groundwater
Energy density [kWh/m^3]	60 – 80	60 – 80 for water 30 – 50 for gravel-water	15 - 30	30 – 40
Cost per unit volume [CAD$/m^3]	160 – 300 (for TTES above 2,000 m^3)	30 – 60 (for PTES above 50,000 m^3)	30 – 60 (for BTES above 50,000 m^3 water equivalent including buffer tank)	75 – 90 (for ATES above 10,000 m^3 water equivalent). Investment costs are highly dependent of the charge / discharge power capacity
Cost per unit capacity [CAD$/kWh]	$3.4 - $11	$0.4 – $7.6	$1.7 – $2.9	$2 - $3
Geological requirements	Above ground: none Buried: stable ground conditions, low groundwater flow, 5 – 15m of depth	Stable ground conditions, low groundwater flow, 5 – 15m of depth	Drillable ground, soil with high heat capacity and thermal conductivity, low groundwater flow, 30 – 100m of depth	Accessible aquifer
Application	Short time / diurnal storage, buffer storage	Long time / seasonal storage, short time for large capacity CHP	Long time / seasonal storage	Long time / seasonal heat and cold storage
Storage temperatures [°C]	5 – 95	5 – 95	5 – 90	7 - 18
Advantages	High charge / discharge capacity	High charge/discharge capacity and low investment costs	Most properties are suitable	Provides heat and cold storage and many geologically suitable sites
Disadvantages	High investment costs	Large area requirements	Low charge/discharge capacity	Low-temperatures and low ΔT

2.5.2 Thermal energy storage in 5GDHC

TES can be extremely useful in 5GDHC systems, particularly in locations with dynamic energy prices, large changes in ambient temperature, and electrical emission factors. The FLEXYNETS project found that using TTES in three reference cities: Rome (Italy), London

(England), and Stuttgart (Denmark) significantly lowered annual CO_2 emissions and heat delivery costs [90]. In this case, the TES was used as a seasonal energy storage to store heat rejected from building cooling processes. Without TES, the heat would be exhausted to ambient unused. Using Heat Recovery Heat Pumps (HRHPs) and TES, the FLEXYNETS system can capture and store the typically wasted heat. Bünning et al. [72] also used seasonal TES with a large volume ($V=2x10^6$ m^3) to balance a bidirectional 5GDHC network's temperature, resulting in a significant decrease in energy consumption and emissions.

2.6 Summary

In conclusion, the 5th generation of DHC is a relatively new field of district energy solutions. With only 40 known installations in Europe and a wide variety of proposed solutions, there is a significant opportunity for new developments. 5GDHC systems offer numerous improvements over previous generations, such as reduced heat losses and increased potential for multiple energy sources because of the low supply temperature.

The Ontario energy market offers a novel situation for an ICE-Harvest system. The unique combination of low electrical average emission factors because of a large supply of emission-free energy sources and dynamic marginal emissions factors creates the opportunity for substantial emissions savings. Also, there is significant potential to replace the existing low-efficiency gas generators with higher efficiency CHP units that use otherwise wasted thermal energy.

The use of distributed energy resources is also a new topic in the field of district energy. Distributed energy resources were introduced in the 4th generation as prosumers, thus creating bidirectional energy networks. Bidirectional energy networks must be explored further to realize their full potential. The ideal design of 5GDHC using distributed energy resources is highly

dependent on the market structure and building energy demands of the system being analyzed. While the thermodynamic principles remain the same across all locations, the quantified potential of these systems remains unknown.

Therefore, there is a need to quantify the potential of 5GDHC systems in the Ontario energy market from an energetic and emission perspective. This work will address this issue by comparing an ICE-Harvest system designed for the Ontario energy market to common energy system alternatives.

3 Methodology and Verification

This section explains the ICE-Harvest system and the methodology used in developing each of the system models. This research's scope is limited to energy-intensive buildings such as data centers, residential towers, and arenas with higher energy use intensity values (GJ/m^2) than single-family residences [42]. This limitation is chosen because the buildings with higher energy use intensity are the most viable candidates for district energy systems [14].

3.1 System schematics

For this research, five different systems are being considered. The energy flow schematics of each system are provided in the figures below.

3.1.1 Conventional system

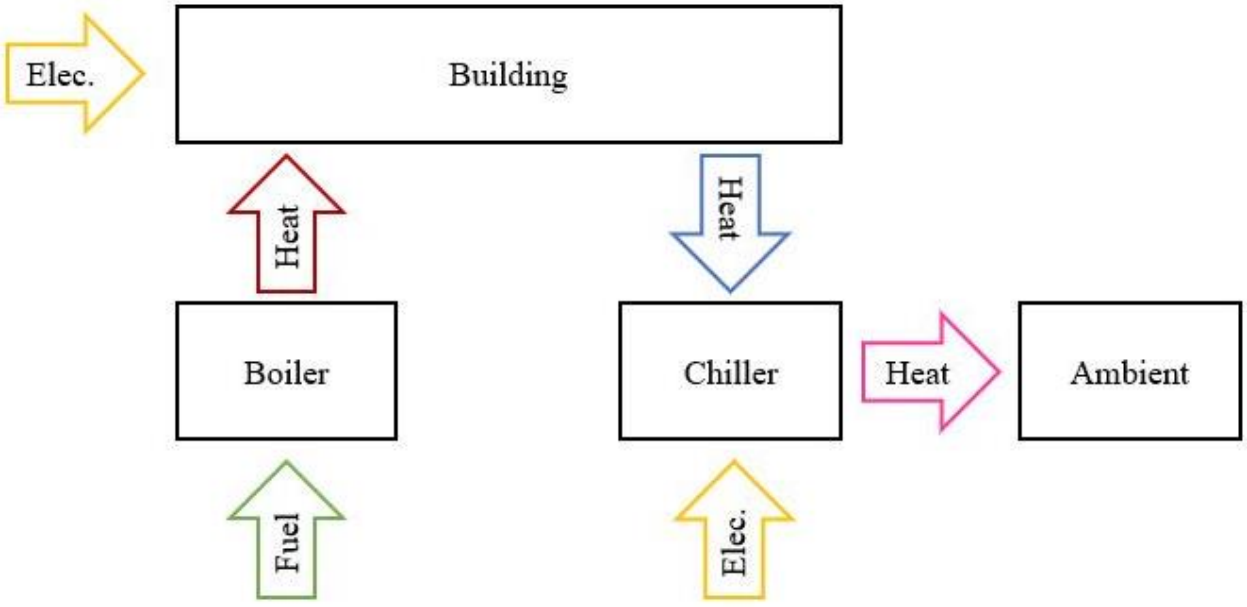

Figure 3.1: Schematic of the conventional system

The first system is referred to as the conventional system. This system represents the typical current heating and cooling equipment found in Canadian buildings. The system consists of a fossil natural gas-based boiler for heating and an electric chiller for cooling. The heating and cooling

equipment is isolated to service a single building. As shown in Figure 3.1, the boiler or furnace consumes fuel to produce the heat that is delivered to the building. The chiller uses electricity in a refrigeration cycle to extract heat from the building, which is rejected to the ambient through a constant return temperature heat exchanger. Electricity is delivered to the building and chiller from the grid. The boiler operates at a constant efficiency where the efficiency describes the ratio of heat delivered to the fuel energy consumed. The chiller COP is calculated using the building Chilled Water Supply (CHWS) temperature and the ambient temperature.

3.1.2 Ground source heat pump system

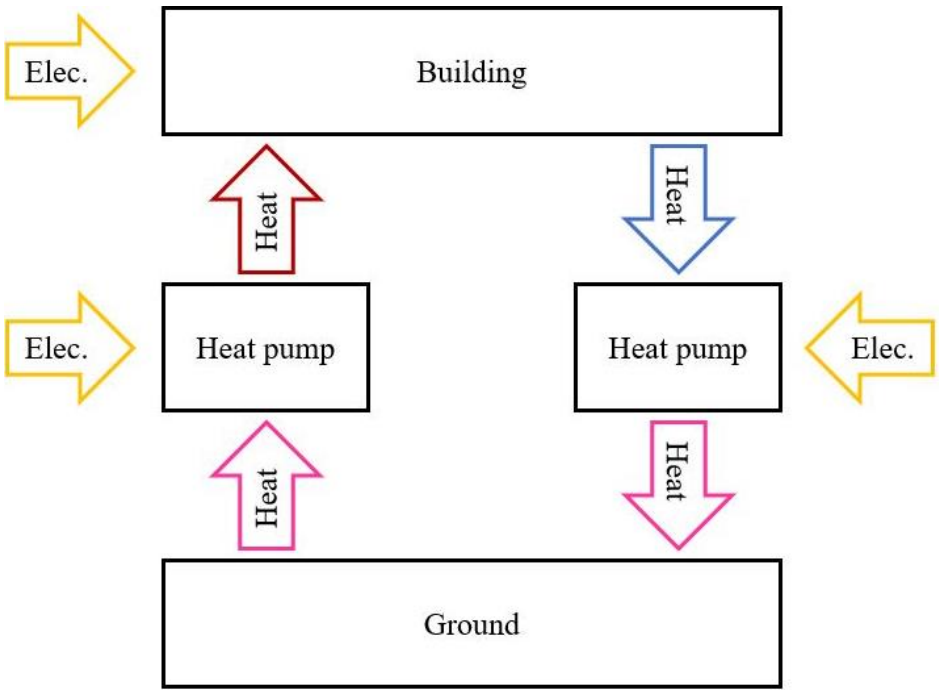

Figure 3.2: Schematic of the GSHP system

The second system is referred to as the GSHP system. This system aims to quantify the effects of electrification on the building sector using current heat pump designs. The system consists of water-to-water heat pumps connected to a borehole field at each building. As shown in Figure 3.2, the heat pumps extract and reject heat into the ground depending on the heating and cooling demand. In this system, the ground boundary is contained to the geothermal borehole field,

which acts as a sink and source for thermal energy. The heat pumps consume electricity to deliver heat to and remove heat from the building using a refrigeration cycle. While a single heat pump could be used for both heating and cooling, the heat pumps were modelled separately for clarity. Also, sometimes a backup boiler is used to increase the heating capacity, but that was excluded from this model. Electricity is delivered to the building and heat pumps from the grid. The COP of the heat pumps is a function of the average soil temperature and the building Hot Water Supply (HWS) and CHWS temperatures.

3.1.3 District heating system

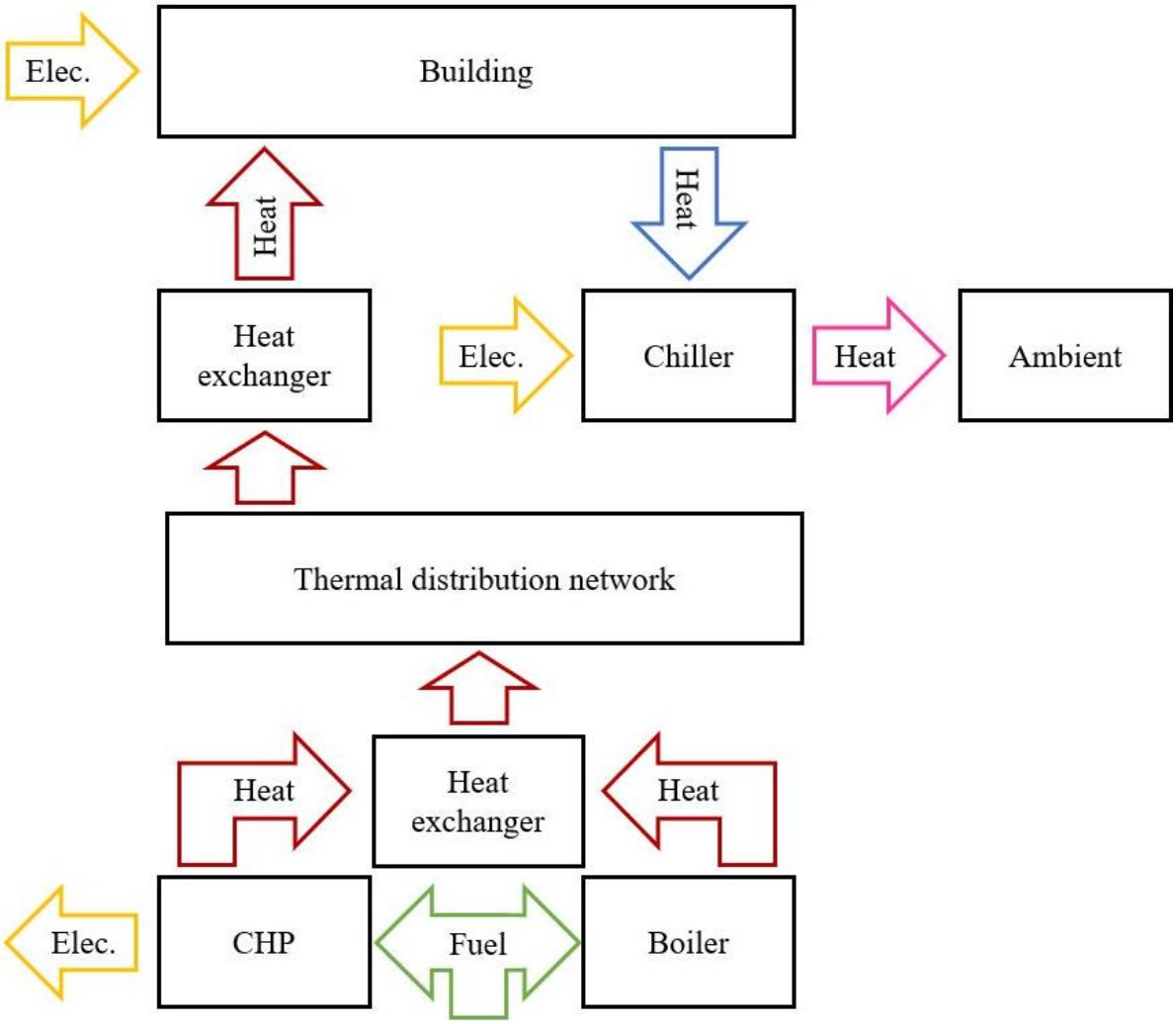

Figure 3.3: Schematic of the DH system

The third system is referred to as the DH system. The DH system serves to quantify the current performance of a modern DH network. As shown in Figure 3.3, the system consists of a centralized generation plant, a thermal distribution network, and building-level heating and cooling equipment. There are multiple buildings connected to the thermal distribution network; however, only one is shown in the figure for clarity.

The centralized generation houses two heat sources, a CHP, and a boiler, both of which are fossil fuel-based. The heat they produce is transferred to the thermal distribution network through a heat exchanger. The CHP is controlled by Following the Thermal Load (FTL) of the network, and the boiler is used to supplement the heating supplied when the heating demand exceeds the CHP capacity. The thermal distribution network is a ring structure with a unidirectional medium and energy flow. The buildings extract heat from the network using heat exchangers. Heat is removed from the buildings and rejected to the ambient at the building level. Electricity for the buildings and chillers comes from the grid. The electricity produced by the CHP is either consumed locally or exported to the grid when the production exceeds the local demand.

The CHP's efficiency is defined as the ratio of the heat and electricity produced to the fuel energy consumed. The CHP's efficiency varies according to the part-load ratio, which is the ratio between the current output and the maximum capacity. Therefore, the part load ratio is 100% when the CHP operates at full capacity and 0% when the CHP is off. The efficiency of the boiler is constant. The COP of the chiller is calculated using the building CHWS temperature and the ambient temperature.

3.1.4 Integrated Community Energy and Harvesting system

3.1.4.1 Low-temperature thermal network

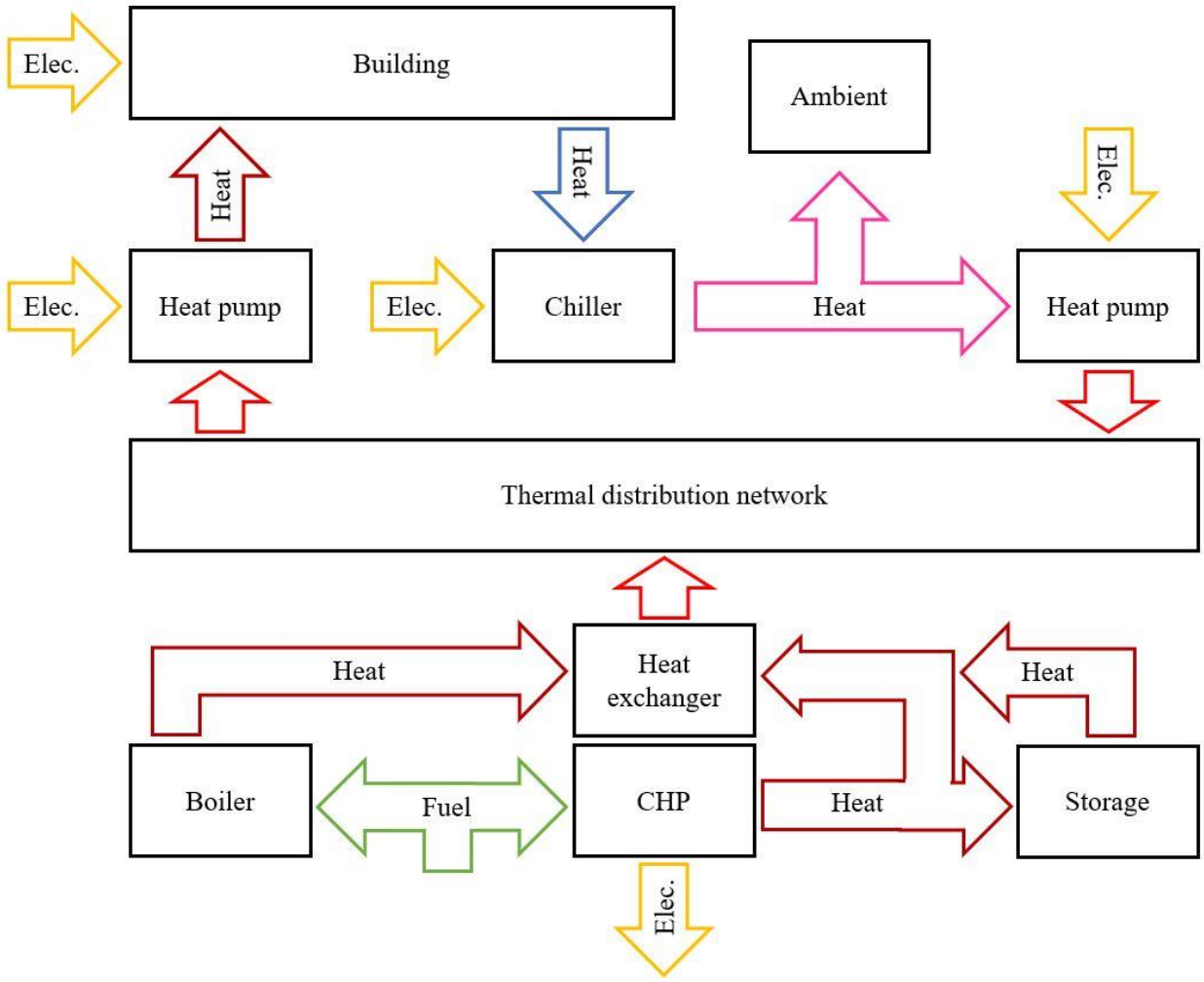

Figure 3.4: Schematic of the ICE-Harvest system

The fourth system is referred to as the Integrated Community Energy Harvesting (ICE-Harvest) system. There are two variants of the ICE-Harvest system presented in this thesis. The first is the low-temperature system (below direct exchange temperatures, assumed 60 °C for building hot water), which uses a heat pump for delivering heat from the network, and the second is a high-temperature system (at or above direct exchange temperatures) that uses a heat exchanger for delivering heat. The low-temperature system is discussed here, and the high-temperature system will be discussed in the next section. As shown in Figure 3.4, the ICE-Harvest system

consists of a centralized generation area, a thermal distribution network, and building-level heating and cooling equipment. At the centralized generation, referred to as the Energy Management Center (EMC), there is a CHP, a boiler, and TES. As the district heating system, there are multiple buildings connected to the thermal distribution network; however, only one is shown in the figure for clarity.

The CHP and boiler are both fossil fuel-based heat generators. The CHP is only operated at full capacity according to an on/off schedule dictated by the historical hourly grid-level gas generation. This operating schedule intends that the ICE-Harvest systems replace the grid-level gas generators, which do not capture waste heat, with more efficient CHPs. The thermal storage is used to capture the CHP's excess heat when the supply exceeds the demand and delivers heat to the network when the CHP does not supply sufficient heat (either due to the CHP being off or insufficient capacity). The boiler is used when both the CHP and thermal storage cannot meet the demand. The heating equipment interfaces the thermal distribution network through a heat exchanger.

The thermal distribution network is a ring structure with bidirectional energy flow and unidirectional medium flow. The building extracts heat from the network using a heating heat pump. Heat is removed from the building using an electric chiller connected to a Heat Recovery Heat Pump (HRHP) and the ambient. The HRHP removes heat from the chiller condenser circuit and transfers it into the thermal distribution network as needed. This configuration allows for waste heat recovery, referred to as energy sharing, where the heat rejected from building space cooling processes can be used to heat other buildings in the network. Whether to send heat to the heat pump or the ambient depends on the network’s heating demand. For example, the HRHP does not inject heat into the network during the summer because there is no heating demand. Electricity is

provided to the buildings, chillers, and heat pumps from the grid. The electricity produced by the CHP is either consumed locally or exported to the grid when the production exceeds the local demand.

The efficiency of the CHP varies according to the part-load ratio discussed in section 3.2.4. The efficiency of the boiler is constant. The COP of the heating heat pump is calculated using the building hot water supply temperature and the thermal distribution network temperature. The COP of the HRHP is calculated using the chiller condenser water temperature and the thermal distribution network temperature. The COP of the chiller is calculated using the building chilled water return temperature and the ambient temperature.

3.1.4.2 High-temperature thermal network

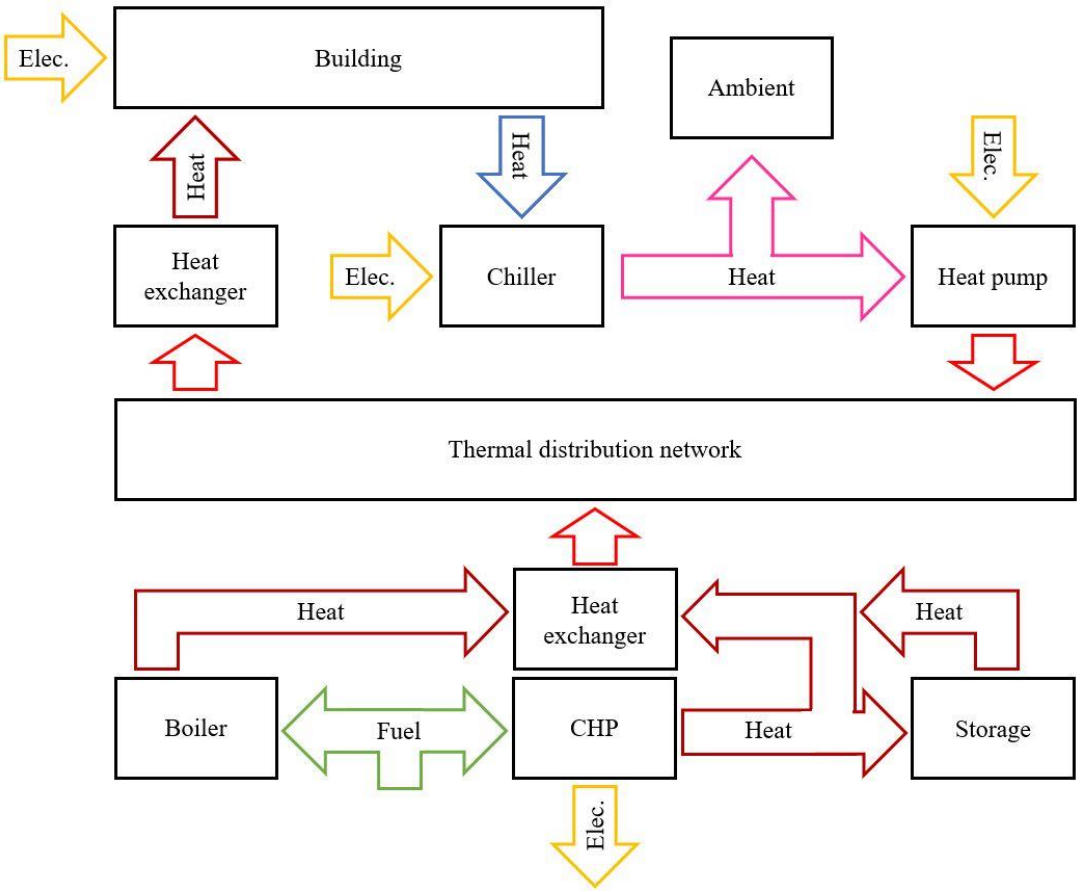

Figure 3.5: Schematic of the high-temperature ICE-Harvest system

The high-temperature variant of the ICE-Harvest system uses all the same equipment as the low-temperature system, with the only exception being a substitution of a heat exchanger in place of a heat pump interfacing the thermal distribution network to the building HWS. A heat exchanger is used to reduce the system's electricity demand by eliminating the need to use a heat pump for HWS. In this system, the network supply temperature is closer to the CHP supply temperature in the EMC. Therefore, by having a higher network supply temperature, less exergy is destroyed when the heat is transferred from the EMC to the network. However, the higher temperature network has higher heat losses from the network pipes and requires more work to inject heat into the HRHP, thus increasing electrical consumption.

Ideally, the network's temperature would be optimized depending on the amount of heat available from cooling heat rejection compared to the total thermal demand. However, this thesis is focused on investigating the limiting cases by only looking at the high and low network temperature cases.

3.2 Model types, architecture, and behaviour

Each of the schematics presented in the previous section was modelled in the Modelica coding language for simulation in Dymola. These models were created using the library of components developed as part of the IEA Annex 60 [26] and IBPSA Project 1 [27] projects. In this research, system models were created that consist of multiple components from these libraries. Before each simulation, system-wide parameters are set to govern the capacity and control of each piece of equipment. The models are separated into three categories: generation models, building demand models, and system models.

3.2.1 Generation models

The generation models are used to represent the central generation equipment used in DHC networks. The primary purpose of these models is to convert fuel and electrical energy into heat delivered to the buildings through the thermal distribution network. The two-generation models developed in this research are the DH FTL and the ICE-Harvest generation station.

3.2.1.1 District heating following the thermal load

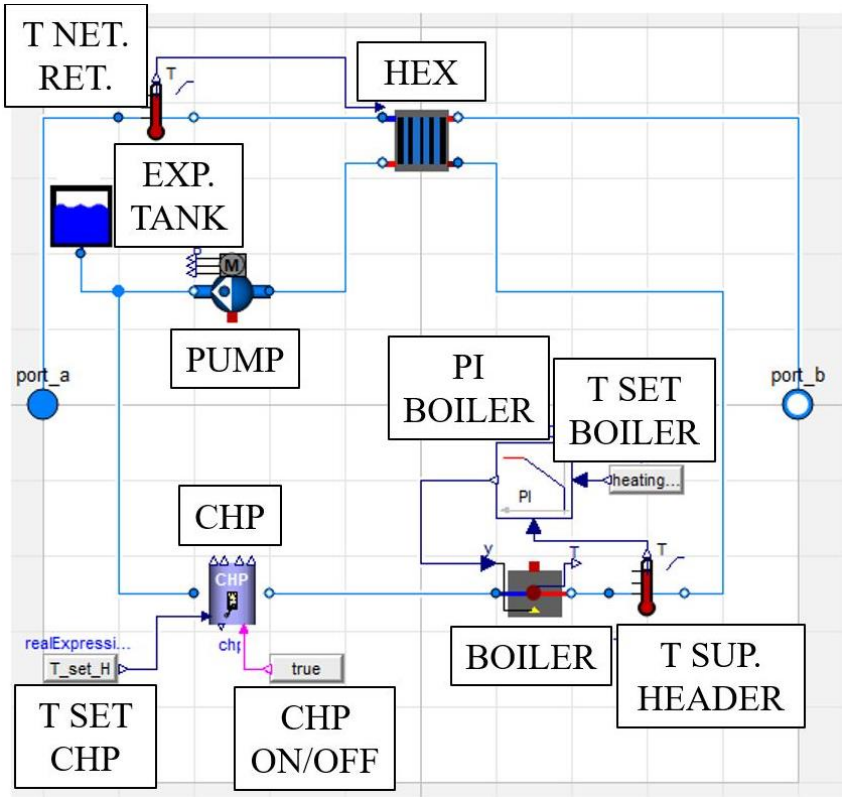

Figure 3.6: DH FTL model

The system diagram of the DH FTL system is shown in Figure 3.6. The system consists of a heat exchanger, CHP, boiler, pump, expansion tank, temperature sensors and controllers. The network return water enters the system through port_a on the left and exits through port_b on the right. The temperature of the return water is measured by the temperature sensor labelled T NET. RET. The temperature reading is used by the heat exchanger, labelled HEX, to determine the

amount of energy that must be added to the network to achieve the desired network supply temperature. The heat exchanger interfaces between the network and the generation model header pipe. Water is circulated in the header pipe at a constant mass flow rate by the header pump, labelled PUMP, with the header pressure defined by the expansion tank, labelled EXP. TANK. The header water is first returned to the CHP, labelled CHP, which controls the supply temperature based on an internal PI controller (k = 10, Ti = 60 s). The supply temperature setpoint is defined by the parameter T SET CHP, and the Boolean expression dictates that the CHP should always be turned on. Next, the header water goes through the boiler, labelled BOILER, which adds heat to the header based on the temperature reading from the temperature sensor, labelled T SUP. HEADER. The boiler is also controlled using a PI controller (k = 0.1, Ti = 60 s). The header's configuration places the CHP before the boiler so that the boiler only supplies heat when the heating demand exceeds the CHP capacity. The water then returns to the heat exchanger from the generation equipment, and the cycle continues. This model adds heat to the network and maintains a specific network supply temperature.

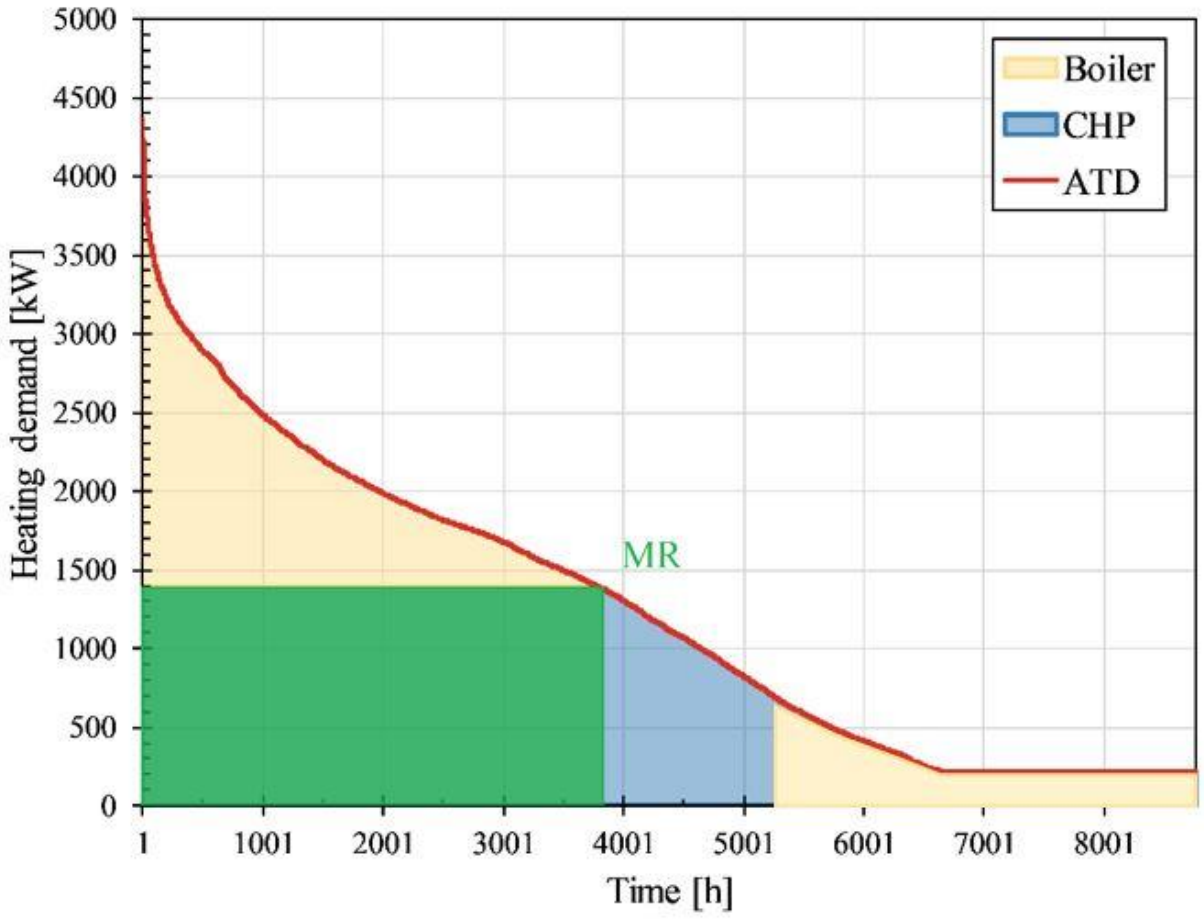

Figure 3.7: Example of the aggregate thermal demand method

As shown in Figure 3.7, the CHP is sized according to the Aggregate Thermal Demand (ATD) method [20]. The ATD method is accomplished by sorting the building heating demand in descending order for each hour of the reference year. For example, the maximum heating demand in this particular year is approximately 4400 kW, and the minimum demand is approximately 200 kW. Next, the CHP's capacity is determined by creating the rectangle with the largest area beneath the ATD curve. This rectangle is referred to as the Maximum Rectangle (MR). In this case, the CHP capacity of 1400 kW with approximately 3800 run hours produced the largest area. The remaining area above the MR area and below the ATD curve is met using the boiler. For example, a heating demand of 2500 kW would require the CHP to operate at full capacity producing 1400

kW and an additional 1100 kW to come from the boiler. The area to the right of the MR area beneath the ATD curve corresponds to heating demands that are lower than the CHP capacity. In systems where the CHP cannot be part loaded, this demand is met using TES or a boiler. In this example, the CHP is assumed to be able to part load from 50% to 100%; thus, the boiler meets the remaining demand.

3.2.1.2 ICE-Harvest Energy Management Center

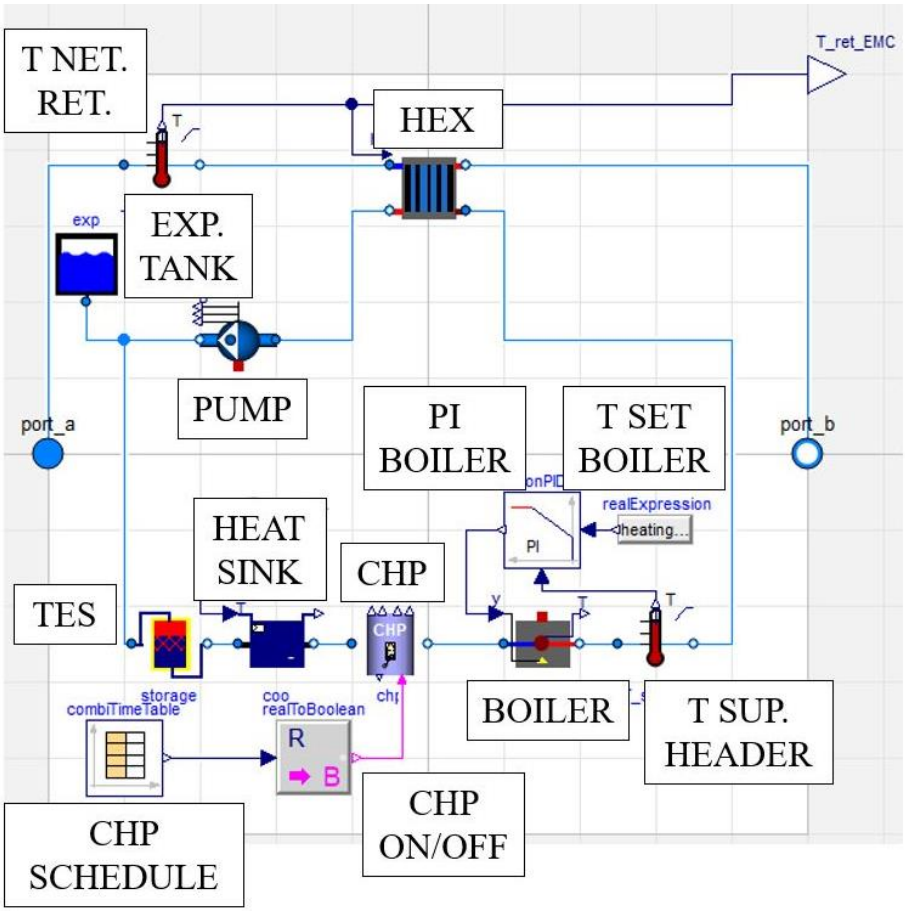

Figure 3.8: ICE-Harvest model

The ICE-Harvest Energy Management Center (EMC) model system diagram shown in Figure 3.8 is like the DH FTL model. The only difference between the two models is the addition of two new components: a TES, labelled TES, a heat sink, labelled HEAT SINK, and a different control strategy for the CHP. In the ICE generation model, the CHP produces heat according to

the historical grid-level gas generation hours stored in the table labelled CHP SCHEDULE. Furthermore, the CHP only operates on an on or off signal, meaning there is no part loading of the CHP in the ICE-Harvest model. Therefore, the CHP's operation is not dependent on the demand for thermal energy in the network. The TES and heat sink are used to manage the heat supplied by the CHP during periods when there is no heating demand. The TES has an internal controller that monitors the header water's return temperature from the heat exchanger. When the temperature is above the setpoint, the storage is used to absorb some of the heat. When the storage is fully charged, the heat sink is used to reject heat from the header that otherwise would have no mechanism of being dissipated. The heat rejected to the heat sink is monitored to determine the amount of wasted heat produced by the CHP, which could instead go into long-term TES. The CHP and TES control strategies will be explained and demonstrated in section 3.3.

The CHP is sized according to the thermal energy demand of the network. In the ICE-Harvest system, the CHP is only allowed to operate when there is gas generation on the grid. For these systems, the capacity of the CHP was calculated using the following equation:

$$CHP\ Capacity\ = \frac{\int Net\ heat\ demand}{Number\ of\ gas\ generator\ run\ hours} \tag{3.1}$$

Where, the net heat demand is the heating demand in the network provided by the EMC and the number of gas generator run hours is the number of hours the grid gas generation was above 1 GW on the Ontario electricity grid.

Using this method of sizing the CHP ensures that the CHP's heat supply is equal to the network's heat demand. Therefore, when the CHP is on with a low network heat demand there will be excess heat, and when the CHP capacity is lower than the network heat demand there will be a heat deficit.

3.2.2 Building models

The building models are used to represent the different options for building level equipment available in different systems. The purpose of these models is to act as the consumers in the system, extracting energy from the thermal distribution network. In the ICE-Harvest model, the option to inject heat into the network is also available. There are five different building demand models: the conventional building, the DH building, the GSHP building, the low-temperature ICE-Harvest building, and the high-temperature ICE-Harvest building.

3.2.2.1 Conventional building

The conventional building model diagram is shown in Figure 3.9. The model is a closed system, meaning it does not interact with any systems outside of the diagram. The building demand model, labelled BUILDING, is in the diagram's center with four fluid ports attached to it.

The building model contains the hourly heating, cooling, and electrical demand data of the sample buildings on text files. According to the text file's demand, the building model adds or removes heat from the hot and chilled water lines. The circuit above the building is the Hot Water Supply and Return (HWSR) line, and the circuit below the building is the Chilled Water Supply and Return (CHWSR) line.

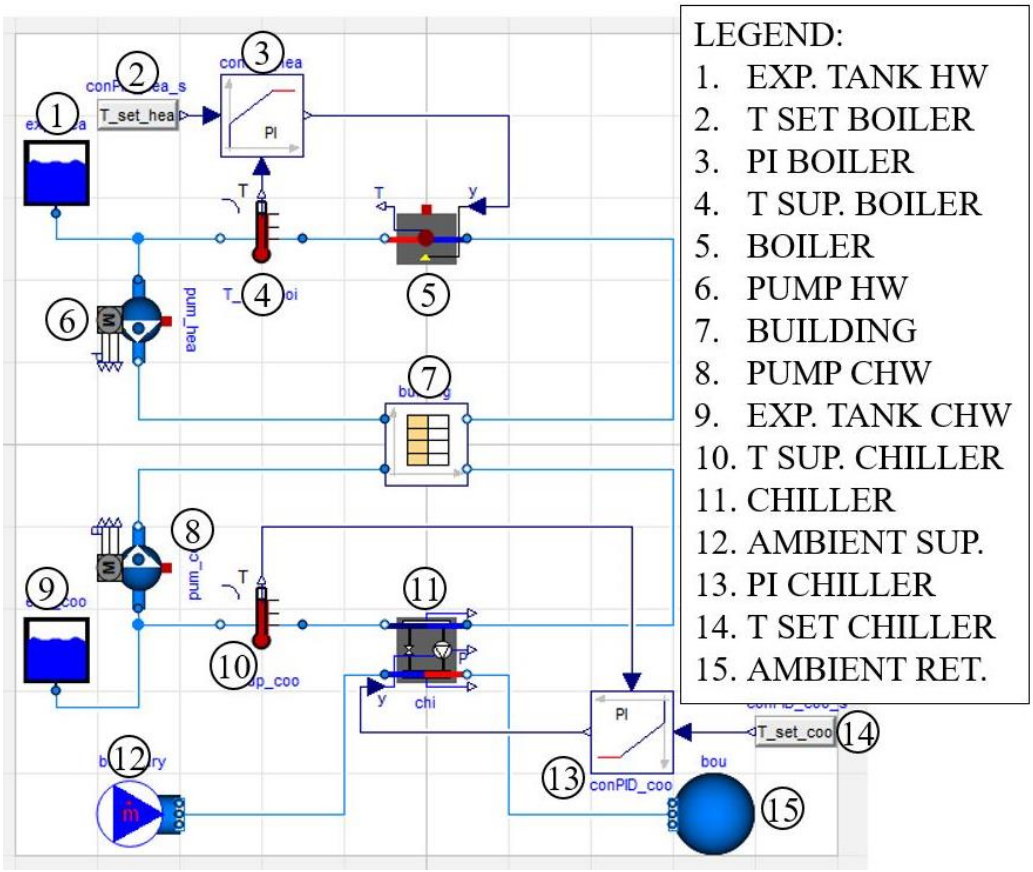

Figure 3.9: Conventional building model

There is a boiler on the HWSR line, labelled BOILER, which heats the water returning from the building. The supply temperature from the boiler is controlled using the temperature sensor, labelled T SUP. BOILER, and a PI controller with a supply temperature setpoint labelled T SET BOILER. The water is circulated at a constant mass flow rate in the HWSR line using the pump, labelled PUMP HW, with the pressure boundary condition defined by the expansion tank, labelled EXP. TANK HW.

There is a chiller on the CHWSR line, labelled CHILLER, which cools the water returning from the building. The supply temperature from the chiller is controlled using the temperature sensor, labelled T SUP. CHILLER, and a PI controller with a supply temperature setpoint labelled T SET CHILLER. The chiller exchanges heat with a constant temperature heat sink, labelled

AMBIENT SUP., which supplies water at constant temperature and mass flow rate. The return water on the cooling side is discharged to a sink, labelled AMBIENT RET. This arrangement was chosen to simulate a cooling tower with a constant return temperature. Ideally, the return water temperature would be a function of the ambient air temperature; however, a constant temperature was chosen due to limitations in the available models. This assumption is justified because all the systems being compared, except for the GSHP system, use the same arrangement for rejecting heat to the ambient. Therefore, when comparing the systems, changing this assumption will affect all the systems in the same way. Also, as shown in section 4.2.4, the electricity demand for cooling is small relative to the other electrical demands. The water is circulated at a constant mass flow rate in the CHWSR line using the pump, labelled PUMP CHW, with the expansion tank's pressure boundary condition, labelled EXP. TANK CHW.

3.2.2.2 District heating building

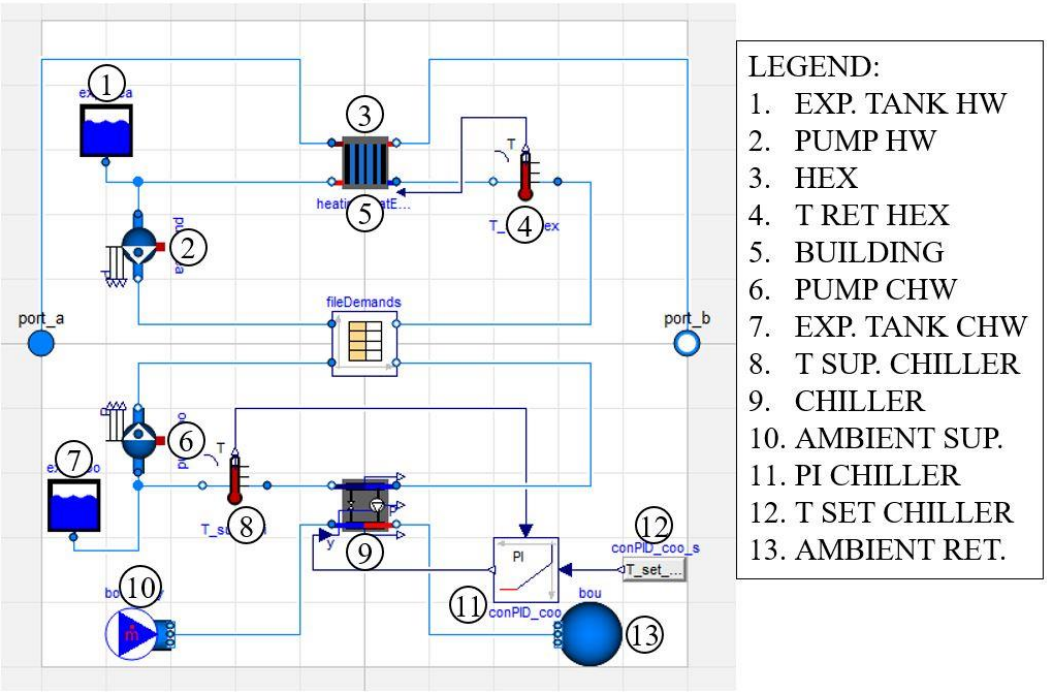

Figure 3.10: DH building model

The DH building model diagram is shown in Figure 3.10. This model is not a closed system and requires a connection to an external pipeline to function. The building demand model and CHWSR line are the same as the conventional system. On the HWSR line, the boiler is replaced with a heat exchanger, labelled HEX, that interfaces with an external pipeline through port_a and port_b. The heat exchanger extracts heat from the external pipeline and adds it to the building HWSR line. The amount of heat exchanged is determined using the temperature sensor, T RET. HEX, and the specified supply temperature to the building from the heat exchanger.

3.2.2.3 Ground source heat pump building

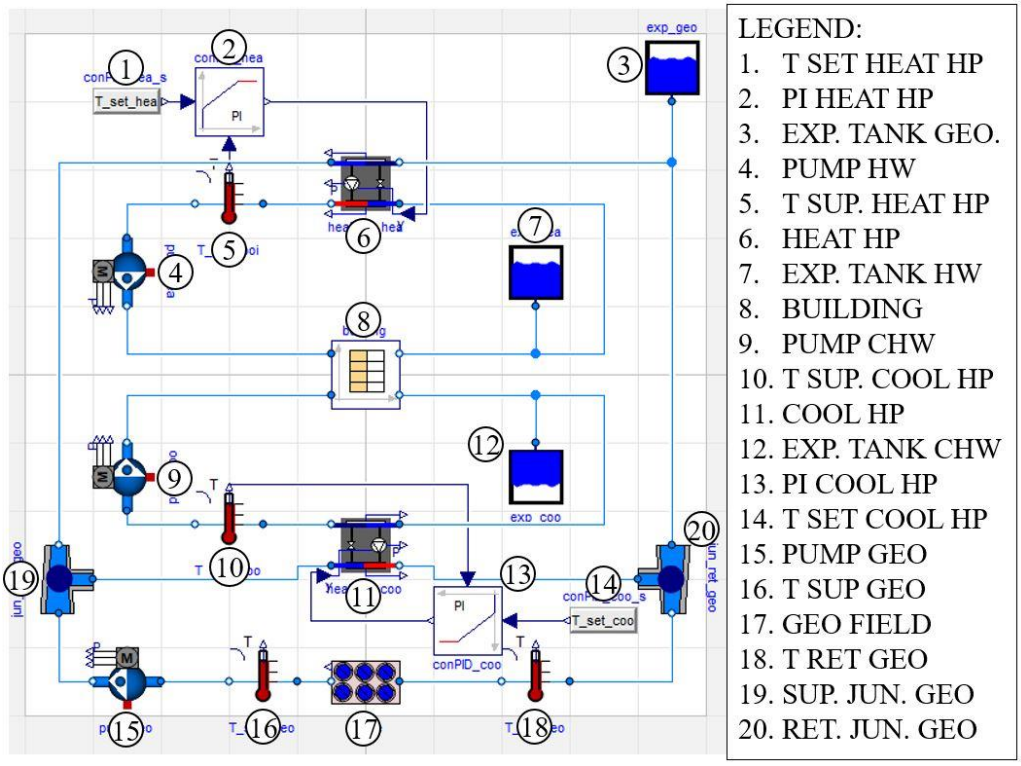

Figure 3.11: GSHP building model

The GSHP building model diagram is shown in Figure 3.11. The model is a closed system and does not require external connections. The building demand model, labelled BUILDING, is identical to the conventional model. There are water-to-water heat pumps, labelled HEAT HP and COOL HP, on the HWSR and CHWSR lines. These heat pumps exchange heat with the geothermal

borehole field, labelled GEO FIELD. The temperature sensors, labelled T SUP. HEAT HP and T SUP. COOL HP, are used with PI controllers to determine the heat pump compressor load and control the amount of heat added or removed from the HWSR and CHWSR lines.

The geothermal borehole field consists of an array of single U-tube boreholes with a specified spacing, depth, and soil properties. Water is circulated through the field at a constant mass flow rate using a pump, labelled PUMP GEO, and is split on the supply and return using two flow junctions, labelled SUP. JUN. GEO and RET. JUN. GEO. The pressure boundary condition is defined by the expansion tank, labelled EXP. TANK GEO. The water from the field is delivered to the evaporator on the HWSR heat pump and the condenser on the CHWSR heat pump. The heat added into and removed from the soil alters the boreholes' soil temperature based on the field's calculated soil volume.

3.2.2.4 Low-temperature ICE-Harvest building

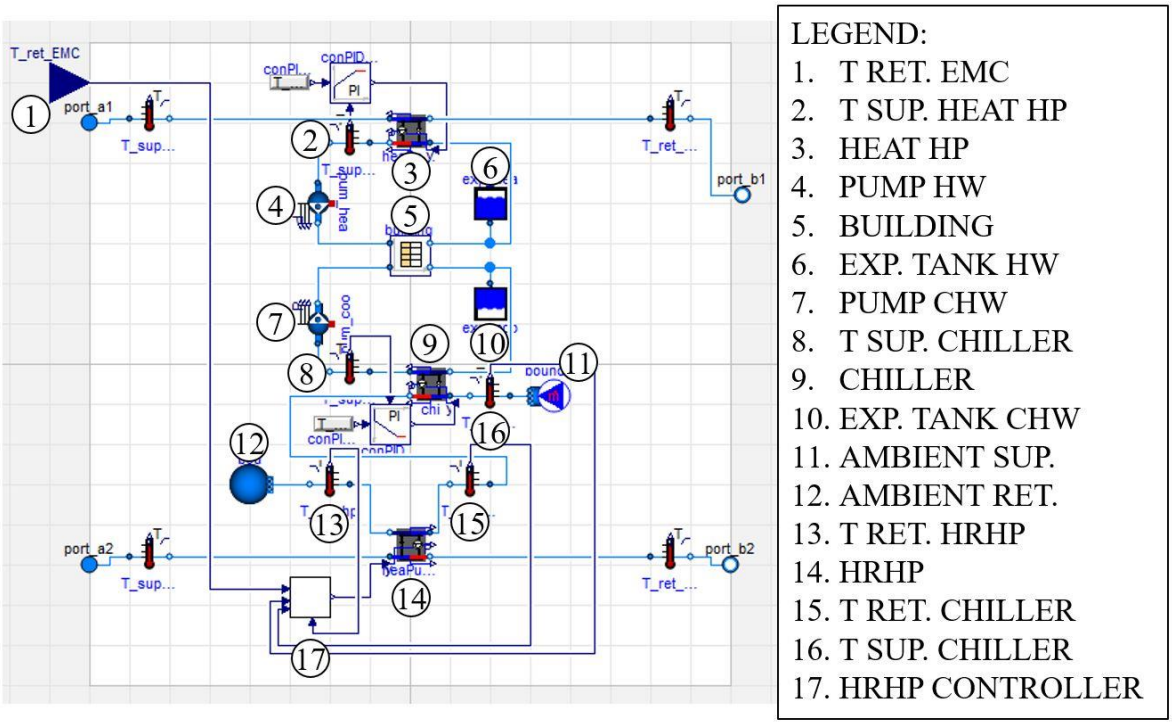

Figure 3.12: Low-temperature ICE-Harvest building model

The low-temperature ICE-Harvest model diagram is shown in Figure 3.12. The model is not a closed system and requires external connections at ports a1, b1, a2, and b2. The building demand model, labelled BUILDING, is identical to the conventional model. The HWSR line and heat pump, labelled HEAT HP, operate the same as the GSHP model; only the geothermal borehole field pipeline has been replaced by the external connection of port_a1 to port_b1. There is a chiller on the CHWSR line, labelled CHILLER, at the building level, which removes heat from the building CHW line and rejects it to the cooling tower return water, labelled AMBIENT SUP. The cooling water leaving the chiller condenser then goes to HRHP, labelled HRHP. The HRHP extracts heat from the chiller cooling water circuit and adds it to the external connection of port_a2 to port_b2. The amount of heat removed is determined by the controller, shown below the port_a2 to port_b2 line, which monitors the supply and return temperatures to the building chiller (labelled T SUP. CHILLER and T RET. CHILLER), the return temperature from the HRHP (labelled T RET. HP), and the return temperature in the network (labelled T RET EMC). The behaviour of this controller will be explained further in section 3.3.

3.2.2.5 High-temperature ICE-harvest building

The high-temperature ICE-Harvest model diagram is shown in Figure 3.13. The model is identical to the low-temperature ICE-Harvest model, with the only difference being the replacement of the HWSR heat pump with a heat exchanger, labelled HEX. The heat exchanger removes heat from the external connection of port_a1 to port_b1 and delivers it to the building HWSR line.

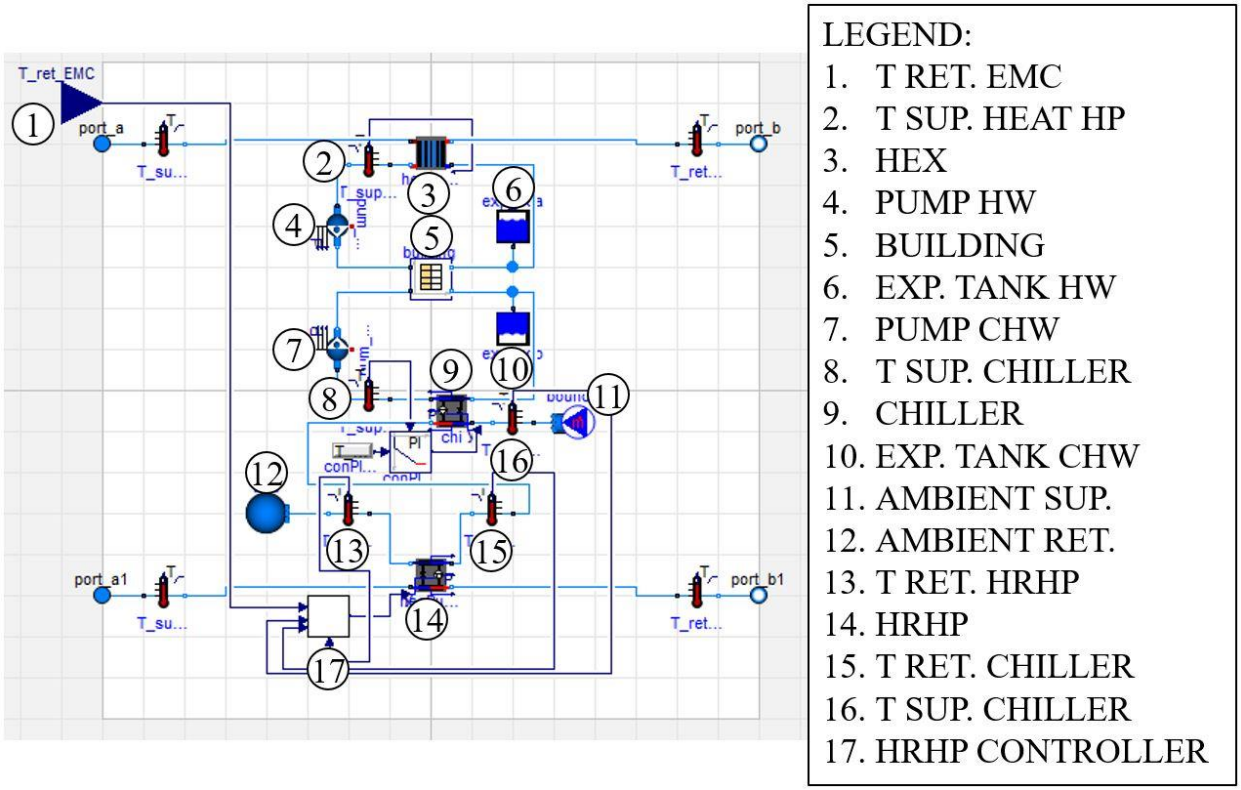

Figure 3.13: High-temperature ICE-Harvest building model

3.2.3 System models

The systems discussed in Section 3.1 are composed of multiple components and models to create system models. The system models are classified into two categories: individual system models and connected system models. The diagram of an individual system model is shown in Figure 3.14, and the diagram of a connected system model is shown in Figure 3.15.

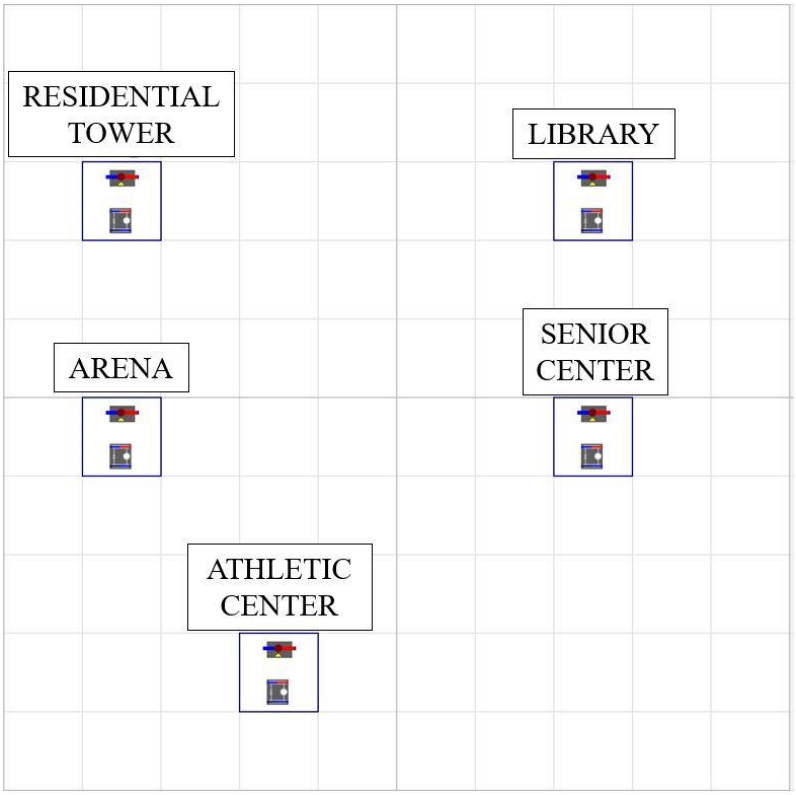

Figure 3.14: Diagram of an individual system model

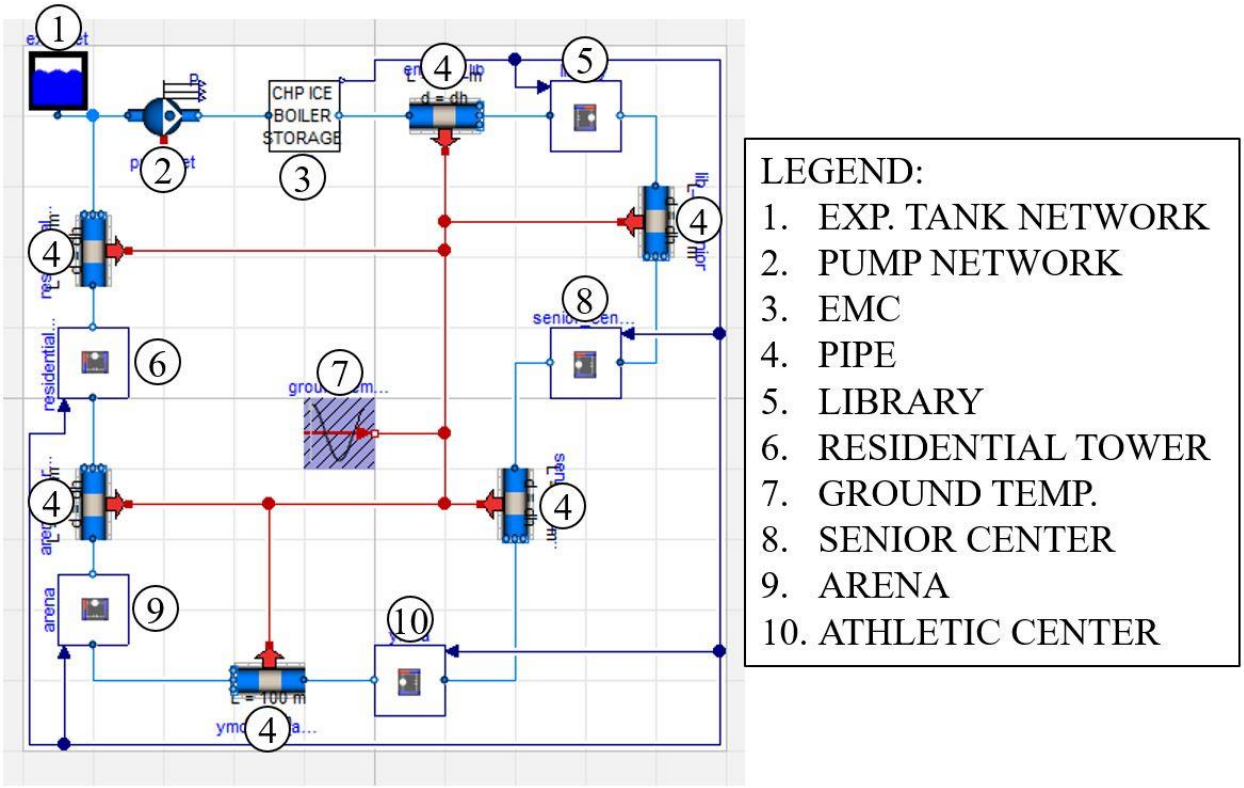

Figure 3.15: Diagram of a connected system model

The individual system model consists of individual building demand models like the ones presented in Section 3.2.2. The individual system does not connect the buildings with a thermal distribution network. Therefore, each building model in an individual system model contains all the equipment necessary to meet the building heating and cooling demands. These systems are isolated and do not have the opportunity for energy sharing or bidirectional energy flow between buildings. The systems that use this model type are the conventional system and the GSHP system. While the GSHP system could be designed as a connected system model, the individual system model was chosen as it is the most common configuration. For future work it is recommended to study a GSHP system as a connected system model. This will add the benefit of waste energy sharing and result in different heating and refrigeration ratios than the ones shown in this research.

The connected system model connects the building models using a thermal distribution network. The building models have external port connections and are connected in series to the network pipes. Thus, these systems are connected and have the opportunity for energy sharing if the building models have the capabilities. The generation model, labelled EMC, provides thermal energy to the network and controls its supply temperature. The network pipes are connected to a ground temperature boundary condition, labelled GROUND TEMP., which provides the temperature boundary condition for conduction heat losses from the network to the surrounding ground. Water is circulated in the network at a constant mass flow rate using a pump, labelled PUMP NETWORK, with a pressure boundary condition provided by the expansion tank, labelled

EXP. TANK NETWORK. The systems that use this model type are the DH system and both the low and high-temperature ICE-Harvest systems.

3.2.4 CHP efficiency

The efficiency of an internal combustion engine-based CHP unit changes depending on the part load ratio of the engine [20]. The part load ratio is typically expressed as a percentage, and it is defined as the ratio between the current CHP output to the maximum CHP capacity. The ratio can be calculated using either the thermal or electrical output and capacity. The efficiency of a CHP can be expressed in three ways: thermal, electrical, or total. The thermal efficiency is the ratio between the useful heat output and the fuel energy input. The electrical efficiency is the ratio between the electrical output and the fuel energy input. The total utilization is the ratio of the sum of the thermal and electrical output to the fuel energy input.

Figure 3.16 and Figure 3.17 show the part-load efficiencies used in this research. The part-load efficiencies are categorized according to the CHP's thermal capacity using data from the AIXLib CHP database [103]. The efficiencies for under 50% part load are excluded because the CHP only operates at a part load of 50% or greater. The CHP units are classified into CHP units with greater than 1 MW_{th} capacity and CHP units with less than 1 MW_{th} capacity.

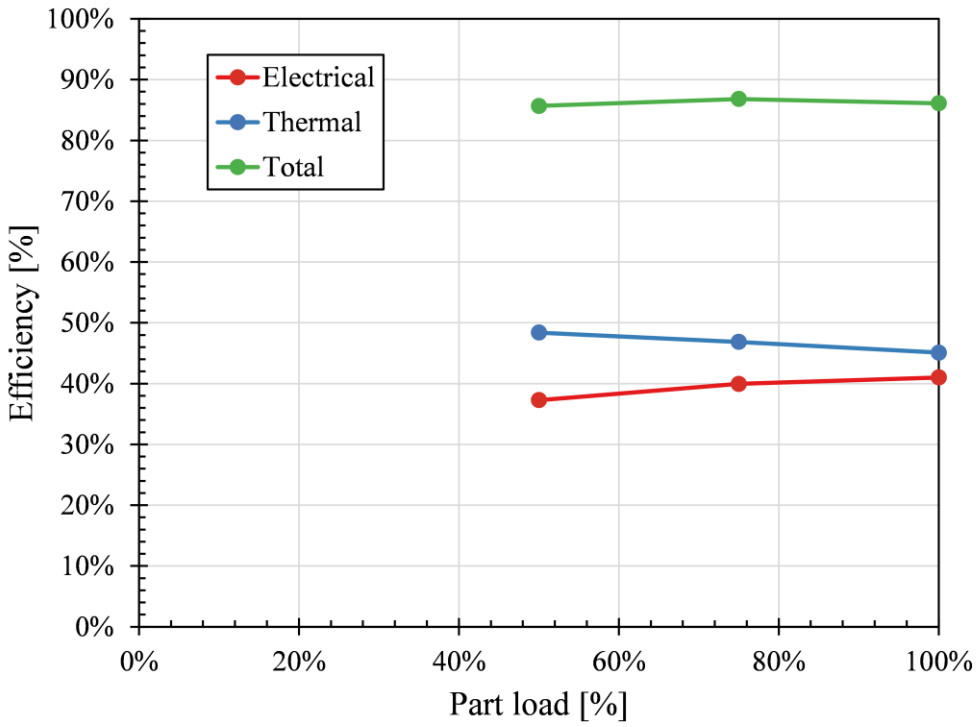

Figure 3.16: Efficiency vs part load for a CHP over 1MW$_{th}$ capacity

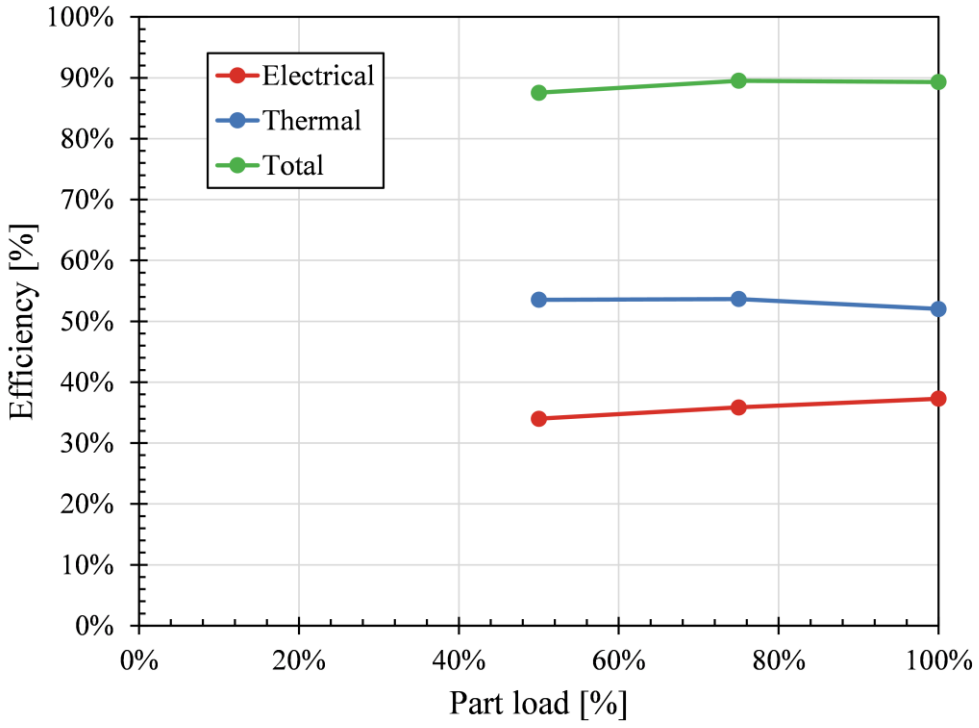

Figure 3.17: Efficiency vs. part load for a CHP under 1MW$_{th}$ capacity

The reason for the distinction is that units over 1 MW_{th} have characteristically lower Heat to Power Ratios (HPR). The HPR defines the ratio of the thermal to electrical output at a given part load ratio. CHP units with capacities greater than 1 MW_{th} have higher electrical efficiencies and lower thermal efficiencies, which decrease rapidly with higher part load ratios approaching an HPR close to unity at full capacity. Conversely, CHP units under 1 MW_{th} consistently produce a larger amount of thermal energy throughout all part load ratios. Therefore, CHP units with capacities greater than 1 MW_{th} are better suited for electricity production, while units under 1 MW_{th} are better for heat delivery.

3.3 Verification

This section will verify the controls of different sub-systems in the presented systems. The sub-systems presented are charging and discharging the TES, a heat exchanger between two headers, and the heating and cooling of a building with waste heat recovery.

The individual components used are verified by the library creators. For example, explanations and examples of the Buildings library models can be found in [102], and descriptions of Modelica and use cases for the Annex 60 Modelica libraries can be found in the project final report [26]. Additional verifications of the CHP and the thermal energy storage can be found in Appendix B.

The purpose of the verifications presented here is to verify the subsystems' response under all the conditions experienced in the ICE Harvest system. This verification will prove that the controllers respond correctly and that the subsystems' components perform as expected.

3.3.1 Charging and discharging of thermal energy storage

3.3.1.1 Background

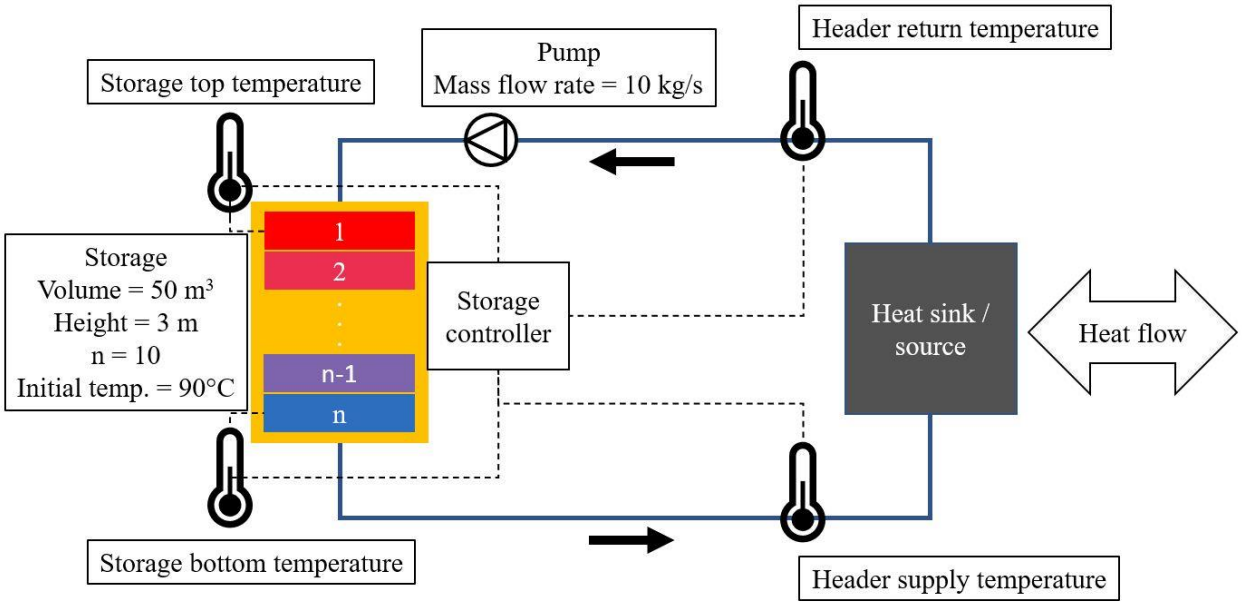

Figure 3.18: System schematic for the thermal energy storage verification

The first sub-system to be verified is the TES. Figure 3.18 shows the system schematic for the test being conducted. For this verification test, the storage has a volume of 50 m^3, a height of 3 m, a uniform initial temperature of 90 °C, and it is discretized into ten nodes. The TES model selected is the stratified storage model from the Buildings library [114]. The TES is connected to the heat sink/source through a piping header. The heat sink/source is assumed to add or remove heat from the header to maintain a specified return temperature. The specified return temperature varies between 50 °C to 90 °C during the test. Water is circulated in the header using a pump with a constant mass flow rate of 10 kg/s. There are four temperature sensors in the header for monitoring the header supply temperature, the header return temperature, the storage top temperature, and the storage bottom temperature. The temperature sensors are connected to the storage controller, which controls the TES charging and discharging.

The heat flow rate is transferred through the heat sink/source according to the profile shown in Figure 3.19. A negative heat flow rate corresponds to heat being removed from the header (header return temperature less than header supply temperature). A positive heat flow rate corresponds to heat being added to the header (header return temperature greater than header supply temperature).

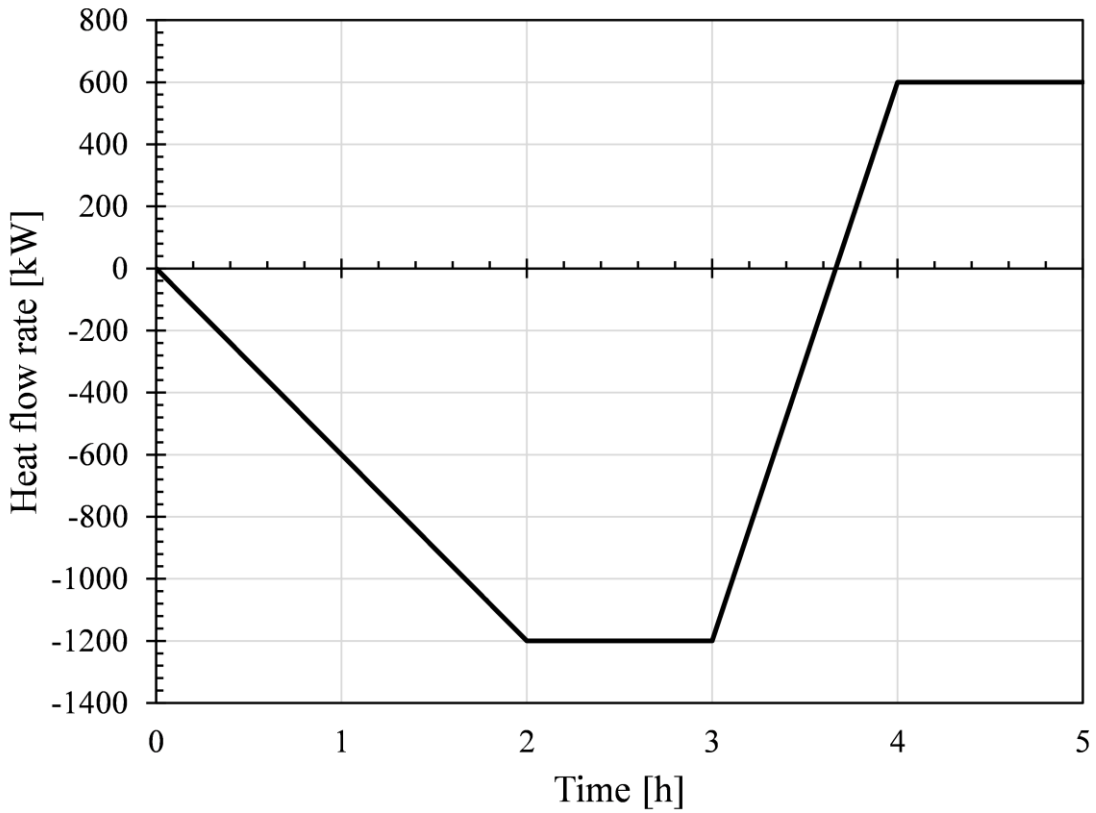

Figure 3.19: Heat flow rate [kW] vs. time [h]. Negative corresponds to heat removed from the header, and positive corresponds to heat added to the header.

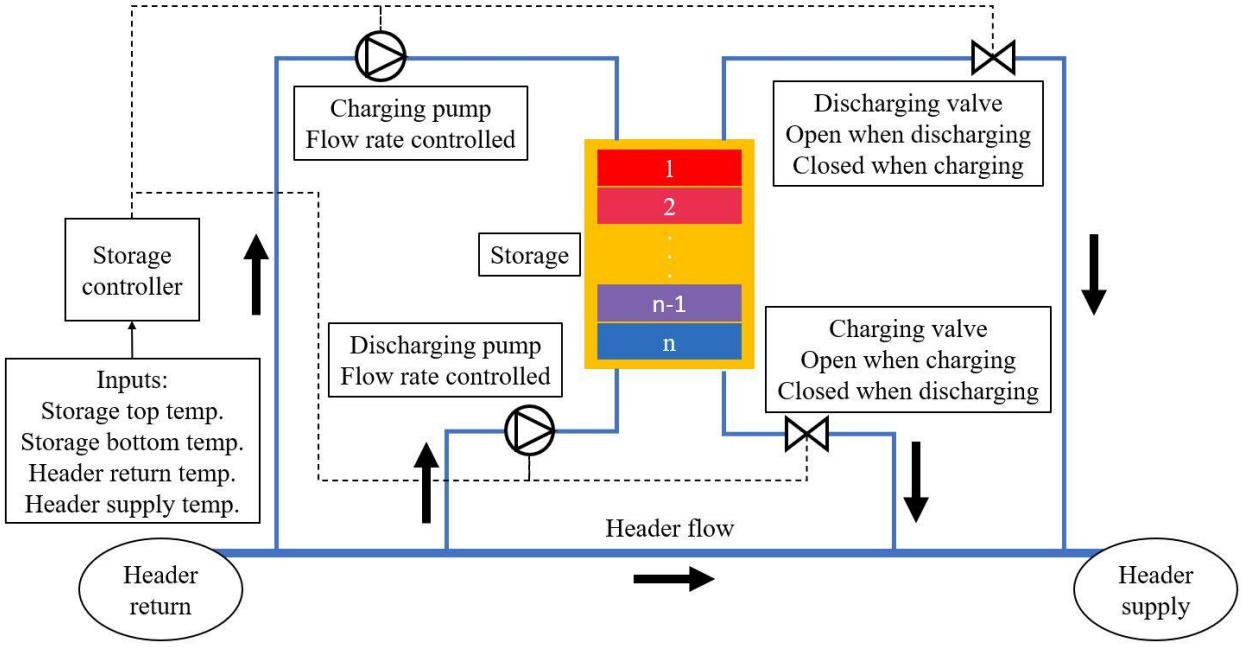

Figure 3.20: Schematic of the thermal energy storage piping and controls

Figure 3.20 shows the schematic of how the TES is piped into the header and how the controller is operated to control the charging and discharging rate. The TES controller controls the header supply temperature to a specified setpoint by varying the charging and discharging pump mass flow rates using PI control. There are four pipes connected to the TES, with two pumps on the supply side and two valves on the return side. The discharging valve is open during discharging and closed during charging and vice-versa for the charging valve.

The controller also monitors the storage top and bottom temperature and the header return temperature to decide when to charge and discharge. For example, when the storage top temperature is lower than the header return temperature, the TES cannot deliver heat to the header. There is a minimum temperature difference between the TES and the header for charging and discharging to avoid cycling the pumps. In this example, the temperature difference is 5 °C.

The header supply temperature is a function of the specified temperature setpoint, the minimum allowed temperature difference between the TES and the header, and the current

temperature of the TES. Table 3.1 explains how the controller adjusts the header supply temperature based on the TES status and temperature conditions.

Table 3.1: TES controller logic

TES status	Condition	Supply temperature
Discharging	$T_{TES,top} >= T_{setpoint} + \Delta T_{min}$	$T_{setpoint}$
	$T_{TES,top} < T_{setpoint} + \Delta T_{min}$	$T_{TES,top} - \Delta T_{min}$
Charging	$T_{TES,bottom} <= T_{setpoint} - \Delta T_{min}$	$T_{setpoint}$
	$T_{TES,bottom} > T_{setpoint} - \Delta T_{min}$	$T_{TES,bottom} + \Delta T_{min}$

3.3.1.2 Results

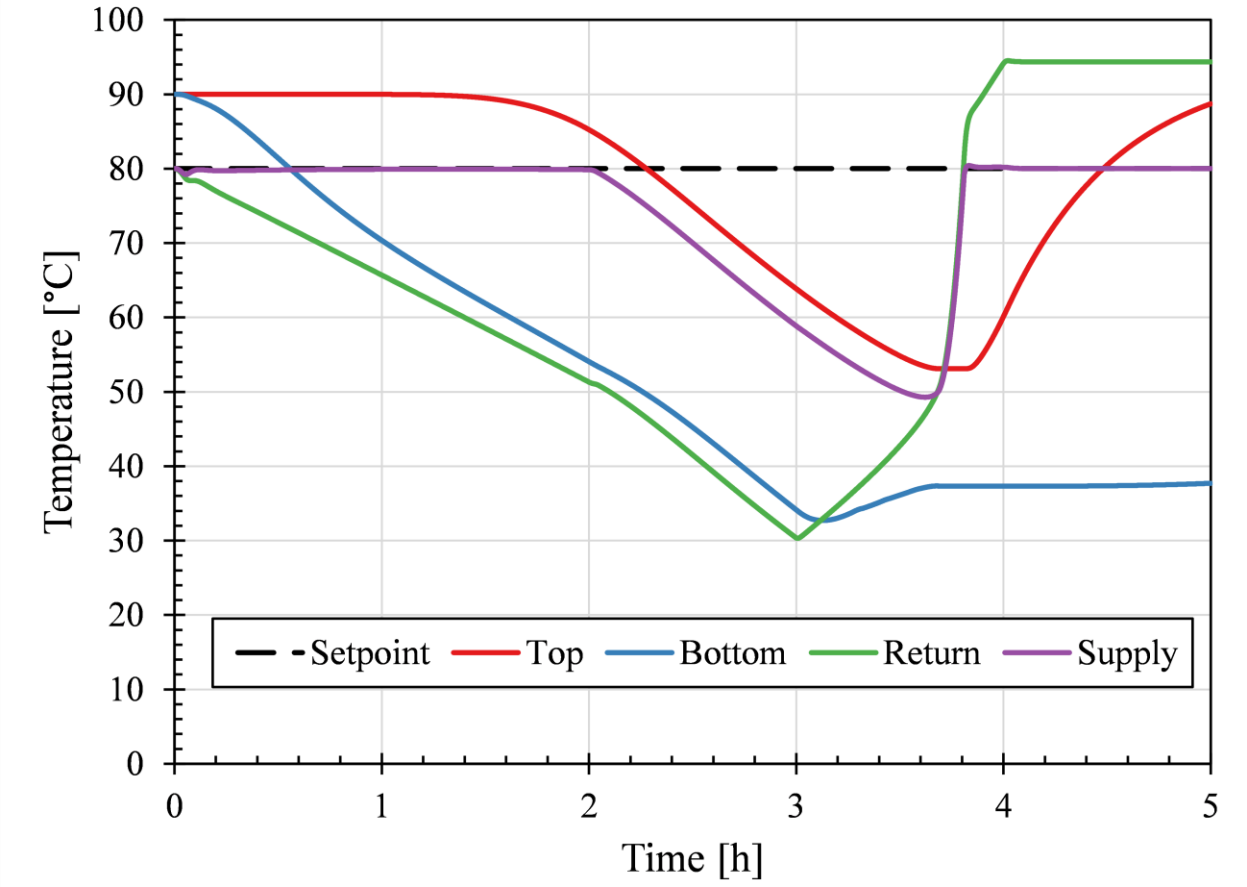

Figure 3.21: TES temperature [°C] vs. time [h] results plot. The supply temperature setpoint (long dash black line), TES top temperature (red line), TES bottom temperature (blue line), header return temperature (green line), and header supply temperature (purple line) are plotted for 5 hours.

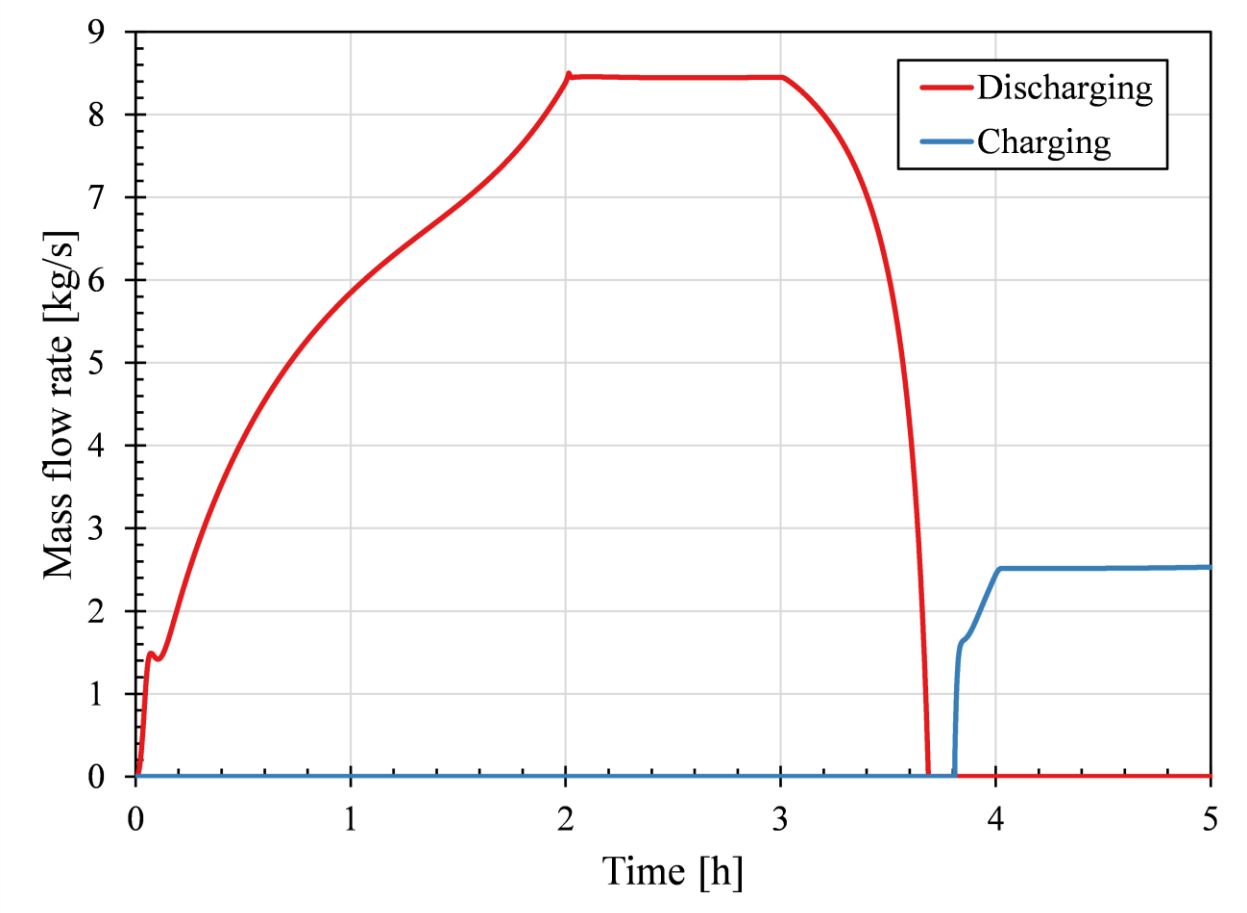

Figure 3.22: The TES mass flow rate [kg/s] during charging and discharging vs. time [h]. The TES charging mass flow rate is plotted in red, and TES discharging mass flow rate is plotted in blue.

Figure 3.21 plots the TES temperature versus the time in hours. The dashed black line is the supply temperature setpoint for the header. The red and blue lines are the temperature measurements at the top and bottom of the TES, respectively. The green and purple lines are the header's temperature measurements returning to and supplying from the TES, respectively. Figure 3.22 plots the mass flow rate versus time in hours. The mass flow rate during charging is shown in red, and during discharging is shown in blue. During the charging process, water flows from the top to the bottom of the TES. During the discharging process, water flows from the bottom to the top of the TES. This control was done to maintain stratification in the TES.

For the first two hours of the simulation, the header's return temperature decreases linearly from 80 °C to approximately 50 °C. While the return temperature decreases, the TES discharges to maintain the supply temperature at the setpoint of 80 °C. Discharging the storage causes an immediate decrease at the bottom of the TES as the lower temperature header water enters from the bottom. The discharging pump's mass flow rate increases during this time because the heat flow rate from the header is increasing. An increase in the heat flow rate from the header means that more flow from the storage is needed to maintain the setpoint. After approximately 1.5 hours, the temperature at the top of the TES decreases as the water entering from the bottom has now reached the top of the storage.

When the temperature at the top of the storage reaches 85 °C, after approximately 2 hours, the controller setpoint changes to the temperature at the top of the TES minus the minimum temperature difference (5 °C). The storage continues discharging, and the temperature at the top of the TES decreases. As the temperature at the top of the TES decreases, so too does the supply temperature. During this time, the heat flow rate from the header is constant; thus, the mass flow rate from the storage is also constant. The constant mass flow rate maintains the temperature difference between the header supply temperature and the TES top temperature at a constant 5 °C, which is the minimum allowed temperature difference specified by the controller.

The storage continues discharging until approximately 3.7 hours when the return temperature increases to match the supply temperature. The storage remains idle for approximately 0.1 hours, as evidenced by zero flow through the charging and discharging pumps, while the return temperature continues to increase. Once the supply temperature reaches the temperature setpoint, the storage begins charging. During charging, the mass flow rate increases while the heat flow rate into the header increases, then remains constant when the heat flow rate is constant. Charging the

storage causes the temperature at the top of the TES to increase first, which shows that the valve controls are working correctly

3.3.2 Heat exchanger between the generation model and the thermal distribution network

3.3.2.1 Background

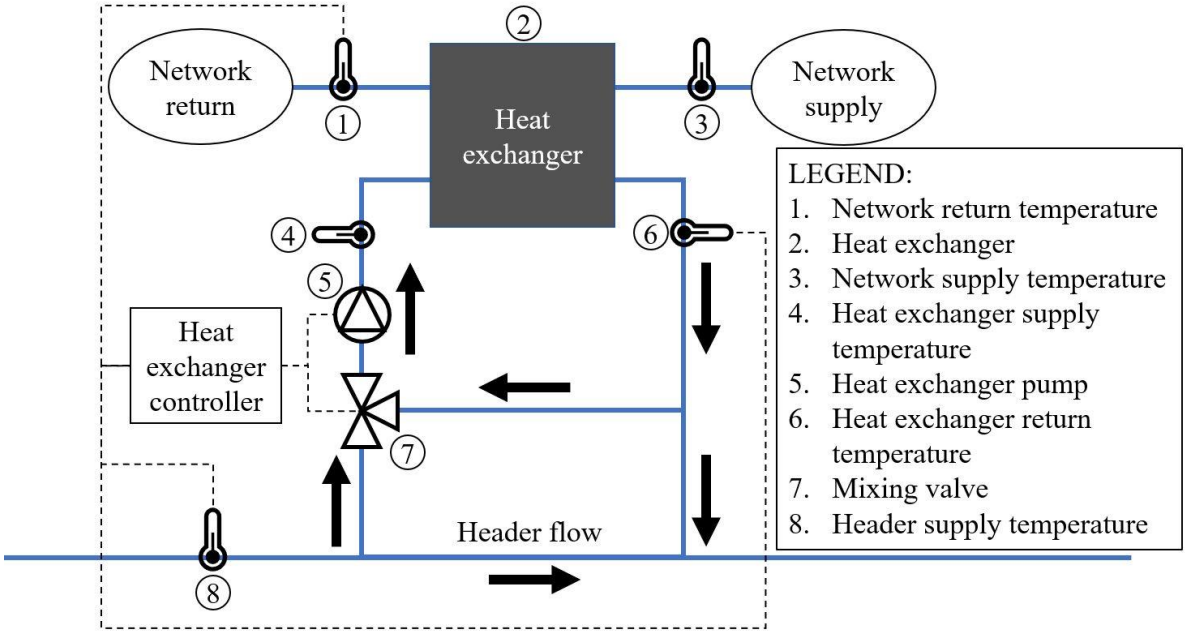

Figure 3.23: System schematic for the heat exchanger verification

Figure 3.23 shows the schematic of the heat exchanger sub-system being verified. The verification will test the heat exchanger controller's performance when the header supply temperature and the network return temperature are varied. The heat exchanger model selected is the ε-NTU model from the Buildings library [115]. The heat exchanger exchanges heat between the network and the header. The heat exchanger's header side has a pump and mixing valve controlled by the heat exchanger controller. The controller receives inputs from the network return temperature, the header supply temperature, and the heat exchanger return temperature. The pump is conditionally operated "on" or "off" while the mixing valve position is varied continuously using

a PI controller. The mass flow rate on the network and header sides are both constant at 10 kg/s. The controller uses the network return temperature and the heat exchanger return temperature to calculate the desired mixing valve position to maintain a specified network supply temperature. The mixing valve mixes the heat exchanger return water with the header supply water to achieve the required heat exchanger supply temperature.

3.3.2.2 Results

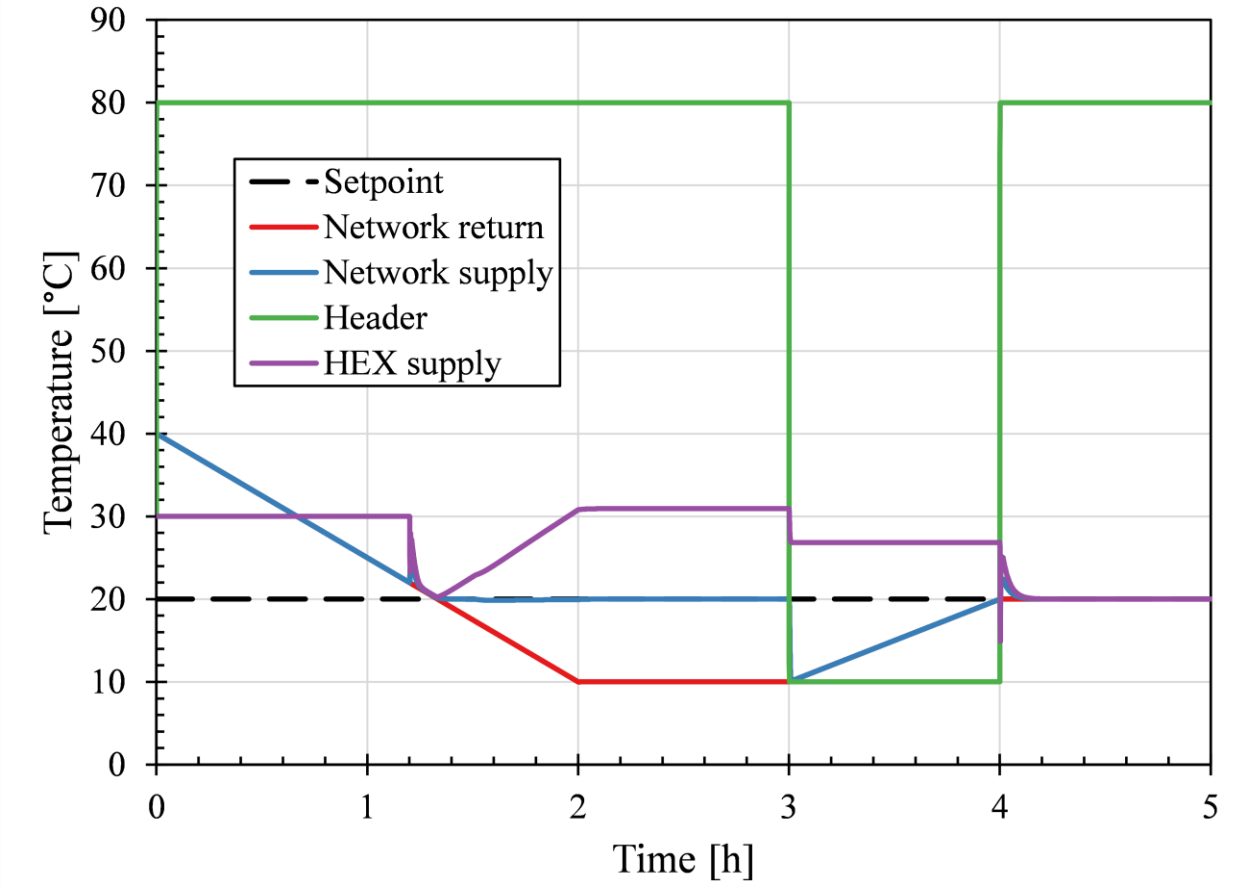

Figure 3.24: Heat exchanger verification temperature [°C] vs. time [h] results plot. The supply temperature setpoint (long dash black line), network return temperature (red line), network supply temperature (blue line), header temperature (green line), and heat exchanger supply temperature (purple line) are for five hours.

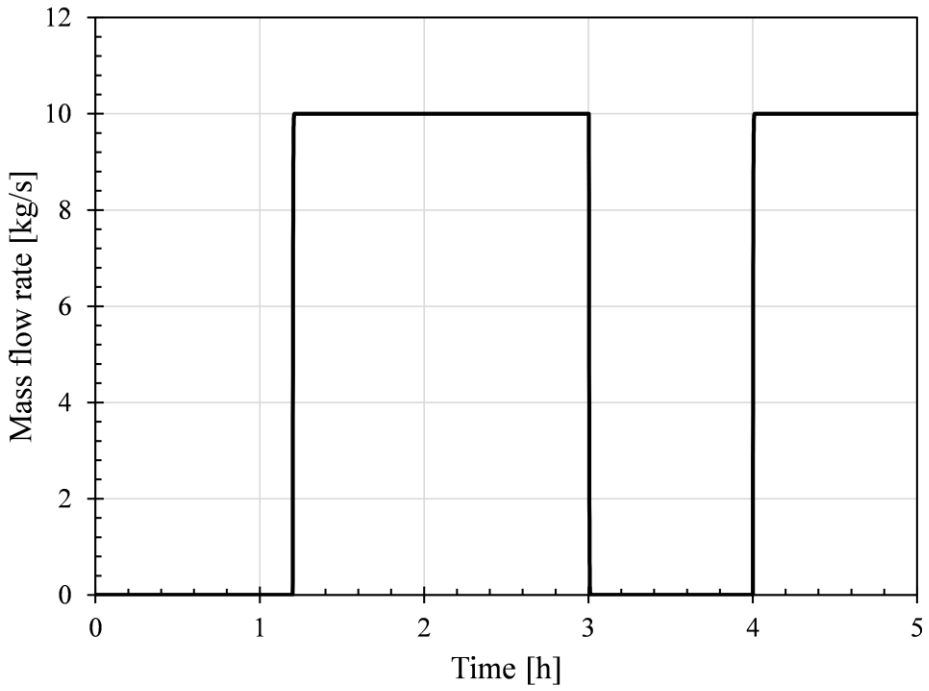

Figure 3.25: Mass flow rate [kg/s] vs. time [h] through the heat exchanger.

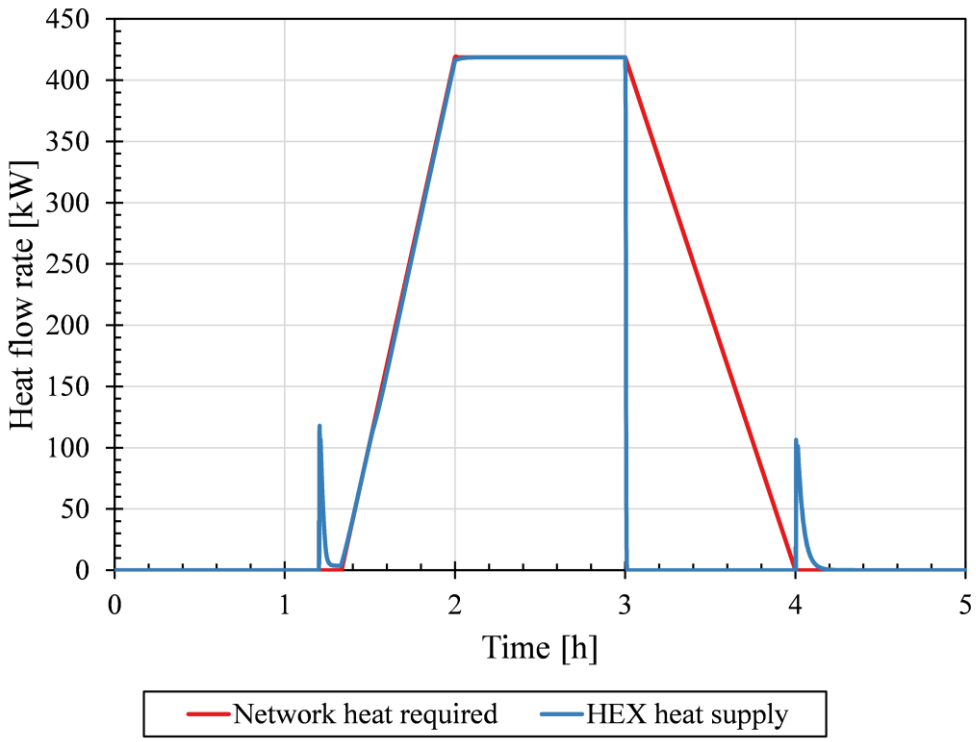

Figure 3.26: Heat flow rate [kW] vs. time [h]

For the first 1.2 hours, the network return temperature is above the setpoint; therefore, the heat exchanger is off, and heat is not exchanged. From 1.2 hours to 2 hours, the return temperature decreases from 20 to 10 °C, where it is held constant for one hour. When the return temperature crosses the setpoint, the mass flow rate increases to 10 kg/s and heat is exchanged. The heat exchanger supply temperature increases as the network return temperature decreases to maintain the required heat transfer rate. Using this control, the heat exchanger can maintain a network supply temperature of 20 °C.

At 3 hours, the temperature in the header decreases from 80 to 10 °C. The temperature in the generation model header is now lower than the network supply temperature setpoint, and the heat exchanger pump turns off. Without heat being supplied from the header, the network supply temperature drops down to 10 °C. The network supply temperature increases back to 20 °C over the next hour only because of the increasing network return temperature. There is still no heat being exchanged, as evidenced by Figure 3.26.

From 4 hours to 5 hours, the header temperature increases back to 80 °C, and the heat exchanger turns back on. Here, the return temperature is very close to the setpoint, and the heat exchanger does not have to deliver much heat to maintain the supply temperature at the setpoint of 20 °C. Therefore, the heat exchanger model and controls are working correctly.

3.3.3 Heating and cooling of a building with waste heat recovery

3.3.3.1 Background

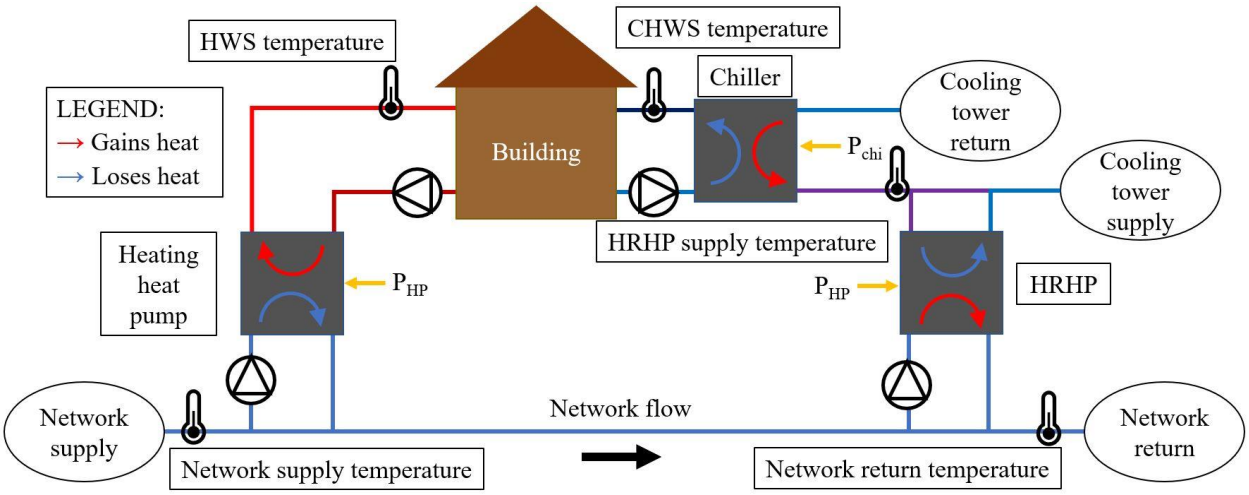

Figure 3.27: System schematic for the heat recovery heat pump verification

Figure 3.27 shows the schematic for the heat recovery heat pump verification in the ICE-Harvest system. The schematic features a building model with HWSR and CHWSR lines going to a heating heat pump and a chiller model, respectively. The heat pump and chiller models are the constant effectiveness model from the Buildings library. Details of the model can be found here [116]. The cooling water is supplied to the chiller by a constant return temperature cooling tower and is rejected to a shared junction for the HRHP and the cooling tower supply. The HRHP has a controller that removes heat from the cooling water when available and required in the network. PI controllers control the HWS and CHWS temperature.

For the verification, the HWS temperature setpoint is 60 °C, the CHWS temperature setpoint is 15.6 °C, and the network return temperature setpoint is 20 °C. For the first hour, the building heating demand is greater than the building cooling demand; therefore, there is more heat required than is available to the HRHP. For the next hour, the heating demand is equal to the cooling demand, and for the last hour, the heating demand is less than the cooling demand. The

HRHP controller will decide how much heat to extract from the chiller cooling water return based on the network supply water temperature after the heating heat pump and the HRHP supply temperature. Also, the HRHP only extracts so much heat such that the HRHP return temperature is not less than the constant return water temperature from the cooling tower.

3.3.3.2 Results

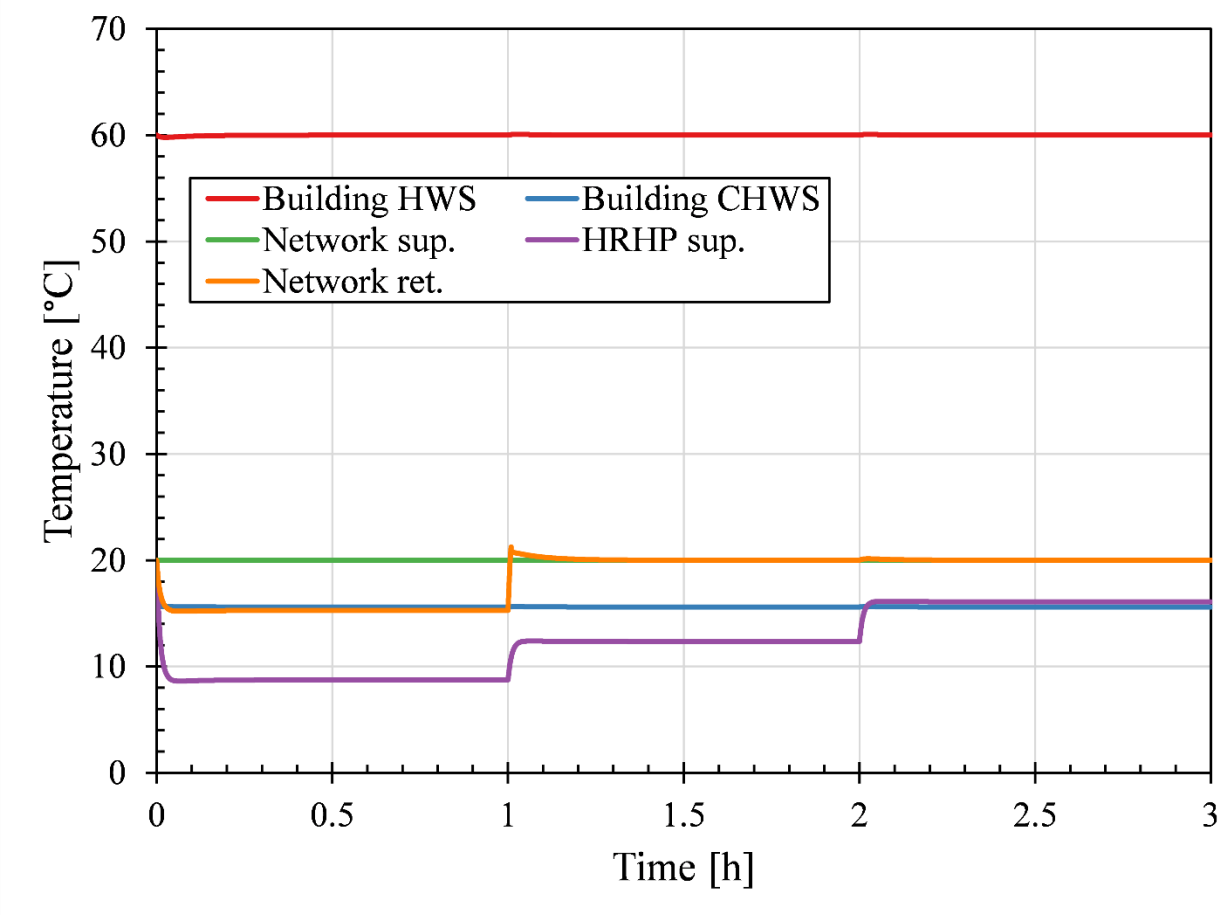

Figure 3.28: ICE-Building model verification temperature plot. Building HWS (red), building CWS supply (blue), network supply to the building (green), HRHP/network return after heating (purple), network return after heat recovery (orange).

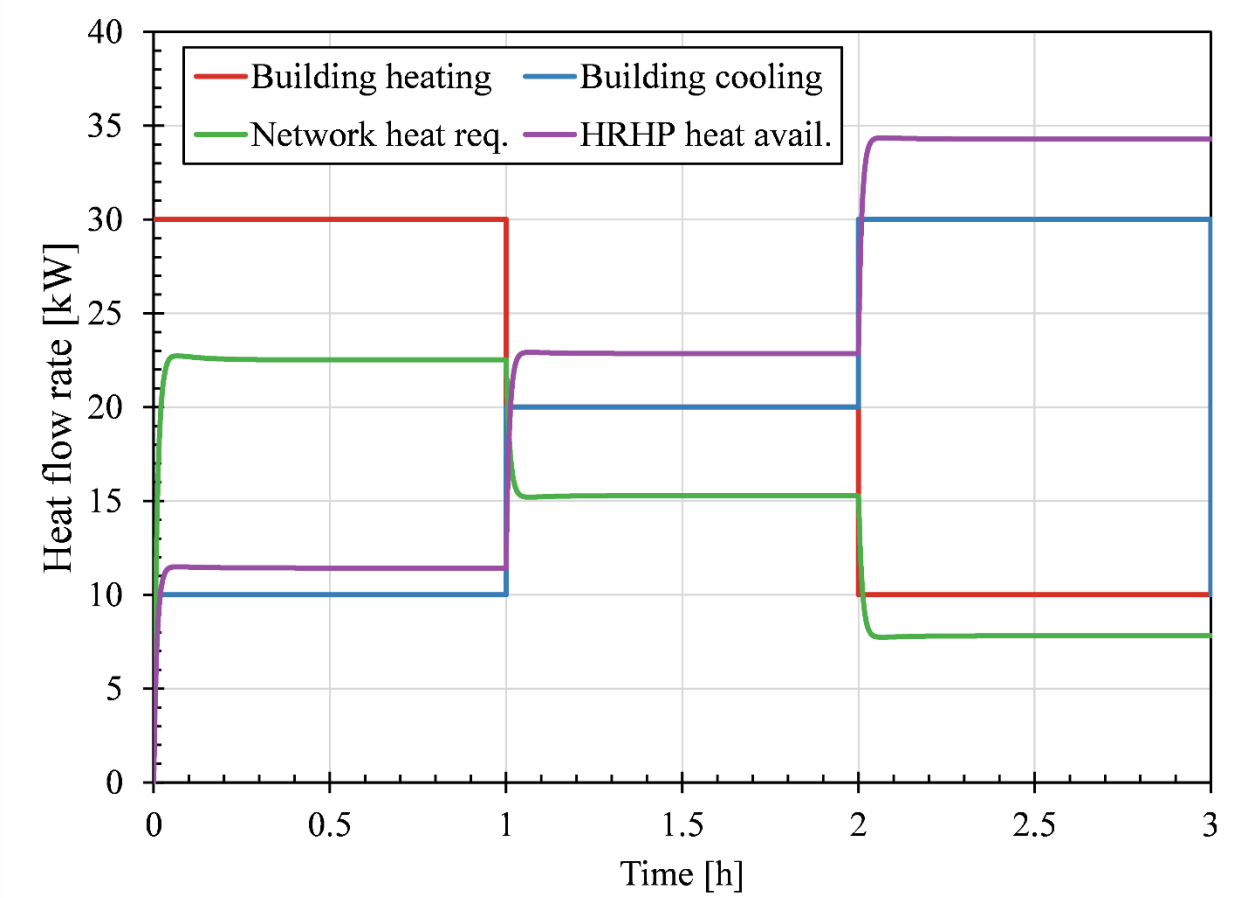

Figure 3.29: ICE-Building model verification heat flow plot. Building heating demand (red), building cooling demand (blue), network heat required / heat removed from the network for building heating (green), HRHP heat available / building condenser heat rejected (purple).

Figure 3.28 and Figure 3.29 show the verification of the HRHP in the ICE-Harvest system. Figure 3.28 shows the building HWS temperature, shown in red, and the building CHWS temperature, shown in blue. The building HWS and CHWS lines exchange heat with the thermal distribution network through the HRHP, shown in purple. The network supply and return temperatures are shown in green and orange, respectively. This verification aims to show how the HRHP operates with variations in building heating and cooling demand. The heat flow rates for the system are shown in Figure 3.29. First, the heating demand, shown in red, is greater than the cooling demand, shown in blue. Therefore, the amount of heat required to raise the network temperature to the supply temperature setpoint, shown in green, is less than the amount of heat

available to the HRHP, shown in purple. When the heating demand is greater than the cooling demand, the network return temperature should be below the supply temperature. When the heating demand is greater than or equal to the cooling demand, the network return temperature will equal the supply temperature.

For the simulation's first hour, the building heating demand is greater than the building cooling demand. The amount of heat required in the network is less than the building heating demand because the heat pump compressor work supplies part of the building heating. The amount of heat available to the HRHP is greater than the building cooling demand because it is on the condenser side of the chiller. Despite this, the HRHP cannot raise the temperature of the network to the desired supply temperature. The network water is supplied to the building at 20 °C. After the heating heat pump evaporator extracts heat, the network's temperature decreases to 9.5 °C, where it is supplied to the HRHP condenser. The HRHP only increases the network return temperature to 16 °C because of the lack of available waste heat.

For the next hour, the building heating demand is equal to the building cooling demand. In this scenario, the amount of heat required is approximately equal to the amount of heat available. The controllers respond correctly by raising the network return temperature to 20 °C. The decrease in building heating demand is shown by the increase in supply temperature to the HRHP from 9.5 °C to 13 °C.

For the final hour, the building heating demand is less than the building cooling demand. Therefore, the amount of heat required is less than the amount of heat available. Here the HRHP does not remove more heat than is required from the chiller condenser circuit and only delivers the required amount of heat to the network. This results in a stable network temperature of 20 °C.

3.3.4 Summary of verifications

In conclusion, there were three verifications shown for the models presented in the methodology section. The first verification was on the charging and discharging of the TES to the generation station header line. The second verification was on the heat exchanger model used to connect the generation station to the network. The third verification was on the functionality of the HRHP under different building heating and cooling demands.

The TES charging and discharging showed that the TES controls the header's temperature by varying the mass flow rate. The pumps also demonstrated that they maintain stratification by charging and discharging to the top of the storage. The TES was able to maintain the header temperature setpoint when the storage temperature was above the setpoint. When the temperature decreased, the TES maintained a 5 °C difference between the top of the storage and the header. When the header temperature increased above the setpoint, the TES began charging.

The heat exchanger verification showed that the heat exchanger correctly responds to temperature changes on both sides to deliver heat in the correct quantity and direction. When the network did not require heat, the heat exchanger did not operate. Once the network temperature was below the setpoint, the heat exchanger was used to maintain the desired supply temperature. When the header temperature was lower than the setpoint, the heat exchanger turned off again to avoid extracting heat from the network. Once the header temperature increased, the heat exchanger was again able to transfer heat into the network. However, because the network return temperature was equal to the network supply temperature setpoint, no heat transfer occurred.

The HRHP recovered the correct amount of heat for three different building heating and cooling demand conditions. When the heat required was greater than the waste heat available, the

HRHP used all the available heat. When the heat required was greater than or equal to the heat available, the HRHP only used the amount of heat required to achieve the desired supply temperature setpoint.

Chapter 4

4 Results

The results section of this thesis focuses on the yearly simulation of five different heating and cooling systems. The systems are quantitatively compared according to their ability to deliver heating, cooling, and electricity to a sample set of buildings. The demands for the buildings are sourced from real hourly energy consumption data collected from the buildings. The evaluation metrics are the system's total energy consumption, greenhouse gas emissions produced, and impact on the hourly electricity market. All of the results presented in this section were produced using the Dymola software and the Annex 60 [26] and IBPSA Project 1 [27] libraries. The simulations were all solved using the DASSL solver with a tolerance of 1E-4, an interval length of 3600 seconds, and for the duration of 1 year.

4.1 Background

The community considered in this study consists of five existing buildings that are within proximity of one another. The buildings are a residential tower, a library, a senior center, an athletic center (referred to as the YMCA), and an arena. The buildings are currently heated using individual boilers and furnaces and cooled using chillers and air conditioners. The hot water and chilled water supply temperatures is 60 °C are 15.6 °C, respectively. The electrical grid provides the electricity they consume for the cooling equipment and plug loads. For the comparison, there will be five systems studied: the conventional, GSHP, DH, low-temperature ICE-Harvest, and high-temperature ICE-Harvest. Two of these systems, the conventional and GSHP, are individual systems where all the heating and cooling equipment is located at the buildings. The other three

systems, the DH, low-temperature ICE-Harvest, and high-temperature ICE-Harvest, are network systems that require a thermal distribution network.

4.1.1 Thermal distribution network layout

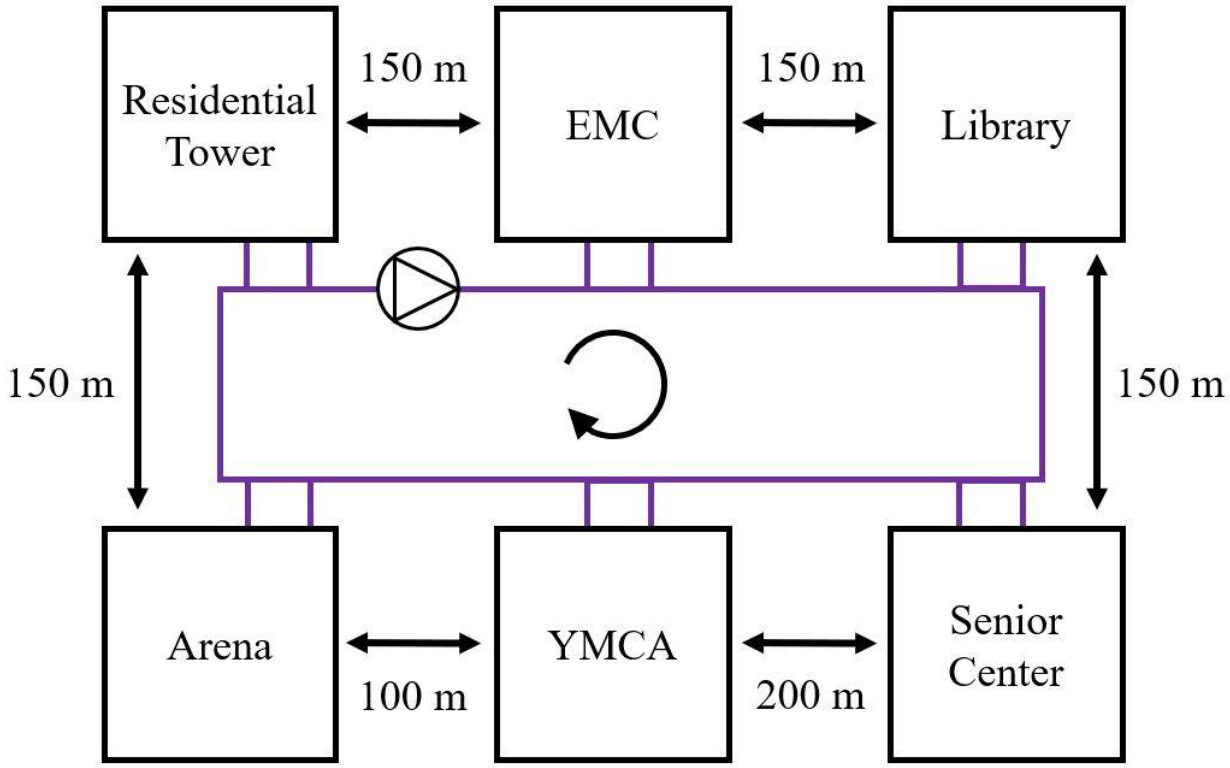

Figure 4.1: Schematic diagram of the network layout.

Figure 4.1 shows the assumed simplified network layout for the buildings and the thermal distribution network. The same network layout is used for all network systems. The network is assumed to be a smooth 18" schedule 40 steel pipe buried at a depth of 4' (1.22m) with an insulation thickness of 6" (0.1524m) and insulation conductivity of 0.04 W/mK. The pipe diameter was chosen to maintain a constant velocity of 1.66 m/s in the network. The water is circulated continuously at a constant mass flow rate by a single network pump. The generation station is referred to as the EMC (Energy Management Centre), and it is assumed to be located between the

residential tower and the library. The total network length is 900 m with a fluid transit time (the time it takes for a fluid element to circulate the network) of approximately 9 minutes (542 seconds).

4.1.2 Building energy demands

The demands are measured on an hourly basis for one year. The heating demand was calculated using the measured natural gas consumption (including space heating and domestic hot water), building temperature setpoint, and the Typical Meteorological Year (TMY) dry bulb temperature. The cooling demand was calculated using the building electricity consumption and TMY dry bulb temperature. The electricity demand was gathered on a 5-minute interval and averaged on an hourly basis. The TMY dry-bulb temperature for the site is shown in Figure 4.2. The highest temperature experienced is 37 °C in July, and the lowest temperature is – 24 °C in December.

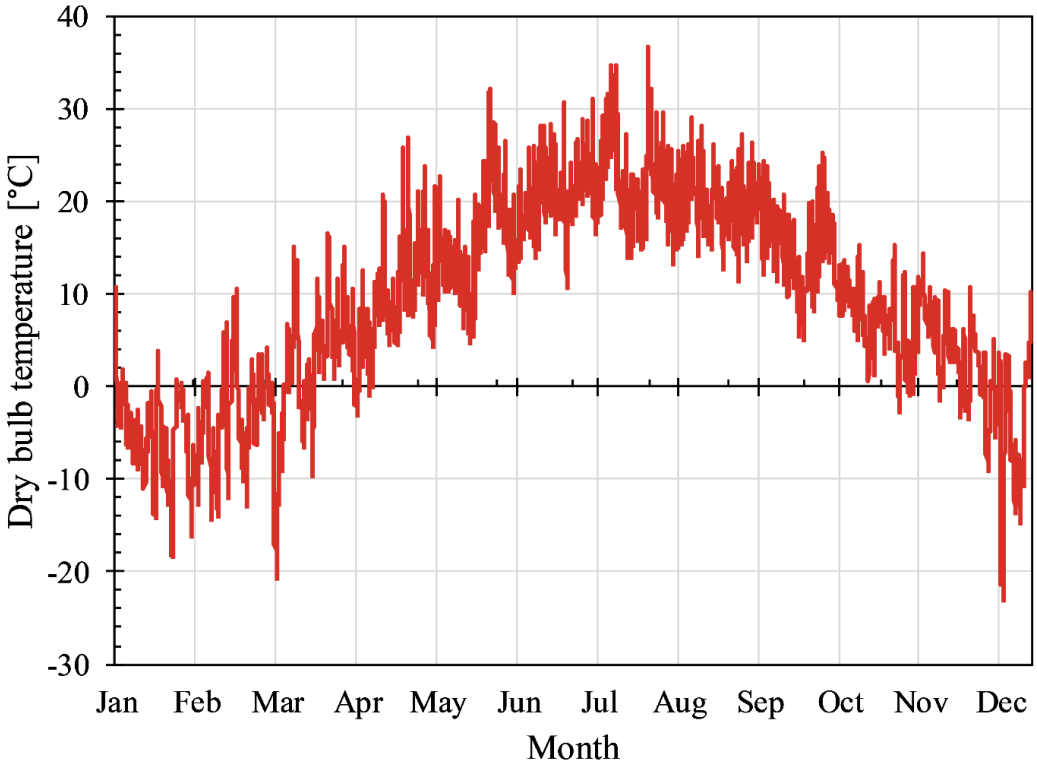

Figure 4.2: TMY dry-bulb temperature for the proposed site

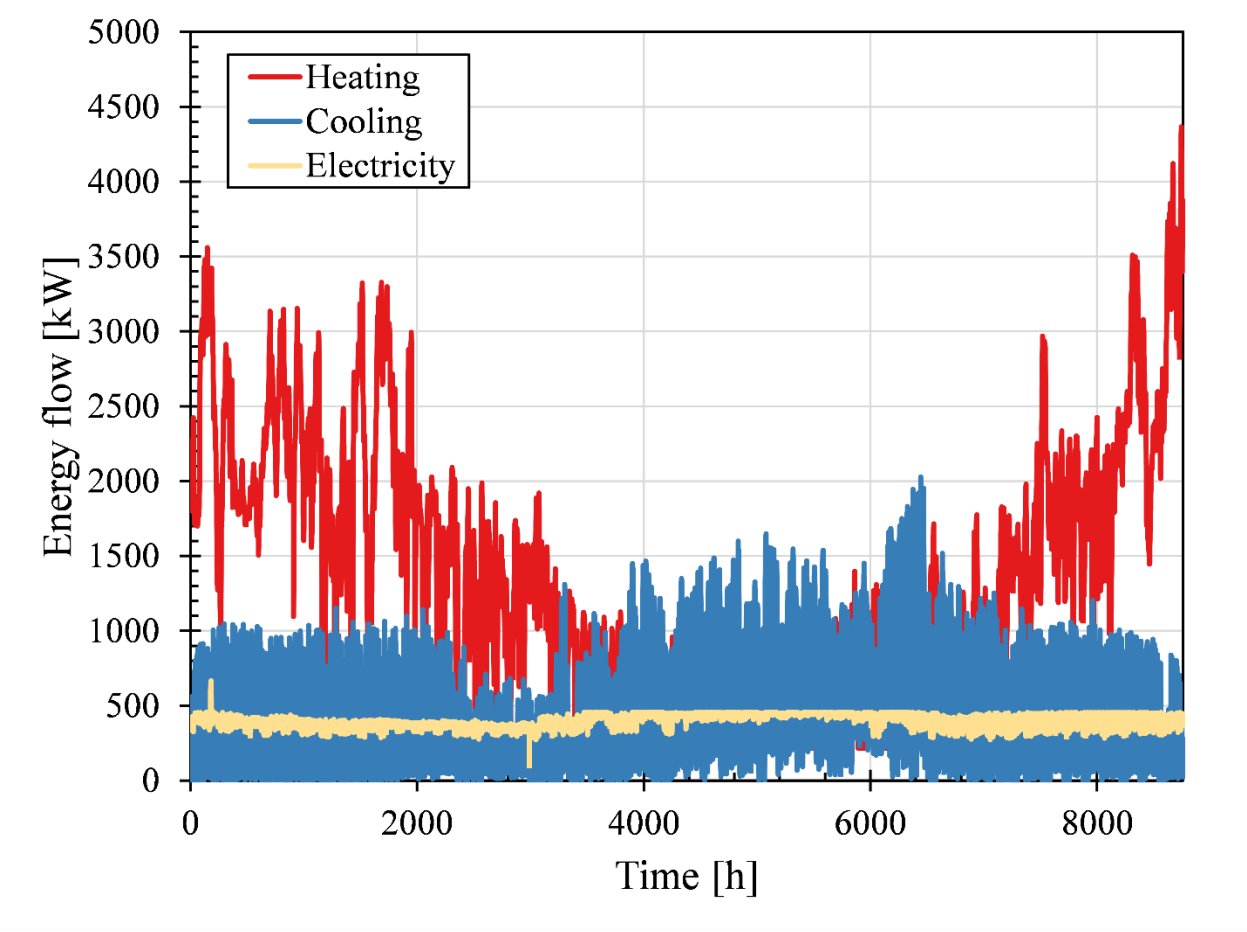

Figure 4.3: Hourly combined heating, cooling, and electricity demands(t=0 coincides with January 1)

Table 4.1: Building demand summary

Building	**Annual heating demand [MWh]**	**Annual cooling demand [MWh]**	**Annual electricity demand [MWh]**	**Peak heating demand [kW]**	**Peak cooling demand [kW]**	**Peak plug load electrical demand [kW]**
Arena	807	1198	165	306	562	20
Library	731	1823	818	332	855	100
Residential tower	5927	273	1123	2697	362	415
Senior center	506	310	286	219	255	35
YMCA	2837	999	1023	837	442	120
Combined	10808	4602	3515	4391	2098	690

Figure 4.3 shows the combined hourly heating, cooling, and plug-load electricity demands of the buildings under study. The electricity demand shown excludes the electricity demands for

cooling equipment because the cooling demand is thermal energy rather than electrical energy. Since the cooling equipment's sub-metered electrical demands were not available, the cooling demand was disaggregated from the electricity demand by assuming a plug load electrical demand limit for each building and a constant COP of 3.3 for the building cooling equipment. The individual energy demands of each building can be found Appendix C. A summary of the individual building energy demands can be found in Table 4.1. The heating demands are higher during the winter months, decreasing to a baseload of domestic hot water during the summer. The cooling demands are highest during the summer months, but there are cooling demands during the winter because of refrigeration loads for the arena and a data center located in the library. The electricity demand is the most stable with few fluctuations.

Table 4.2: Summary of heating, cooling, and electricity demands

	Min	**Max**	**Average**	**Std. deviation**
Heating [kWth]	216	4366	1234	938
Cooling [kWth]	0	2028	525	392
Electrical [kWe]	106	667	401	44

Table 4.2 presents a summary of the combined heating, cooling, and electricity demands. The heating demand has the highest standard deviation with high heating demands during the winter and low heating demands during the summer. The minimum heating demand is 216 kW_{th} during the summer months for domestic hot water purposes. The maximum heating demand is 4366 kW_{th} during the winter months, with the absolute maximum occurring in December. Unlike the heating demand, the cooling demand minimum is 0 kW_{th}, despite year-round cooling demands in the arena and library data center. The cooling demand has a maximum of 2028 kWth in September when the buildings have the greatest space cooling demands. For most of the year, a cooling demand exists because of the refrigeration requirements at the arena for ice production and at the library for data center cooling. The electricity demand is the plug loads of the buildings,

excluding all cooling equipment. Examples of plug loads are lighting, appliances, servers, and computers. The cooling equipment is excluded because the cooling demand is discussed as thermal energy rather than electrical energy in this research. The standard deviation of the electricity demand is much smaller than the heating and cooling demands. The small standard deviation indicates that the electricity demand is relatively stable and does not experience significant hourly fluctuations.

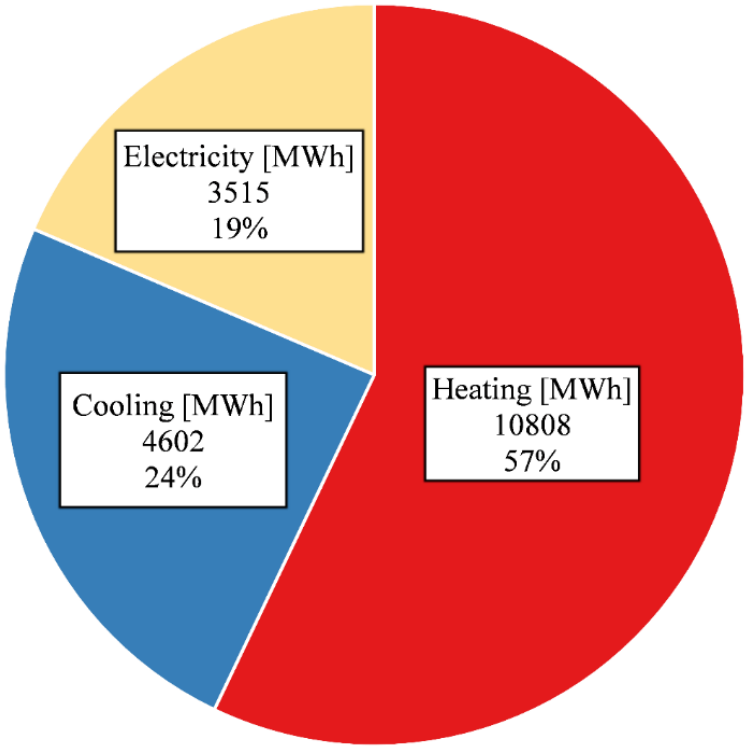

Figure 4.4: Annual total heating, cooling, and electricity demand

Figure 4.4 shows the annual total heating, cooling, and electricity demand. The annual total heating demand is 10808 MWh, and it represents 57% of the total energy demand. The heating demand is the majority of the thermal energy requirements; therefore, this group of buildings can be classified as heating demand dominant. The cooling demand is 4602 MWh, and it represents 24% of the total energy demand. The electricity demand is the smallest energy demand at 3515 MWh per year. This building group's thermal demands (heating and cooling) are 4.4 times greater

than the electricity demands. Therefore, the buildings require 4.4 times more thermal energy added or removed from the buildings than electrical energy. This is an important metric to predict the increase in electrical demand caused by meeting the thermal demands using electricity.

4.1.3 Network heat losses and pumping power

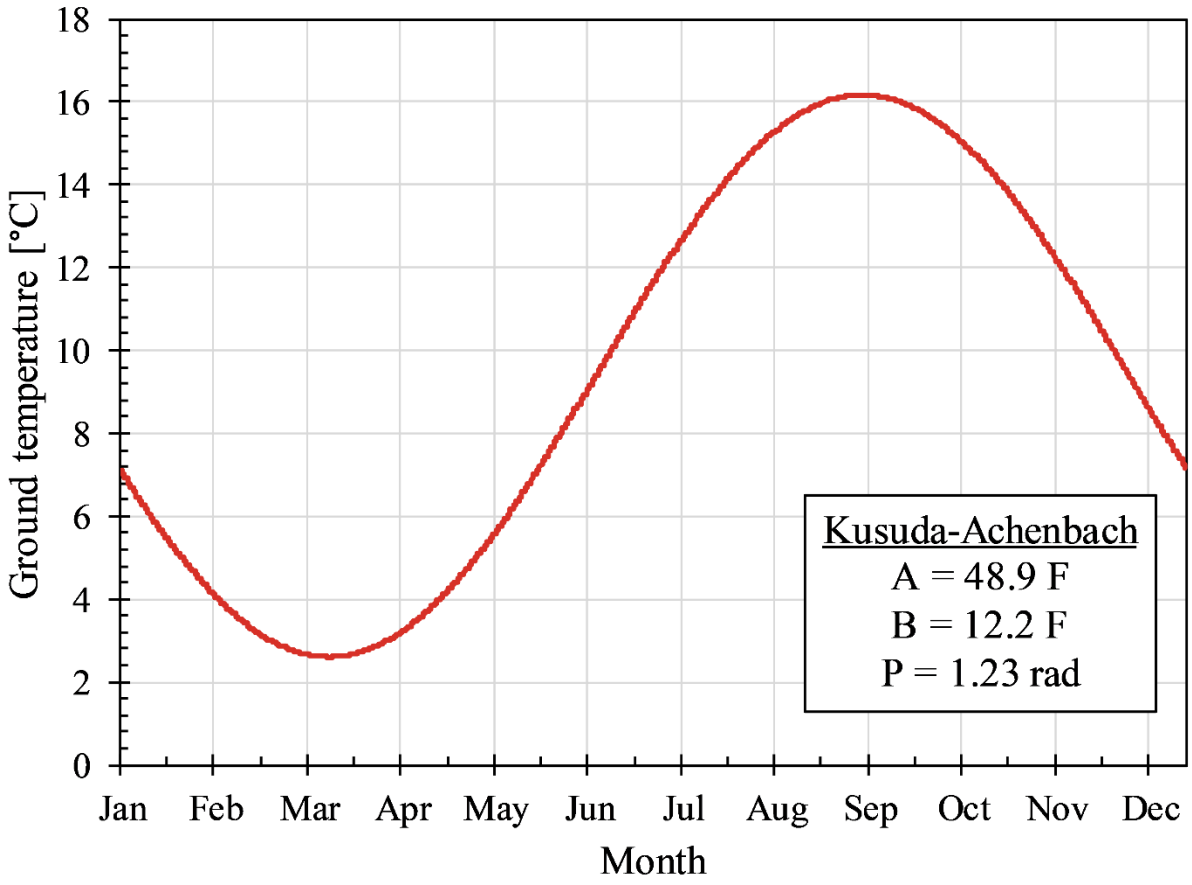

Figure 4.5: Ground temperature used for simulation

The Kusuda-Achenbach equation [117] was used for the ground temperature in the network. Figure 4.5 shows the yearly ground temperature at the chosen depth of 4'. The parameters for Ithaca, New York, were chosen as it is the closest region to the area under study.

The network's pumping power can be calculated using the Darcy Weisbach equation [118] using the pipe parameters defined earlier. Assuming a pumping efficiency of 80%, the annual

pumping power is 15.4 MWh, which is only 0.4% of the annual electricity consumption. Therefore, the pumping power will be ignored in this discussion.

4.1.4 Geothermal borehole fields for ground source heat pumps

Table 4.3: Geothermal borehole field parameters

Building	Number of boreholes	Depth [m]	Spacing [m]	Arrangement
Arena	100	300	7.5	Square
Library	100			
Residential tower	196			
YMCA	144			
Senior center	100			

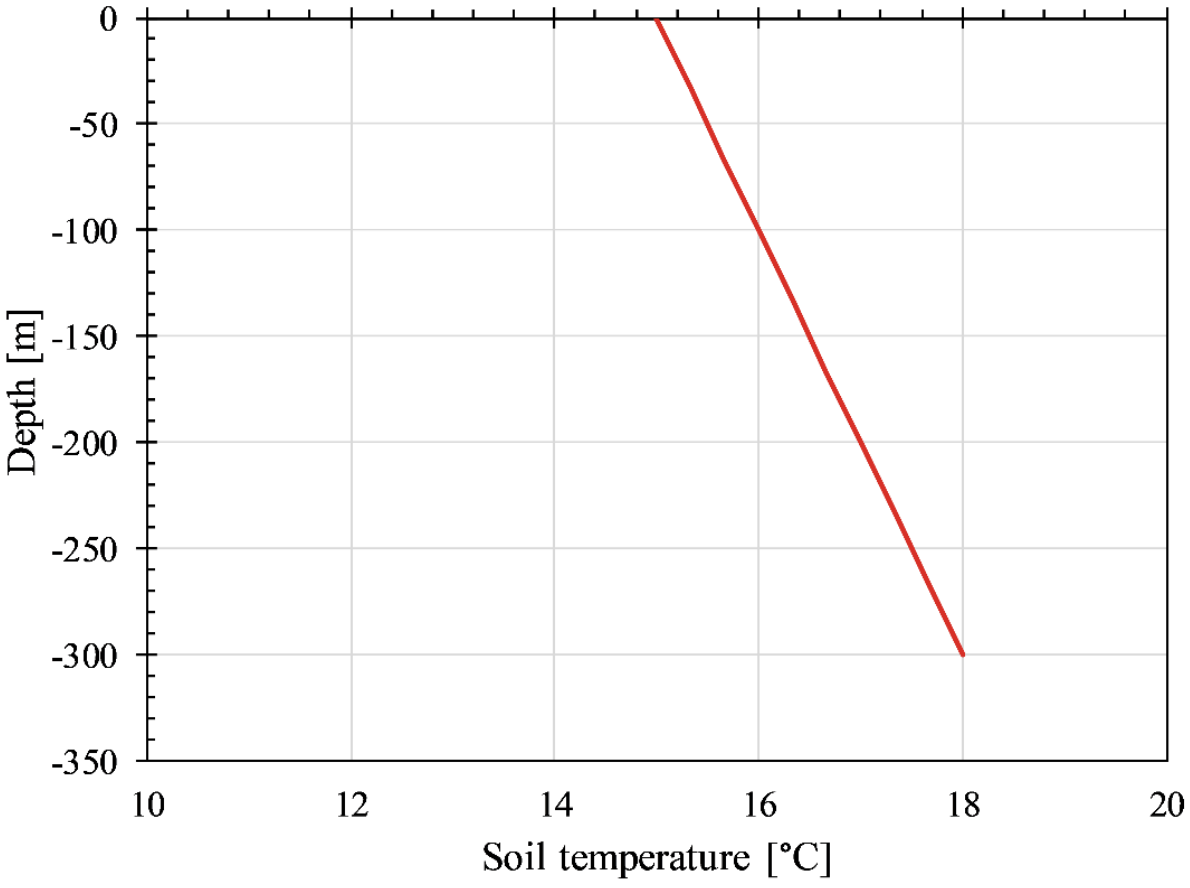

Figure 4.6: Geothermal borehole field initial temperature distribution

The geothermal borehole fields used for the GSHP system were sized to avoid significant seasonal soil temperature fluctuations. Table 4.3 provides the borehole field

parameters used for each building. The number of boreholes varies from 100 to 196 boreholes depending on the energy demands of the building. Buildings with larger energy demands required more boreholes than buildings with lower demands. The depth, spacing, and arrangement were kept constant for all the buildings. The depth refers to the distance in which the borehole is buried beneath the surface. The depth was chosen to be 300 m. The spacing of the boreholes was chosen as 7.5 m, and it refers to the distance between borehole centers. The boreholes are arranged in a square array. Figure 4.6 shows the assumed initial soil temperature in the borehole field. The temperature at the surface is assumed to be 15 °C, and it increases linearly to 18 °C at a depth of 300 m. A portion of the heat that is injected into the borehole field is unrecoverable due to heat dissipation. These losses are referred to as far-field losses. The far-field is assumed to be at a constant temperature of 15 °C.

4.1.5 The electrical grid and hourly emission factor

The electrical supply mix and hourly emission factor data were taken from the Ontario IESO. The historical supply data for the year 2016 was used in these results. Figure 4.7 shows the hourly emission factor for 2016. The peak emission factor is around 0.06 kg CO_{2e}/kWh and an average of 0.02 kg CO_{2e}/kWh. In 2016, over 1 GW of gas generation on the Ontario electrical grid for 8205 hours (i.e., 94% of the year). The number of gas generation hours is used for calculating the CHP capacity and the CHP run hours in the ICE-Harvest system.

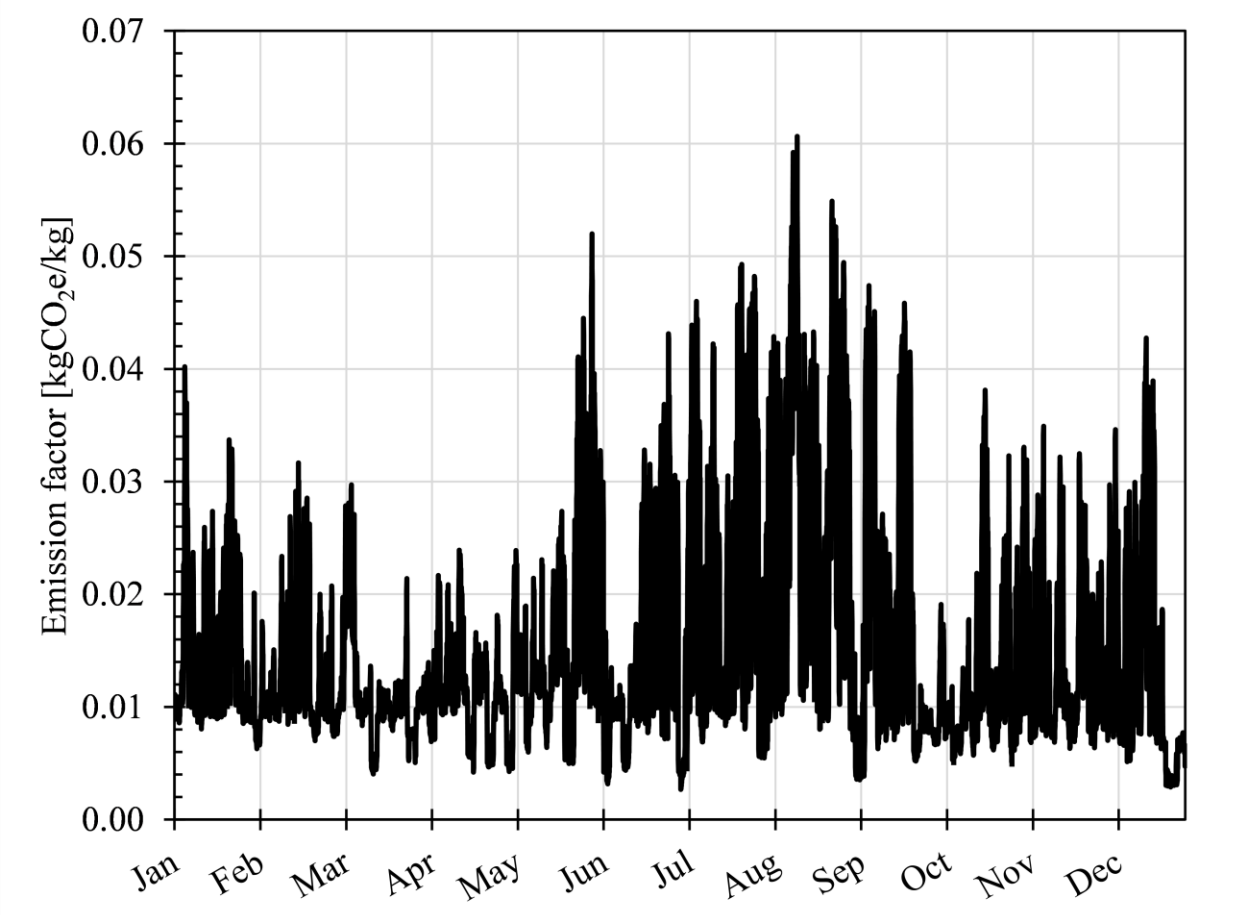

Figure 4.7: Hourly emission factor for the Ontario electrical grid in 2016

4.2 System comparison

This set of simulation results compares the conventional, DH, GSHP, and ICE-Harvest systems' performance in their ability to meet the building's thermal and electrical energy requirements. The ICE-Harvest system is simulated at three different network supply temperatures: 20 °C, 35 °C, and 70 °C. The systems are compared according to their electricity supply mix, annual and hourly electricity demand, heating supply mix, utilization of cooling heat rejection, CO_2e emissions, and equipment capacities. All systems are assumed to have a building level hot water supply temperature of 60 °C and chilled water supply temperature of 15.6 °C.

4.2.1 Heating supply

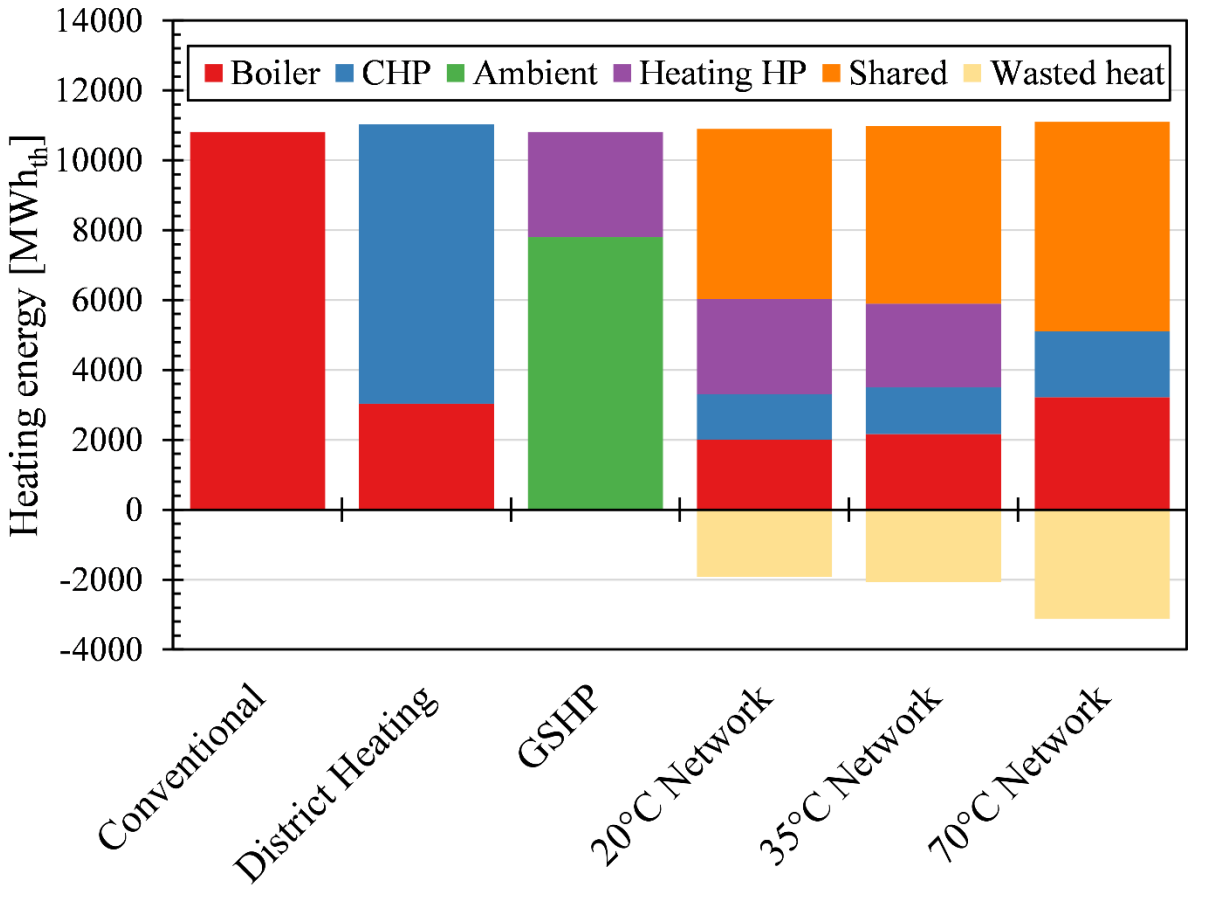

Figure 4.8: Annual total heating thermal energy supplied of each system divided into the boiler (red), CHP (blue), ambient (green), heat pump power (purple), sharing (orange), and wasted heat (yellow)

Figure 4.8 shows the annual total heating supply in each of the six systems. The conventional system's heating supply comes entirely from the boiler because it is the only heating equipment available. The annual total heating delivered totals 10808 MWh, which is equal to the buildings' heating load. The DH system supplies heat from both the boiler and the CHP. The heat supplied in the DH system is slightly greater than the conventional system because of network heat losses. The network heat losses accounted for an additional 222 MWh of heat over the year, which is 2% of the annual heating demand. The CHP accounted for 72% of the supplied heat, and the boiler supplied the remaining 28%. The GSHP has the same total heat supplied as the conventional

system because there are no distribution losses. 72% of the heat came from the geothermal borehole field (referred to as the ambient in the figure), and 28% of the heat is from the compressor work. Therefore, the heating HP in the GSHP system has an annual average COP of 3.59, which is reasonable for the study's geographic region. Also, note that the boiler and CHP are not part of the GSHP system; thus, they do not contribute to the heat supply.

The ICE-Harvest systems have a multitude of heat sources resulting in more subcategories. In the ICE-Harvest systems, heat can be supplied by a CHP, a boiler, the compressor work in the heating HP, and by harvesting heat from cooling processes (referred to as sharing). Unlike the GSHP system, the ICE-Harvest system does not pull heat from the ambient.

Starting with the 20 °C network, the thermal distribution network's annual heat losses are small, measuring only 39 MWh (0.3% of the total heat demand). A significant portion of the heat comes from sharing (44.5%), which is the heat harvested from other buildings' cooling processes. Therefore, energy sharing reduced the required energy from other sources to only 65.5% of the conventional system. The heating heat pump provided 2720 MWh from compressor work, comparable to the GSHP system at 3011 MWh, signifying a similar heating COP between the two systems. The annual average COP of the heating heat pump in the 20 °C network is 3.99. The remaining heat supply is provided by the CHP and boiler located at the EMC. The CHP is only operating when natural-gas generators are connected to the grid, and the capacity of the CHP is 394 kW, which is lower than the average heating demand. Therefore, the boiler is used to supply heat when the CHP capacity is insufficient or when the CHP is off. The wasted heat (which appears as a yellow bar in Figure 4.8) is heat produced by the CHP when the heat production is greater than the heat demand. In practice, it is unlikely that a plant operator would turn the CHP on when

there is no heat demand; however, this parameter has been quantified to estimate the available CHP heat potential for TES.

There is little difference between the 35 °C network and the 20 °C network besides a decrease in heating HP power and an increase in waste heat and heat losses from the thermal distribution network. The heat losses increased to 95 MWh from 39 MWh in the 20 °C network. The decrease in heating heat pump power results in an annual average COP of 4.51, which is a 26% improvement over the GSHP system. There are also slightly higher losses in the 35 °C network and slightly more shared energy. The amount of shared energy increased because the higher COP of the heating heat pump in the 35 °C system results in more heat being extracted on the heat pump's evaporator (network) side.

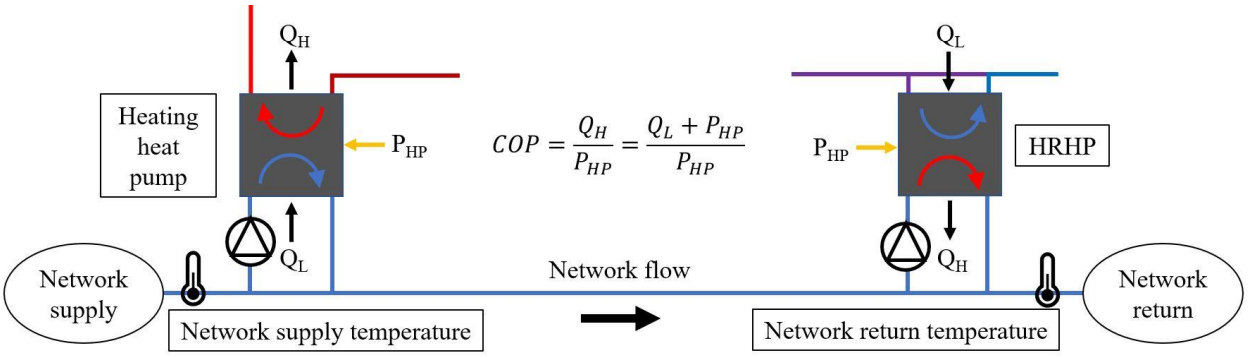

Figure 4.9: Explanation of increased sharing potential caused by a higher heating HP COP.

Figure 4.9 explains this concept in more detail. The COP of the heating HP is a measure of the heat delivered, Q_H, to the electrical power used, P_{HP}. Since Q_H is constant, the same amount of heat is delivered in both the 20 °C and 35 °C systems, the power consumed must decrease for the COP to increase. However, the COP is also related to the heat extracted at the evaporator, Q_L. As the equation in Figure 4.9 shows, for Q_H to remain constant with a lower P_{HP}, Q_L must increase. Therefore, more heat is extracted from the network with increasing heating HP COP. When more heat is extracted from the network, the HRHP (which transfers recovered heat into the network)

can recover more heat from the chiller cooling water, thus increasing the sharing. As explained in section 3.3.3, the HRHP controller calculates the heat transfer rate to the loop using the specified network return temperature. When the network return temperature decreases, due to more heat being extracted from the network, there is more potential for the HRHP to recover heat.

Lastly, the 70 °C network substitutes a heat exchanger in place of the heating heat pump, eliminating a heating energy supply source. This loss of energy is made up for by an increase in heating supplied by the EMC. Both the boiler and CHP supply more heat over the year and the waste heat increases because of the increased CHP capacity. The energy sharing also increases because more heat is extracted from the network, resulting in more waste heat recovery opportunities, as explained earlier. The higher network supply temperature also leads to an increase in heat losses from the thermal distribution network. The heat losses increased to 223 MWh from 95 MWh and 39 MWh in the 35 and 20 °C systems, respectively.

4.2.2 Cooling heat rejection

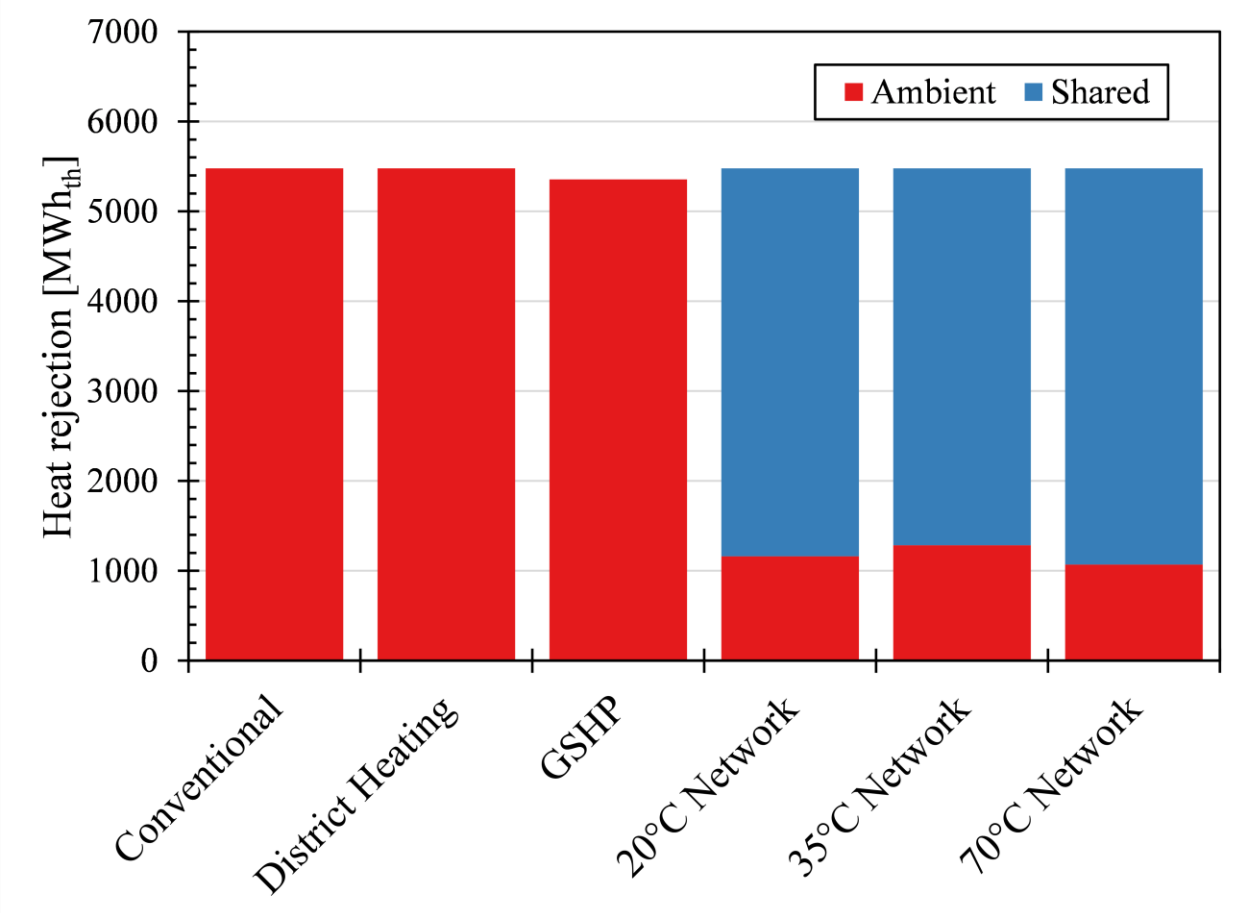

Figure 4.10: Annual total heat rejection in each system divided into heat rejected to the ambient (red) and heat recovered for sharing (blue)

Figure 4.10 shows the annual total heat rejection in each of the six systems. The heat rejection refers to the cooling water line at the building level chillers. Therefore, for the ICE-Harvest system, this is Q_L on the HRHP shown in Figure 4.9, whereas in Figure 4.8, the sharing refers to Q_H of the HRHP. In some systems, the cooling water can only reject heat to the ambient through the cooling tower. In the ICE-Harvest system, however, some of the cooling water heat is harvested in the HRHP. This figure aims to see if it is possible to replace the cooling tower capacity using a HRHP. In the conventional and DH system, the condenser heat is rejected to the ambient through the cooling tower.

The conventional and DH systems reject the same amount of heat because they have the same chiller water systems with the same CHWS and cooling water return temperatures. The GSHP system rejects slightly less heat because the GSHP has a higher cooling COP than the other systems. The heat in the GSHP system is rejected to the geothermal borehole field rather than a cooling tower like in the conventional and DH system. This heat is used to increase the geothermal borehole field's soil temperature to minimize the thermal drift. The ICE-Harvest systems can use the rejected heat for energy sharing when there is a heating demand, reducing the amount of heat sent to the ambient. The 35 °C network system has the least amount of energy recovered for sharing; however, Figure 4.8 shows increased shared energy over the 20 °C network system. This is because the COP of the HRHP is higher in the 20 °C network than in the 35 °C network. Therefore, the 35 °C network system removes less heat from the building chilled water condenser stream but rejects more heat into the network from the HRHP electrical work. For further clarification, the 35 °C network system uses 322 MWh less electricity than the 20 °C network system in the heating heat pump because of the higher network temperature. However, the 35 °C network system consumes 318 MWh more electricity than the 20 °C network system in the HRHP, making the annual balance appear equal. The 70 °C network system had increased shared heat rejection over the 35 °C system because the heat exchanger removed more heat from the network.

Greater amounts of shared energy lead to less heat being sent to the ambient, reducing the need for heat rejection equipment such as cooling towers, radiators, and dry coolers. None of the ICE-Harvest systems could harvest all the heat despite the buildings' heating load being significantly larger than the cooling load. This is because there are periods when heat rejection is available, but there is no heating load to service. During these periods, TES could potentially store the heat; however, that is outside this research scope.

4.2.3 Electricity supply

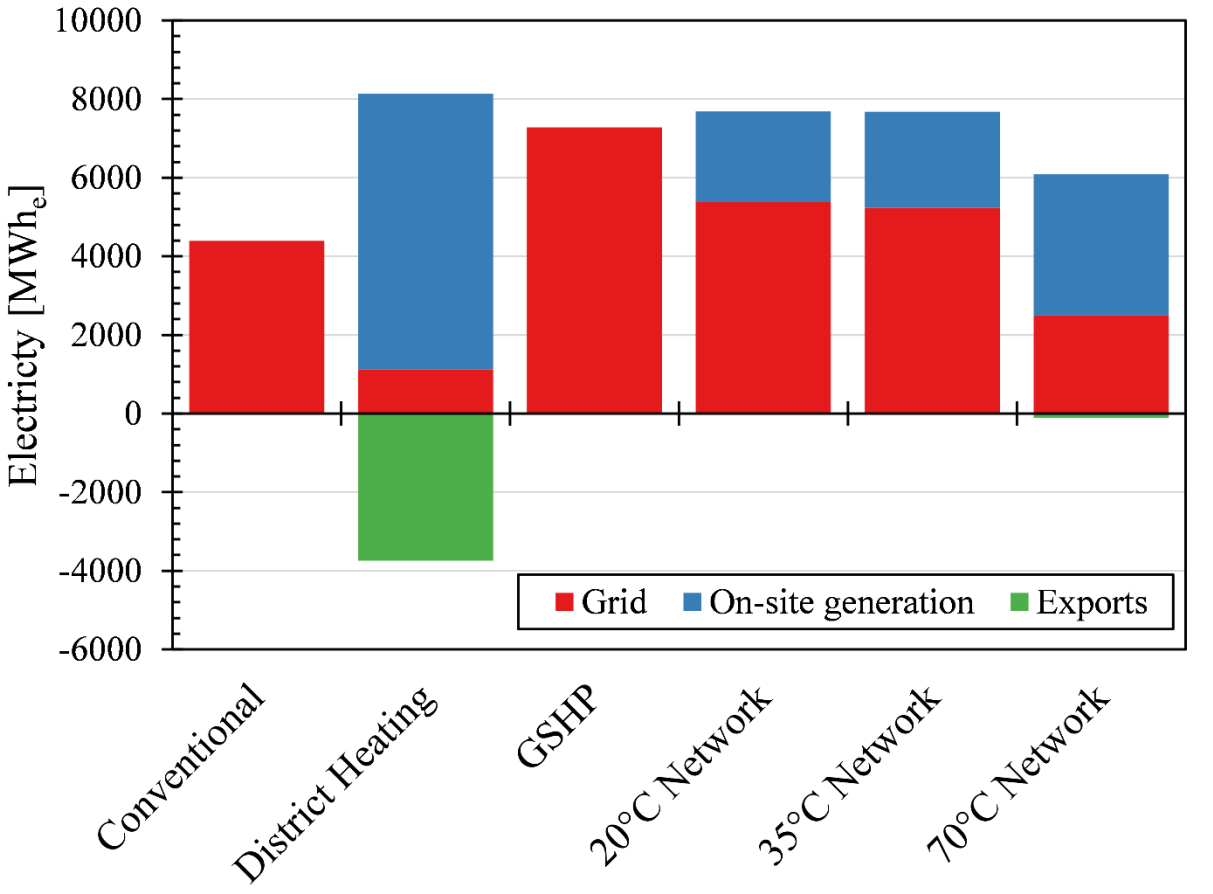

Figure 4.11: Annual electricity supply of each system divided into electricity imported from the grid, exported to the grid, and generated on-site

Figure 4.11 shows the annual electricity supply in each of the six systems. The conventional and GSHP systems import 100% of the electricity from the grid. The DH and ICE-Harvest systems have on-site power generation from the CHP. When the CHP's electricity supply is greater than the building electricity demands, the system must export electricity. The amount of exported electricity is greatest in the DH system. Since the CHP is operated to follow the thermal demand, the CHP produces both heat and electricity simultaneously even though there might not be corresponding electricity demand. This can be problematic for electricity system operators because the supply must be handled by the transmission infrastructure which can overload the local

grid. If the electricity cannot be exported, then the CHP must decrease its output in the absence of a battery, thus reducing the heat supply. To make up for the thermal deficit either a boiler must be used, which will increase the emissions, or a TES must be discharged. Therefore, systems that do not export electricity are preferred to systems that export electricity. While the ICE-Harvest system does export some electricity, it is considerably less than the DH system. The amount of on-site generation and exports increases with increasing network temperature in the ICE-Harvest system because the CHP capacity increases with higher network temperatures.

4.2.4 Electricity demand

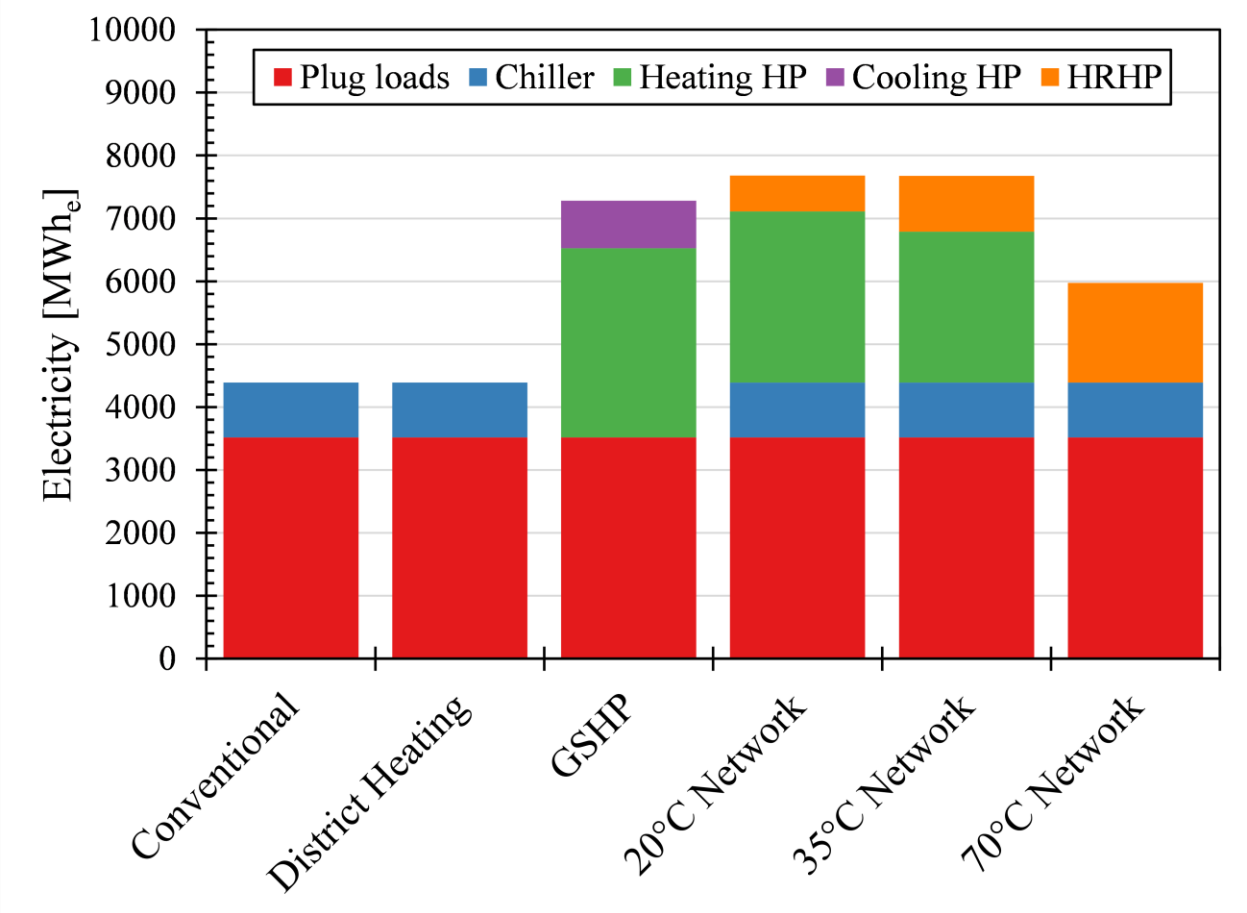

Figure 4.12: Annual electricity demand of each system divided into electricity demands for the plug loads (red), the chiller (blue), the heating heat pump compressor work (green), the cooling heat pump compressor work (purple), and the HRHP (orange).

Figure 4.12 shows the annual total electricity demand in each of the six systems. The red bar shows the plug loads of the buildings, which are constant for each system. The chiller electricity demand, shown in blue, is the same in the conventional, DH, and ICE-Harvest systems because the building chilled water systems are identical and have the same COPs. The GSHP replaces the chiller with a cooling GSHP and electrifies the heat supply using a heating GSHP. The heating GSHP uses significantly more electricity than the cooling GSHP totalling 3011 MWh and 753 MWh, respectively. The heating GSHP delivers 10808 MWh of heat, resulting in an average COP of 3.6, and the cooling GSHP delivers 4602 MWh of cooling resulting in an average COP of 6.1. The electricity demand increases from 4391 MWh in the conventional system to 7279 MWh in the GSHP system.

The 20 °C and 35 °C ICE-Harvest systems have electricity demands for the chiller, the heating HP, and the HRHP. In the 20 °C system, the heating HP consumes 2720 MWh of electricity, 291 MWh less than the GSHP system. However, the total electricity demand is greater than the GSHP system because of the electricity consumed by the HRHP. The HRHP does not use much electricity because the network's low temperature creates a high COP for waste heat recovery. While the HRHP does not heat or cool the building directly, it contributes by reducing the heat required from the CHP and boiler and reducing the heat rejected to the ambient.

The 35 °C system has a comparable total electricity consumption to the 20 °C system, totalling 7675 MWh and 7680 MWh, respectively. However, the differences appear in the proportions of electricity used by the heating HP and the HRHP. The 35 °C system uses less electricity in the heating HP but more electricity in the HRHP for waste heat recovery showing the trade-off between network temperature and electricity consumption. As the network temperature increases, the COP of the heating HP increases, decreasing the electricity consumption for heating.

Conversely, the COP of the HRHP decreases, increasing the electricity consumption for waste heat recovery. As explained in section 4.2.1, this created an interesting scenario where the amount of heat shared increased but the amount of heat removed from the chiller cooling water decreased. Therefore, increasing the network temperature does not always reduce the need for a cooling tower despite increasing the heat delivered by sharing.

The 70 °C ICE-Harvest system increases the electricity demand to 5975 MWh, a 1584 MWh increase over the conventional. The high-temperature ICE-Harvest system has a lower electricity demand than the other ICE-Harvest systems because there is no heating heat pump electricity demand. This highlights the potential for the ICE-Harvest system to control the electrical demand by changing the network temperature. For example, the 20 °C network and the 70 °C had an annual electricity consumption of 7680 MWh and 5974 MWh, respectively. Therefore, a potential 1706 MWh of electricity can be modified by changing the temperature between 20 °C and 70 °C representing a large potential for demand management, which could benefit electricity system operators. Commercially available heat pumps are rated for temperatures of 10 to 32 °C for heating and cooling [119], and heat exchangers could be installed for direct heating at higher temperatures. Therefore, there is no technical reason that the network cannot be operated across such a wide temperature range, and the designer of the system should explore the benefit of such operation.

4.2.5 Hourly electricity demands

4.2.5.1 Annual

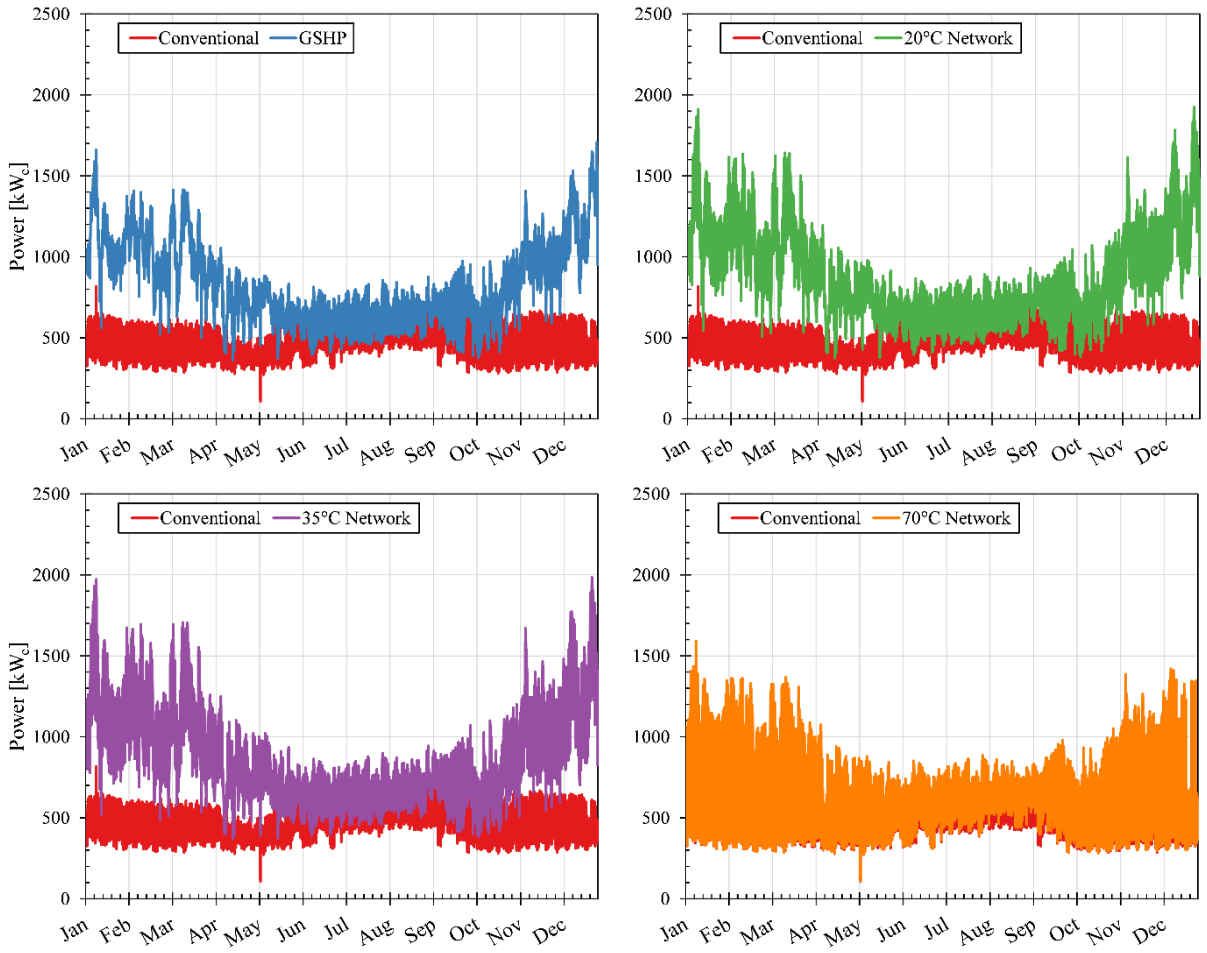

Figure 4.13: Hourly electricity demands of each system divided into conventional (red), GSHP (blue), 20 °C network (green), 35 °C network (purple), and 70 °C network (orange). The district heating system is excluded because the hourly electricity demand is identical to the conventional system.

Figure 4.13 shows the hourly electricity demands of four different systems compared against the conventional system, which serves as the baseline for comparison. The conventional system hourly electricity demand is relatively level throughout the year with high-frequency daily fluctuations and a low amplitude annual frequency. The electricity demands peak during the summer months due to an increase in the cooling demands. Taking the annual average electricity demand (501 kW) as the base, the conventional system has a peak above the base of 422 kW. The

peak above base measurement estimates the electrical power generation capacity required to meet the peak demand. Systems with a lower peak above base require less capacity to meet their electricity demands.

Table 4.4: Summary of hourly electricity demands of simulated systems

System	Average [kW]	Peak [kW]	Peak above base [kW]
Conventional	501	923	422
GSHP	831	1708	878
20 °C network	877	1926	1049
35 °C network	876	1986	1110
70 °C network	682	1592	910

Table 4.4 summarizes the average, peak, and peak above base electricity demands in each simulated system. The GSHP system increased the average electricity demand by 66% and the peak electricity demand by 85%. The phase of the annual electricity demand also shifted, resulting in a winter peak demand rather than a summer peak demand, as seen in the conventional system. This is because the heating demands of the buildings in this study are much greater than the cooling demands. Therefore, transitioning to a GSHP system would result in 85% greater electricity demand capacity and 66% greater average electricity demand. The 20 °C and 35 °C network systems have a similar effect on the hourly electricity demand. These systems increase the average electricity demand by 75% and increase the peak electricity demand by 109% and 115%, respectively. Also, both systems shift the peak electricity demand from the summer to the winter. Therefore, the 20 °C and 35 °C network considerably increase the average electricity demand and peak electricity demand. The 70 °C has the lowest average and peak electricity demand increase over the conventional system of the four systems considered. This is because the 70 °C network system uses a heat exchanger instead of a heat pump, reducing the electricity demand during the winter. In conclusion, the 70 °C network increases the average electricity demand by 36% and the

peak electricity demand by 66%. The next section will show the electricity demands for a single winter day.

4.2.5.2 Winter

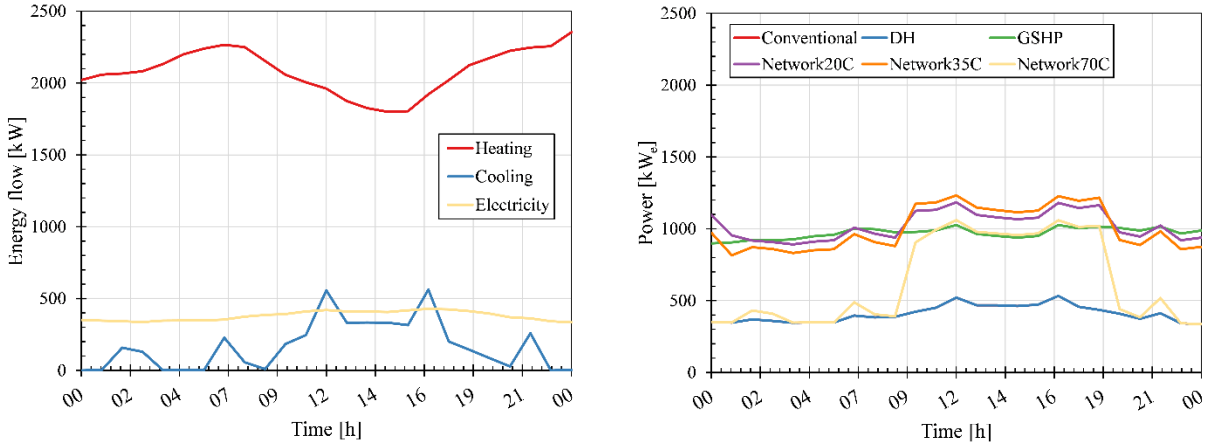

Figure 4.14: Hourly heating, cooling, and electricity demands for a winter's day (left). Hourly electricity demands of each system (right)

Figure 4.14 shows the hourly heating, cooling, and electricity demands on the left and the corresponding hourly electricity demands for each system on the right. Both plots are for the same 24 hour period during the winter. Looking at the left figure, the heating demands are high and there is an intermittent cooling demand that peaks towards the middle of the day. The electricity demand (which consists of all electricity demands minus electricity used for cooling equipment) is relatively flat throughout the day. Looking at the right figure, the conventional and DH electricity demands are identical; thus, the two curves overlap. The electricity demand for both of these systems has intermittent spikes throughout the day in response to the building cooling demands. The GSHP system has a higher average electricity demand as electricity is used to provide heating and cooling through the heat pumps.

The ICE-Harvest systems have significantly different hourly demand profiles depending on the network temperature. The 20 °C and 35 °C network systems have similar demand profiles

to the GSHP system when the demand is heating dominant. However, when the cooling demand increases, the ICE-Harvest system has a higher electricity demand because the HRHP turns on to inject recovered heat into the network. The increase in electricity demand contributes to reducing the heat required from the EMC due to energy sharing. Therefore, the 20 °C and 35 °C network systems have the highest average electricity consumption during this winter day. The 70 °C ICE-Harvest system has the same electricity demand as the conventional and DH systems when there are only heating demands in the network. The electricity demand increases whenever there is cooling because of the HRHP. During the peak cooling period of this day (approx. 9 AM-7 PM), the electricity demand of the 70 °C network system increases to a level comparable to the GSHP system.

Comparing the 20 °C network system at 0 hr to 8 hr and 19 hr to 24 hr profiles with the 70 °C 8 hr to 19 hr profile demonstrates the potential to level the electricity demands of the ICE-Harvest system during the winter season by changing the network temperature in response to the building energy demands. By removing the peaks and valleys from the electrical demand, the ICE-Harvest system will contribute to levelling the electrical grid. Also, by increasing the electrical demand at night by lowering the network's temperature, the ICE-Harvest systems can be used for demand management. This is beneficial to electricity system operators because large electrical demand peaks require a large reserve capacity to service. If the peaks only occur for a short period each year, the asset remains idle for the remaining time. Likewise, valleys create a problem where renewable generators must be curtailed (ordered to bypass power generation) from the grid resulting in renewable generators shutting down. Currently, curtailment amounts to 22% (2,581 GWh) of Ontario's annual electrical demand, and it mainly occurs during winter nights and

shoulder seasons [7]. The ICE-Harvest system can use this power by adjusting the network's temperature according to the availability of renewable energy resources.

4.2.5.3 Summer

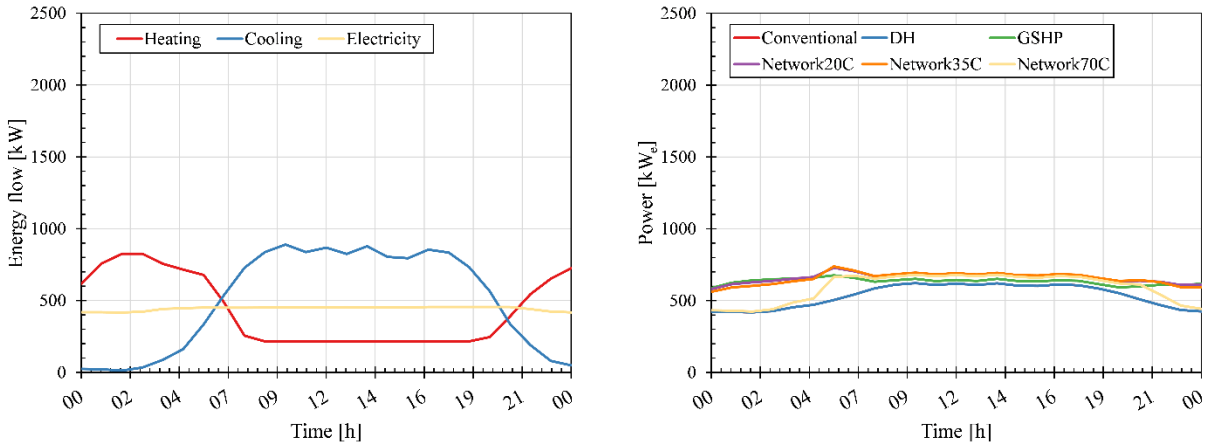

Figure 4.15: Hourly heating, cooling, and electricity demands for a summer's day (left). Hourly electricity demands of each system (right)

Figure 4.15 shows hourly heating, cooling, and electricity demands on the left and the corresponding hourly electricity demands for each system on the right. Both plots are for the same 24 hour period. Looking at the left figure, the cooling demands are high and rise from 0 kW to 900 kW over 7 hours, where they remain near constant from 9 AM to 9 PM before decreasing back to near zero by midnight. There is also an overnight heating demand that decreases towards mid-day before reaching a constant minimum for domestic hot water, then rising again in the evening and into midnight. The electricity demand is fairly constant throughout the day. Looking at the right figure, the electricity demands are fairly similar across all systems. The electricity demand in the conventional and DH systems are identical. The electricity demand in the GSHP, 20 °C network and 35 °C network are nearly indistinguishable outside of a small increase in the ICE-Harvest systems between 4 AM and 7 AM. The 70 °C network has a similar demand profile to the conventional and DH systems when the heating demand is greater than the cooling demand. The

70 °C network has a slightly higher electricity demand as the cooling demand increases. The differences between each system's electricity demands are not as drastic in the summer as they are in the winter because there is minimal opportunity for energy sharing and the COP of all of the cooling systems are very similar. Therefore, when there is a low potential for energy sharing, possibly due to a lack of simultaneous heating and cooling demands, the ICE-Harvest systems have similar performance to a GSHP system. Also, because the cooling demand is greater than the heating demand during the summer, the EMC does not have to supply heat to the network. Therefore, TES is necessary to use the heat available from gas generators during the summer months.

4.2.6 Annual CO_2e emissions

4.2.6.1 Total

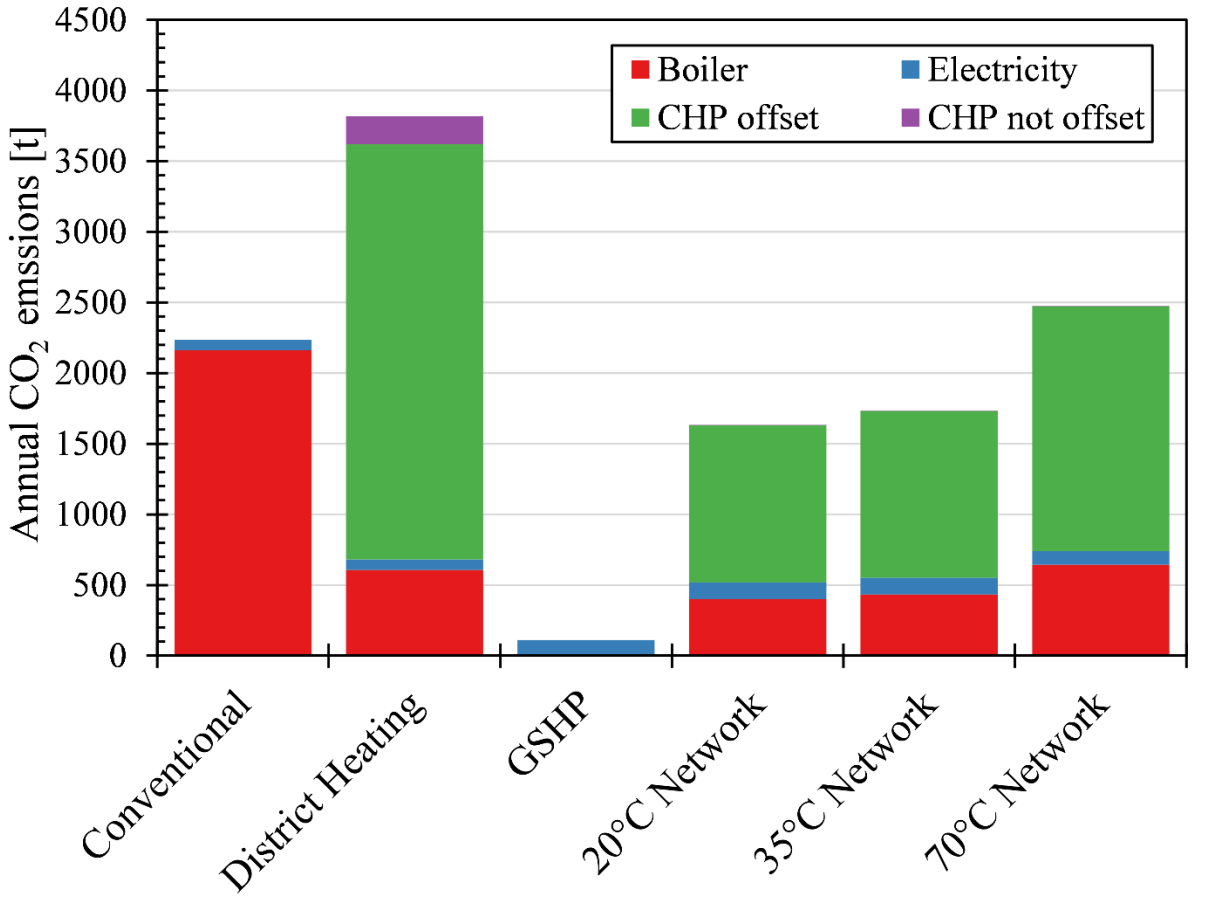

Figure 4.16: Annual total CO_2e emissions of each system divided by boiler (red), electricity (blue), CHP operation during gas generator hours (green), and CHP operation outside of gas generator hours (purple).

Figure 4.16 shows the annual total CO_2e emissions in each of the six systems. In the conventional system, the boiler accounts for most of the total emissions. The boiler is used only for heating purposes. The remainder of the emissions come from the buildings' electricity for plug loads and cooling equipment. In total, the conventional system produces 2234 tonnes of CO_2e per annum. The emissions are calculated using the carbon intensity factors of natural gas for the heating equipment and the Ontario Hourly Average Emissions Factor (AEF) for the electricity emissions. The AEF was assumed to remain constant across all systems despite the electrical

demand changing between the systems. Typically, in Ontario, additional demands at night are managed by hydro whereas additional demands during the day are managed by gas generators. Therefore, additional electrical loads could increase the grid emission factor if they are not coordinated properly. However, modifying the AEF is outside the scope of this research, thus the same hourly AEF is used for all systems.

The DH system has fewer emissions from the boiler than the conventional system because, as shown in Figure 4.8, most of the heat is supplied by the CHP. The CHP has a lower thermal efficiency than the boiler (45% in the CHP vs. 90% in the boiler); therefore, the total emissions are greater when the CHP is used as the primary heat source. The CHP emissions are divided into two categories: CHP emissions that occurred when gas generation was on the grid (offset) and CHP emissions that occurred when gas generation was not on the grid (not offset). For the year simulated in these results (2016), gas generation was abundant on the Ontario electricity grid. Grid level gas generators have approximately the same electrical efficiency as distributed CHP engines. Therefore, if a CHP is operating at the same time as a gas generator, the electrical output of the CHP could be used to offset the gas generator output. The CHP would provide the same electricity, but at a higher total efficiency because the thermal energy from the exhaust can be used for heating rather than being wasted. The emissions coming from the CHP while it is offsetting a gas generator can, therefore, be discounted because the CHP system simply enables the utilization of an otherwise wasted resource. However, this is not to say that the emissions from the increased electricity consumption of the ICE-Harvest system are ignored. All emissions are calculated by multiplying the total electrical demand by the grid hourly emission factor just as before. Only the emissions produced by the CHP when it offsets a gas generator are subtracted because it is assumed

that the CHP is replacing the gas generator and burning the same amount of fuel but with higher utilization.

The GSHP system has the lowest annual total CO_2e emissions because it does not use a fossil fuel-based energy source. The Hourly Emissions Factor in Ontario is very low because of a large baseload generation from nuclear and hydro. Therefore, in Ontario, electricity-based heating systems have much lower emissions than fossil fuel-based systems. The GSHP reduces the annual emissions to 111 tonnes, which is a 95% reduction. The ICE-Harvest systems all have annual total emissions less than the DH system. Most of the emissions come from the CHP; however, it all contributes to offsetting gas generation because the ICE-Harvest control strategy requires that the CHP only operates when there is gas generation on the grid. The boiler accounts for the next largest share of emissions. Both the 20 °C and 35 °C have lower total emissions than the conventional system. They reduce the annual emissions to 1632 tonnes and 1731 tonnes, providing a 27% and 23% reduction, respectively.

4.2.6.2 Excluding CHP that coincides with gas generation

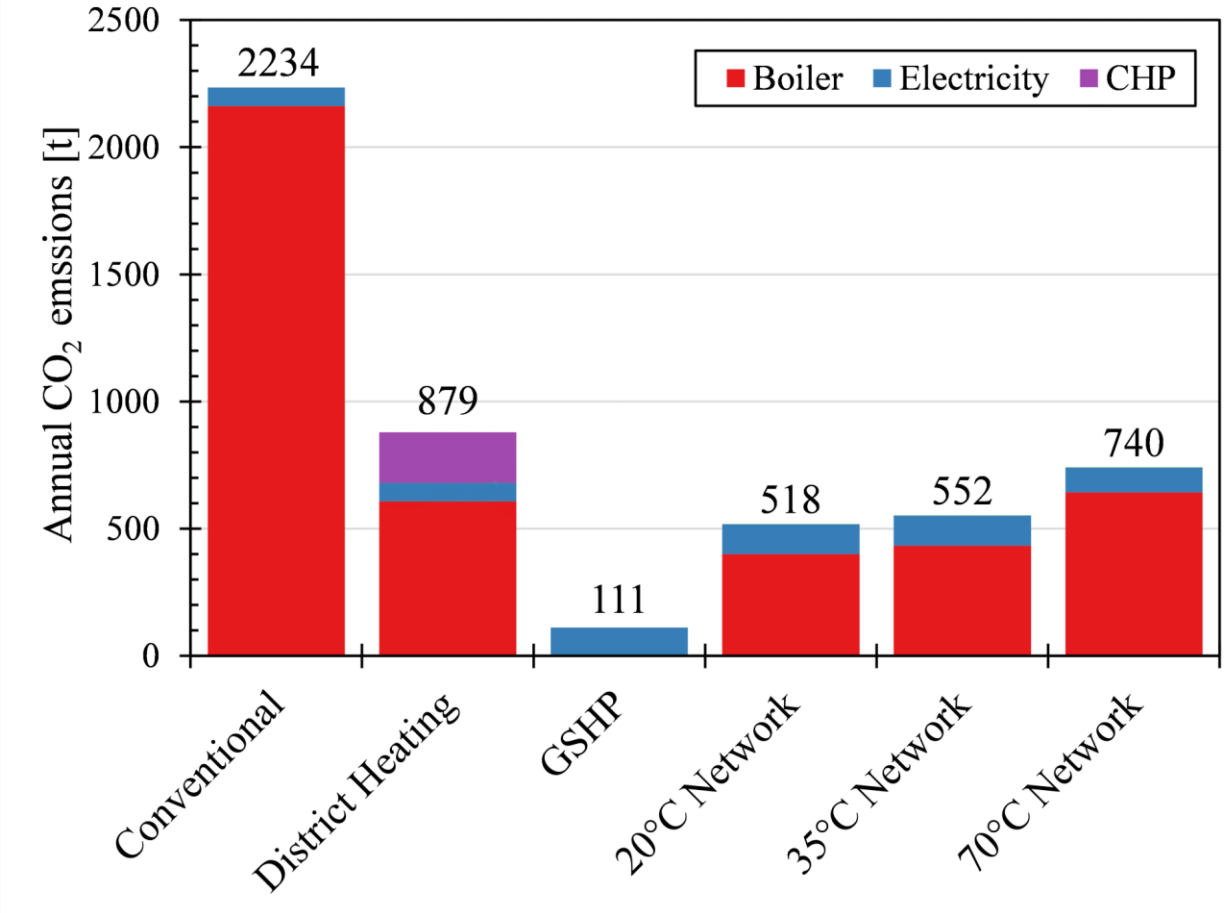

Figure 4.17: 2016 annual total CO_2e emissions of each system divided by boiler (red), electricity (blue), CHP (purple). It does not include emissions produced by the CHP when gas generators are operating.

Figure 4.17 shows the annual total CO_2e emissions in each of the six systems, not including emissions from the CHP when centralized gas generators would have been operating. This figure aims to show the difference in emissions when the CHP is integrated with the electricity market. By recognizing that the CHP can provide the same service as a peak energy provider, which provides intermittent electricity in response to demand fluctuations, the emissions can be discounted when the CHP is used to replace a centralized gas generator. This assumption significantly reduces the emissions of the ICE-Harvest systems, where the CHP only operates when there are gas generators on the grid. Because of this constraint, the CHP emissions are zero,

and the only sources of emissions are the boiler and electricity demand. There are still CHP emissions in the DH system because the CHP does not have the constraint only to operate when there are gas generators on the grid.

Nonetheless, the DH system's emissions decreased from 3818 t to 879 t because, coincidentally, the CHP electricity supply correlated with the grid level gas generator electricity supply. This represents a significant decrease compared to the conventional system, but it depends on the gas generator schedule. The emissions from the GSHP system do not change because there is no CHP in the GSHP system. The ICE-Harvest systems eliminate CHP related emissions because the CHP only operates when there are gas generators on the grid. Therefore, the total emissions are reduced drastically, and the boiler becomes the new largest source of emissions.

4.2.6.3 Annual CO_2e emissions for 2015, 2017, and 2018

For the sake of comparison, Figure 4.19, Figure 4.20, and Figure 4.21 show the annual emissions for the years 2015, 2017 and 2018. As shown in Figure 4.18, 2015 had a similar amount of gas generator run hours to 2016, while 2017 and 2018 had considerably fewer hours. Therefore, according to equation 3.1, the CHP capacity will also vary depending on the number of gas generator hours. The years 2015, 2017, and 2018 have 8528, 3347, and 5413 natural gas generator run hours, respectively. The grid emission factor for each year can be found in Appendix D.

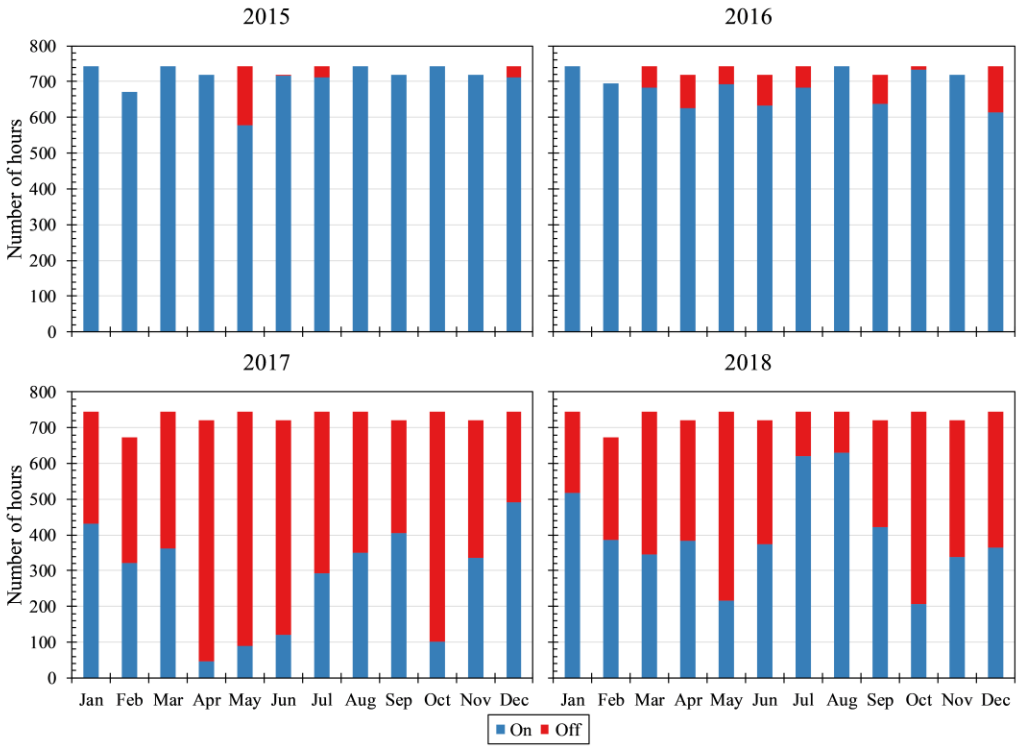

Figure 4.18: IESO gas generator operating hours in Ontario for the years 2015 through 2018.

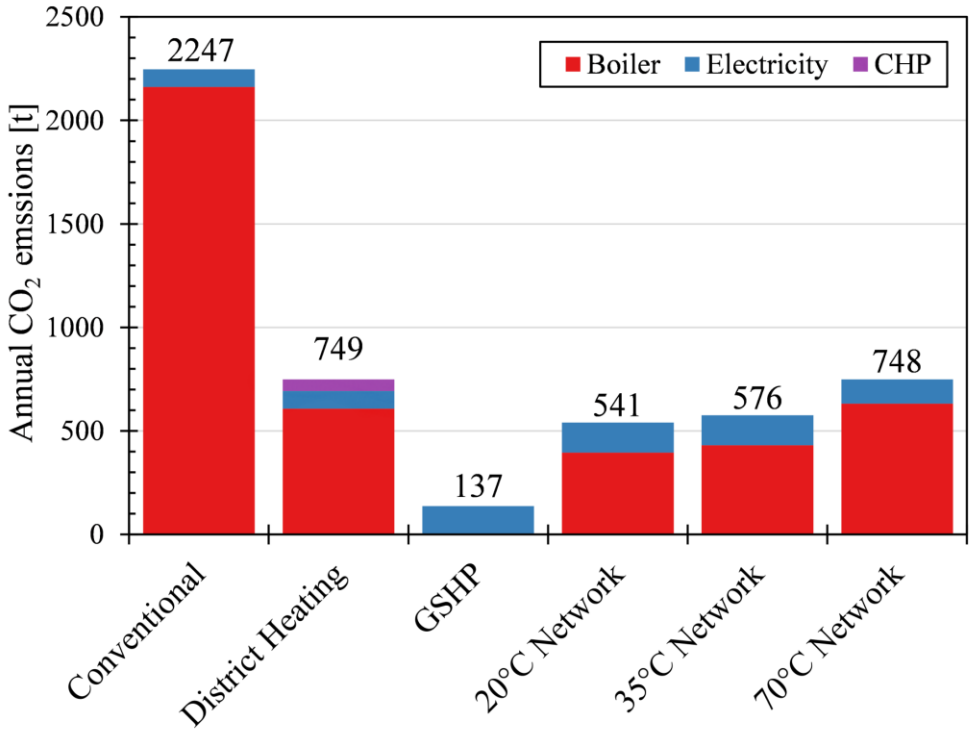

Figure 4.19: 2015 annual total CO_2e emissions of each system divided by boiler (red), electricity (blue), CHP (purple). It does not include emissions produced by the CHP when gas generators are operating.

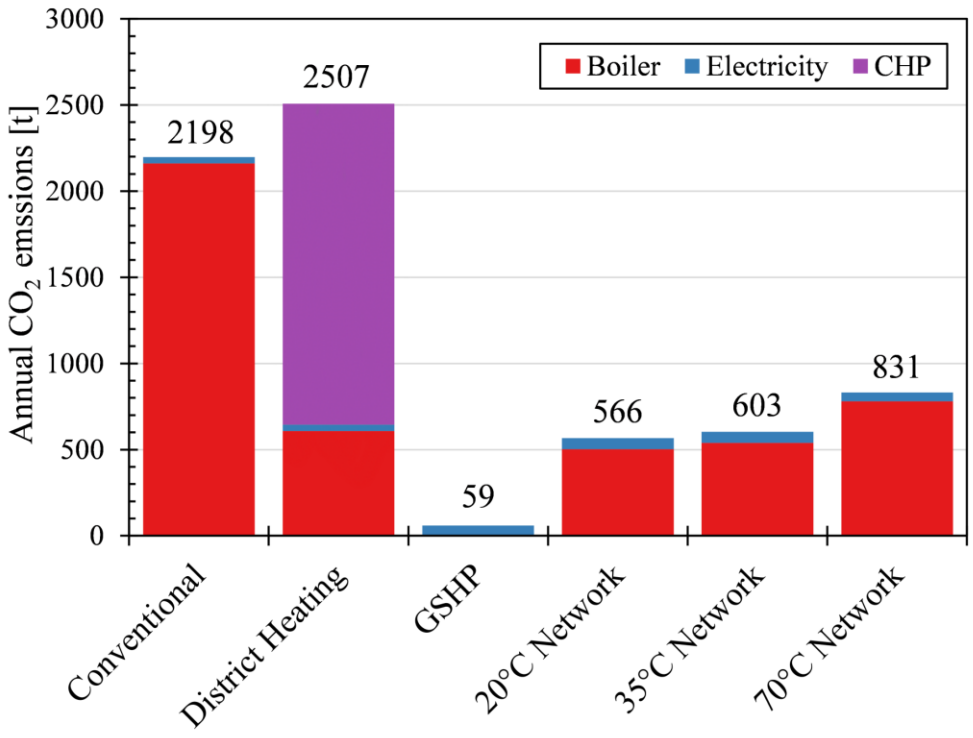

Figure 4.20: 2017 annual total CO_2e emissions of each system divided by boiler (red), electricity (blue), CHP (purple). It does not include emissions produced by the CHP when gas generators are operating.

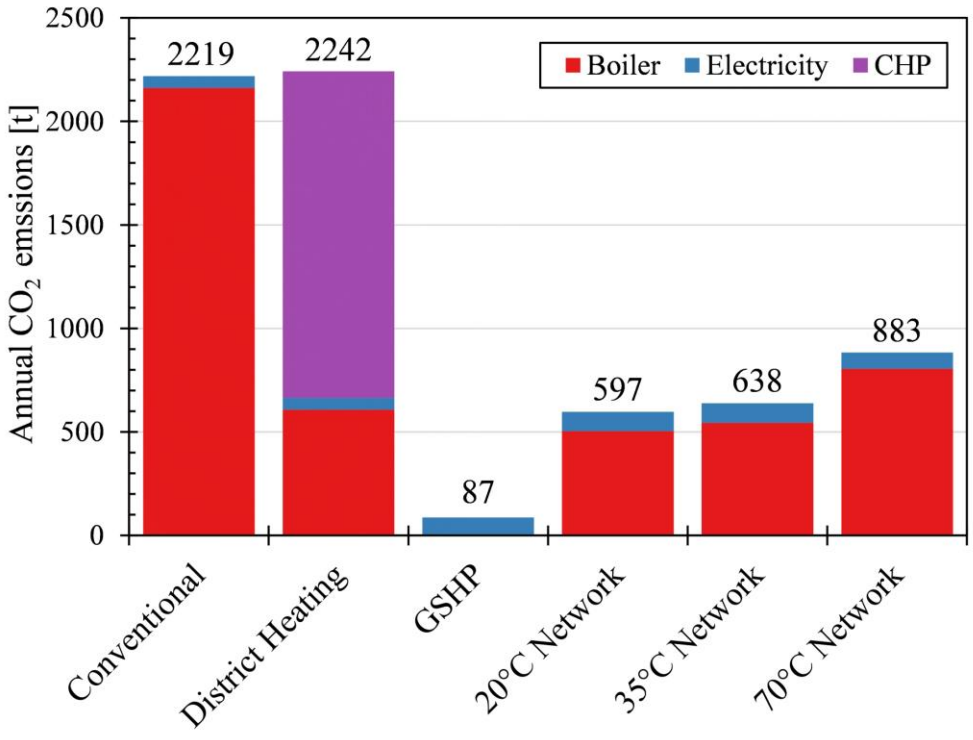

Figure 4.21: 2018 annual total CO_2e emissions of each system divided by boiler (red), electricity (blue), CHP (purple). It does not include emissions produced by the CHP when gas generators are operating.

Comparing Figure 4.17, Figure 4.19, Figure 4.20, and Figure 4.21, the natural gas generator run hours and grid emission factors greatly impact the annual total CO_2e emissions. The conventional system emissions only change slightly as the electrical emissions factor fluctuations are outweighed by a large amount of emissions coming from the boiler. The boiler emissions are constant for every year and insensitive to the changes in the grid emission factor. The district heating system emissions vary from 749 t in 2015 to 2507 t in 2017. This is because 2017 had the fewest gas generator run hours, resulting in considerably fewer CHP emission offsets for the district heating system. The CHP emission offsets were fewer because the CHP is Following the Thermal Load and is not influenced by the grid level natural gas generator operation. The GSHP system emissions vary from 59 t in 2017 to 137 t in 2015. The years of least and greatest emissions are the opposite of the district heating system's lowest and highest emissions because the GSHP produces lower emissions when fewer natural gas generators are operating. Every year the GSHP system offers considerable emissions reductions from the conventional system indicating the benefits of electrifying the heating supply in grids with low emissions factors such as Ontario.

Lastly, the ICE-Harvest system emissions vary from 518, 552, and 740 t in 2016 to 597, 638, and 883 t in 2018 for the 20, 35, and 70 °C network systems, respectively. The boiler emissions were greater in the years when there were fewer natural gas generator hours (i.e., 2017 and 2018). With fewer natural gas generator hours, the CHP has fewer opportunities to provide heat, and therefore more heat must come from the boiler to compensate. The ICE-Harvest system still significantly reduced the emissions during these years, however, because of the use of heat pumps to electrify the heating supply. It is also worth noting that the emissions from electricity consumption amounted to 93, 94, and 78 t during 2018 in the 20, 35, and 70 °C network systems, respectively. These annual total emissions indicate that if the boiler is replaced with a TES that

stores heat from the CHP, the ICE-Harvest system can achieve emissions reductions comparable to or greater than the GSHP system.

4.2.7 Equipment capacities

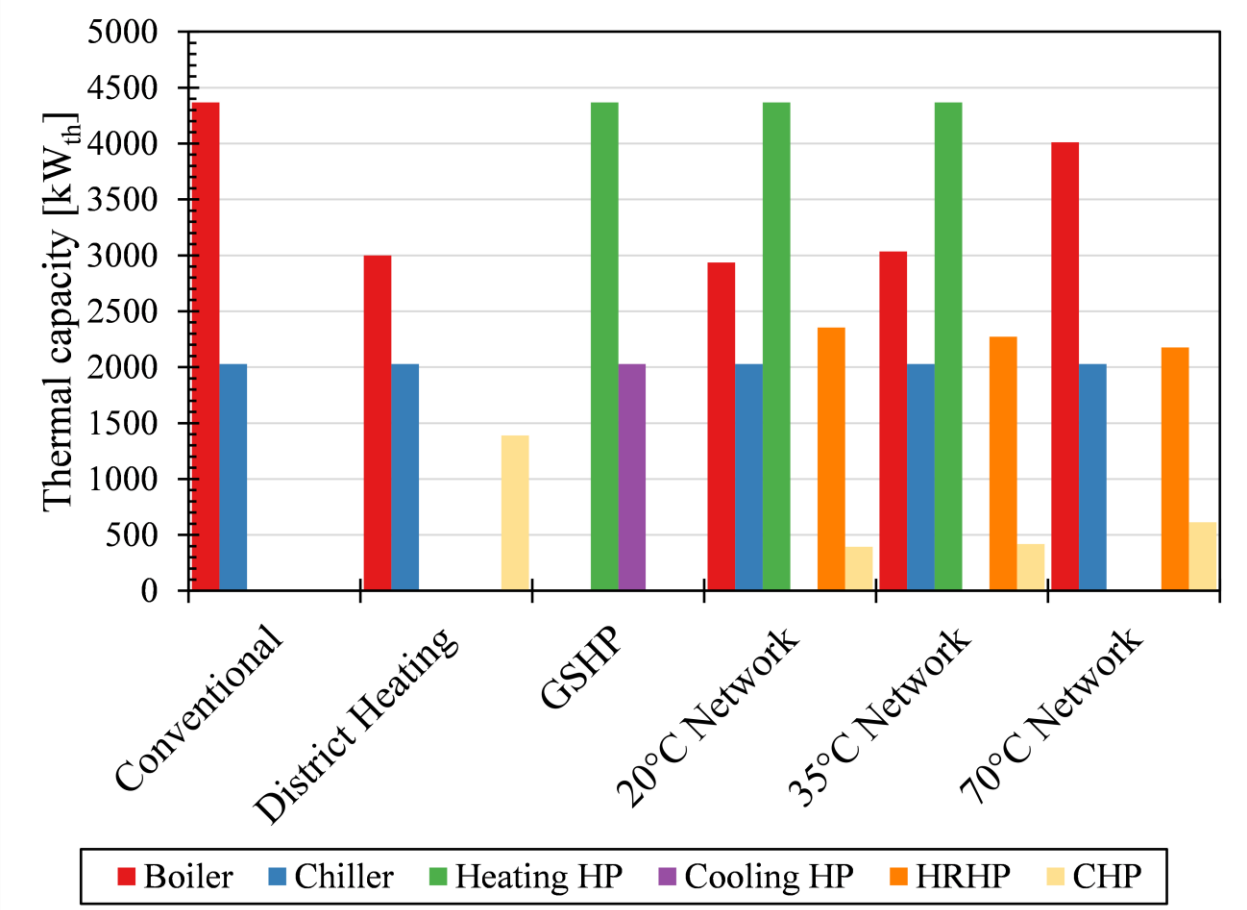

Figure 4.22: Thermal capacities of each piece of equipment of each system divided by boiler (red), chiller (blue), heating heat pump (green), cooling heat pump (purple), HRHP (orange), and CHP (yellow).

Figure 4.22 shows the capacity of each piece of heating and cooling equipment in each of the six systems. The capacity is measured in kW_{th} and it refers to the amount of thermal energy (heating or cooling) that the equipment can deliver. The equipment's capacity is determined by measuring the maximum load the piece of equipment must deliver over the simulation period. To maintain an accurate comparison between equipment that services a single building (ex. individual boilers) and equipment that services a network (ex. CHP), the capacity refers to the maximum

combined load across all the buildings. The conventional system consists of a boiler for heating and a chiller for cooling. The equipment's capacity in the conventional system is equal to the maximum heating and cooling demand is shown in Table 4.2. The DH system has a smaller boiler capacity than the conventional system because the CHP provides additional heat supply capacity. The combined capacity of the boiler and CHP is greater than the boiler capacity in the conventional system. The chiller capacity is the same as the conventional system. The GSHP system has replaced the boiler and chiller of the conventional system with GSHPs. The capacity of the heat pumps is also equal to the maximum heating and cooling demand, respectively.

The ICE-Harvest systems have a more diverse set of generation equipment. The diverse set of generation equipment affords flexibility, but it also introduces numerous redundancies. For example, the ICE-Harvest system has four heat supply sources: the boiler, CHP, heating heat pump, and Heat Recovery Heat Pump (HRHP). In the 20 °C network system, the boiler capacity is less than the conventional and DH systems, but the capacity increases as the network temperature increases. The chiller demand is constant across all network temperatures and it is equal to the conventional and DH systems. The heating heat pump capacity is the same as in the GSHP system and is independent of the network temperature.

The 70 °C network system does not need a heat pump; however, there must be heat exchangers of equivalent capacity installed in the network. The capacity of the HRHP decreases slightly with increasing network temperature. The CHP capacity in all the ICE-Harvest systems is much lower than the DH system. The CHP capacity is calculated by dividing the annual total network heating demand by the number of gas generator run hours for a chosen year. The CHP capacity increases with increasing network temperature because the higher temperature networks have a greater annual total network heating demand. The total network heating demand is greater

because more heat is extracted from the network at higher temperatures, as explained in Figure 4.9. More heat is extracted because the COP of the heating HP increases; therefore, more heat is transferred at the evaporator. When the heat pump is replaced with a heat exchanger, more heat is removed from the network because there is no heat contribution from the compressor work.

4.2.8 System comparison conclusions

In conclusion, the conventional system has the lowest electrical demand, is 100% dependent on electricity from the grid, only receives heat from a boiler, has a low average electricity demand and peak above the base with a summertime peak for cooling equipment, has high annual emissions because of fossil fuel-based heating, and requires equipment to be sized to the peak energy demands.

The DH system has the same electrical demand as the conventional system, has onsite generation from the CHP, exports electricity when the CHP is operated to follow the thermal load, has a low average electricity demand and peak above the base with a summertime peak for cooling equipment, has high annual emissions because of fossil fuel-based heating, and can reduce the capacity of heating equipment but does not affect the capacity of cooling equipment.

The GSHP system increases the electrical demand, is 100% dependent on electricity from the grid, receives heat from the ambient, which requires a geothermal borehole field or lower efficiency air source system, has a high average electricity demand and peak above the base with a wintertime peak due to high heating demands, has low annual total emissions because of the low emission electricity grid in Ontario, and requires the heat pumps to be sized to the peak energy demands.

The 20 °C and 35 °C ICE-Harvest systems have high electrical demands, have onsite generation from the CHP, do not export electricity because of their small CHP capacity, have a high average electricity demand and peak above the base with a wintertime peak due to high heating demands, have low emissions because the CHP reduces boiler usage and operates to intentionally offset gas generators, and have a diverse set of equipment which are sized to meet the demands accordingly.

The 70 °C ICE-Harvest system has a lower electrical demand than other ICE-Harvest systems but higher than the conventional system, has onsite generation from the CHP, occasionally exports a small amount of electricity, has a low average electricity demand peak above the base with a wintertime peak due to energy sharing, has higher emissions because of increase boiler usage due to higher network heating demands, and has a diverse set of equipment.

Table 4.5: Summary of system comparison results

	Conventional	DH	GSHP	20 °C ICE	35 °C ICE	70 °C ICE
Electricity supply	Grid	Grid, CHP	Grid	Grid, CHP	Grid, CHP	Grid, CHP
Electricity exports	N/A	Yes, when CHP follows thermal demand	N/A	Possible, usually none because of small CHP capacity	Possible, usually none because of small CHP capacity	Likely, however, not very much total energy
Electricity demands	Low average, low peak above base, summer peak	Low average, low peak above base, summer peak	High average, high peak above base, winter peak	High average, high peak above base, winter peak	High average, high peak above base, winter peak	Low average, low peak above base, winter peak
Heating supply	Boiler	Boiler, CHP	Heat pump	Boiler, CHP, heat pump	Boiler, CHP, heat pump	Boiler, CHP
Cooling heat rejection	Cooling tower / ambient	Cooling tower / ambient	Ground / ambient	Energy sharing, cooling tower / ambient	Energy sharing, cooling tower / ambient	Energy sharing, cooling tower / ambient
Emissions	High	High, can be lower if CHP offsets gas gen.	Low, can be higher if the power grid is fossil fuel-based.	Medium, CHP offsets gas gen. by design	Medium, CHP offsets gas gen. by design	Medium/high, CHP offsets gas gen.by design
Equipment	Boiler, chiller. Sized to peak	Boiler, CHP, chiller. Diverse heating, cooling sized to peak	Heat pumps. Sized to peak	Boiler, CHP, heat pumps, chiller. Diverse sources for both heating and cooling	Boiler, CHP, heat pumps, chiller. Diverse sources for both heating and cooling	Boiler, CHP, heat pump, chiller. Diverse sources for both heating and cooling

4.3 Storage volume sweep

The results presented in section 4.2 did not include any TES integrated with the ICE-Harvest system. As shown in Figure 4.8, there is a considerable amount of heat wasted (18 to 29% of the total heat demand) in the ICE-Harvest systems when the CHP heat supply does not correspond to the building heat demands. To see how TES can benefit the ICE-Harvest system a series of simulations was performed with varying storage volumes. The motivation behind this exercise is to roughly estimate the volume of storage needed to capture this energy and to quantify the benefits that TES can provide. The TES selected for this application is a water reservoir tank TES. Figure 4.23 shows where the TES is inserted into the header pipe of the generation model.

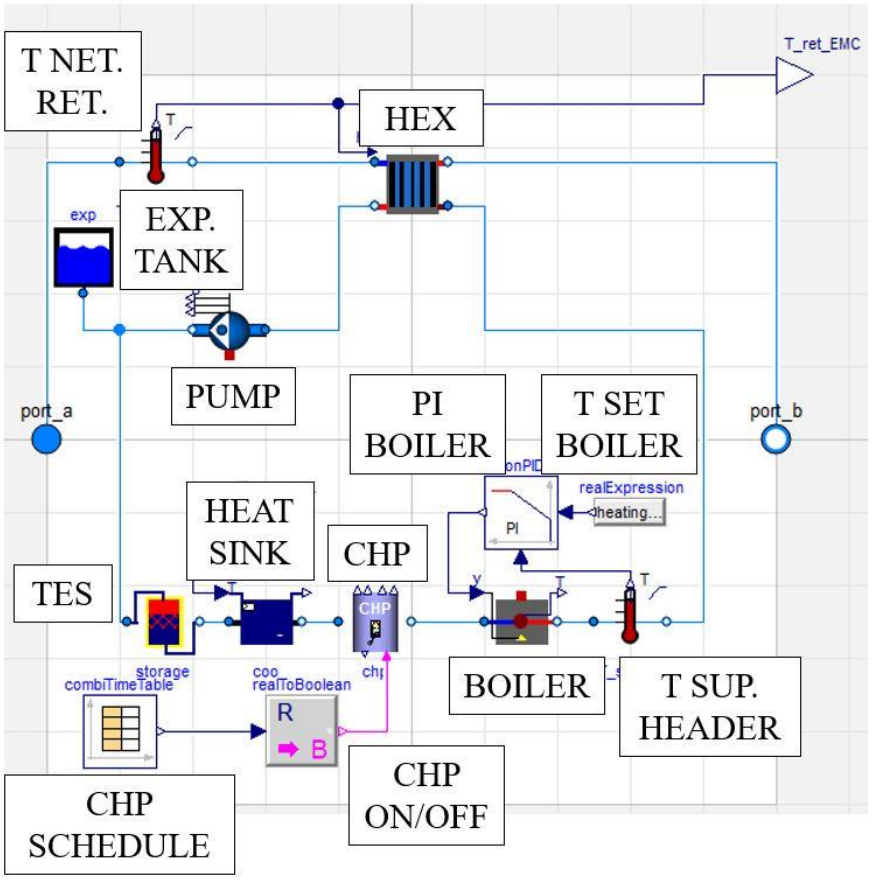

Figure 4.23: ICE-Harvest model. Repeated from Figure 3.8.

The TES is located after the heat exchanger and before the heat sink. Therefore, if there is excess energy after the heat exchanger, the TES will capture it before the heat sink removes it. The TES is also located before the CHP and boiler so that the stored heat will be used first before either piece of heating equipment adds heat. The storage volumes included in the parameter sweep are 1, 10, 100, 1000, 5000, 10000, 20000, and 50000 m^3 water reservoirs. TES is expected to reduce the amount of heat wasted from the CHP and reduce boiler usage. Two new parameters are proposed to capture the impact of adding TES. The first is the Boiler Utilization Ratio (BUR), and the second is the Energy Utilization Ratio (EUR). The BUR is calculated as follows.

$$BUR = \frac{E_{boiler}}{E_{supplied}} \times 100 \tag{4.1}$$

where, E_{boiler} is the annual amount of heat delivered to the system by the boiler [J]

$E_{supplied}$ is the annual amount of heat supplied to the network by the generation model, i.e., the heat transferred across the HEX in Figure 4.23 [J]

If no heat is supplied to the system by the boiler, the BUR is 0%. If all the heat supplied to the system is from the boiler, the BUR is 100%. The EUR is calculated as follows.

$$EUR = 1 - \frac{E_{wasted}}{E_{CHP}} \times 100 \tag{4.2}$$

where, E_{wasted} is the annual amount of heat wasted in the generation model to the ambient [J]

E_{CHP} is the annual amount of heat produced by the CHP [J]

If no heat is wasted from the CHP, the EUR is 100%. If all the heat is wasted from the CHP, the EUR is 0%.

The TES has a fixed aspect ratio of 3, insulation thickness of 6” and ten vertical nodes. The TES is initialized with a uniform temperature distribution at 80 °C.

4.3.1 Boiler Utilization Ratio

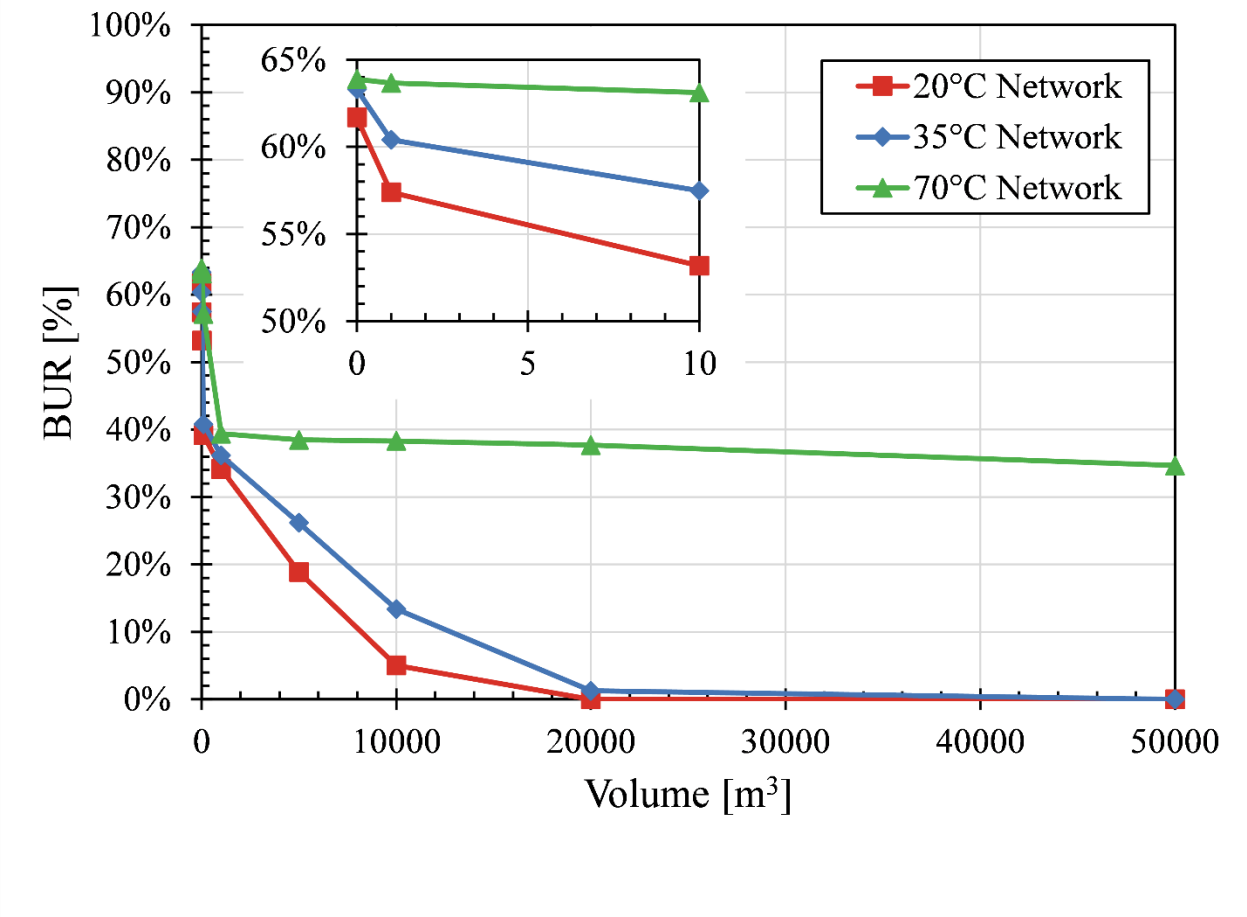

Figure 4.24: BUR versus storage volume (m^3). The points are grouped by network temperature with 20 °C (red), 35 °C (blue), and 70 °C (green).

Figure 4.24 shows the BUR versus storage volume in m^3 for each network temperature under investigation. The BUR is a measure of the quantity of energy supplied by the boiler to the buildings in an ICE-Harvest system. Lower BUR values correspond to lower annual emissions in ICE-Harvest systems. Without TES, each system has a BUR from 60% to 65%. Higher network temperatures have greater BURs, agreeing with the results presented in Figure 4.8. The 20 °C network has the greatest reduction in BUR per unit of storage volume. Just 10 m^3 of storage volume reduces the BUR from 62% to 53%. The BUR reaches 0% with a storage volume of 20000 m^3; however, because the storage volumes are arbitrarily selected, the exact volume needed to achieve

a 0% boiler reduction could be anywhere between 10000 and 20000 m^3. The 35 °C network follows a similar trend to the 20 °C network. The reduction in BUR per unit volume is less than the 20 °C network. For example, a storage volume of 10 m^3 reduced the BUR from 63% to 57%, a 6% reduction versus the 9% reduction in the 20 °C network system for the same storage volume. The BUR reaches 0% with a storage volume of 50000 m^3. The BUR is near 0% at 20000 m^3 (1%); therefore, the minimum volume required to achieve a BUR of 0% is likely closer to 20000 m^3 than 50000 m^3.

The 70 °C network system behaves differently from the other two systems. In the 70 °C network system the BUR plateaus between 30% and 40%, where it hardly changes for large increases in TES volume. The BUR plateaus in the 70 °C network system because the TES discharge temperature setpoint is greater than the boiler temperature setpoint from January to May. The TES top and bottom temperature can be seen in Figure 4.25.

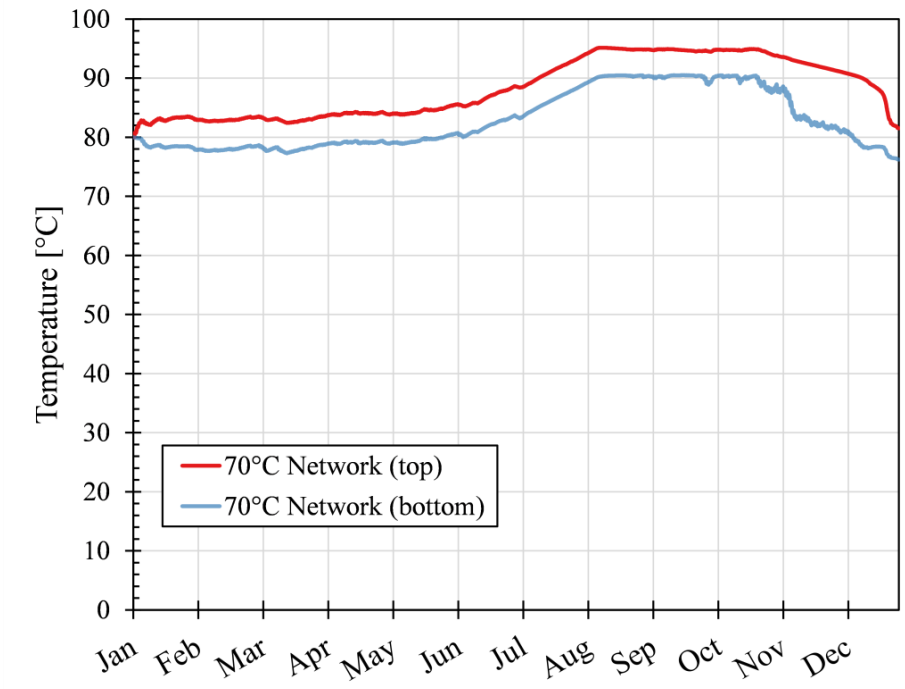

Figure 4.25: Hourly TES temperatures for one year measured at the top and bottom of the tank for the 70 °C network system. The TES volume is 50000 m^3.

As explained in section 3.3.1, the TES discharge temperature setpoint is the minimum of the EMC header supply temperature and the TES top temperature minus the minimum temperature difference (5 °C). Therefore, with an initial storage temperature of 80 °C, the TES discharge temperature setpoint is 75 °C. The boiler temperature setpoint is determined by the minimum allowed temperature difference between the EMC header and network return temperatures. For all systems, the minimum allowed temperature difference is 10 °C. Therefore, when the network temperature is 70 °C, the minimum EMC header temperature, and thus the boiler temperature setpoint, is 80 °C. Since the boiler setpoint is greater than the TES discharge temperature the boiler has priority in providing heat to the EMC header, increasing the boilers utilization. The boiler retains this priority until June when the TES top temperature exceeds 85 °C and the TES discharge setpoint becomes 80 °C.

This problem could have been solved with a different control strategy for the 70 °C system simulations with large storage volumes. For example, the TES controller's minimum temperature difference could have been decreased to encourage the storage to discharge before the boiler turns on. However, for the sake of consistency throughout the parameter sweep, the control strategy was kept constant across all of the systems and storage volumes. The result is important because it highlights the difficulties in controlling a TES across various temperature levels and storage volumes.

4.3.2 Energy Utilization Ratio

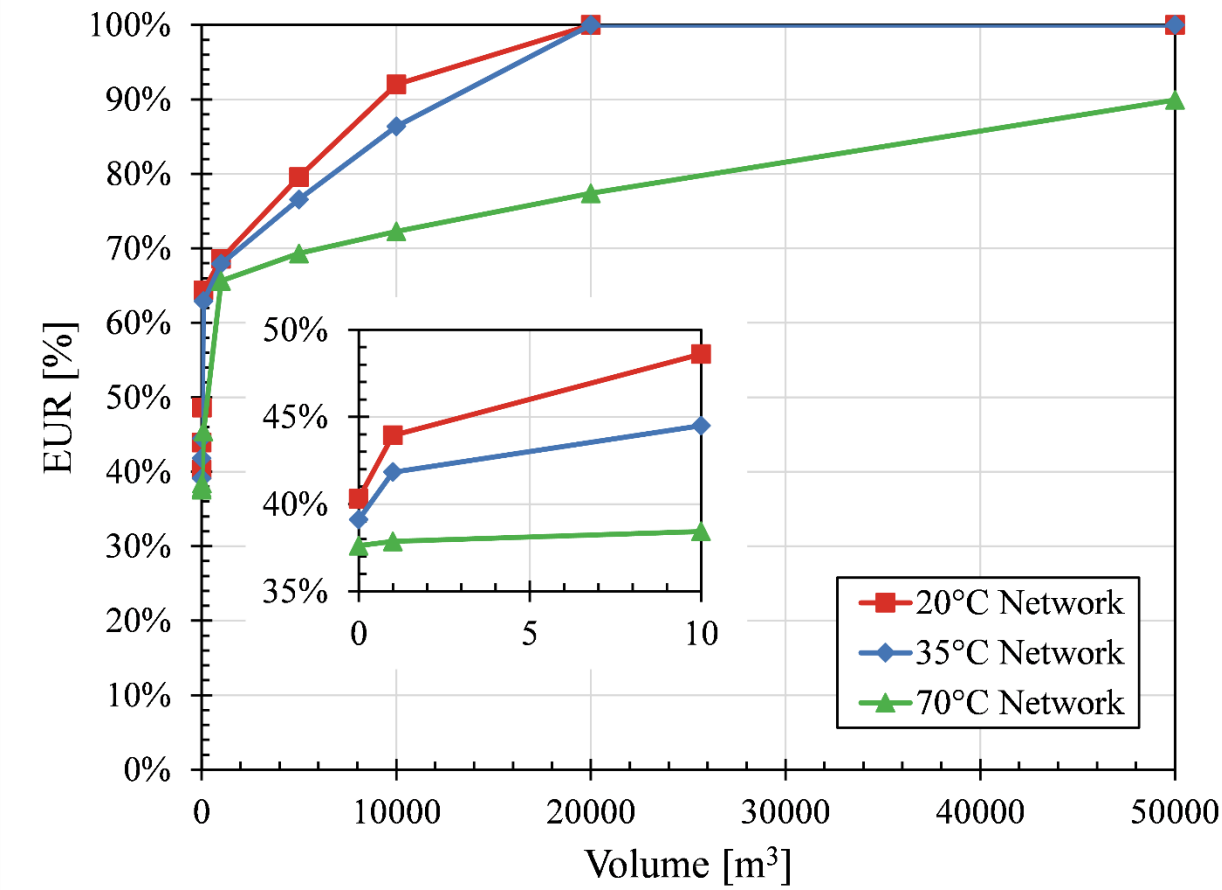

Figure 4.26: EUR versus storage volume (m3). The points are grouped by network temperature with 20 °C (red), 35 °C (blue), and 70 °C (green).

Figure 4.26 shows the EUR versus storage volume in m^3 for each network temperature under investigation. The EUR is a measure of the utilization of heat available from the CHP in an ICE-Harvest system. Higher EUR values correspond to less heat being wasted / unused in ICE-Harvest systems. Without TES, each system has a EUR value from 35% to 40%. Higher temperature networks have lower EURs corresponding to more waste heat coming from the CHP, which agrees with the results presented in Figure 4.8. In the ICE-Harvest systems, the BUR and EUR are inversely correlated. Reduced boiler utilization is a direct consequence of more waste heat being utilized. Therefore, the curves presented in Figure 4.26 have similar characteristics to

those presented in Figure 4.24. The biggest difference between the two figures is in the 70 °C network curve. The EUR for this system does not plateau like the BUR curve does. Therefore, the storage is charging with waste heat, but the heat is not being used to offset the boiler. The explanation for the TES not discharging properly can be found in section 4.3.1.

4.3.3 Annual CO_2e emissions

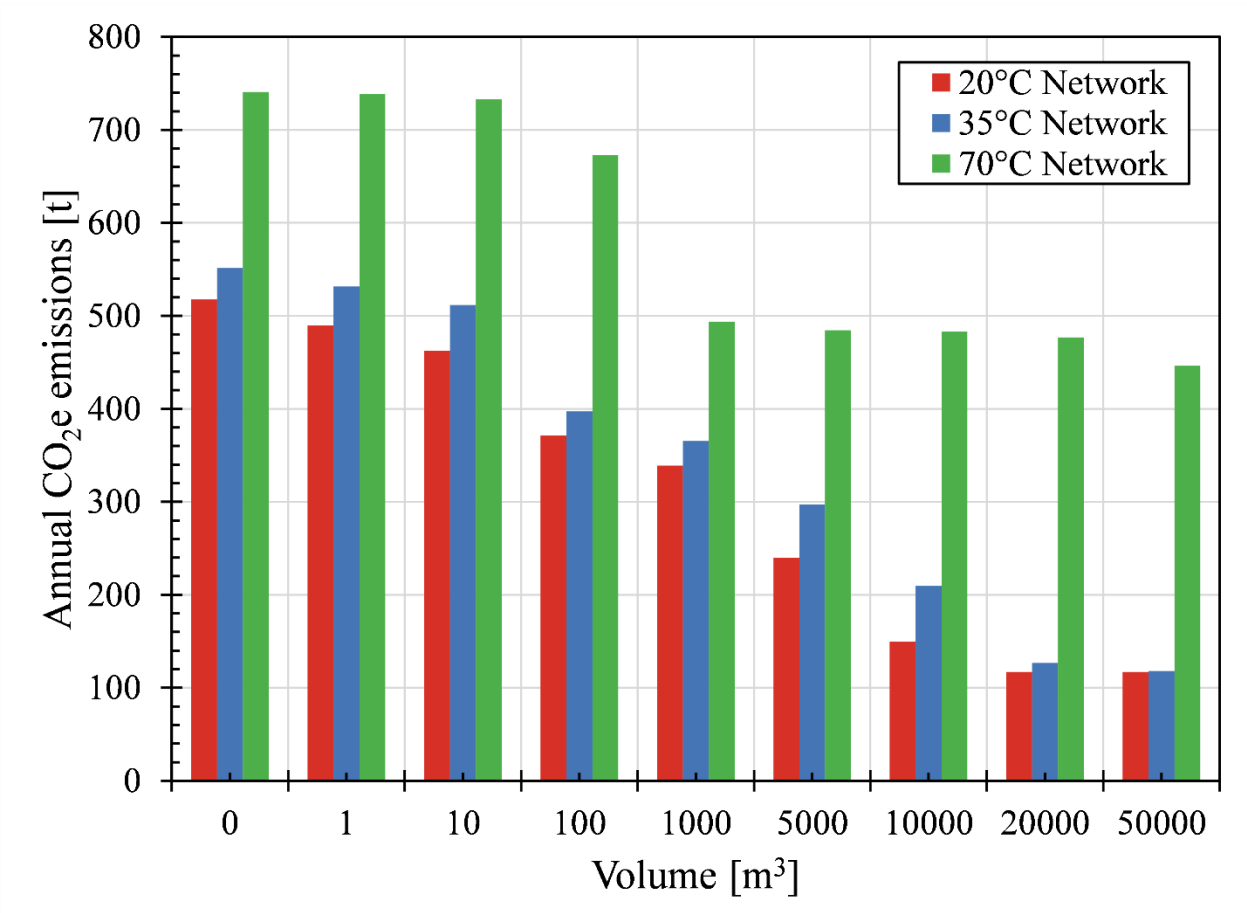

Figure 4.27: Annual total CO_2e emissions in each system versus thermal storage volume (m^3). The bars are grouped by network temperature with 20 °C (red), 35 °C (blue), and 70 °C (green).

Figure 4.27 shows the annual total CO_2e emissions in each system versus the thermal storage volume in m^3 for each network temperature under investigation. Without TES, the annual CO_2e of the 20 °C, 35 °C, and 70 °C network systems are 518, 551, and 741 tonnes, respectively. This agrees with the results presented in Figure 4.17. As expected, the annual CO_2e emissions

decrease with declining boiler utilization. At the largest volume of 50000 m^3, the emissions of the 20 °C, 35 °C, and 70 °C network systems are 117, 118, and 446 tonnes, respectively. As per Figure 4.17, the annual CO_2e emissions of the conventional and GSHP systems are 2234 and 111 tonnes, respectively. Therefore, ICE-Harvest systems that do not require any heat from a boiler, such as the 20 °C and 35 °C systems with large TES, have similar annual CO_2e emissions as GSHP systems and offer a 95% reduction in annual CO_2e emissions over the conventional system.

4.3.4 Storage volume sweep conclusions

The storage volume sweep showed that TES could be used to reduce the boiler utilization, waste heat, and emissions of the ICE-Harvest system. The volume of thermal storage required to eliminate the boiler varies depending on the network temperature because higher temperature networks require more energy and have smaller temperature operating ranges for TES. With very large TES, the ICE-Harvest system's emissions can be reduced to a level comparable with GSHP systems and 95% lower than conventional systems.

Chapter 5

5 Discussion

The discussion section of this research will focus on the ICE-Harvest system's ability to address specific challenges currently facing 5GDHC systems in Ontario. In particular, the objective of the proposed system was to reduce emissions at a provincial level by making use of the heat produced by gas generators, eliminating peaks in the electrical grid, thereby reducing the standby hours for fossil-fuel peaking generators, and introducing energy sharing between buildings to reduce heating and cooling equipment energy consumptions.

5.1 Reducing emissions

The ICE-Harvest system aims to reduce the building sector's emissions by utilizing waste heat from gas generators and building cooling processes. As discussed earlier, the building sector is one of the largest producers of emissions in Canada. Meanwhile, emissions from the electrical sector have been steadily declining due to increased shares of renewable resources. Despite having a sufficient capacity of non-emissive resources, gas generators are still used on the grid to respond to changes in supply and demand quickly. The ICE-Harvest system uses the waste heat produced by gas generators by including it as part of a thermal distribution network.

Even without TES, the ICE-Harvest system offered significant emissions reductions over the conventional system that is currently installed. Most of the conventional system emissions come from the boiler used to deliver heat to the buildings. The boiler is used to produce heat despite an abundance of heat available from grid-level gas generators. Conventional heating systems cannot use this heat because it is not feasible to connect grid-level gas generators to single building heating systems.

Using large scale TES, the ICE-Harvest systems had comparable emissions to the GSHP system. The emissions in the ICE-Harvest system with large-scale TES are produced entirely by the electricity consumed in the system. The amount of electricity consumed in the ICE-Harvest system depends on the COP of the heat pumps used for heat delivery and waste heat recovery. Using different network temperatures, the ICE-Harvest system can control its electrical demand. Controlling the electrical demand is beneficial because the ICE-Harvest system can increase its demand during periods with low hourly emission factors or when there is a curtailment of renewable energy sources and decrease its demand when the hourly emission factor is high. This type of control is not available to GSHP systems because they do not control the soil temperature in the borehole field. This disadvantage leads to significant electrical demand peaks during the winter as the borehole field temperature and thus, COP, decrease. Therefore, wintertime electrical demand peaks are inevitable if more GSHPs are used for heating.

The ICE-Harvest system's ability to control the electrical demand is extremely advantageous in the province of Ontario, where renewable generation is abundant [7]. Using 2016 hourly emission factor data, the ICE-Harvest system reduced the annual emissions by 67% to 77% over the conventional system without TES. With large TES, the annual emissions can be reduced by up to 95%, which is similar to the results shown by the FLEXYNETs project [90]. Therefore, the ICE-Harvest system is a viable option for reducing emissions from the Ontario building sector. It should be noted, however, that these emissions reductions are calculated using the current grid average emissions factor. If the electrical demand is not managed appropriately the electrification of heating will lead to a significant nighttime winter peak approximately 5 to 10 times greater than the current peak demand. If this demand is met using gas generators then there will not be a significant net benefit of using heat pumps for emissions reductions.

5.2 Electrical demand management

One of the greatest advantages of the ICE-Harvest system is the ability to control the electrical demand of the system by changing the network temperature. Electrical grids of the future are looking for ways to integrate more intermittent renewable energy resources into the supply mix. One of the largest barriers to adoption facing these assets today is the variability in their generation. When renewable energy resources are unable to respond to increases in demand, fossil-fuel generation must be used, which is the primary source of GHG emissions on the Ontario electrical grid. When renewable energy resources produce more power than is demanded, the electricity must be curtailed or sold at a loss, which is a waste of clean energy resources.

Demand management affords electricity systems operators the flexibility to control the demand of the market they are servicing. System operators do this by offering incentives to consumers to switch loads on or off at a time that is convenient for the grid. Most electrical demands are not flexible, meaning they do not respond to these incentives. Some of the largest electrical loads come from industrial consumers who cannot afford to halt a process even with significant incentives from the system operator. Fortunately, thermal loads are much more flexible and, therefore are a prime opportunity for demand management.

The ICE-Harvest system proposes the electrification of thermal loads using heat pumps. As shown in Figure 4.13, the ICE-Harvest system's electrical demand is significantly greater than the conventional system at all network temperatures. However, the benefit of electrifying the thermal loads using the ICE-Harvest system is that the demand can be controlled by changing the network temperature. Increasing the network temperature results in lower electricity demands during the winter months. This is because the heating demand is greater than the cooling demand during the winter, and therefore, the benefit of increasing the COP of the heat pumps in heating

mode outweighs the penalty for the heat pumps in cooling mode. Changing the network temperature from 20 °C to 70 °C reduced the wintertime (January to May and October to December) electricity consumption by over 50%. This flexibility is of great value to electricity systems operators as it offers an alternative to electrical energy storage at a much lower cost. Furthermore, demand management strategies can contribute to levelling the electrical demand, which allows for higher capacity factors on baseload generators such as nuclear, hydro, and wind.

For example, in 2016 the peak natural gas consumption used for space heating and domestic hot water reported by Enbridge was 90000 MW and the peak electricity consumption was 22000 MW [120]. Therefore, if space heating and domestic hot water demands are met using GSHPs, assuming an average annual COP of 3, there will be an increase of 30000 MW during the wintertime peak. Historically, peaks have occurred during the summer, however, wintertime peaks of up to 24979 MW have occurred in the past and typically the demand fluctuates from 15000 to 20000 MW during the winter [121]. Therefore, an additional demand of approximately 30000 MW will increase the peak demand to approximately 45000 to 55000 MW which exceeds the current installed capacity of 38600 MW. To meet this demand new generation must be built. Since the heating demands are seasonal, the capacity factor for the generators will not be high enough for nuclear or hydro to be economically viable. Therefore, the demand will likely be met using centralized gas generators. Assuming an average capacity of 500 MW, this amounts to approximately 30 new gas generators in the province [48]. Also, the efficiency of the gas generators is approximately 30% meaning that, if the electricity is used in a heat pump with a COP of 3, the same amount of natural gas will be burned as in a conventional system with a high efficiency boiler or furnace. Therefore, for the electrification of heating to be realized, it is essential that the demand be levelized to allow for emission free, high capacity factor, generation to be used.

5.3 Reducing energy consumption

5.3.1 Energy sharing

The ICE-Harvest system allows for the sharing of energy through the single pipe network design. Energy sharing occurs when the heat that is rejected from one building's cooling process is used to heat another building. Typically, heat rejected from building cooling systems is at too low of a temperature to be used for space heating resulting in it being wasted. However, the ICE-Harvest system allows for energy sharing because both the heating and cooling systems are connected to the same thermal distribution network.

This research focused on a community campus of five buildings, two of which had large cooling demands. These buildings served as excellent sources of waste heat year-round, significantly reducing the heat required from the EMC. As shown in Figure 4.8, the shared energy in the ICE-Harvest system accounted for 48% to 57% of the total heating energy supplied. Therefore, waste heat recovery from space cooling processes can significantly reduce the heating demands of 5GDHC systems. The amount of energy shared increased as the network temperature increased because of the lower COP on the HRHP. As the network temperature increased, the COP of the HRHP decreased, resulting in greater electrical power consumption. While this does increase the electrical demand, the compressor work is still being converted to heat in the compressor; thus, the energy is not wasted. As explained earlier, this allows system operators to control the system's electrical demand using the network temperature by monitoring the ratio of heating to cooling demands in the network. The system operators can run a high temperature when the heating demands outweigh the cooling demands and a low temperature when the cooling demands are greater, thus harvesting more rejected heat.

When TES is integrated with the ICE-Harvest system the amount of heat energy supplied does not increase significantly over the conventional system. The heat stored from the CHP can be used later, which eliminates any wasted heat and allows the boiler to be removed from the system. Depending on the amount of insulation in the TES, the heat losses can be controlled to manageable levels. Also, since the network can be operated at lower temperatures than typical DH systems, the distribution heat losses are very small.

5.3.2 Utilization of waste energy

As shown in Figure 4.10, the ICE-Harvest system is the only system that can use rejected heat from cooling processes. The conventional, DH, and GSHP systems all reject this energy to the ambient, preventing it from being recovered for other purposes. For the buildings considered in this study, that is approximately 5500 MWh of thermal energy each year. With cooling demands predicted to increase in the future, it is very important to make use of this energy. The ICE-Harvest systems can capture up to 80% of the cooling heat rejected in this study. The cooling heat is used in the thermal distribution network to provide heat to other buildings, reducing the fuel consumption of the CHP and boiler. The remaining cooling heat rejection that was not captured occurred when there was insufficient heating demand for sharing. This heat rejection comes from the building space cooling demands during the summer. GSHP system inherently uses this energy as the cooling heat rejected goes towards heating the ground during the summer. An ICE-Harvest system would need either another heat pump to store the heat in the EMC TES or a TES installed in the thermal distribution network to store this energy. As both of these options increase system complexity, it is recommended that ICE-Harvest systems are installed primarily in locations where significant simultaneous heating and cooling demands are present. As space cooling currently only represents 3.4% of Ontario’s energy demand, harvesting energy from space cooling processes has

not been a primary focus [31]. Instead, the ICE-Harvest system focuses on harvesting energy from cooling dominant buildings, such as arenas, grocery stores, and data centers.

5.4 GSHP heat balance

The heat balance of the geothermal borehole field, or borefield, is important for the long-term performance of GSHP systems. Ideally, the amount of heat transferred out of the ground for heating plus the losses to the far-field will be close to the amount of heat transferred into the ground from cooling to maintain a stable ground temperature year over year. If too much heat is extracted from the borefield, as is the case in heating demand dominate buildings, the ground temperature will decrease, thus decreasing the COP of the GSHP. Likewise, if too much heat is transferred into a borefield, the temperature will increase, and the cooling performance will suffer.

Figure 5.1 through Figure 5.5 plots the heat added, heat removed, and heat balance of each building in the study. The heat added to the borefield (from building cooling processes) is shown in red, the heat removed from the borefield (from building heating processes) is shown in blue, and the heat balance (heat added minus heat removed) is shown in green. Ideally, the GSHP systems would be simulated for multiple years to allow the far-field losses to stabilize. However, this research only considers the first year of operation.

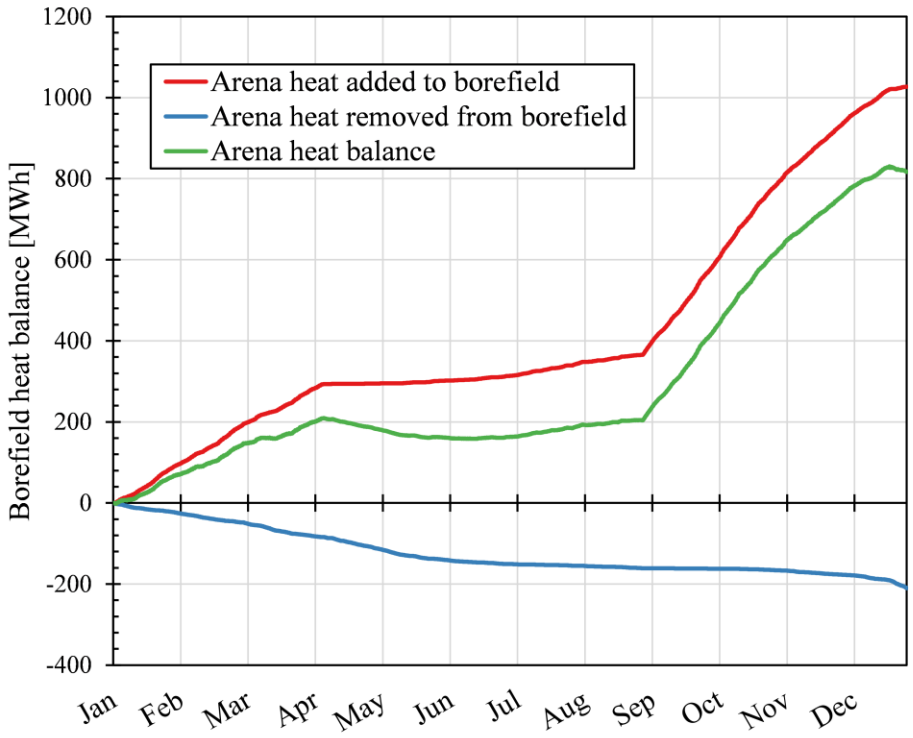

Figure 5.1: Arena geothermal borefield cumulative heat balance [MWh] vs. time.

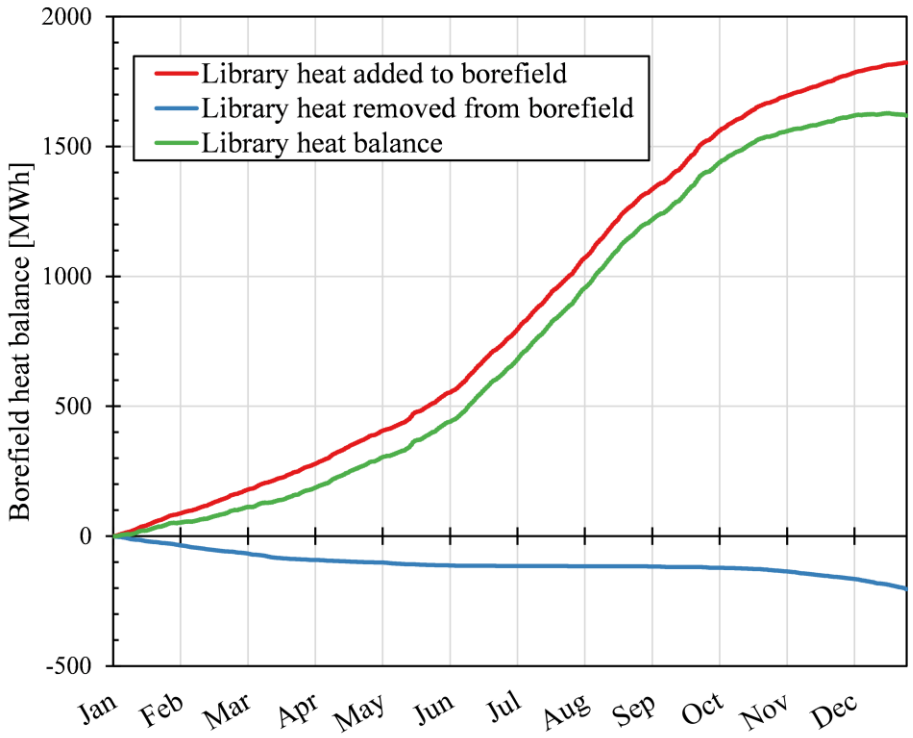

Figure 5.2: Library borefield cumulative heat balance [MWh] vs. time.

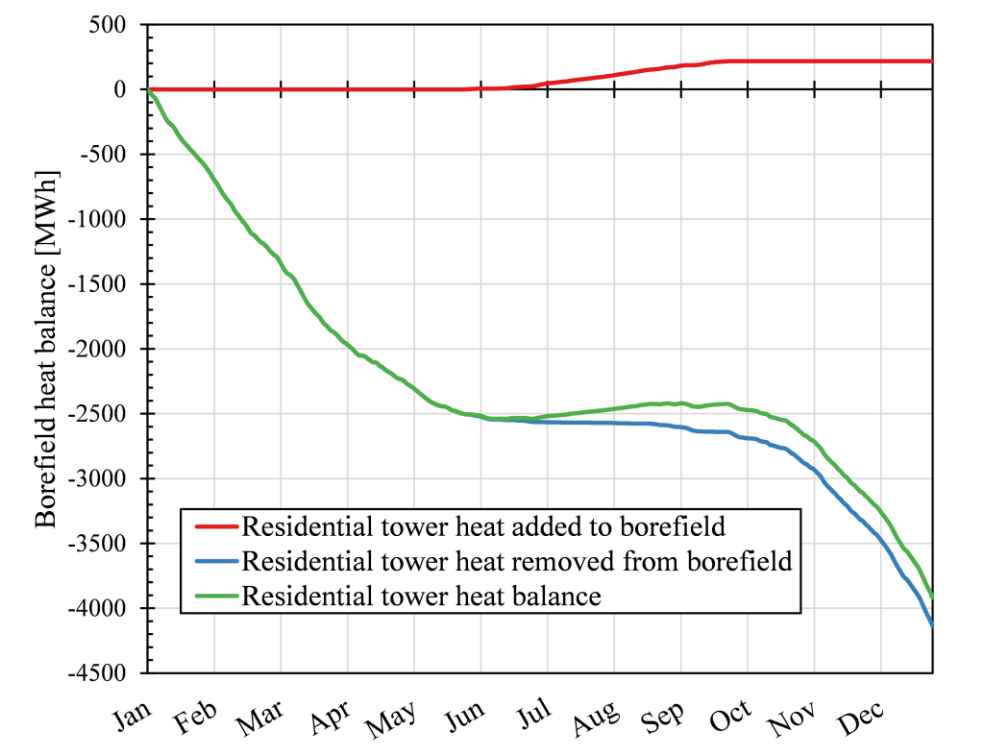

Figure 5.3: Residential tower cumulative borefield heat balance [MWh] vs. time.

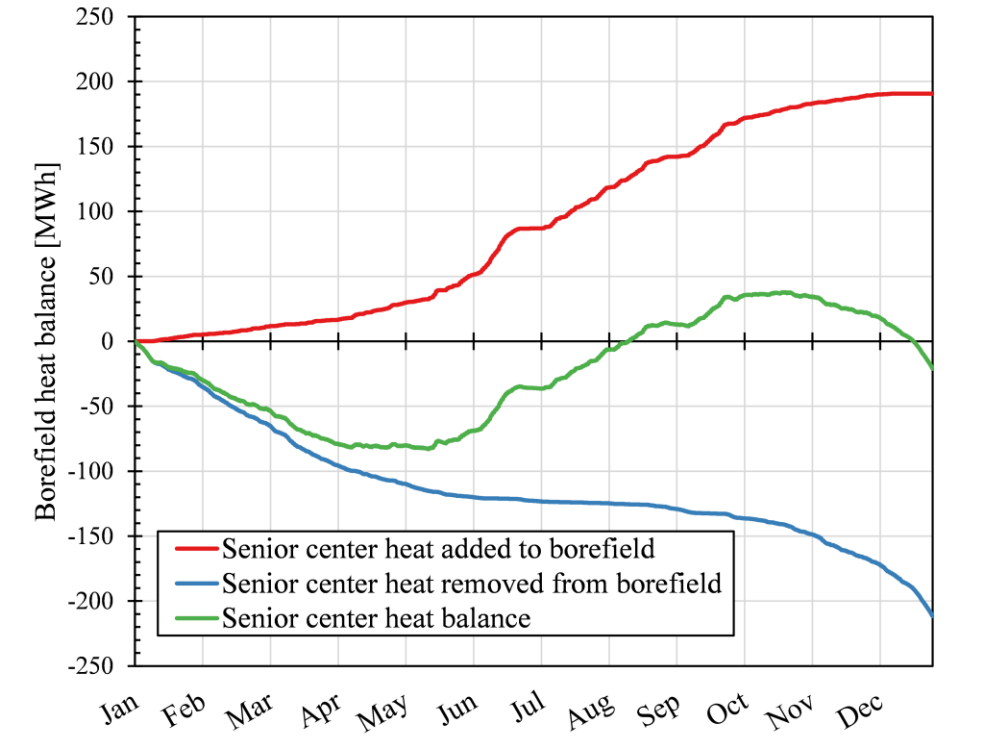

Figure 5.4: Senior center borefield cumulative heat balance [MWh] vs. time.

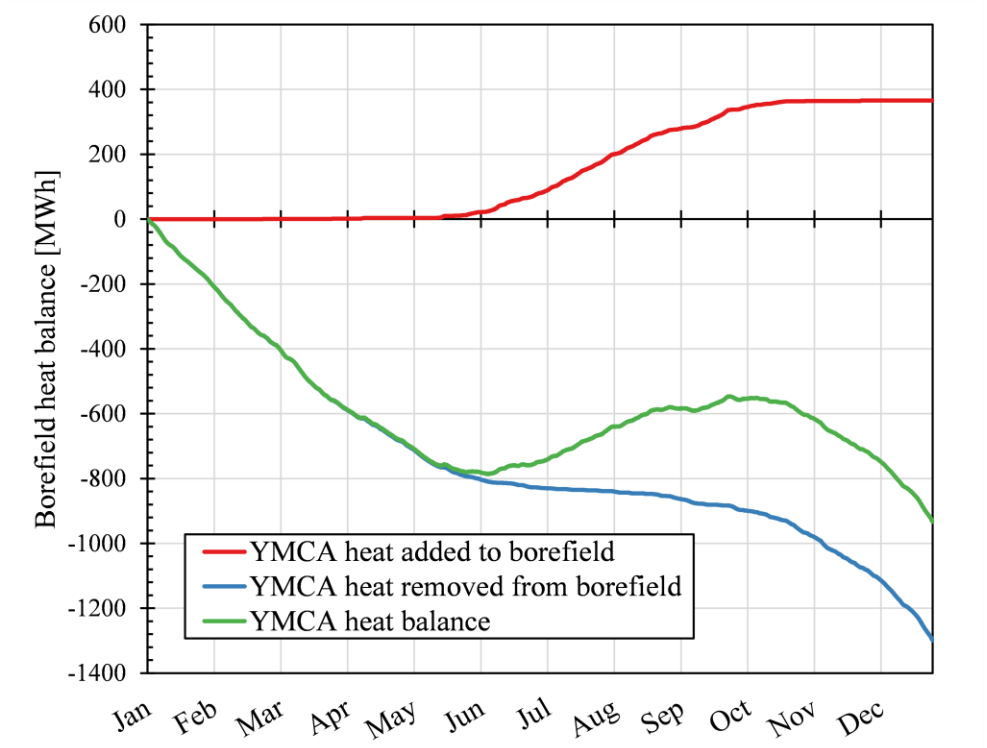

Figure 5.5: YMCA borefield cumulative heat balance [MWh] vs. time.

Figure 5.1 shows the arena borefield cumulative heat balance. The arena is cooling dominated with 1026 MWh of heat added to the borefield from cooling and 209 MWh of heat removed for heating for a net heat balance of 816 MWh. The largest amount of cooling heat rejection occurred from January to April and September to December, which corresponds with when the arena is refrigerated for ice sports.

Figure 5.2 shows the library borefield cumulative heat balance. The library is also cooling dominated with 1822 MWh of heat added to the borefield from cooling and 204 MWh of heat removed for heating for a net heat balance of 1619 MWh. The cooling demand is more constant in the library than in the arena, with an increase during the summer months corresponding to an increase in ambient temperature.

Figure 5.3 shows the residential tower borefield cumulative heat balance. The residential tower is heating dominated with 217 MWh of heat added to the borefield from cooling and 4136

MWh of heat removed for heating for a net heat balance of -3919 MWh. The residential tower is extremely heating dominant with hardly any heat added to the borefield from January to June.

Figure 5.4 shows the senior center borefield cumulative heat balance. The senior center is marginally heating dominant with 191 MWh of heat added to the borefield from cooling and 212 MWh of heat removed for heating for a net heat balance of -21 MWh. The senior center has the smallest energy demands of all the buildings, and the energy flows are nearly balanced over the year.

Figure 5.5 shows the YMCA cumulative borefield heat balance. The YMCA is heating dominant with 366 MWh of heat added to the borefield from cooling and 1299 MWh of heat removed for heating for a net heat balance of -933 MWh. The YMCA has large baseload heating demands for heating an indoor heating pool. Like the residential tower, there is hardly any heat added to the borefield from January to June. A GSHP system operating under these conditions would consistently remove more heat from the field than is recovered year over year.

In conclusion, two of the buildings are cooling dominant, one building is close to balanced, and two buildings are heating dominant. For the sake of comparison, Figure 5.6 shows the combined heat added, heat removed, and heat balance for all of the buildings combined. The objective is to visualize the heat balance of a hypothetical borefield connected to the heat pumps of all of the buildings. This hypothetical borefield gives an idea of the net heat balance of the entire network, which tests the hypothesis that a GSHP system's thermal drift can be managed by connecting heating dominant buildings with cooling dominant buildings.

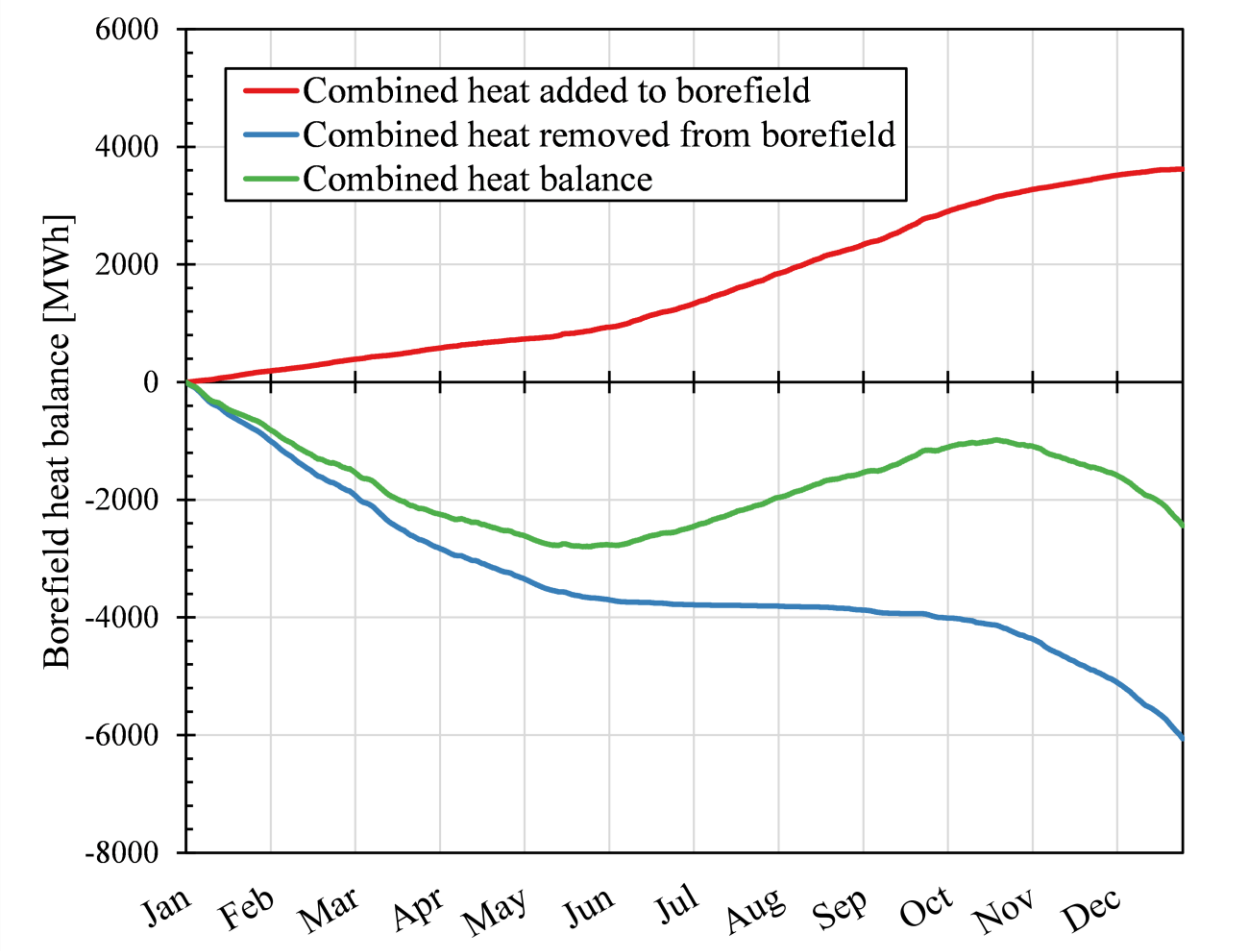

Figure 5.6: All buildings combined geothermal borefield cumulative heat balance [MWh] vs. time.

Figure 5.6 shows the combined borefield cumulative heat balance. Altogether the buildings are heating dominant with 3622 MWh of heat added to the borefield from cooling and 6061 MWh of heat removed for heating for a net heat balance of -2439 MWh. Overall, the system is much more balanced, but there is still more heat removed than added, leading to the average temperature decreasing year over year. The benefit of this arrangement is that the buildings that are cooling dominant will offset the buildings that are heating dominant. Therefore, the net heat load on the borefield will decrease, allowing for a smaller field with fewer boreholes than if the systems were designed individually.

5.5 Thermal energy storage

The TES is an important part of reducing the ICE-Harvest system energy consumption and emissions. The TES is used to capture the CHP's heat when there is insufficient heat demand and deliver the heat back into the network during high demand periods. The performance of the TES depends on the size, controls, and design of the tank. These points will be discussed in this section.

5.5.1 Controls

As shown in section 3.3, the TES is controlled to charge and discharge according to the EMC header temperature. The TES is designed to maintain stratification by pumping high-temperature water to the top of the tank during charging and pumping cold water to the bottom of the tank during discharging. The maximum charging temperature is determined by the CHP maximum allowed supply temperature, and the minimum discharging temperature is determined by the supply temperature in the network. Therefore, TES in systems with lower network temperatures can operate across a larger temperature range than TES in systems with higher network temperatures.

To demonstrate this, Figure 5.7 through Figure 5.15 show the temperature at the top and bottom of the TES for a 1 m^3, 1000 m^3, and 50000 m^3 storage volume. Each figure plots the temperature at the top and bottom of the storage versus time for one year. The red series corresponds to the top temperature, and the blue series corresponds to the bottom temperature.

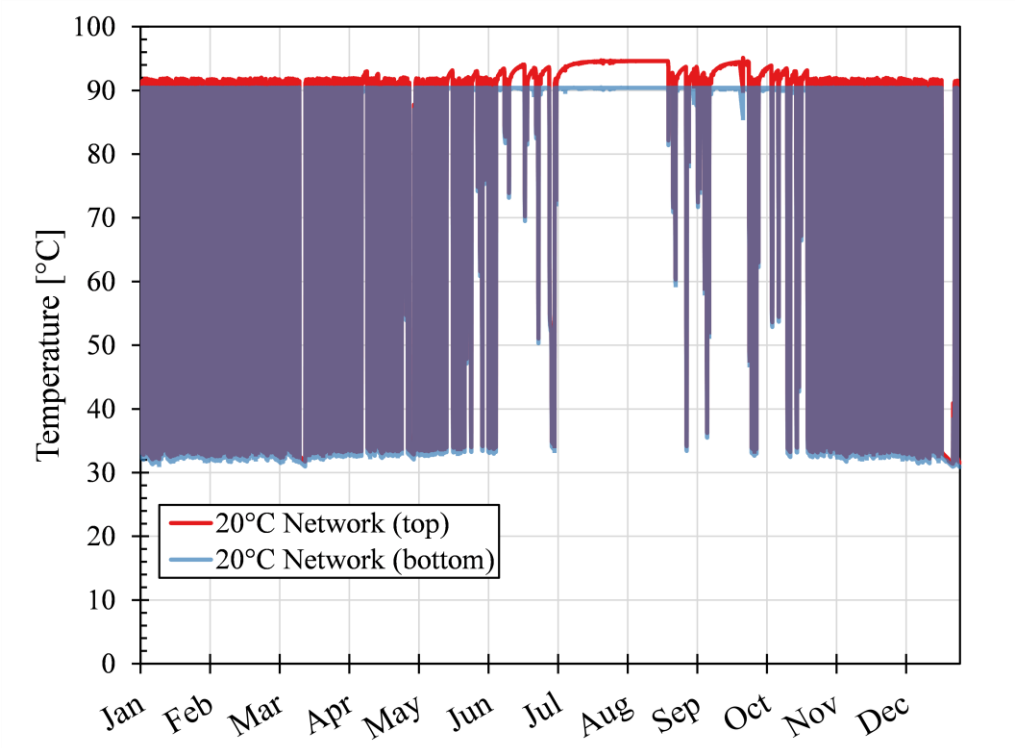

Figure 5.7: Hourly TES temperatures for one year measured at the top and bottom of the tank for the 20 °C network system. The TES volume is 1 m³.

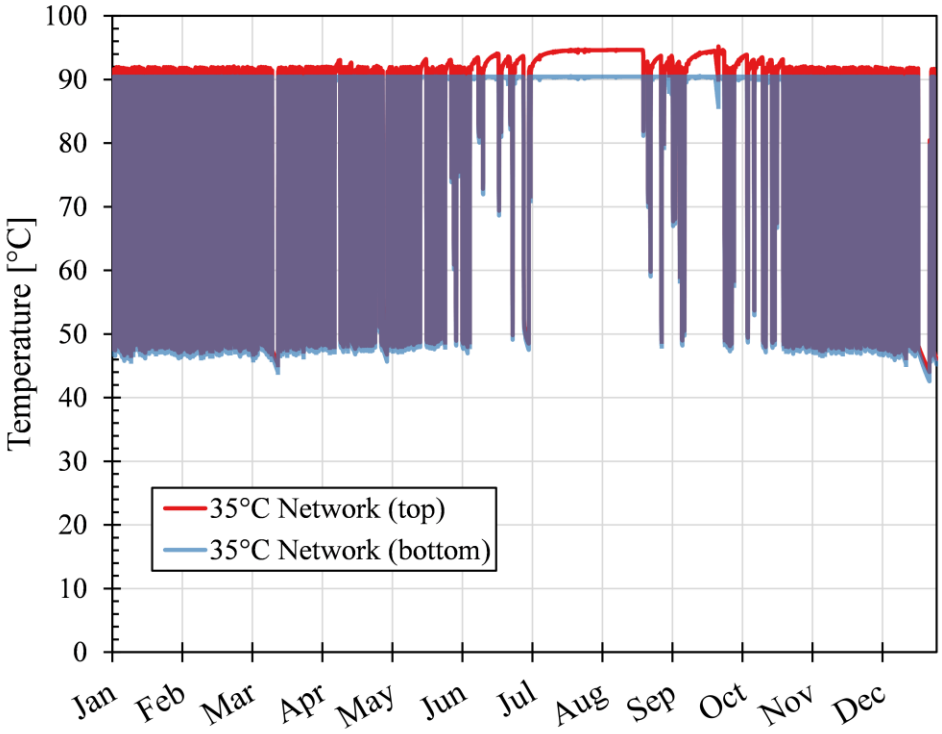

Figure 5.8: Hourly TES temperatures for one year measured at the top and bottom of the tank for the 35 °C network system. The TES volume is 1 m³.

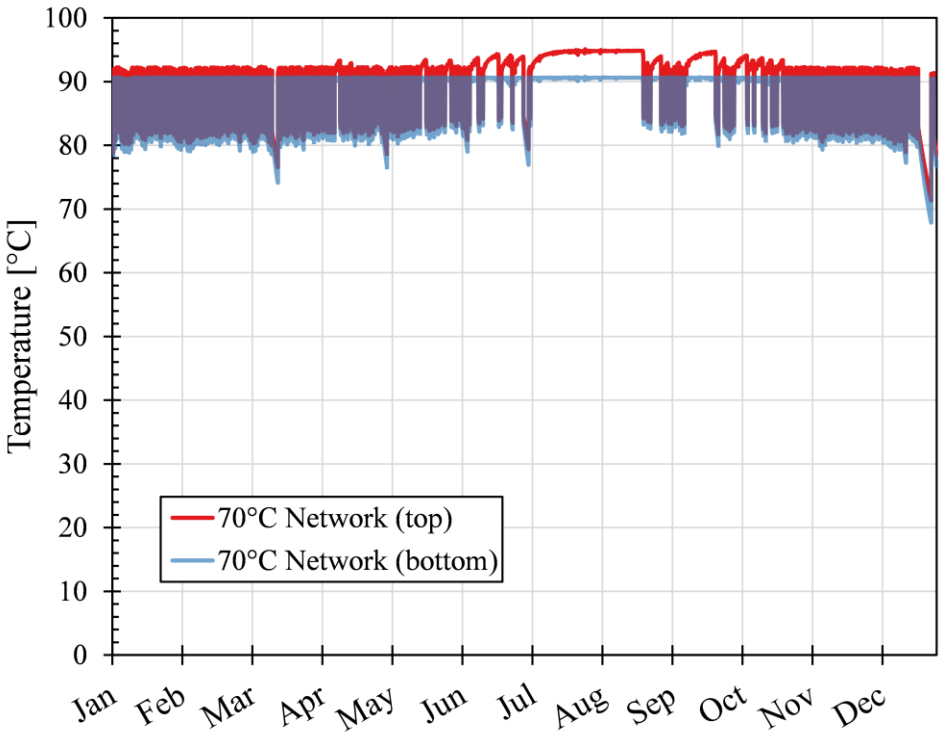

Figure 5.9: Hourly TES temperatures for one year measured at the top and bottom of the tank for the 70 °C network system. The TES volume is 1 m^3.

Looking at Figure 5.7, the TES is cycled frequently throughout the year. The TES's minimum temperature is 32 °C when the storage is fully discharged, up to a temperature of 95 °C when the storage is fully charged. Therefore, the operating temperature range is 63 °C, corresponding to an energy density of 73 kWh/m^3. The storage temperature does not change during the peak of the summer months (July to mid-August) because there is a very low heating demand during this period.

Figure 5.8 shows that the 35 °C network series has a smaller TES temperature difference between fully discharged and fully charged because of a higher network temperature. The lowest temperature is 47 °C, and the highest is 95 °C giving an operating temperature range of 48 °C and an energy density of 55.8 kWh/m^3. The series exhibits the same seasonal behaviour as the 20 °C series. Finally, the 70 °C network series, shown in Figure 5.9, has the smallest operating

temperature range of only 16 °C with a low temperature of 79 °C and a high temperature of 95 °C. This results in an energy density of 18.6 kWh/$m^{3,}$ which is low for a water TTES system.

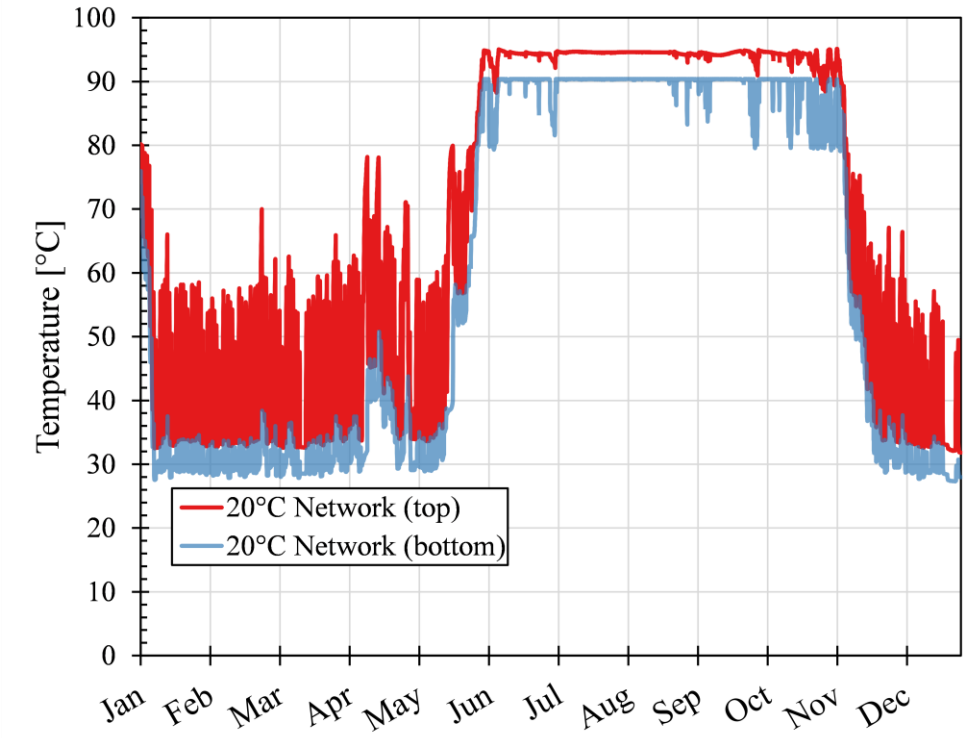

Figure 5.10: Hourly TES temperatures for one year measured at the top and bottom of the tank for the 20 °C network system. The TES volume is 1000 m^3.

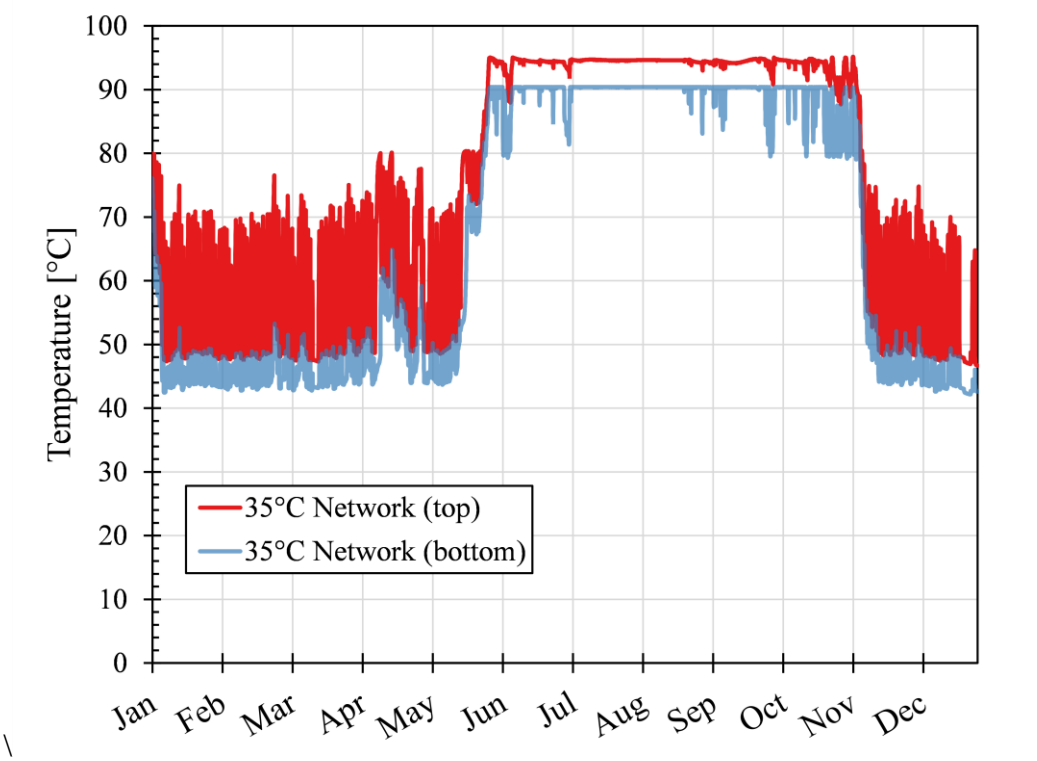

Figure 5.11: Hourly TES temperatures for one year measured at the top and bottom of the tank for the 35 °C network system. The TES volume is 1000 m³.

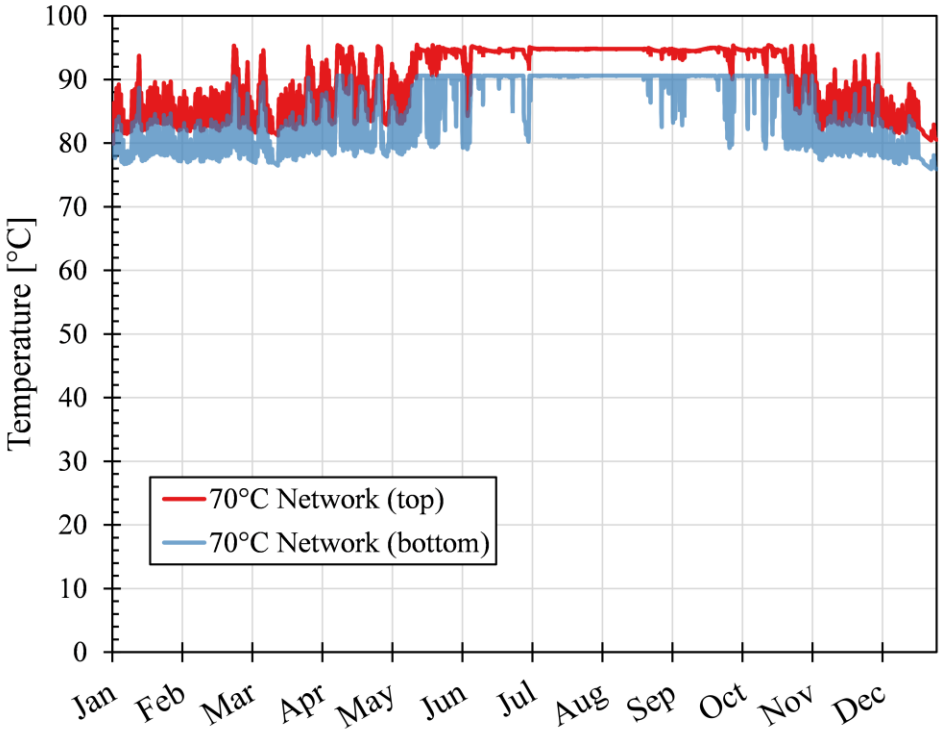

Figure 5.12: Hourly TES temperatures for one year measured at the top and bottom of the tank for the 70 °C network system. The TES volume is 1000 m³.

Figure 5.10, Figure 5.11, and Figure 5.12 show the same series as before but for a storage volume of 1000 m^3. The series had the same high and low temperature as the 1 m^3 storage as they all experienced a full charging and discharging cycle throughout the year. Here, the effects of stratification in the storage are more prominent as the TES top temperature separates away from the bottom temperature. Therefore, the controller, which is designed to promote stratification, is working correctly. During the winter months, the 20 °C and 35 °C TES bottom temperatures hover around the fully discharged temperature. This indicates that the heat being added to the storage is being used before reaching the bottom. Once the heating season ends, the TES temperature rapidly rises and does not decrease until the following winter.

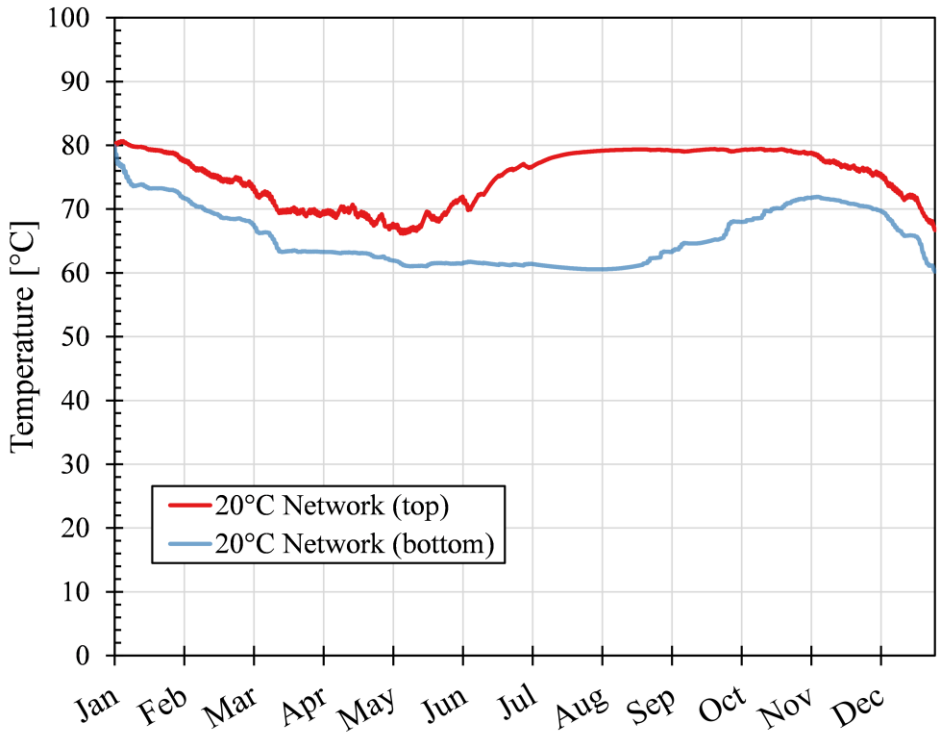

Figure 5.13: Hourly TES temperatures for one year measured at the top and bottom of the tank for the 20 °C network system. The TES volume is 50000 m^3.

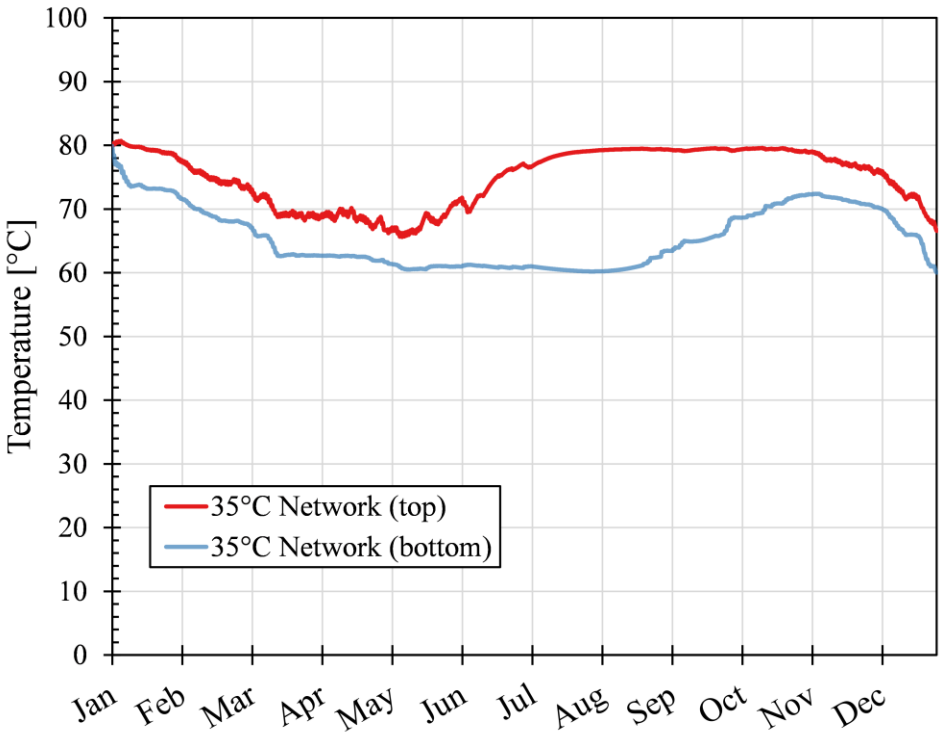

Figure 5.14: Hourly TES temperatures for one year measured at the top and bottom of the tank for the 35 °C network system. The TES volume is 50000 m^3.

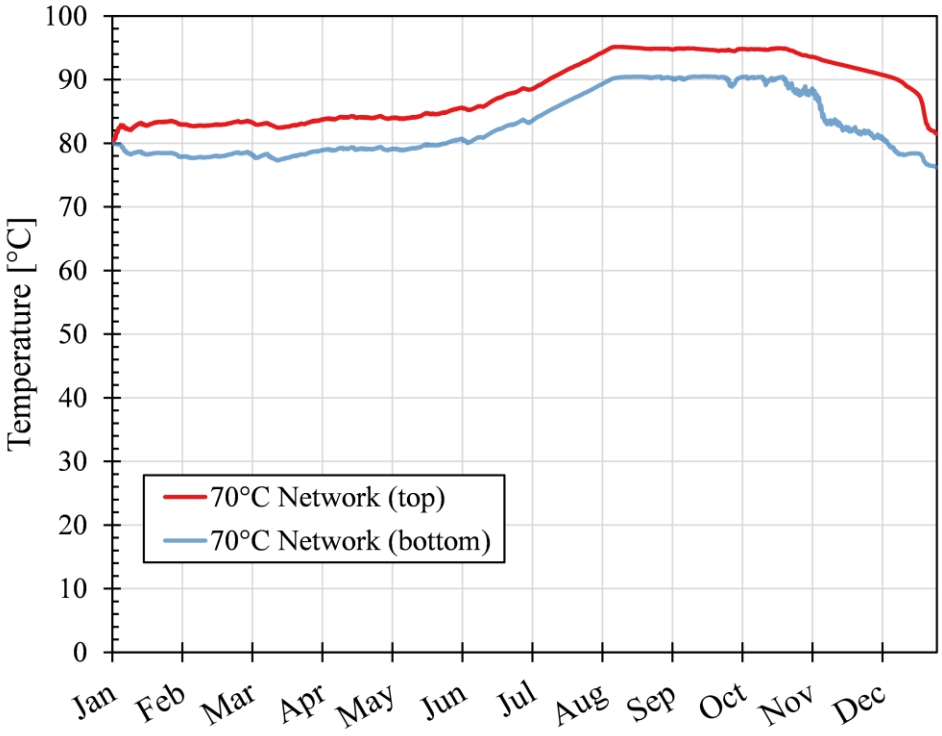

Figure 5.15: Hourly TES temperatures for one year measured at the top and bottom of the tank for the 70 °C network system. The TES volume is 50000 m^3.

Figure 5.13, Figure 5.14, and Figure 5.15 are again the same series but for a storage volume of 50000 m^3. In this case, the 20 °C and 35 °C network TESs did not reach a fully discharged or charged state during the year. By the end of the year, both systems' average storage temperature is approximately 65 °C, which is lower than the initial temperature of a uniform 80 °C. This indicates that the storage has lost heat during the year. Since the amount of heat charged to the storage is equal to the amount of heat extracted, this can only be attributed to heat losses from the storage to the ambient. The maximum amount of stratification is 20 °C, and it occurs at the beginning of August. In the 70 °C system, the TES does not provide much heat from January to June as the TES discharge temperature is greater than the boiler setpoint during this time. For a more detailed explanation of the controller behaviour, refer to section 4.3.1. During the summer months, the TES charges to a maximum temperature of 95 °C, followed by discharging during the winter.

5.5.2 Heat loss

Figure 5.16 shows the TES's annual total heat loss for different storage volumes and different network temperatures. The TES was assumed to be an insulated tank with an insulation thickness of 6” and an insulation conductivity of 0.04 W/mK located in a 25 °C environment. The figure shows that the higher network temperatures resulted in larger heat losses because the water is stored at a higher average temperature. For storage volumes under 100 $m^{3,}$ the annual total heat losses are under 2.5% of the system's annual heating demand. Therefore, up to this size, 6” of insulation is sufficient to mitigate heat losses.

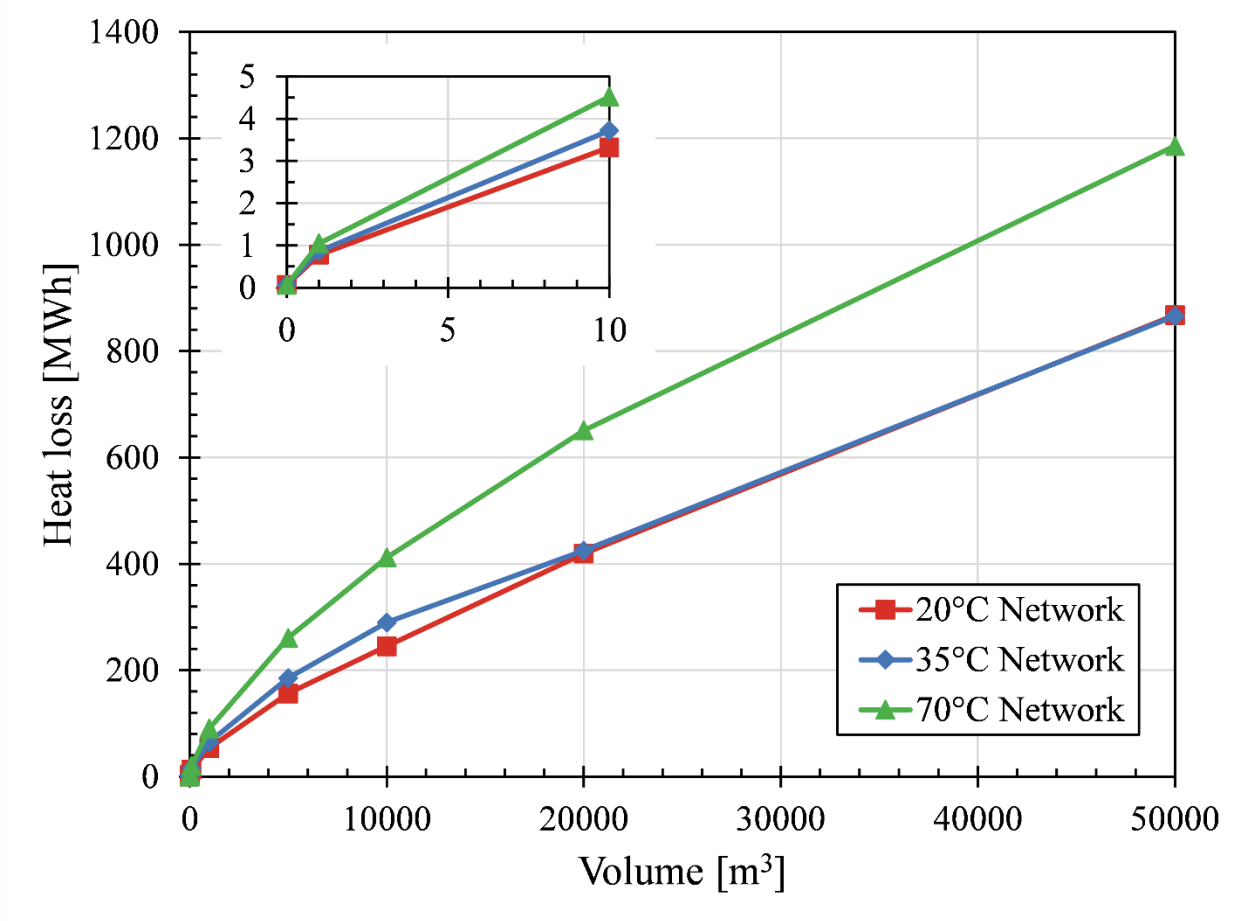

Figure 5.16: Annual total heat loss from TES versus storage volume (m^3). The curves are separated by network temperature; 20 °C network (red), 35 °C network(blue), and 70 °C network(green).

As the storage size increases, however, the heat losses increased to as high as 12% of the annual heating demand, which is a significant amount of lost heat. For reference, the heat losses from the thermal distribution network are 39, 95, and 223 MWh for the 20, 35, and 70 °C network systems, respectively. The heat loss could be reduced in larger storage volumes by increasing the insulation thickness or exploring other TES technologies. For example, using a small high-temperature storage and a large low-temperature storage would reduce the average temperature, thus reducing heat losses.

Chapter 6

6 Conclusions and Recommendations

The electrification of space heating is crucial in reducing Canada's greenhouse gas emissions and increasing the share of renewable energy resources. 5th generation district heating and cooling systems offer enormous potential to implement community-level energy solutions that holistically integrate the electrical and thermal energy sectors in a way that the previous generations of district heating do not offer. These systems will provide great benefits to electricity system operators, distribution companies, and communities. In this work, a modified 5th generation district heating and cooling system was proposed to make the best use of the Ontario energy markets to reduce emissions, increase energy utilization, and stabilize the electricity grid. To accomplish this a background was provided outlining the Ontario energy markets and establishing the current state of the art in the buildings sector. Next, district heating and cooling were discussed which led to the introduction of 5th generation district heating and cooling systems and the ICE-Harvest system. A series of simulations were conducted to compare five different heating and cooling systems using the Modelica coding language. The performance of the simulated systems was verified, and the results were discussed.

6.1 Performance of the ICE-Harvest system

A series of simulations were performed to compare the ICE-Harvest system against conventional, district heating, and ground source heat pump systems. The simulations were done using actual building heating and cooling data for a proposed community site in Ontario. The results showed that the ICE-Harvest system reduced the annual greenhouse gas emissions over the conventional system by 67% to 95% while providing the same level of thermal comfort to the

occupants. This proved the assumption that waste heat from grid-level gas generators can be used as part of a modified 5th generation district heating and cooling framework to provide reliable heating and cooling to buildings.

The concept of energy sharing was also proven to be an effective method of reducing the network's heating demand. It was shown that the heating energy required could be reduced by as high as 57% by capturing waste heat from building cooling processes. The use of a low-temperature single pipe network also did not incur significant heat losses during distribution.

Lastly, it was proven that the ICE-Harvest system could electrify the buildings sector without straining the electricity generation and distribution infrastructure. Through controlling the network temperature, the ICE-Harvest system offers a higher degree of flexibility over 5th generation district heating and cooling systems. It was demonstrated that the total electricity consumption is a function of the network temperature. The network temperature can be modified to benefit the electrical system operators, thus unlocking a large demand management resource through the coupling of electrical and thermal energy markets.

6.2 Recommendations for future work

The work presented in this thesis was limited to system-level simulations. Therefore, the results could be improved through experimentation on a physical system. As with any computational work, numerous assumptions were made, which may not capture the system's correct behaviour. While the underlying technologies presented in this work are well established, it is still unknown if they will work as expected in practice.

For example, it was assumed that the CHP in the ICE-Harvest system operates on an on or off signal at full capacity. This resulted in considerable amounts of wasted energy in the cases

where TES was unavailable or insufficient. In future research, a comparison should be made between running the CHP at full capacity and using TES versus allowing the CHP to part load, thus reducing its output when the heat demand is lower. The situation where the CHP is part loaded is also more realistic of real-world operation of CHP units as operators would not generate excess heat if they knew there was no demand for it.

In this research, the network temperature was held constant throughout the year at three different temperature levels: 20, 35, and 70 °C. It is recommended that future researchers design a controller capable of controlling the network temperature between 20 and 70 °C. The temperature setpoint should be determined by considering the impact on heat losses in the network, available energy sources, and the COPs of the distributed heat pumps and heat recovery heat pumps.

Another potential energy delivery system to be explored is a hybrid GSHP system. The system would use GSHPs at each building connected in series to a thermal distribution network like the one presented in the ICE-Harvest system. The hybrid component of the system would come from using auxiliary energy sources such as air-source, solar thermal, or industrial waste heat, to balance the borefield net energy flow and avoid temperature drift. The benefit of using this system is that the buildings could still share energy because of the thermal distribution network but sites that are heating dominant would be able to maintain a stable ground temperature with only minor heat additions.

This research was limited to waste energy recovery from cooling and refrigeration processes. It is recommended that industrial waste heat sources are explored in future research. These sources sometimes exist near community centers and they represent a large untapped thermal resource for waste heat recovery.

The emissions were calculated using the historical average emission factors. However, the emission factor is likely to change in the future with an increase in electric vehicles and heating equipment. Therefore, it is recommended to explore a variety of predicted future grid emission factors based on the forecasted demand changes and electrical generation options.

As mentioned in the introduction, approximately 2581 GWh of renewable generation was curtailed in the province of Ontario in 2017. This energy represents electricity that could have been produced by renewable generators, however, there was no demand for them to service so it went unused. Therefore, it is recommended to explore using the ICE-Harvest system to increase the electrical demand during periods of curtailment to make use of this power. This could be accomplished by decreasing the network temperature as it was shown in this work to increase the electrical demand of the system.

The addition of decentralized TES should also be explored at the building level to introduce more flexibility to the heat pump power consumption. For example, during the heating season, the heat pumps could be used to charge a local TES during the off-peak periods and avoid increasing the electrical demand during the day. This would offer the system operator another degree of flexibility that is not available in the current configuration.

The TES should be explored further with potential technologies explored in greater depth. This work showed that TES could significantly reduce greenhouse gas emissions in the Ontario market, but its design assumptions were rudimentary. A proper assessment should be performed on large-scale storage technologies such as BTES and PTES to better understand their viability in 5GDHC systems. Also, the TES's operating temperature ranges make it a viable candidate for latent thermal energy storage technologies such as PCM. Using PCMs, the storage could be maintained within a stable temperature range around the material's melting temperature. For

example, water has a specific heat capacity of 4.2 kJ/kgK, and paraffin wax, a commonly used PCM, has a heat of fusion of 200 kJ/kg [122], which is 48 times the specific energy storage capacity. This represents a great opportunity to reduce the TES volume so that it can be better situated within the community.

Finally, a better understanding of the time constants and sizing constraints of the system is recommended to provide insights into an ICE-Harvest system's overall size limit. Since this research was on a relatively small network size, with a residence time of 9 minutes, it remains to be seen if the ICE-Harvest system is viable on the larger district energy scale. The key area of interest in this will be whether or not the Energy Management Center can control the network temperature to reduce energy consumption and emissions effectively.

7 Bibliography

[1] Natural Resources Canada, “Energy Fact Book 2019-2020,” 2020.

[2] M. Brander, “Greenhouse Gases , CO2 , CO2e , and Carbon : What Do All These Terms Mean?,” *Ecometrica*, no. August, p. 3, 2012.

[3] E. and C. C. Canada, “National Inventory Report 1990-2018: Greenhouse gas sources and sinks in Canada,” Ottawa, 2020.

[4] Government of Canada, “Progress towards Canada’s greenhouse gas emissions reduction target,” *Greenh. gas Proj.*, p. 14, 2019.

[5] H. Lund, P. A. Østergaard, D. Connolly, and B. V. Mathiesen, “Smart energy and smart energy systems,” *Energy*, vol. 137, pp. 556–565, 2017.

[6] The Government of Ontario, “Archived - The End of Coal,” 2017. [Online]. Available: https://www.ontario.ca/page/end-coal. [Accessed: 25-Nov-2019].

[7] IESO, “2019 Year in Review,” 2020. [Online]. Available: http://www.ieso.ca/Corporate-IESO/Media/Year-End-Data#yearenddata. [Accessed: 11-Jun-2020].

[8] B. Aust and A. Horsch, “Negative market prices on power exchanges: Evidence and policy implications from Germany,” *Electr. J.*, vol. 33, no. 3, p. 106716, 2020.

[9] Independent Electricity System Operator, “IESO Report : Energy Storage,” *Energy Rep.*, no. March, 2016.

[10] S. Werner, “The new European heating index,” *10th Int. Symp. Dist. Heat. Cool.*, no. September, 2006.

[11] J. Collins, John F., “The History of District Heating,” in *District Heating*, 1959, pp. 154–161.

[12] S. Werner, “International review of district heating and cooling,” *Energy*, vol. 137, pp. 617–631, 2017.

[13] H. Lund *et al.*, “4th Generation District Heating (4GDH). Integrating smart thermal grids into future sustainable energy systems.,” *Energy*, vol. 68, pp. 1–11, 2014.

[14] S. Buffa, M. Cozzini, M. D’Antoni, M. Baratieri, and R. Fedrizzi, “5th generation district heating and cooling systems: A review of existing cases in Europe,” *Renew. Sustain. Energy Rev.*, vol. 104, pp. 504–522, Apr. 2019.

[15] IESO, “Reliability Outlook,” no. December, p. 48, 2018.

[16] A. I. Report, E. Ontario, and N. Fleet, “Together to Deliver the Future of Nuclear in Ontario.”

[17] G. Vishwanathan, J. P. Sculley, A. Fischer, and J. C. Zhao, “Techno-economic analysis of high-efficiency natural-gas generators for residential combined heat and power,” *Appl. Energy*, vol. 226, no. November 2017, pp. 1064–1075, 2018.

[18] D. Lindley, “The energy should always work twice,” *Nature*, vol. 458, no. 7235, pp. 138–141, 2009.

[19] IESO, “2018,” 2020. [Online]. Available: http://www.ieso.ca/en/Corporate-IESO/Media/Year-End-Data/2018.

[20] E. Masood and A. Keshavarz, *Combined Cooling, Heating and Power: Decision-Making, Design and Optimization*. 2014.

[21] S. Martínez-Lera and J. Ballester, “A novel method for the design of CHCP (combined heat, cooling and power) systems for buildings,” *Energy*, vol. 35, no. 7, pp. 2972–2984, Jul. 2010.

[22] R. Evins, “Multi-level optimization of building design, energy system sizing and operation,” *Energy*, vol. 90, pp. 1775–1789, Oct. 2015.

[23] T. Wakui and R. Yokoyama, “Optimal sizing of residential gas engine cogeneration system for power interchange operation from energy-saving viewpoint,” *Energy*, vol. 36, no. 6, pp. 3816–3824, Jun. 2011.

[24] J. Wang, Z. (John) Zhai, Y. Jing, and C. Zhang, “Particle swarm optimization for redundant building cooling heating and power system,” *Appl. Energy*, vol. 87, no. 12, pp. 3668–3679, Dec. 2010.

[25] J.-J. Wang, Y.-Y. Jing, and C.-F. Zhang, “Optimization of capacity and operation for CCHP system by genetic algorithm,” *Appl. Energy*, vol. 87, no. 4, pp. 1325–1335, Apr. 2010.

[26] International Energy Agency, M. Wetter, and C. Van Treeck, *New Generation Computational Tools for Building & Community Energy Systems (Annex 60 final report)*, no. September. 2017.

[27] International Building Performance Simulation Association (IBPSA), “IBPSA Project 1 Participation,” 2019. [Online]. Available: https://ibpsa.github.io/project1/. [Accessed: 16-Sep-2018].

[28] O. Lucon *et al.*, “IPCC - Climate Change 2014 - WG III - Buildings,” *Clim. Chang. 2014 Mitig. Clim. Chang. Contrib. Work. Gr. III to Fifth Assess. Rep. Intergov. Panel Clim. Chang.*, vol. 33, pp. 1–66, 2014.

[29] IEA, “IEA Online Data Services,” 2013. [Online]. Available: http://data.iea.org/ieastore/statslisting.asp. [Accessed: 16-Jun-2020].

[30] Statistics Canada, “Census of Population Reference Guide Structural Type of Dwelling and Collectives Reference Guide,” *Stat. Canada Cat. no. 98-500-X2016001*, no. 98, 2017.

[31] Natural Resources Canada, “Residential Sector Ontario1 Table 2: Secondary Energy Use and GHG Emissions by End-Use,” 2017. [Online]. Available: https://oee.nrcan.gc.ca/corporate/statistics/neud/dpa/showTable.cfm?type=CP&sector=res&juris=on&rn=2&page=0. [Accessed: 16-Jun-2020].

[32] Ontario Energy Board, “Potential Projects to Expand Access to Natural Gas Distribution,” 2019. [Online]. Available: https://www.oeb.ca/industry/policy-initiatives-and-consultations/potential-projects-expand-access-natural-gas. [Accessed: 16-Jun-2020].

[33] Statistics Canada, “Table 38-10-0286-01 Primary heating systems and type of energy,” 2017. .

[34] U.S. Department of Energy, “Furnaces and Boilers.” [Online]. Available: https://www.energy.gov/energysaver/home-heating-systems/furnaces-and-boilers. [Accessed: 16-Jun-2020].

[35] Government of Canada, “Energy Savings Rebate program,” 2019. [Online]. Available: https://www.canada.ca/en/environment-climate-change/news/2019/08/energy-savings-rebate-program.html. [Accessed: 16-Jun-2020].

[36] Natural Resources Canada, “Commercial/Insitutional Sector Ontario1 Table 2: Secondary Energy Use and GHG Emissions by End Use,” 2017. [Online]. Available: https://oee.nrcan.gc.ca/corporate/statistics/neud/dpa/showTable.cfm?type=CP&sector=com&juris=on&rn=2&page=0.

[37] P. Dalin, J. Nilsson, and A. Rubenhag, “The european cold market, WP2 report from the Ecoheatcool project,” Brussels, 2005.

[38] Government of Canada, “Guide to Canada’s Energy Efficiency Regulations,” 2020. [Online]. Available: https://www.nrcan.gc.ca/energy-efficiency/energy-efficiency-regulations/guide-canadas-energy-efficiency-regulations/6861. [Accessed: 16-Jun-2020].

[39] IEA, “The Future of Cooling,” Paris, 2018.

[40] M. Isaac and D. P. van Vuuren, “Modeling global residential sector energy demand for heating and air conditioning in the context of climate change,” *Energy Policy*, vol. 37, no. 2, pp. 507–521, 2009.

[41] L. W. Davis and P. J. Gertler, “Contribution of air conditioning adoption to future energy use under global warming,” *Proc. Natl. Acad. Sci. U. S. A.*, vol. 112, no. 19, pp. 5962–5967, 2015.

[42] Energy Star, “Technical Reference: Technical Reference Canadian Energy Use Intensity by Property Type,” 2013.

[43] CanmetENERGY, *Comparative study of refrigeration systems for ice rinks*. 2013.

[44] E. Masanet, A. Shehabi, N. Lei, S. Smith, and J. Koomey, “Recalibrating global data center energy-use estimates,” *Science (80-.).*, vol. 367, no. 6481, pp. 984–986, Feb. 2020.

[45] Arman Shehabi *et al.*, “United States Data Center Energy Usage Report | Energy Technologies Area,” no. June, p. 65, 2016.

[46] “Amazon, data center turn hot idea into cool technology | The Seattle Times.” [Online]. Available: https://www.seattletimes.com/business/real-estate/amazon-towers-will-be-heated-by-neighbors-excess-energy/. [Accessed: 16-Oct-2019].

[47] IESO, “Hourly Ontario Energy Price (HOEP),” 2020. [Online]. Available: http://www.ieso.ca/Power-Data/Price-Overview/Hourly-Ontario-Energy-Price. [Accessed: 16-Jun-2020].

[48] Ontario Power Authority, “A Progress Report On Contracted Electricity Supply - 2014,

Quarter 3," 2014.

[49] IESO, "Power Data," 2020. [Online]. Available: http://www.ieso.ca/Power-Data. [Accessed: 16-Jun-2020].

[50] A. Nittenberg, "Performance of Ontario Hydro's CANDU nuclear generating stations: an outlook for the future," in *Nuclear power performance and safety*, 1987, pp. 185–203.

[51] Navigant, "Conservation Behind the Meter Generation Potential Study," Toron, 2016.

[52] A. Purvins, A. Zubaryeva, M. Llorente, E. Tzimas, and A. Mercier, "Challenges and options for a large wind power uptake by the European electricity system," *Appl. Energy*, vol. 88, no. 5, pp. 1461–1469, 2011.

[53] European Wind Energy Association, "Large scale integration of wind energy in the European power supply: Analysis, issues and recommendations," pp. 1–172, 2005.

[54] A. R. Razani and I. Weidlich, "A genetic algorithm technique to optimize the configuration of heat storage in DH networks," *Int. J. Sustain. Energy Plan. Manag.*, vol. 10, no. 0, pp. 21–32, 2016.

[55] R. Hledik, R. Lueken, C. Mcintyre, and H. Bishop, "Stacked Benefits: Comprehensively Valuing Battery Storage in California," no. September, 2017.

[56] J. Sotes, "A clearer view on Ontario's emissions," 2019.

[57] M. A. Lozano, M. Carvalho, and L. M. Serra, "Operational strategy and marginal costs in simple trigeneration systems," *Energy*, vol. 34, no. 11, pp. 2001–2008, Nov. 2009.

[58] P. J. Mago and A. K. Hueffed, "Evaluation of a turbine driven CCHP system for large office buildings under different operating strategies," *Energy Build.*, vol. 42, no. 10, pp. 1628–1636, Oct. 2010.

[59] C. B. Heendeniya, A. Sumper, and U. Eicker, "The multi-energy system co-planning of nearly zero-energy districts – Status-quo and future research potential," *Appl. Energy*, vol. 267, no. April, p. 114953, 2020.

[60] C. Edison, "Steam energy," 2017.

[61] S. Kelly and M. Pollitt, "An assessment of the present and future opportunities for combined heat and power with district heating (CHP-DH) in the United Kingdom," *Energy Policy*, vol. 38, no. 11, pp. 6936–6945, 2010.

[62] T. R. Casten and F. Pena, *Turning off the heat: why America must double energy efficiency to save money and reduce global warming*. Prometheus Books New York, 1998.

[63] Euroheat, "District Heating and Cooling Statistics 2015," no. September, p. 2013, 2015.

[64] L. G and J. Donev, "Oil crisis of the 1970s," 2016. [Online]. Available: https://energyeducation.ca/encyclopedia/Oil_crisis_of_the_1970s. [Accessed: 18-Jun-2020].

[65] S. Frederiksen and S. Werner, "District heating and cooling," *Lund Studentlitteratur*, 2013.

[66] IEA and AIE, "World energy balances (Edition 2019).," *IEA World Energy Stat. Balanc.*, 2020.

[67] H. Lund, B. Möller, B. V. Mathiesen, and A. Dyrelund, "The role of district heating in future renewable energy systems," *Energy*, vol. 35, no. 3, pp. 1381–1390, 2010.

[68] J. P. Painuly, "Barriers to renewable energy penetration: A framework for analysis," *Renew. Energy*, vol. 24, no. 1, pp. 73–89, 2001.

[69] D. Connolly, H. Lund, and B. V. Mathiesen, "Smart Energy Europe: The technical and economic impact of one potential 100% renewable energy scenario for the European Union," *Renew. Sustain. Energy Rev.*, vol. 60, pp. 1634–1653, 2016.

[70] F. Ruesch and M. Haller, "Potential and limitations of using low-Temperature district heating and cooling networks for direct cooling of buildings," *Energy Procedia*, vol. 122, pp. 1099–1104, 2017.

[71] N. Vetterli, M. Sulzer, and U.-P. Menti, "Energy monitoring of a low temperature heating and cooling district network," *Energy Procedia*, vol. 122, pp. 62–67, 2017.

[72] F. Bünning, M. Wetter, M. Fuchs, and D. Müller, "Bidirectional low temperature district energy systems with agent-based control: Performance comparison and operation optimization," *Appl. Energy*, vol. 209, pp. 502–515, Jan. 2018.

[73] F. Ruesch, M. Rommel, and J. Scherer, "Pumping Power Prediction in Low Temperature District Heating Networks," *Proc. Int. Conf. CISBAT 2015*, pp. 753–758, 2015.

[74] A. Prasanna, V. Dorer, and N. Vetterli, "Optimisation of a district energy system with a low temperature network," *Energy*, vol. 137, pp. 632–648, 2017.

[75] R. Li, R. Ooka, and M. Shukuya, "Theoretical analysis on ground source heat pump and air source heat pump systems by the concepts of cool and warm exergy," *Energy Build.*, vol. 75, pp. 447–455, 2014.

[76] H. Averfalk, P. Ingvarsson, U. Persson, M. Gong, and S. Werner, "Large heat pumps in Swedish district heating systems," *Renew. Sustain. Energy Rev.*, vol. 79, no. June 2016, pp. 1275–1284, 2017.

[77] P. L. Younger, "Ground-Coupled Heating-Cooling Systems in Urban Areas: How Sustainable Are They?," *Bull. Sci. Technol. Soc.*, vol. 28, no. 2, pp. 174–182, Apr. 2008.

[78] K. Rafferty, "Design aspects of commercial open loop heat pump systems," *Geo-Heat Cent. Q. Bull.*, vol. 4, no. March, pp. 16–24, 2001.

[79] M. Sulzer and D. Hangartner, "Kalte Fernwärme (Anergienetze)-Grundlagen-/Thesenpapier," *Horw Hochschule Luzern, Zent. für Integr. Gebäudetechnik*, 2014.

[80] K. M. Heissler, J. Metz, W. Lang, T. Auer, and I. Nemeth, "Potenziale von Niedrigtemperaturnetzen zur Steigerung des Anteils erneuerbarer Energien in Quartieren," 2017.

[81] L. Brange, J. Englund, and P. Lauenburg, "Prosumers in district heating networks - A Swedish case study," *Appl. Energy*, vol. 164, pp. 492–500, 2016.

[82] T. Netze, “Fallbeispiele „ Thermische Netze “,” pp. 1–136, 2019.

[83] V. K. Vanoli, D. Christoffers, and G. Rockendorf, “Solarsiedlung am Ohrberg,” 2000.

[84] I. P. Pattijn and A. Baumans, “Fifth-generation thermal grids and heat pumps: A pilot project in Leuven, Belgium,” *HPT Mag.*, vol. 35, no. 2, pp. 53–57, 2017.

[85] “Home - Flexynets,” 2020. [Online]. Available: http://www.flexynets.eu/en/Home. [Accessed: 19-Jun-2020].

[86] “Horizon 2020,” 2020. [Online]. Available: https://ec.europa.eu/programmes/horizon2020/en. [Accessed: 19-Jun-2020].

[87] “EURAC research,” 2020. [Online]. Available: http://www.eurac.edu/en/pages/default.aspx. [Accessed: 19-Jun-2020].

[88] F. Bava, A. Hussein, and M. Cozzini, “Report on Early Adopters case studies,” 2018.

[89] R. Fedrizzi *et al.*, “Project Booklet: Fifth generation, low temperature, high exergy district heating and cooling networks,” 2018.

[90] D. Trier, L. Laurberg Jensen, F. Bava, I. Ben Hassine, and X. Jobard, “Large Storage Systems for DHC Networks,” 2019.

[91] “Home - life4heatrecovery,” 2020. [Online]. Available: http://www.life4heatrecovery.eu/en/. [Accessed: 22-Jun-2020].

[92] N. Vetterli, M. Sulzer, and U. P. Menti, “Energy monitoring of a low temperature heating and cooling district network,” *Energy Procedia*, vol. 122, pp. 62–67, 2017.

[93] D. Connolly, H. Lund, B. V. Mathiesen, and M. Leahy, “A review of computer tools for analysing the integration of renewable energy into various energy systems,” *Appl. Energy*, vol. 87, no. 4, pp. 1059–1082, 2010.

[94] Aalborg University, “EnergyPLAN.” [Online]. Available: https://www.energyplan.eu/. [Accessed: 03-Jul-2020].

[95] EnergySoft, “Energy Pro,” 2020. [Online]. Available: http://www.energysoft.com/. [Accessed: 03-Jul-2020].

[96] HOMEREnergy, “HOMER - Hybrid Renewable and Distributed Generation System Design Software,” 2020. [Online]. Available: https://www.homerenergy.com/. [Accessed: 03-Jul-2020].

[97] TRNSYS, “TRNSYS: Transient System Simulation Tool,” 2020. [Online]. Available: http://www.trnsys.com/. [Accessed: 03-Jul-2020].

[98] S. Udomsri, C. Bales, A. R. Martin, and V. Martin, “Decentralized cooling in district heating network: System simulation and parametric study,” *Appl. Energy*, vol. 92, pp. 175–184, 2012.

[99] H. Torío and D. Schmidt, “Development of system concepts for improving the performance of a waste heat district heating network with exergy analysis,” *Energy Build.*, vol. 42, no. 10, pp. 1601–1609, 2010.

[100] H. Ahmadisedigh and L. Gosselin, "Combined heating and cooling networks with waste heat recovery based on energy hub concept," *Appl. Energy*, 2019.

[101] The Modelica Association, "The Modelica Association," 2020. [Online]. Available: https://www.modelica.org/. [Accessed: 03-Jul-2020].

[102] M. Wetter, W. Zuo, T. S. Nouidui, and X. Pang, "Modelica Buildings library," *J. Build. Perform. Simul.*, vol. 7, no. 4, pp. 253–270, 2014.

[103] D. Müller, M. Lauster, A. Constantin, M. Fuchs, and P. Remmen, "AixLib - An Open-Source Modelica Library withi the IEA-EB Annex 60 Framework," *BauSIM*, no. September, pp. 3–9, 2016.

[104] UdK Berlin, "BuildingSystems," 2019. [Online]. Available: https://modelica-buildingsystems.de/. [Accessed: 03-Jul-2020].

[105] F. Jorissen, G. Reynders, R. Baetens, D. Picard, D. Saelens, and L. Helsen, "Implementation and Verification of the IDEAS Building Energy Simulation Library," *J. Build. Perform. Simul.*, vol. 11, no. 6, pp. 669–688, 2018.

[106] R. Rogers, "Unidirectional low temperature thermal networks: enabling thermal distributed energy resources," McMaster university, 2019.

[107] R. Zarin Pass, M. Wetter, and M. A. A. Piette, "A thermodynamic analysis of a novel bidirectional district heating and cooling network," *Energy*, vol. 144, pp. 20–30, Feb. 2018.

[108] I. Dincer and M. A. Rosen, *Thermal Energy Storage: Systems and Applications*. John Wiley & Sons, 2002.

[109] M. Y. Abdelsalam, H. M. Teamah, M. F. Lightstone, and J. S. Cotton, "Hybrid thermal energy storage with phase change materials for solar domestic hot water applications: Direct versus indirect heat exchange systems," *Renew. Energy*, vol. 147, pp. 77–88, 2020.

[110] R. Hirmiz, H. M. Teamah, M. F. Lightstone, and J. S. Cotton, "Performance of heat pump integrated phase change material thermal storage for electric load shifting in building demand side management," *Energy Build.*, vol. 190, pp. 103–118, 2019.

[111] H. M. Teamah and M. F. Lightstone, "Numerical study of the electrical load shift capability of a ground source heat pump system with phase change thermal storage," *Energy Build.*, vol. 199, pp. 235–246, 2019.

[112] D. Mangold and T. Schmidt, "The next generations of seasonal thermal energy storage in Germany," p. 8, 2009.

[113] Energistyrelsen, "Udredning vedrørende varmelagringsteknologier og store varmepumper i fjernvarmesystemet," no. November, 2013.

[114] M. Wetter, "Buildings.Fluid.Storage," 2020. [Online]. Available: https://simulationresearch.lbl.gov/modelica/releases/latest/help/Buildings_Fluid_Storage.html#Buildings.Fluid.Storage.Stratified. [Accessed: 15-Sep-2020].

[115] M. Wetter, "Buildings.Fluid.HeatExchangers," 2020. [Online]. Available: https://simulationresearch.lbl.gov/modelica/releases/latest/help/Buildings_Fluid_HeatExc

hangers.html#Buildings.Fluid.HeatExchangers.DryCoilEffectivenessNTU.

[116] M. Wetter, "Buildings.Fluid.HeatPumps." [Online]. Available: https://simulationresearch.lbl.gov/modelica/releases/latest/help/Buildings_Fluid_HeatPumps.html#Buildings.Fluid.HeatPumps.Carnot_y. [Accessed: 25-Jul-2020].

[117] T. Kasuda; and P. R. Achenboch, "Earth temperature and thermal diffusivity at selected stations in the United States," 1965.

[118] N. De Nevers, *Fluid Mechanics*. 1970.

[119] Nordic, "WH Series." [Online]. Available: https://www.nordicghp.com/product/nordic-products/high-temp-water-to-water/wh-series/. [Accessed: 25-Jul-2020].

[120] Enbridge Gas, "Strategic Energy for Ontario," Toronto, 2016.

[121] Independent Electricity System Operator, "Historical Demand," 2020. [Online]. Available: https://www.ieso.ca/en/Power-Data/Demand-Overview/Historical-Demand.

[122] R. C. Weast, *Handbook of Chemistry and Physics*, 62nd ed. Boca Raton, Florida: CRC Press Inc., 1981.

[123] PlanEnergi, "Long term storage and solar district heating: A presentation of the Danish pit and borehole thermal energy storages in Braedstrup, Marstal, Dronninglund and Gram," Aalborg.

[124] V. Arpaci, *Conduction heat transfer*. Addison-Wesley, 1966.

Chapter 7

8 Appendices

8.1 Appendix A: List of international TES projects

Table 8.1: List of international thermal storage systems [123]

Project Name	Location	Capacity	Temperature range	Notes
Bradytroph District Heating	Bidstrup, Denmark	48 boreholes heating 19000 m^3 of soil 2 steel tanks: 1x 2500 m^3, 1x 5500 m^3 (total: 8000 m^3)	Heated to 60 °C during summer and cooled to 15 °C during winter (45 °C)	Borehole depth of 45 m 18600 m^2 of solar collectors Two boilers (13.5 MW, 10 MW) Two engines (4.1 MW) One electric boiler (10 MW) One heat pump (1.2 MW)
SUNSTORE 4	Marsal, Denmark	75000 m^3 pit storage 2100 m^3 of steel tank water storage	Heated to 85 °C during summer and cooled to 10 °C during winter (75 °C)	18300 + 15000 m^2 of solar collectors 8.3 MW bio-oil boilers 4.0 MW wood chip boiler 750 kWe ORC 1.5 MWth heat pump
SUNSTORE 3	Droning, Denmark	60000 m^3 of pit water storage	Heated to 85 °C during summer and cooled to 10 °C during winter (75 °C)	37573 m^2 of solar collectors 8 MW boiler 6 MW engines 2.1 MW cooling bio-oil boiler driven heat pump
Gram Fervor	Gram, Denmark	122000 m^3 of pit water storage 2300 m^3 of steel tank water storage	Heated to 85 °C during summer and cooled to 10 °C during winter (75 °C)	44800 m^2 of solar collectors two 10 MW boiler 6.5 MW engine 8 MW electric boiler 900 kW heat pump

The Well	Toronto, Canada	7600 m^3 of pit water storage	Heated to 85 °C during summer and cooled to 10 °C during winter (75 °C)	-
Drakes Landing Solar Community	Okotoks, Canada	2x 120 m^3 steel tanks 144 boreholes at 35 m depth 34000 m^3 of soil	Heated to 80 °C during summer and cooled to 40 °C during winter (40 °C)	798 – 2.45m x 1.18 m solar collectors
Strugar		1500 m^3 of pit water storage	Heated to 60 °C during summer and cooled to 35 °C during winter (25 °C)	
SUNSTORE 2	Marsal, Denmark	10000 m^3 of pit water storage	Heated to 90 °C during summer and cooled to 35 °C during winter (55 °C)	
Ovens		210000 m^3 of pit water storage	Heated to 90 °C during summer and cooled to 40 °C during winter (50 °C)	
Toft Lund		85000 m^3 of pit water storage	Heated to 90 °C during summer and cooled to 20 °C during winter (70 °C)	
Griesheim		37500 m^3 of soil	Heated to 70 °C during summer and cooled to 20 °C during winter (50 °C)	
Berringer				A temperature difference of 8 °C with a capacity of 1500 kW
Large scale hot water tanks		1500 to 5000 m^3	30 to 60 °C	Many installations worldwide
Small scale hot water tanks		50 to 300 L	30 to 60 °C	

8.2 Appendix B: Component verifications

The model being tested: CHP

Test: Water is supplied at 70 °C and a flow rate of 3 kg/s. The CHP is turned on and outputs 82 kWth at a constant rate. Temperature measurements are taken before and after the CHP. The purpose of this test is to verify that heat is added correctly under stable conditions.

Expected result: The temperature at the outlet will be 76.5 °C.

$$T = 70\,°C + \frac{82000W}{3\frac{kg}{s} \times 4178\frac{J}{kgK}} = 76.5°C$$

Simulated result: The simulation results agree with what is expected.

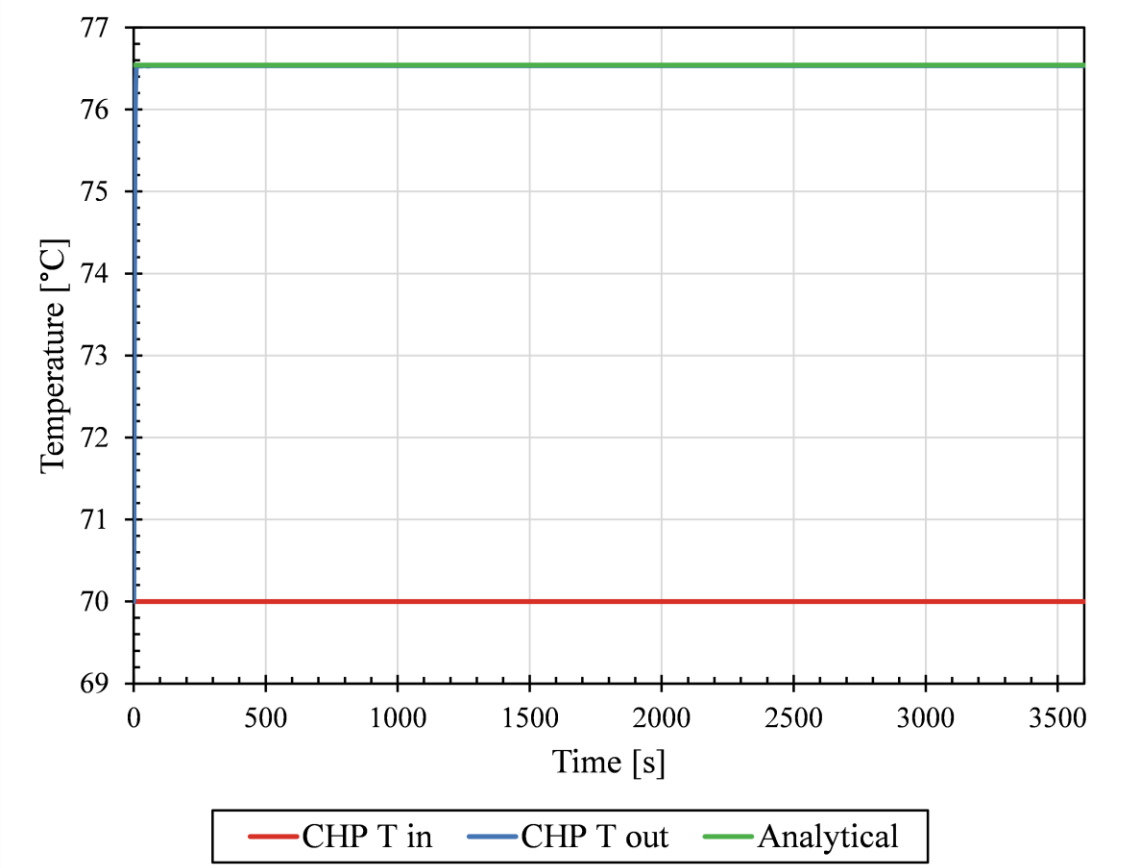

Figure 8.1: Verification of the CHP model in heating water from an inlet temperature of 70 °C to 76.5 °C

The model being tested: CHP

Test: Water is supplied at a mass flow rate of 3 kg/s. The temperature of the supply water increases linearly from 40 °C to 60 °C for one hour. The temperature is held constant for one hour before decreasing linearly back to 40 °C. The CHP adds 82 kWth to the flow. The purpose of this test is to verify that heat is added to flow steam correctly under varying inlet temperatures.

Expected result: The outlet temperature will increase linearly from 46.5 °C to 66.5 °C in one hour then remain constant at 66.5 °C for one hour before returning to 46.5 °C.

$$T = 40\,°C + \frac{82000W}{3\frac{kg}{s} \times 4178\frac{J}{kgK}} = 46.5°C$$

Simulated result: The simulation results agree with what is expected.

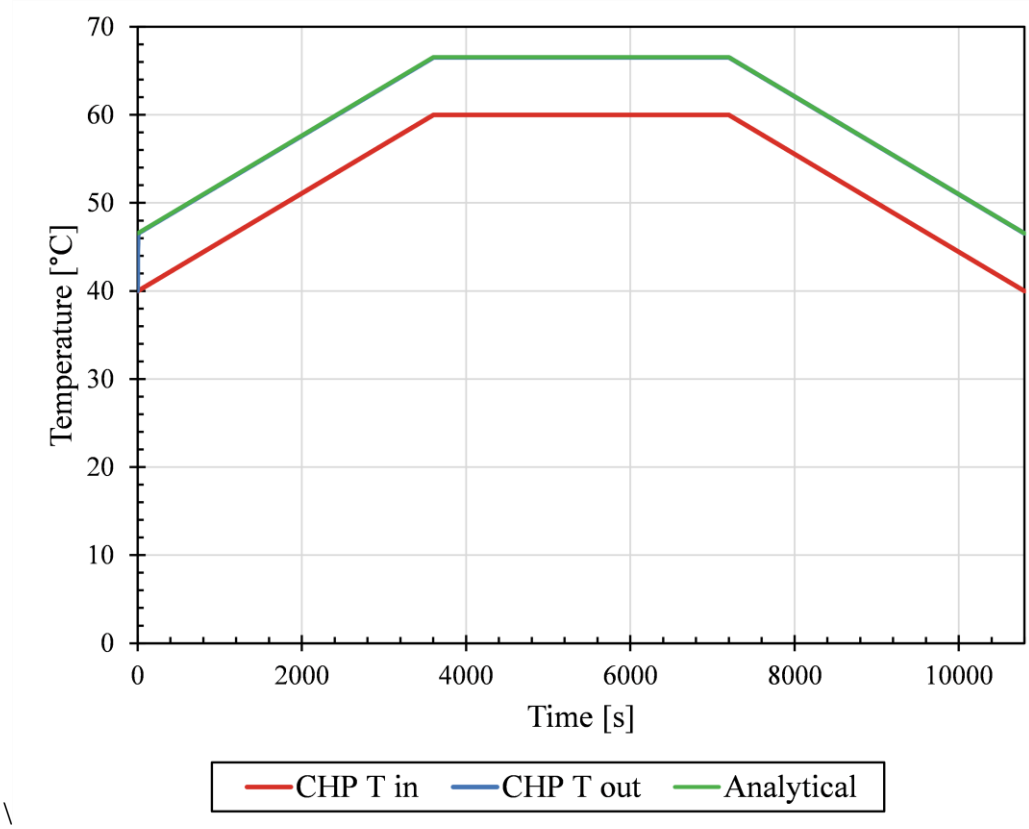

Figure 8.2: Verification of the CHP for constant heat addition under variable inlet temperature

The model being tested: Thermal energy storage

Test: A hot water tank is initially at 70 °C. The height of the tank is 3 m, and the volume is 1 m^3. The insulation thickness is 10 cm, with a thermal conductivity of 0.04 W/mK. The tank is subject to an ambient temperature of 20 °C at the wall boundary. The purpose of this test is to verify the heat loss model from the tank.

Expected result: The temperature should drop non-linearly from 70 °C to 20 °C. The equation for the rate of heat loss is as follows.

$$\frac{dT}{dt} = \frac{T - T_{inf}}{\tau}$$

Where,

$$\tau = \frac{m \times c_p}{UA}$$

$$T(t) = T_{inf} - (T_{inf} - T_o)e^{-\frac{t}{\tau}}$$

Simulated result: The simulation results agree with what is expected.

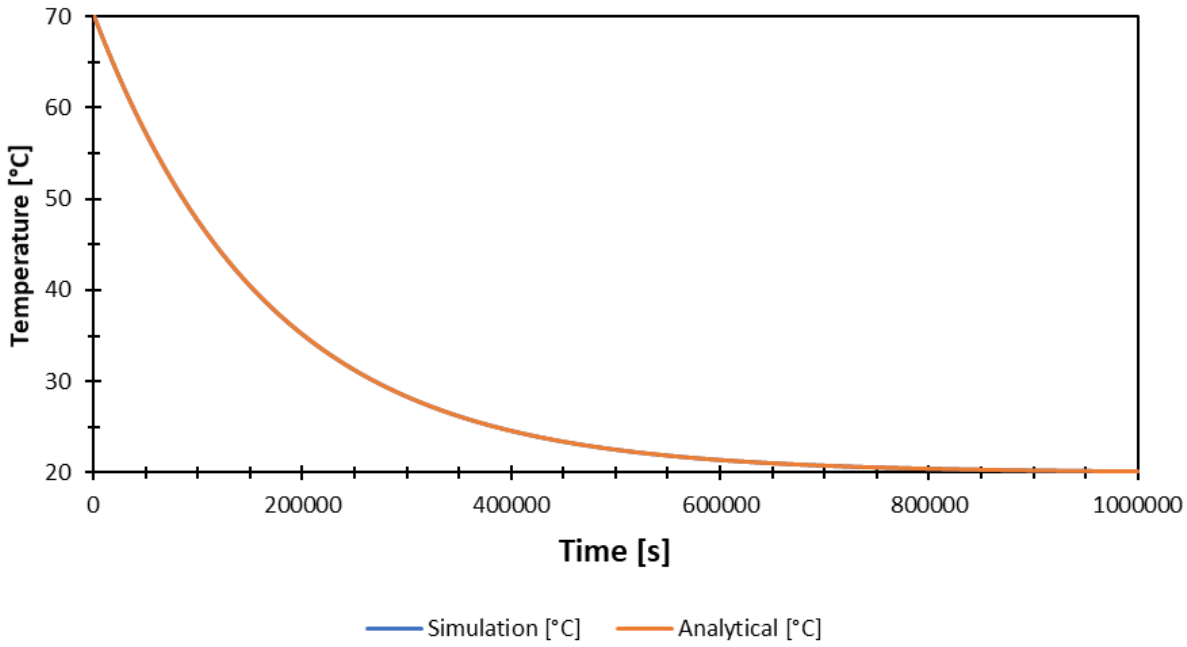

Figure 8.3: Average temperature of the hot water tank model vs. analytical solution

The model being tested: Thermal energy storage

Test: A hot water tank is initially at 20 °C. The height of the tank is 3 m, and the volume is 1 m^3. Water at 70 °C flows into the tank at a mass flow rate of 0.1 kg/s from the top fluid port. Water exits the tank to an infinite sink. The tank is assumed to be perfectly insulated. The purpose of this test is to verify the stratification of the tank during charging.

Expected result: According to Arpaci [124], the solution for unsteady heat conduction to a semi-infinite solid between a source at Tinf and a solid initially at T0 is as follows:

$$\frac{\mathrm{T(x,t)\ -\ Tinf}}{\mathrm{T0\ -\ Tinf}} = \mathrm{erf}\left[\frac{\mathrm{x}}{2(\alpha \mathrm{t})^{1/2}}\right]$$

Where α is the thermal diffusivity. There is numerical diffusivity due to the flow of fluid in the tank. Therefore,

$$\alpha = \alpha + \frac{1}{2} \times u \times \frac{H}{N}$$

Where u is the fluid velocity, H is the tank height, and N is the number of control volumes.

For fluid below the thermocline, the equation is:

$$\frac{T(x,t) - Tave}{T0 - Tave} = \text{erf}\left[\frac{x - C}{2(\alpha t)^{1/2}}\right]$$

Where C is the thermocline location, and Tave is the thermocline temperature.

The equation for fluid above the thermocline is:

$$\frac{T(x,t) - Tave}{Tinf - Tave} = \text{erf}\left[\frac{C - x}{2(\alpha t)^{1/2}}\right]$$

Simulated result: The simulation results agree with what is expected.

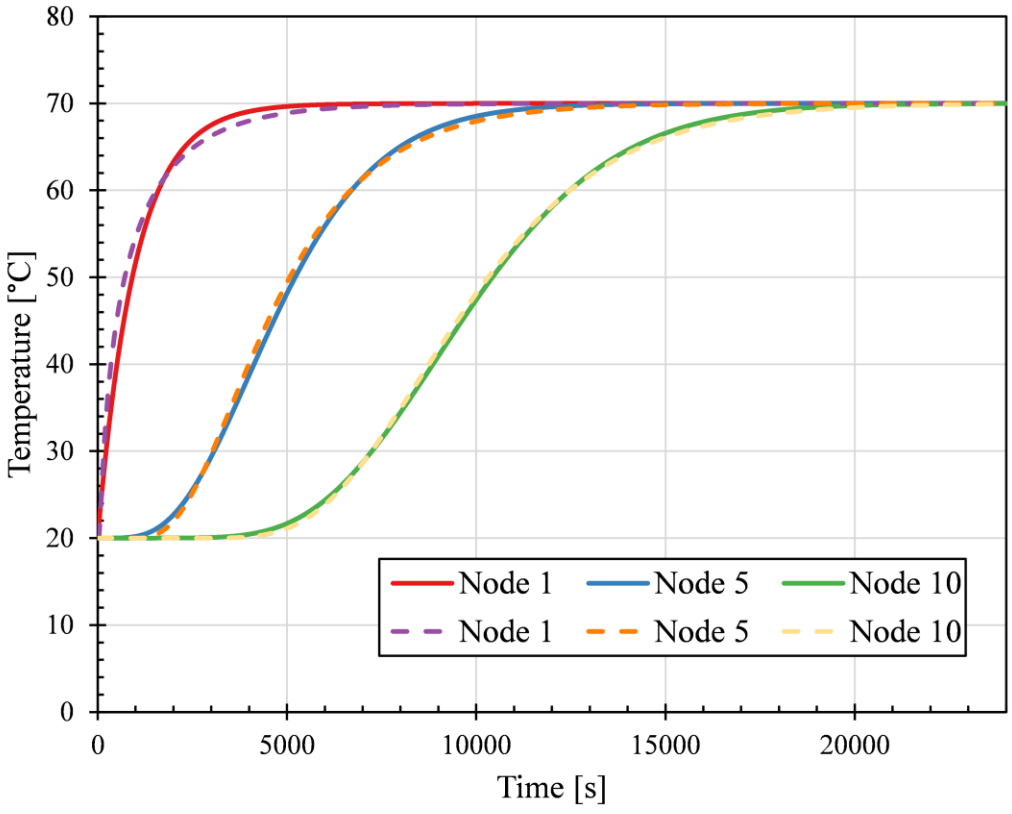

Figure 8.4: Temperature [°C] vs. time [s]. The simulated average temperatures are plotted as solid lines. The analytical average temperatures are plotted as dashed lines.

8.3 Appendix C: Building energy demands

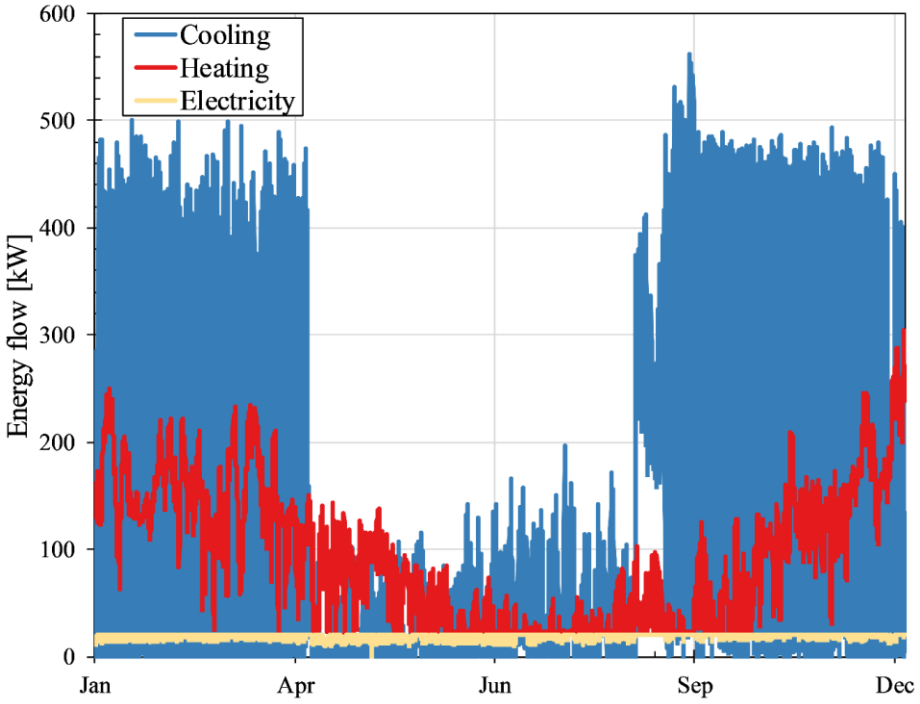

Figure 8.5: Arena hourly energy demands

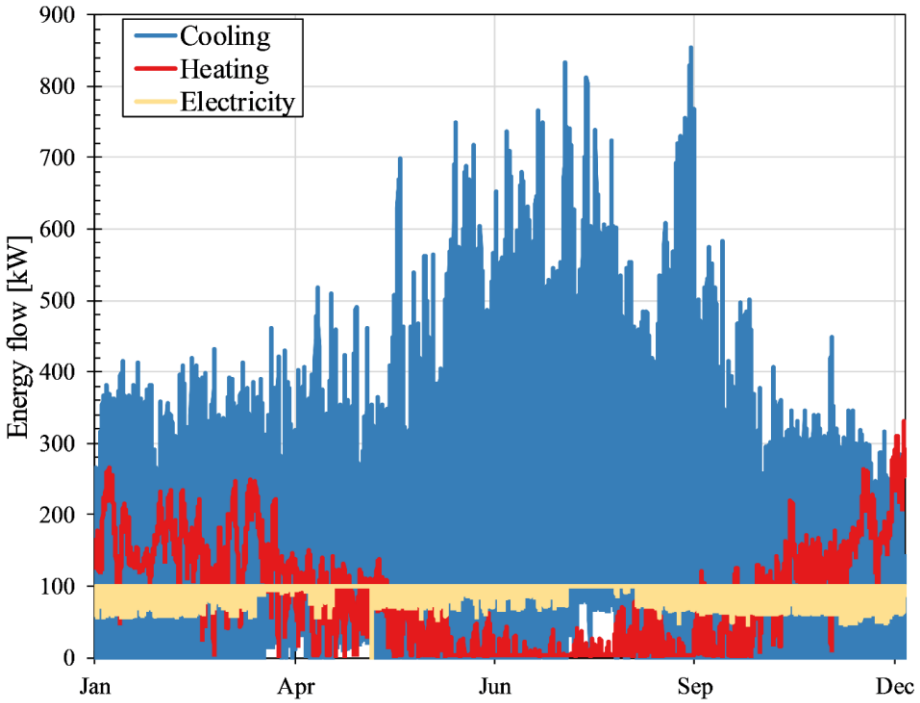

Figure 8.6: Library hourly energy demands

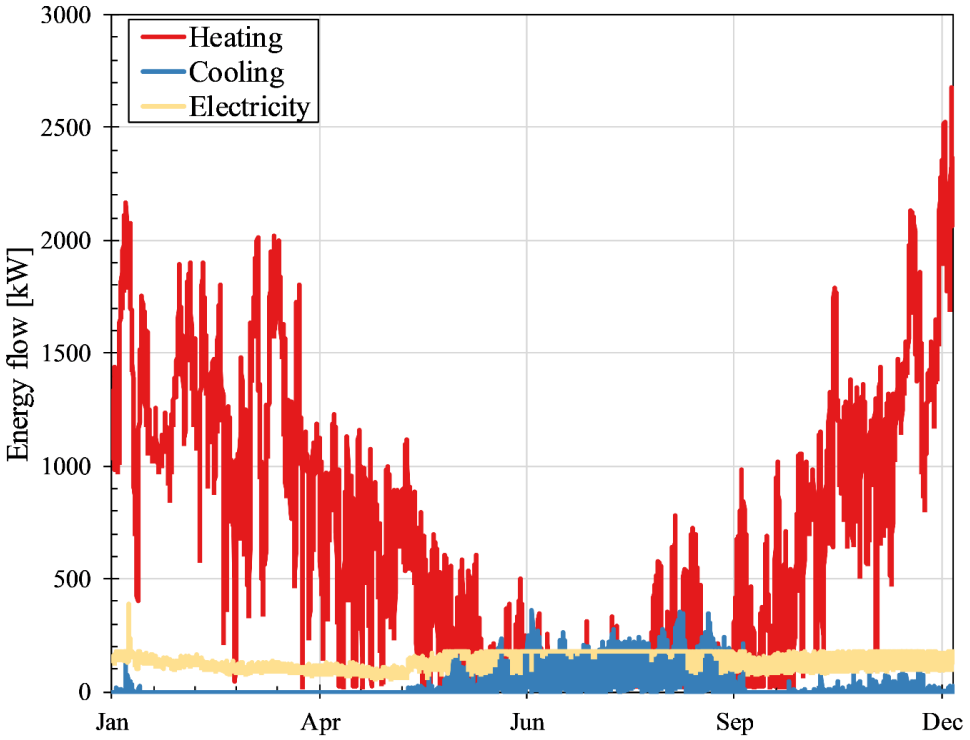

Figure 8.7: Residential tower hourly energy demands

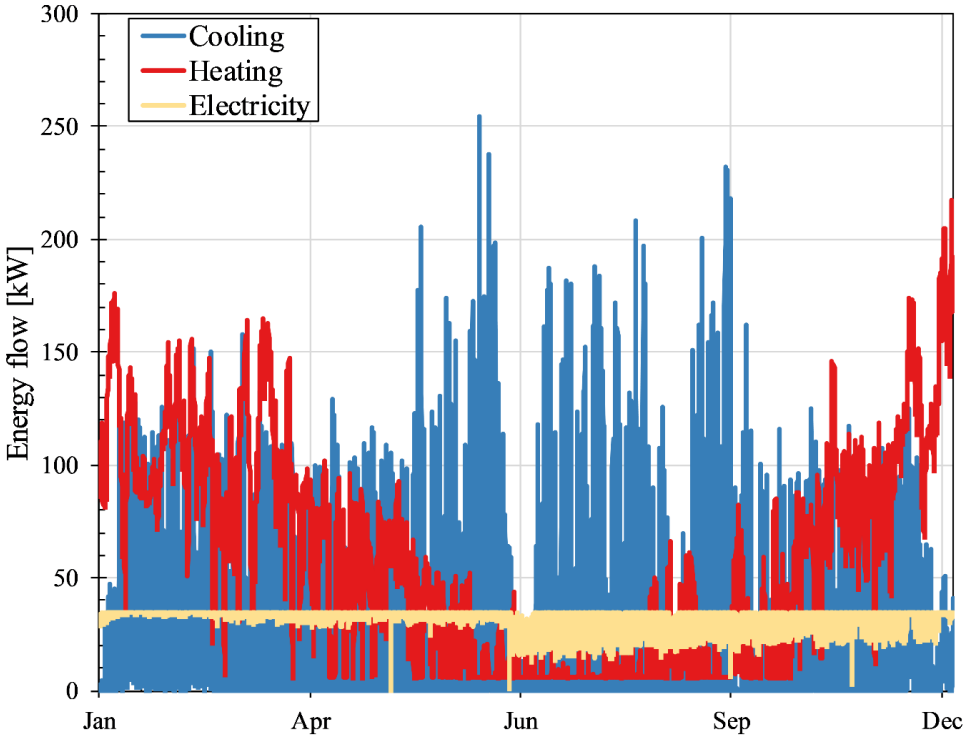

Figure 8.8: Senior center hourly energy demands

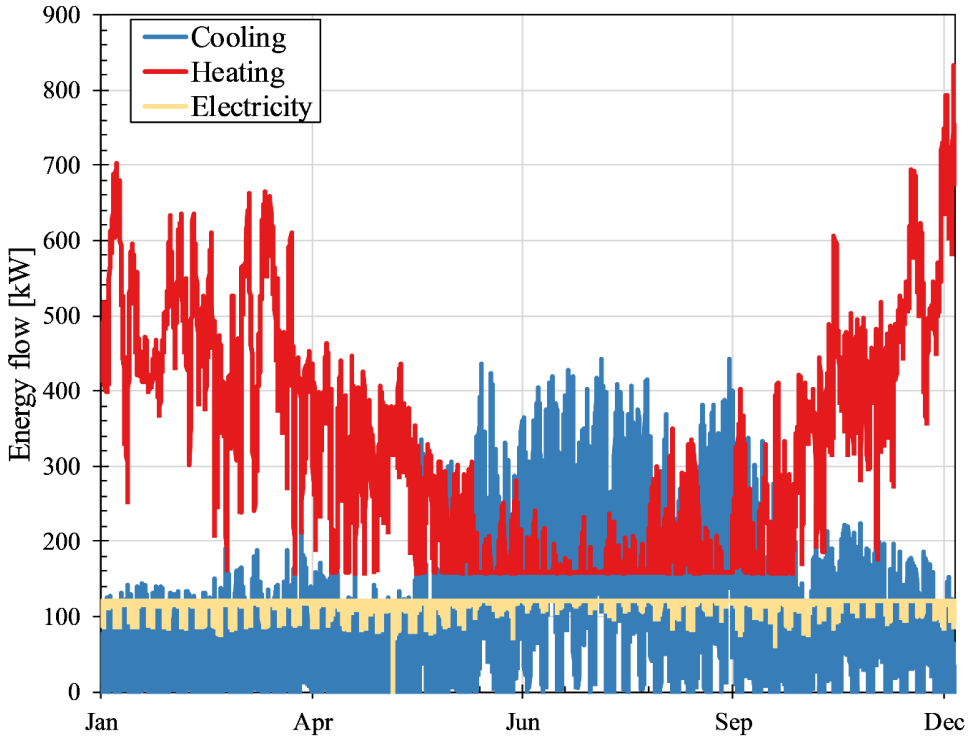

Figure 8.9: YMCA hourly energy demands

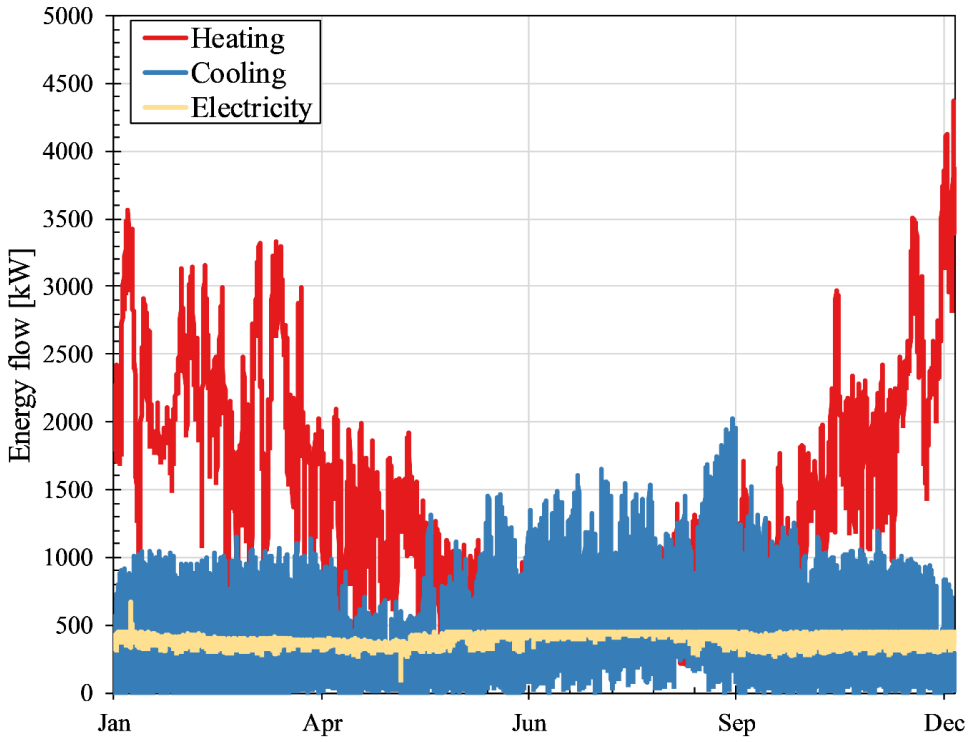

Figure 8.10: Total hourly energy demand

8.4 Appendix D: Ontario electrical grid hourly emission factor

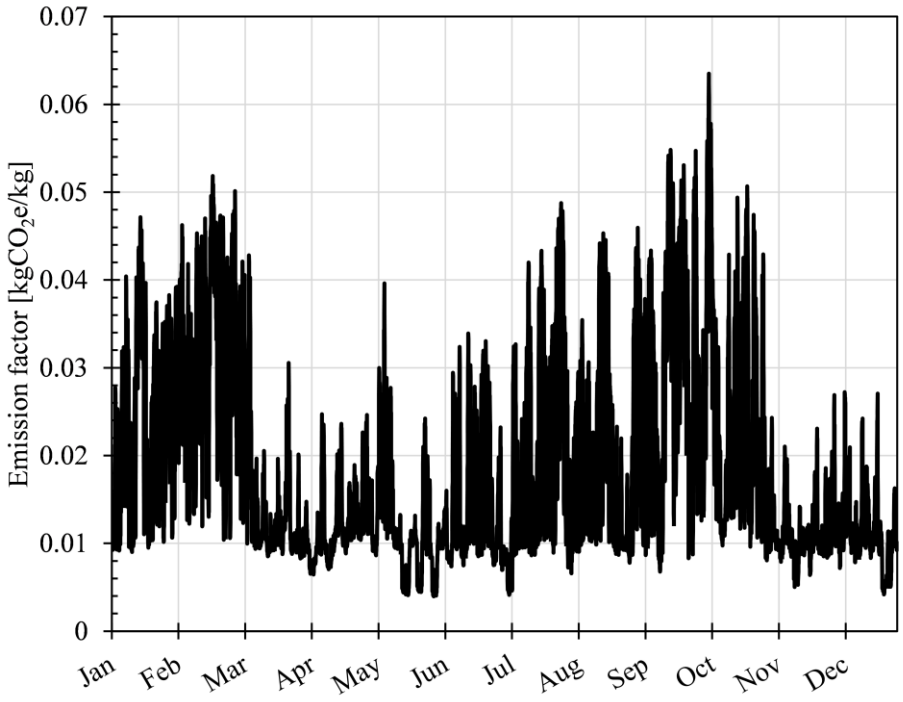

Figure 8.11: Ontario 2015 grid hourly emission factor

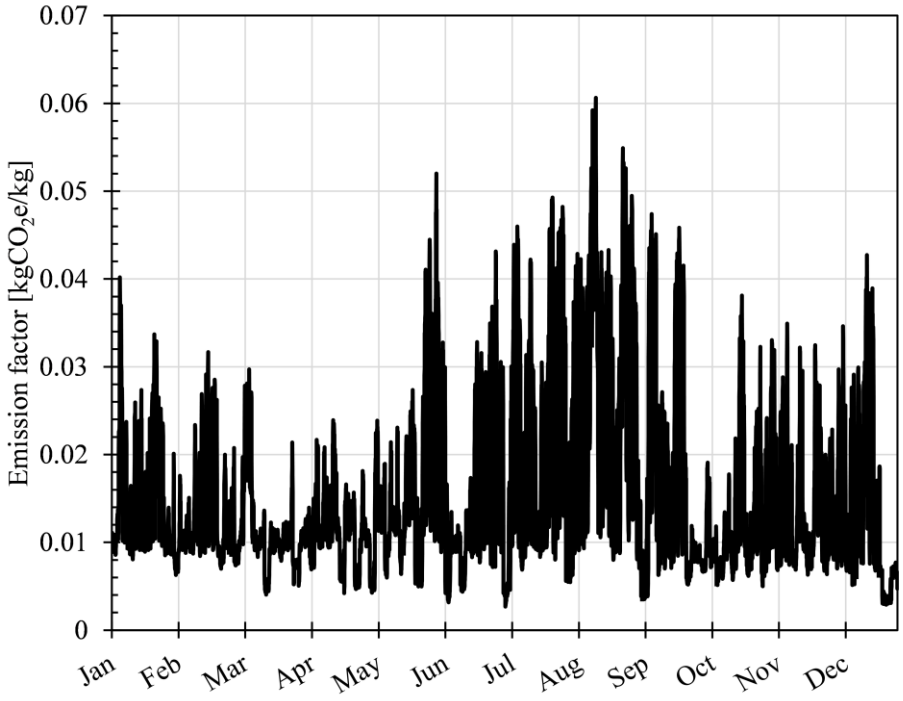

Figure 8.12: Ontario 2016 grid hourly emission factor

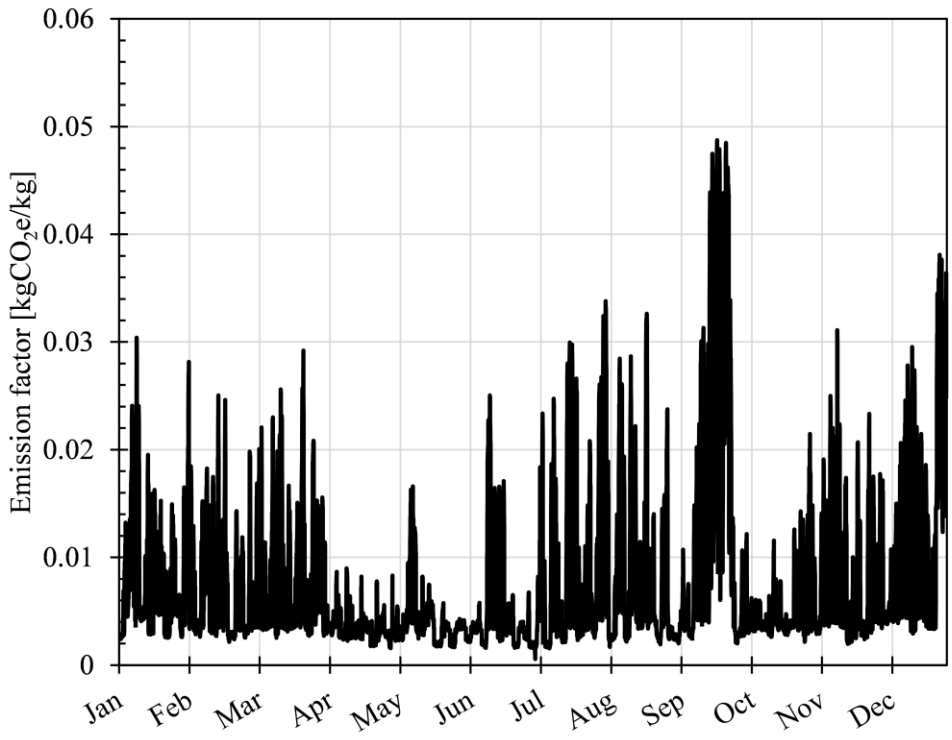

Figure 8.13: Ontario 2017 grid hourly emission factor

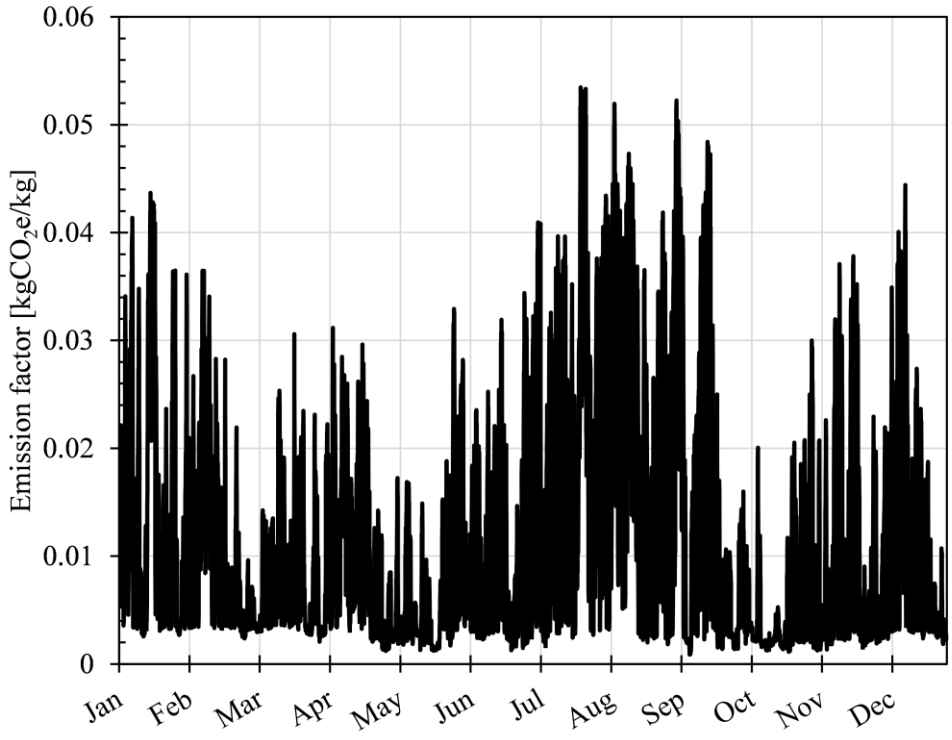

Figure 8.14: Ontario 2018 grid hourly emission factor